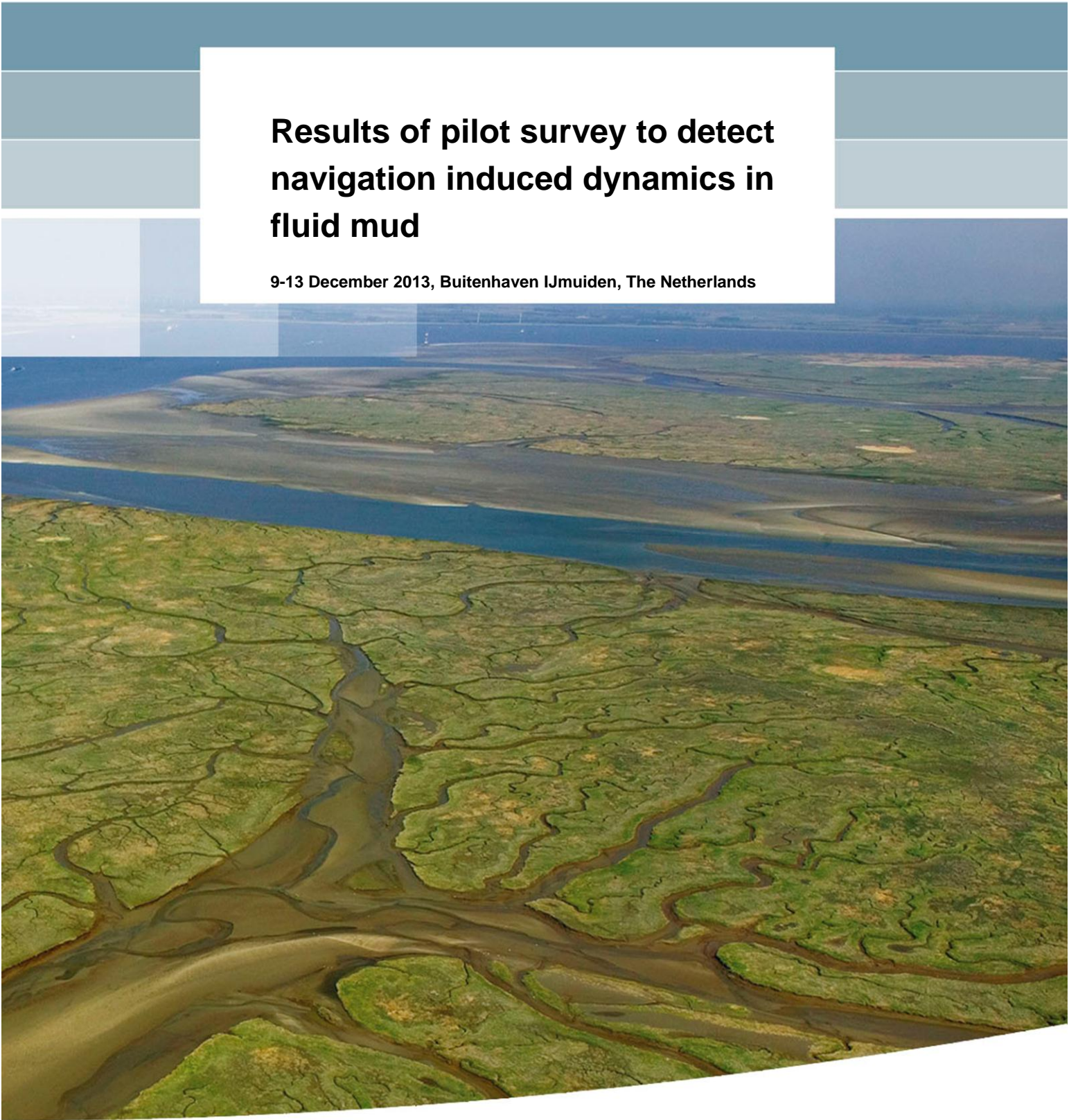


**Results of pilot survey to detect
navigation induced dynamics in
fluid mud**

9-13 December 2013, Buitenhaven IJmuiden, The Netherlands



Results of pilot survey to detect navigation induced dynamics in fluid mud

9-13 December 2013, Buitenhaven IJmuiden, The Netherlands

Pauline Kruiver
Han Winterwerp
Chris Mesdag
Giovanni Diaferia
Ane Wiersma

1209402-000

Title

Results of pilot survey to detect navigation induced dynamics in fluid mud

Client	Project	Reference	Pages
Rijkswaterstaat Corporate Dienst	1209402-000	1209402-000-BGS-0001	36

Keyword




Fluid mud, internal wave, mud flow, acoustic measurements, Side Scan Sonar, multibeam, ADCP, SILAS, density profiles

Summary

RWS and Deltares performed a pilot survey in the harbour of IJmuiden, the Netherlands, in December 2013. The goal of this pilot survey, as a first trial, was to detect the dynamics of the mud layer caused by everyday navigation with sufficient accuracy to be able to convert observations to mud properties through inverse modelling. Acoustic measurements were performed during the passage of 23 vessels; 7 of them were analysed. The swath bathymetry sonar data, acquired to monitor the water/fluid mud interface beneath and close to the passing vessel, appeared to be too noisy in the first interpretation. More advanced processing is needed to extract information on the internal wave beneath the passing vessel. Acoustic measurements beneath the survey vessel, at considerable distance from the passing vessel, showed that the internal structure of the mud changed during the passage. The observed disturbance of the mud can be a manifestation of internal waves inside the mud, mud flow and/or artefacts from horizontal movement of the survey vessel. The current data and level of processing do not allow firm conclusions on the mechanism observed. ADCP measurements suggest that the entire water column flows during passage of a vessel, which supports flow in the mud layer. The ADCP signal, however, does not penetrate the mud and provides flow velocities of the water layer only. The results of this first pilot are promising with regard to the possibilities of designing an operational system of navigability based on in situ and continuous measurements in harbours with muddy water bottoms. Recommendations are made with respect to processing, experiments and modelling for the next step in this line of research.

Reference

RWS KPP project "Alternatieve parameters en nieuwe meettechnieken voor vaargeuldieptes bij zachte slibbodems"

Version	Date	Author	Paraaf Review	Paraaf Goedkeuring	Paraaf
3	22 April 2014	dr. P.P. Kruiver	 ir. Joh.G.S. Pennekamp	 dr. R.M. Hoogendoorn	
		prof. dr. ir. J.C. Winterwerp			
		drs. C.S. Mesdag			
		G.Diaferia MSc			
		dr. A.P. Wiersma			

Title

Results of pilot survey to detect navigation induced dynamics in fluid mud

Client

Rijkswaterstaat Corporate Dienst

Project

1209402-000

Reference

1209402-000-BGS-0001

Pages

36

Version	Date	State	Comments
1	27 March 2014	Draft	Draft document for internal use
2	31 March 2014	Draft	Internally reviewed draft document, released to RWS
3	17 April 2014	Final	Comments of RWS incorporated

State

final

Contents

1 Introduction	3
2 Measurement techniques	5
3 Selection of vessel passages	7
4 Results	9
4.1 Effect of passing vessel on water level	9
4.2 RWS Multibeam bathymetry	10
4.3 ADCP – Vessels 6a, 6 and 6b	11
4.4 X-star – Vessel 15	15
4.5 SILAS – Vessel 15	16
4.6 Hydrochart – Vessel 6	17
4.7 Point measurements of density	20
5 Interpretation	23
5.1 Internal waves at the water/ mud interface	23
5.2 Interpretation of reflections in SILAS	23
5.3 Derivation of observation parameters for vessel 6a	25
5.4 Derivation of observation parameters for all vessels	27
5.5 Accuracy	32
6 Conclusions	33
7 Recommendations	35
 Appendices	
A References	A-1
B Short survey report	B-1
C Instruments	C-1
C.1 ADCP	C-1
C.2 Hydrochart	C-2
C.3 Multibeam RWS	C-3
C.4 X-star (subbottom profiler)	C-3
C.5 SILAS	C-4
D Summary processing	D-1
D.1 Simple processing	D-1
D.2 SILAS processing	D-1
E Screenshots of measurements of all selected vessels	E-1
F Navitracker density profiles	F-1

G Interpretation of SILAS data

G-1

1 Introduction

From 9 to 13 December 2013, Deltares performed a pilot survey in part of the harbour of IJmuiden (Buitenhaven), the Netherlands. The survey was carried out on Ms. Zirfaea, a survey vessel of RWS.

The background of this pilot is described in Deltares reports Kruiver et al. (2013a) and Versteeg and Kruiver (2013). Summarised, RWS is looking for new ways to determine the nautical depth and the thickness of soft mud layers in the areas of their responsibility in the Netherlands, i.e. the Maasgeul (entrance of Port of Rotterdam) and IJmond (entrance to harbour of IJmuiden). A new approach was proposed by J.C. Winterwerp from Deltares. This approach is based on observation of the internal wave generated at the water/mud interface by the passage of ships followed by an analysis and interpretation of such measurements in terms of key mud properties.

The goal of the pilot is to observe the dynamics of the fluid mud caused by the passage of a deep draught vessel for the first time in a systematic way. From the measurements, it should be possible to determine the amplitude, wavelength, velocity and damping of the internal wave. These parameters would form the input for numerical modelling of internal waves aimed at determining the properties of the fluid mud (e.g. density and viscosity) in the same mix and interaction as they govern the navigability. Collection of more internal wave parameters, forward modelling, inverse modelling and building a decision support system will be the next steps towards an operational system of navigability based on in situ and continuous measurements in harbours with muddy water bottoms (Kruiver, 2013b).

Model calculations of a two layer model (water and fluid mud) with a moving vessel showed that internal waves are expected to be excited in IJmuiden with measurable effects (Kruiver et al., 2013a, chapter 5). The survey plan for this pilot is described in Versteeg and Kruiver (2013). Additionally, X-star measurements were performed. It was expected that 5 to 10 vessel passages would be measured.

During the survey, ship traffic was more busy than anticipated. In total, 23 measurements were acquired during vessel passages, using varying acoustic instruments. This resulted in a larger and possibly richer dataset than anticipated. During the survey days RWS performed regular point measurements of density by Navitracker. Additionally, point measurements were performed on the line of passage (in general on the "lichtenlijn") before and after passage of a deep draught vessel. On two of the five survey days, DotOcean performed Graviprobe measurements. These are reported separately (van Roeyen, 2013). Their results are not integrated in this study.

This study is performed within the Corporate Innovation Program (CIP) of Rijkswaterstaat.

In chapter 2, a short description of the measurement techniques is given. A more extensive overview of the instruments and the processing steps are provided in Appendix C and D. Chapter 3 describes the selection of the vessels that were analysed. In Chapter 4, the results of the various techniques are illustrated showing the vessel passage with the best results. Results of all vessel passages are included in Appendix E. The interpretation of results in terms of observation parameters is given in chapter 5. Chapters 6 and 7 include conclusions and recommendations.

2 Measurement techniques

The survey consisted of two parts: (i) Navitracker measurements of the regular IJmuiden monitoring grid and (ii) the internal wave experiment with a variety of acoustic instruments and additional Graviprobe measurements (DotOcean). Table 2.1 summarises the specifications of the instruments and their purpose. The memo of the survey report is included in Appendix B. This is a shorter and anonymised version of Kruiver (2013d). More detailed specifications are included in Appendix C.

Table 2.1 Summary of instruments used during the survey

Instrument	Owner	Specifications	Purpose
Navitracker	RWS	Nuclear density probe	Measurements of density profiles: <ul style="list-style-type: none"> Regular monitoring grid Before and after passage of vessels
ADCP	RWS	600 kHz	Measure water flow velocities in water column up to just above the water-mud interface.
Multibeam	RWS	Kongsberg EM3002 single head	Determination of bathymetry, measuring top of the mud, swath too small to look beneath passing vessel.
X-star Subbottom profiler	Deltares	Edgetech X-star SB424, frequency sweep of 2 to 24 kHz	Determine structures within the mud directly below the survey vessel, visual.
SILAS	RWS	33 kHz penetrating echosounder with SILAS acquisition software	Determine structures within the mud directly below the survey vessel by analysing different density levels (calibration needed).
Hydrochart	Deltares	Klein Hydrochart 5000 Swath Bathymetry Sonar System, frequency 455 kHz	<ul style="list-style-type: none"> Side scan sonar: structures in top of the mud Bathymetry (inferometric): determine top of the mud similar to multibeam, but with much larger swath (able to look beneath passing vessel).
Graviprobe	DotOcean	Free fall penetrometer	<ul style="list-style-type: none"> Indication of density of the mud Indication of viscosity of the mud

During the first two days, a different survey vessel carried out a multibeam survey to determine the bathymetry of the entire IJmuiden harbour. RWS West Nederland Noord provided the interpreted multibeam grids and nautical depth grid to Deltares.

Before raw data can be interpreted, processing is necessary. The processing steps are explained in appendix D.

3 Selection of vessel passages

Vessel names have been omitted in order to guarantee privacy of the vessel. This is a prerequisite to use AIS data (navigation data) of passing vessels provided by Marin and Kustwacht.

During the survey, measurements were performed while vessels with sufficient draught (> 6 m) passed Ms. Zirfaea. There was more ship traffic during the survey, not all vessels were measured. In total, data were collected during approximately 23 passages.

Table 3.1 gives an overview of the vessel passages and measurements. Vessels are referred to by sequential numbers related to the data files. In some cases, one or more vessels that could influence the measurements passed Ms. Zirfaea before or after the main vessel. This is indicated with an a or b. Speed and draught are given, because these parameters are important for the selection of the vessels to be analysed. For most vessels, all measuring systems were operational. The operational measuring systems are indicated by the crosses. The survey vessel Ms. Zirfaea was stationary during most of the vessel passages. For some early measurements, the best measurement strategy needed to be found. Therefore, for passing vessels 2 and 3, Ms. Zirfaea moved to the passing vessel. Later on, it was decided to put Ms. Zirfaea on dynamic positioning and stay as stationary as possible. We decided to do a sailing experiment with the passage of vessel 10, letting it pass and then sailing along for some distance.

Due to limited time and budget for data processing, only approximately 5 vessel passages could be analysed. These passages are selected using several rules of thumb. Theoretically, the height of internal waves scales with the square of the vessel speed and exponential with the reciprocal of keel clearance of the vessel. For the ranges of keel clearances in this experiment, this is more or less linear. In the IJmuiden setting, with more or less fixed water depths, this means that the height of the internal wave will be larger for deeper draughts (smaller keel clearance). Based on the rules of thumb, the effect of vessel speed dominates that of the draught, because of the quadratic relation.

Using the vessel speed and draught to do the selection. Vessel 6 and 18 are chosen because of their large draught of almost 17 m. However, entering the harbour their speed was already reduced to moor at the quay of Tata Steel. Vessels 6a and 6b passed Ms. Zirfaea just before and just after the main vessel 6. The data are in the same files. Consequently, 6a and 6b were included in the analysis. Vessels 3, 15 and 20 have intermediate draught and high speeds. In total, 7 vessels were analysed. The sizes of the selected vessels and the shortest distance to Ms. Zirfaea are included in Table 3.2.

Table 3.1 Details of vessels for selection

Date (Dec 2013)	Vessel identification	Speed (knots)	Draught (m)	Time of passage (UTC)	Survey vessel Ms. Zirfaea stationary?	IMB	ADCP	Hydrochart	SILAS	X-star	Navitracker before	Navitracker after
09	1	8.7	13.9	17:52-17:54	yes	x	x	x	x		0?	5
10	2		6.2	08:20	no		x				0	0
10	3	11.8	11.6	11:15-11:17	no	x	x	x	x		5	
10	3a			11:18	yes	x	x	x	x			5
10	5a	7.1	7.1	18:10	yes	x	x	x			0	0
10	5	5.6	10.4 5	18:16-18:18	yes	x	x	x			0	0
11	6a	7.1	8.4	05:12	yes	x	x	x	x		5	
11	6	3.8	16.9	5:31-5:33	yes	x	x	x	x			
11	6b	9	7.3	5:44-5:45	yes	x	x	x	x			5
11	7	10.6	7.3	06:24	no			x			0	0
11	8	12.7	8	7:53-7:54	no		x	x			0	0
11	9			10:04	no			x			0	0
11	10	7.4	13.7	11:32-11:36	sailing	x	x	x	x		0	5
11	11	8.6	7	13:40	?			x			0	0
11	12	9.7	10.5	16:06	?	x	x	x	x	x	0	0
12	13	10	6.2	8:45?	no					x	0	0
12	14	5.5	13.6	09:10	yes	x	x	x	x	x	5	5
12	15	9.7	11.5	09:20	yes	x	x	x	x	x	0	0
12	16	9.2	10.4	12:29	yes	x	x		x	x	0	0
12	17	5.3	13.4	13:22	yes	x	x	x	x	x	0	0
12	18	4.9	16.8	19:02	yes	x	x	x	x	x	3	3
13	19	13	6.2	08:27	yes	x	x	x	x	x	0	0
13	20	11.2	8	10:10-10:12	yes	x	x	x	x	x	0	3

Table 3.2 Dimensions of vessels selected for analysis

Date	Id.	Time of passage (UTC)	Speed (knots)	Speed (m/s)	Length (m)	Length/speed = expected duration of passage (s)	Width (m)	Draught (m)	Shortest distance according to Side Scan Sonar (m)
10-12-13	3	11:15-11:17	11.8	6.07	289	48	45	11.6	76
11-12-13	6a	05:12	7.1	3.65	183	50	32	8.4	90
11-12-13	6	5:31-5:33	3.8	2.00	289	145	45	16.9	68
11-12-13	6b	5:44-5:45	9	4.63	185	40	32	7.3	90
12-12-13	15	09:20	9.7	5.00	183	37	32.2	11.5	136
12-12-13	18	19:02	4.9	2.52	289	115	45	16.8	78
13-12-13	20	10:10-10:12	11.2	5.76	250	43	38	8	144

4 Results

Before showing the results, the effect of a passing vessel on the water level at Ms. Zirfaea needs to be explained. This is described in section 4.1.

The results of the multibeam survey performed for RWS and processed by them are included in section 4.2. The results of the different acoustic systems are illustrated in sections 4.3 through 4.6 using the vessel passage that best illustrates the technique. The results of the point measurements of density by Navitracker are described in section 4.7. The screenshots for the all vessels containing vessel route, GPS height information, density information and acoustic results are included in Appendix E. The Navitracker density profiles of all point measurements of the regular monitoring grid in the survey area are included in Appendix F.

4.1 Effect of passing vessel on water level

Sailing vessels induce a water return flow proportional to the vessel size and speed. Because of the increased flow velocity, the water level will drop (Bernoulli-effect). It is expected that the water level around Ms. Zirfaea will lower by the passage of (large) vessels. Normal heave motion of the vessel is on a time scale of seconds, while the effect on water level caused by the passage of a large vessel is in the order of minutes. The motion sensor of the vessel that measures heave by vertical acceleration is not able to detect the very slow vertical movement induced by the Bernoulli-effect. In order to properly interpret the top of the mud during and after passage, this water level effect is accounted for.

Due to the expected lowering of Ms. Zirfaea during passage, the distance between the water level and the top of the mud decreases. This will show as an apparent decrease in water depth in the various acoustic measurements.

The height of Ms. Zirfaea is registered by two GPS antennas, one at port and one at starboard side. The GPS signal gives the height relative to the WGS84 ellipsoid. The heights were not converted to NAP, since this analysis is qualitative only. Figure 4.1 shows the port and starboard antenna heights on the left axis. On the right axis, the top of the mud (according to SILAS) in m-NAP reflects the apparent water depth. The top of the mud seems to be lifted during passage (smaller water depths, see e.g. Figure 4.7). For plotting purposes, however, the right y-axis has been inverted so that the apparent lift in the top of the mud shows as a dip, similar to the dip in GPS height. From Figure 4.1 we infer that the apparent lift in top of the mud corresponds excellently with the drop in GPS height. This pattern is similar for all other analysed vessels. The differences in water level and the difference in apparent top of the mud before and during passage are summarised in Table 4.1.

The error in GPS heights is ca. 3 cm, the error in top of the mud level according to SILAS is approximately 5 cm. Differences between SILAS and GPS heights are -3 to + 2 cm. From Figure 4.1 and Table 4.1 we conclude that the apparent lift in top of the mud is entirely due to the effect of lowering of the water level and hence Ms. Zirfaea during passage of the large vessels. Therefore, in the interpretation of levels (e.g. depths of reflections) this is corrected for.

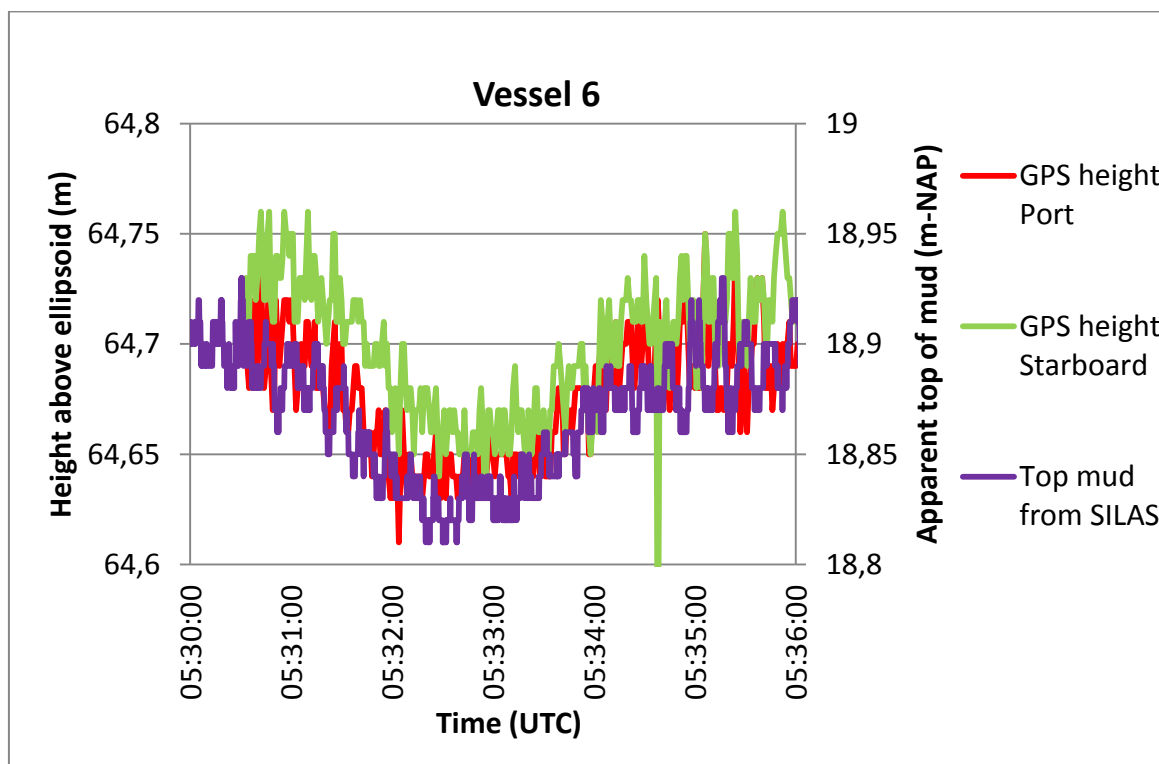


Figure 4.1 GPS height and apparent water depth (top of the mud) according to SILAS for vessel 6. GPS height is given relative to WGS84 ellipsoid on the left axis. The water depth (top of the mud) relative to NAP is given on the right axis. Note that the values for the apparent water depth are plotted inversely, so that the graphs overlap.

Table 4.1 GPS heights and apparent top of the mud before and during passage of vessels.

Vessel	SILAS top of mud before passage (m-NAP)	SILAS maximum level of top mud during passage (m-NAP)	SILAS difference in top mud (m)	Maximum drop in starboard/port GPS height (m)	Difference GPS and SILAS (m)
3	18.98	18.55	0.43	0.4	-0.03
6a	18.41	18.35	0.06	0.08	0.02
6	18.43	18.35	0.08	0.07	-0.01
6b	18.43	18.32	0.11	0.11	0.00
15	19.22	19.11	0.11	0.12	0.01
18	18.21	18.11	0.1	0.1	0.00
20	18.94	18.82	0.12	0.12	0.00

4.2 RWS Multibeam bathymetry

During the survey with Ms. Zirfaea, a small survey vessel performed a multibeam survey for RWS West-Nederland Noord. RWS processed the data and provided the multibeam grid of bathymetry. The bathymetry for the harbour of IJmuiden is shown in Figure 4.2. The survey location is situated between the old and the new piers. The colour coding of bathymetry is chosen to emphasise visualisation of differences in height in the survey area. The water way is clearly visible. In the red box, the water depth is generally around 21.5 m (with additional tide range of ± 1 m). There are some localised shallower spots, shown in yellow. During measurement with the multibeam in the internal wave experiment, these small “bumps” were visible in the multibeam record.

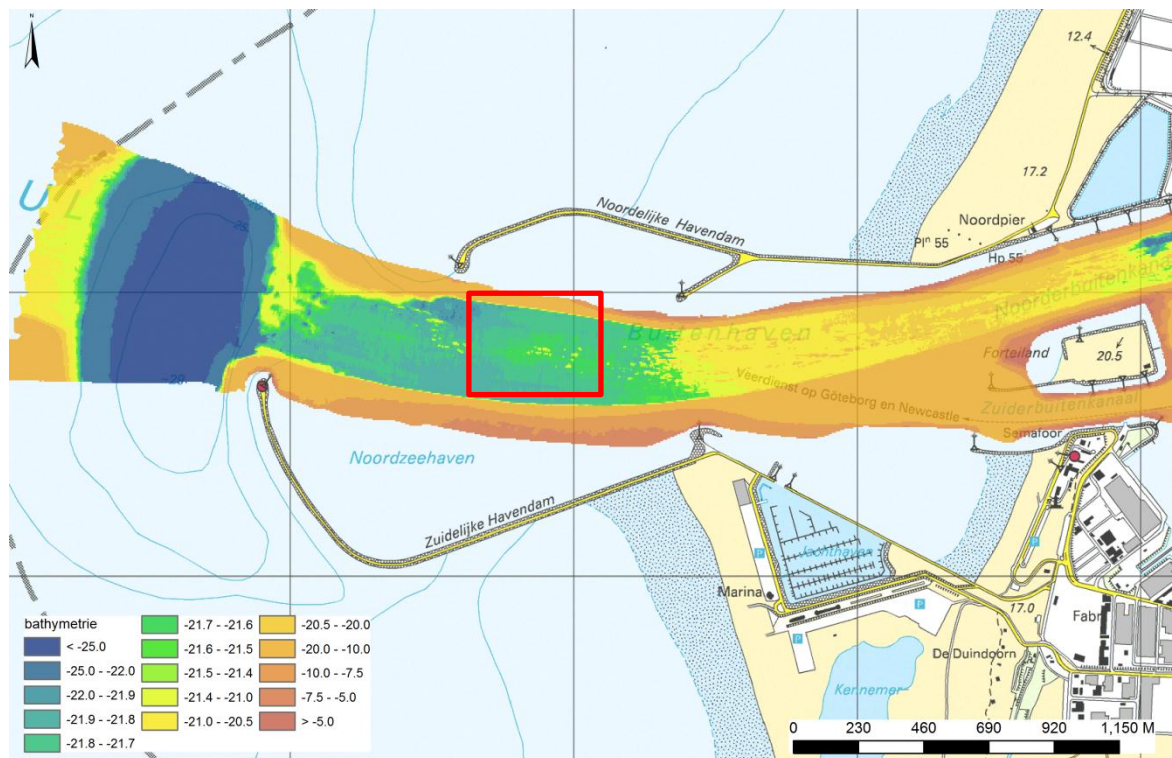


Figure 4.2 RWS bathymetry grid for IJmuiden, 9-10 December 2013. The survey area for the internal wave experiment is indicated by the red square.

4.3 ADCP – Vessels 6a, 6 and 6b

The ADCP data which were collected during this survey contain a lot of noise. The noise level is in the order of 5 cm/s, while the signal to be analysed is around 25 cm/s. This noise level is related to the frequency of ADCP, grid cell size and the fact that no averaging over time was applied. With higher ADCP frequency, the bottom would not be reached due to attenuation. It was expected that the possible effect of passing vessels on the water flow could not be detected using larger cell sizes and averaging over time. Because of the noise, the flow near the bottom cannot be quantified with sufficient accuracy. However, flow patterns can be distinguished in the ADCP data.

The ADCP results are illustrated using the vessel passages around vessel 6 (Figure 4.3, Figure 4.4 and Figure 4.5). The screen dumps for the other vessels are included in Appendix E. The top panel of Figure 4.3 shows the magnitude of flow velocity. Before and after passage of a vessel, the water column is quite stationary. Two velocity anomalies are visible, corresponding to passage of vessels 6 and 6b. At those moments, the flow is around 15 to 35 cm/s over the entire water column. For fixed or sandy bottoms, the velocity profile is generally logarithmic. In this case, however, the entire water column moves with approximately the same velocity. The velocity right above the water/mud interface, however, cannot be determined because of the noise. At the time of passage of vessel 6a, no clear velocity anomaly is visible, due to the high noise level.

The middle panel of Figure 4.3 shows the direction of the flow. Before and after passage of a vessel, flow scatters in all directions. During passage, however, the flow is directional. In the record, we observe three directional events, corresponding to the passage of vessels 6a, 6 and 6b. In addition, there seem to be two more anomalies present, indicated by the blue arrows. The timing of these ADCP velocity direction anomalies correspond to the timing of the

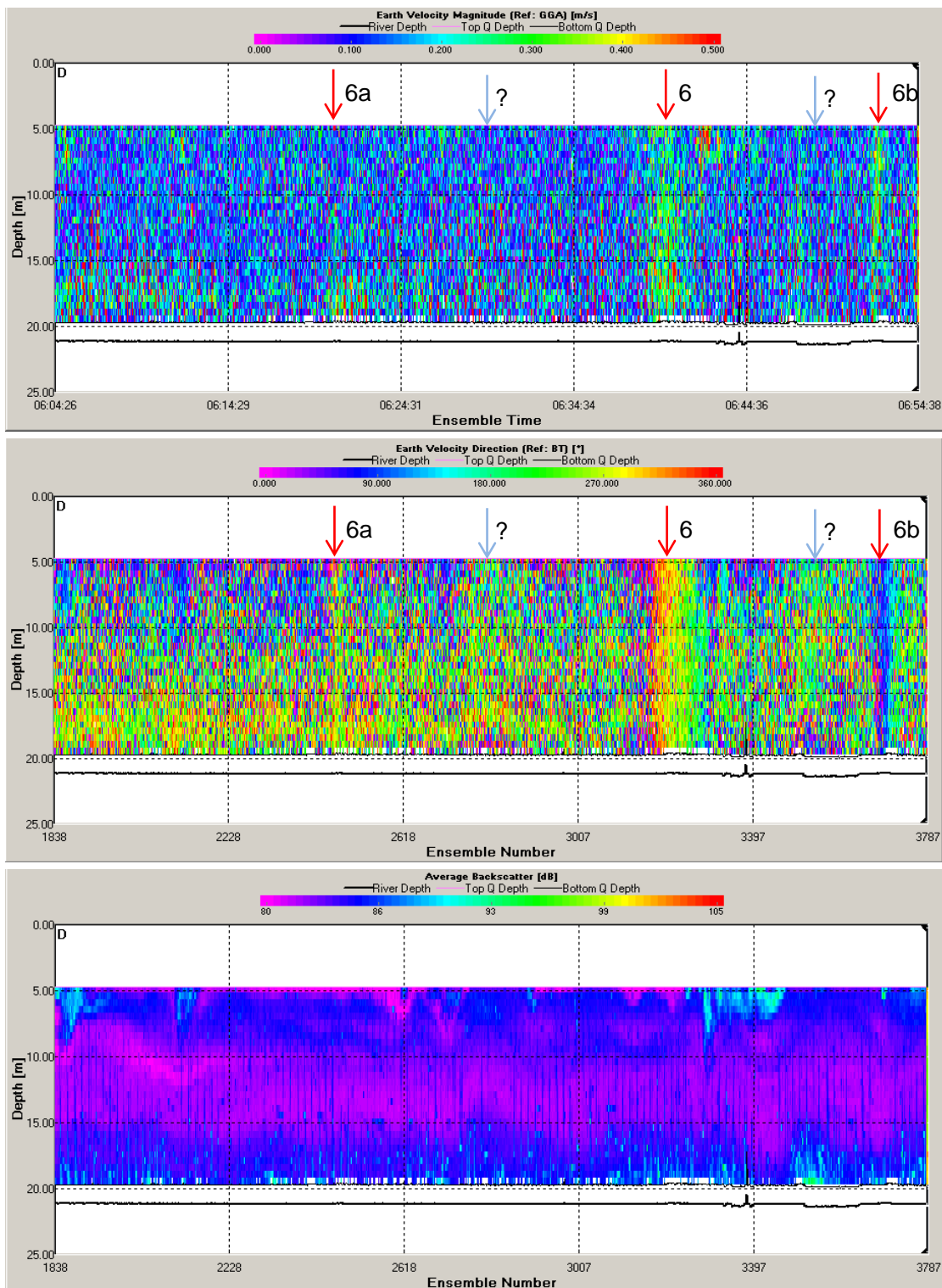


Figure 4.3 Example of ADCP result, for record 6, containing passage of vessels 6a, 6 and 6b. Reference system: GPS coordinates. Top: magnitude of velocities, middle: direction of velocities, bottom: backscatter intensity. The events of passage are indicated by red arrows. Two more anomalies are identified in the direction of velocities (middle panel), shown by blue arrows. Note that there was a shift of approximately 1 hour and 8 minutes in internal ADCP instrument time relative to UTC. Record lengths of top (showing time), middle and bottom (showing ensemble number) are equal.

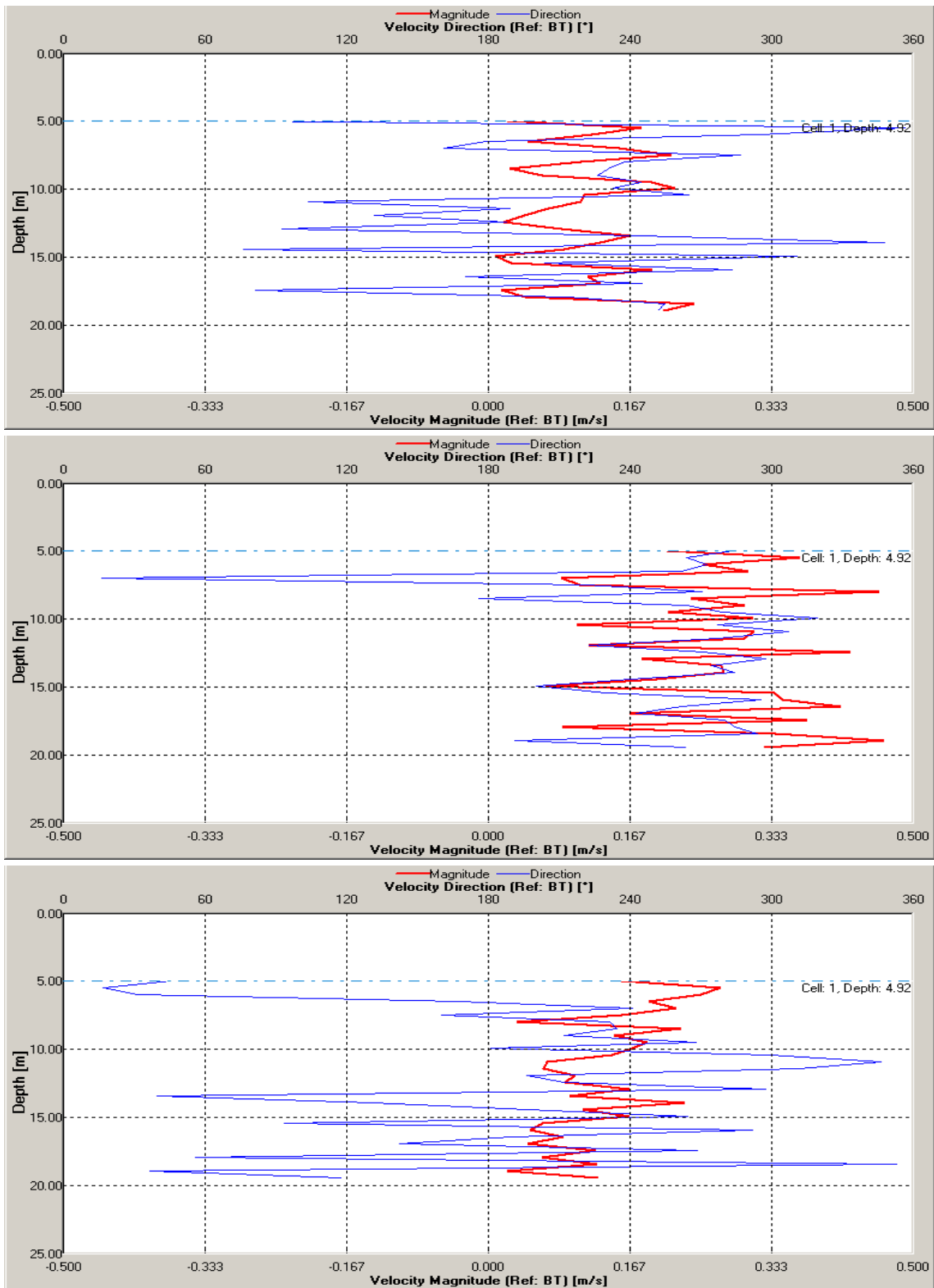


Figure 4.4 ADCP velocity profiles for vessel 6. From top to bottom: before passage (ensemble 3077), during passage (ensemble 3235) and after passage (ensemble 3325).

anomalies in the SILAS data (included in Appendix G, but not interpreted). For one of them, passage of a small vessel was noted in the log. For the other, there was no entry in the log, but a small vessel might have passed as well.

The bottom panel of Figure 4.3 shows the backscatter intensity of the signal. In general, backscatter is related to the distribution of particles in the water column. Particles can consist of sediment, algae or organisms. Mud clouds, the transition between salt and fresh water and bubbles caused by propulsion of passing vessels can also be distinguished. Backscatter anomalies in Figure 4.3, bottom panel, do not seem to be related to the passage of vessels 6a, 6 and 6b.

The magnitude and direction of flow can be visualised by plotting the profile at any chosen time (corresponding to an ensemble number). The vertical profiles of magnitude and direction of flow are plotted before, during and after passage of vessel 6 in Figure 4.4. Before and after passage, the direction of the flow (blue line, top and bottom panel) shows no clear direction. During passage (middle panel), the flow is much more directional. The velocity magnitude shows a lot of noise in all panels. Looking through the slit of your eye, it appears that during passage there is a constant velocity through the entire water column, rather than a logarithmic profile. There seems to be no deceleration towards the bottom, which is normally observed over a fixed or sandy water bottom. Although the ADCP is not able to detect flow within the mud, the fact that there is still flow above the top of the mud suggests that it is possible that the mud itself might be flowing. Additional flow measurements using P-EMS facilitating determination of flow within the fluid mud are recommended. P-EMS is a sensor that measures flow using electromagnetic principles, instead of acoustics principles used in ADCP.

Another way to check for movement of the water bottom is to plot the coordinates of the ADCP by GPS signal and by bottom tracking. If the water bottom is stationary, the two tracks plot on top of each other. If the water bottom is moving, the two tracks diverge. Figure 4.5 shows the movement of Ms. Zirfaea for vessel 6 (left panel) and vessel 20 (right panel). The GPS coordinates and bottom tracking coordinates almost coincide for vessel 6. The difference after passage is well within 1 m. For vessel 20, however, the difference is in the order of 25 m. Therefore, it is likely that the bottom was not stationary during passage of vessel 20. In this case, there seems to be a two layer system of flow (see screenshot in Appendix E), possibly related to salt and fresh water layering due to drainage at the sluices.

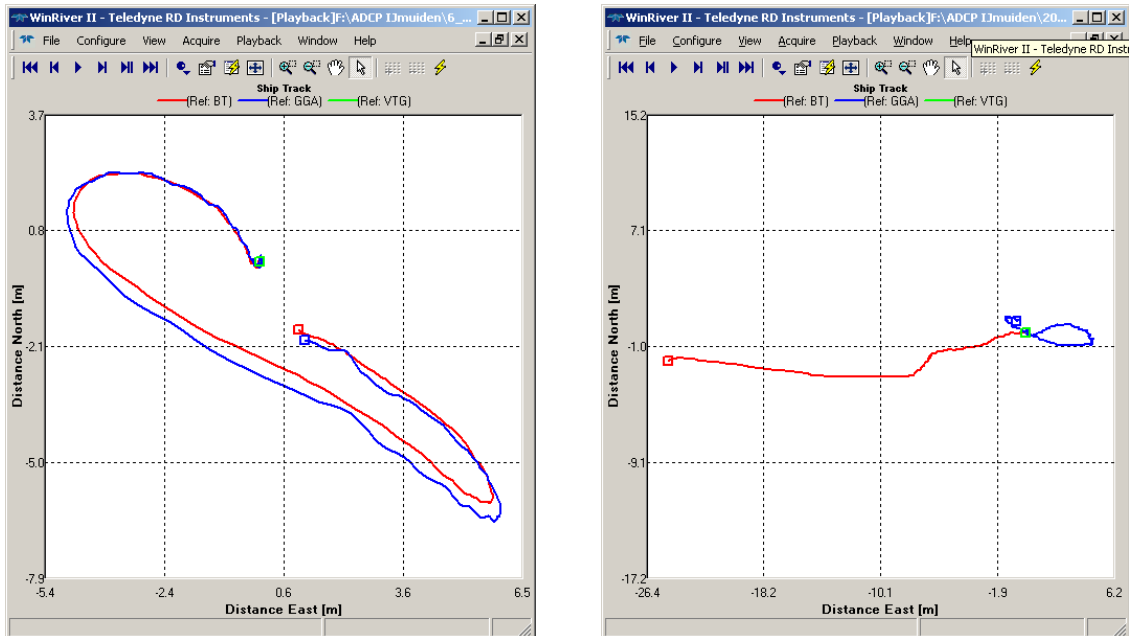


Figure 4.5 ADCP coordinates with green box: position at start of graph, red line the position according to bottom tracking and blue line according to GPS antenna (RTK-GPS). Left: for vessel 6 between ensembles 3075 - 3325. Right: for vessel 20 between ensembles 180 - 330. Note the difference in horizontal and vertical scale of the two panels.

4.4 X-star – Vessel 15

Figure 4.6 shows a typical X-star subbottom profiler image, in this example for vessel 15. In the figure, the top of the mud is only just visible as a faint reflection indicated by the red arrow. The bottom of the mud is visible as a much clearer reflection. In between, the internal structure of the mud is visible by faint reflections.

At the passage of vessel 15, the top of the mud seems to be lifted slightly. This is an artifact related to the water displacement cause by the large vessel as explained in section 4.1. Additionally, the internal structure of the mud seems to alter during passage of the vessel. Due to the limited vertical resolution of the X-star (at best 0.1 m), the image is not very clear.

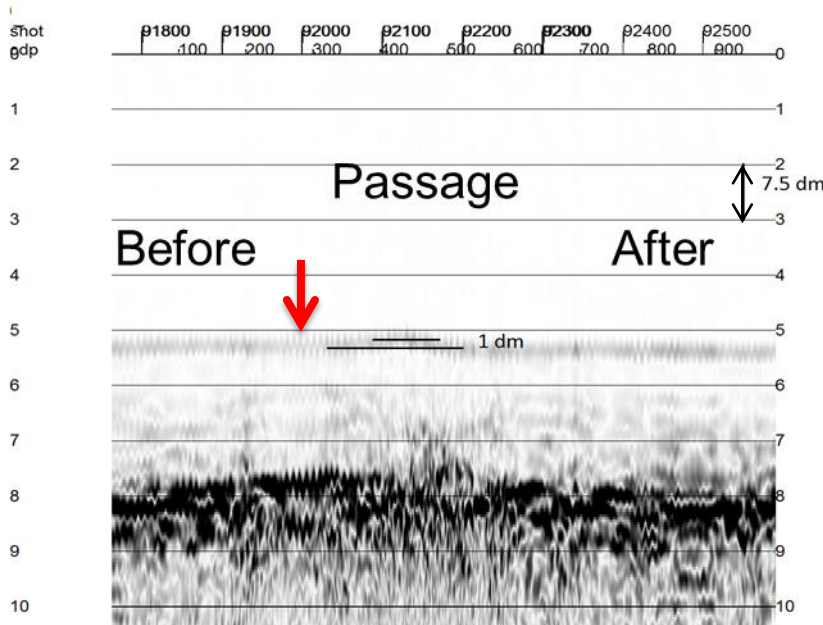


Figure 4.6 Example of X-star result, showing the internal structures of the mud (reflections), for vessel 15. The y-axis shows two-way travel time (TWT) in ms (with an offset). The vertical double sided arrow indicates distance: 1 ms TWT corresponds to 0.75 m. The x-axis shows the traces progressing in time. Shot numbers correspond to time in UTC (shot 91800 means 9:18:00 UTC). The top of the mud is indicated by red arrow. During passage, the top of the mud seems to rise 1 dm. This effect is discussed in section 4.1.

4.5 SILAS – Vessel 15

The penetrating echosounder of the SILAS system has a higher frequency than the X-star: 33 kHz compared to a sweep of 4 to 24 kHz of the X-star. Therefore, we can expect that the vertical resolution of the SILAS system will be better than the X-star. Figure 4.7 shows an example of SILAS data, for approximately the corresponding time as for X-star in Figure 4.6. Indeed, the resolution of the SILAS is much better.

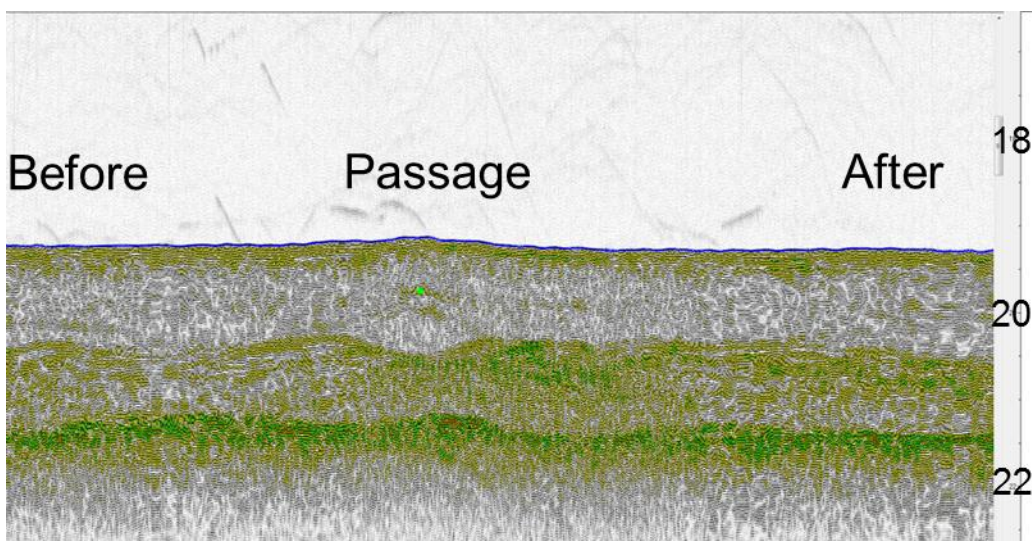


Figure 4.7 Example of SILAS result, showing the internal structures of the mud (reflections), for vessel 15. The y-axis shows depths relative to NAP (calculated from two-way travel times using the sound speed in water), the x-axis shows the traces progressing in time. The image corresponds to approximately 2 minutes acquisition time.

In the SILAS result, we observe the same as in the X-star result:

- Apparent lift in top of the mud during passage of vessel 15, due to lowering of the water level caused by water displacement (section 4.1).
- Internal structures in the mud before, during and after passage of vessel 15.

Moreover, in the SILAS image, there seems to be a wave like structure during the passage of vessel 15. This can be related to internal waves, mud flow, movement of the survey vessel or a combination of factors. This will be discussed in section 5.1. Because of the good resolution of the SILAS data, we will use these data in the interpretation in chapter 5.

4.6 Hydrochart – Vessel 6

The Hydrochart acquires both intensity and travel time (two-way) of the backscattered signal. The travel time can be translated into bathymetric data. However, this can only be done when (i) there is a clear reflection and (ii) the signal is reflected on the top of the mud. Before performance of the experiment, we expected to be able to detect internal waves in the mud by undulations of the top of the mud as seen in Side Scan Sonar images (SSS) and bathymetric information. Because of the smaller swath of the RWS Multibeam, we expected that these undulations would not be visible on the RWS Multibeam (out of range), but would be visible on the Hydrochart data.

The analysis in sections 4.1 through 4.5 shows that the top of the mud beneath Ms. Zirfaea does not move vertically during and after passage of large vessels. However, the top of the mud directly below the passing vessel up to a certain distance from the vessel might show movement that might be related to internal waves.

The Hydrochart data proved to be less useful at the first instance than anticipated. This will be illustrated using Figure 4.8 and Figure 4.9. Processing of the raw data, however, might give useful results.

Figure 4.8 shows a SSS image, in which the various reflections can be recognised. In general, in a SSS image the intensity of the backscattered signal is plotted on a grey scale. Reflections from objects in the water column (e.g. a vessel) plot as if the object were on the water bottom.

In Figure 4.8, time is on the vertical axis, progressing from bottom to top. The reflections from the vessel and its bow wave at the water-air interface can be recognised very clearly. Additionally, the echoes appear in the image. These reflections are not related to the top of the mud at all. Reflections that originate at the water bottom are visible before the vessel appears (bottom of the picture), showing an undisturbed top of the mud. After the vessel has passed, the backscatter is different from before passage. This is either caused by disturbance the mud, or by artefacts such as bubbles from vessel propulsion. During passage, signals of the vessel and bow wave are dominant, masking information of the water bottom below and next to the vessel. After passage, hidden within the noise, there might be information on the internal wave. The description of the backscatter signal before, during and after passage is qualitative information only. This will be illustrated in Figure 4.9.

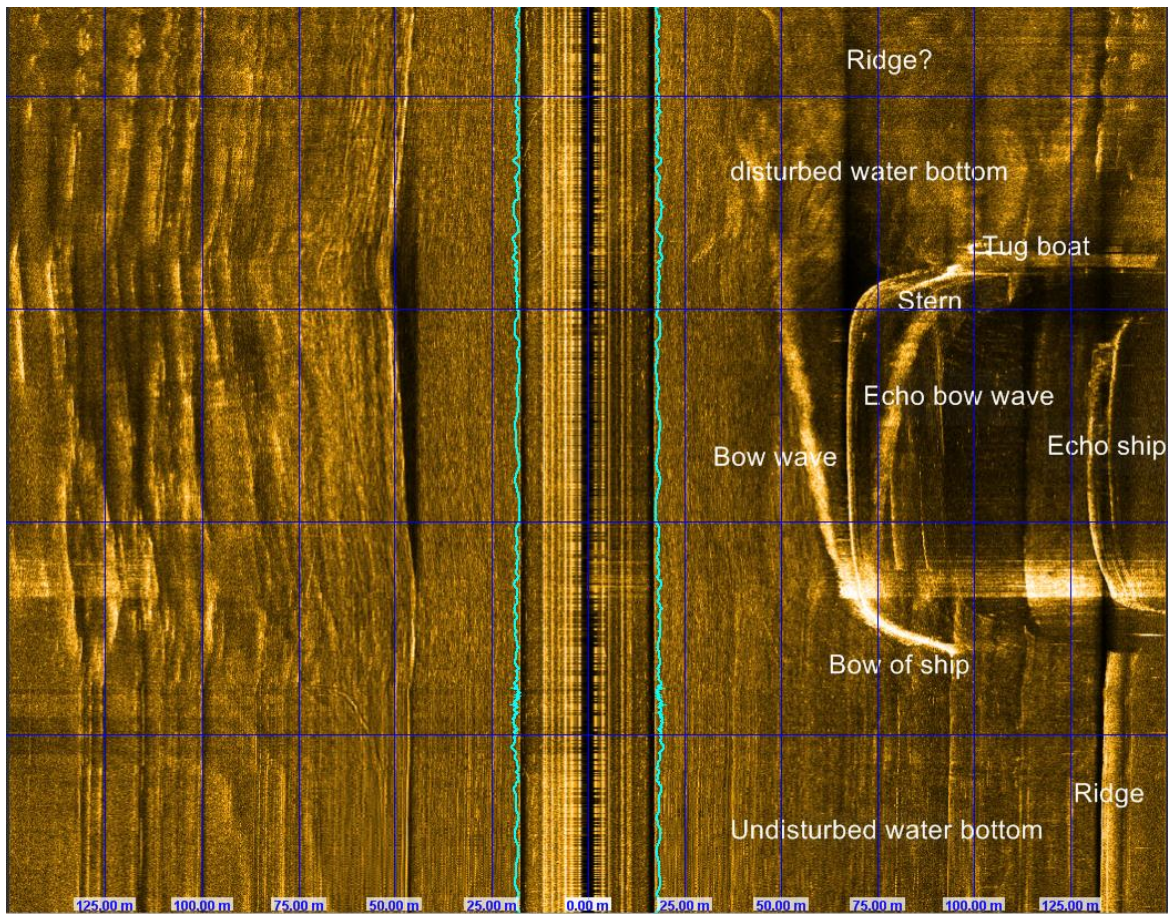


Figure 4.8 Hydrochart Side Scan Sonar image showing the passage of vessel 6. The black line in the middle is the location of the survey vessel Ms. Zirfaea. At the left side, the slope of the waterway is detected. On the right side, vessel 6 passed. The pale blue line indicates the water depth near Ms. Zirfaea.

In Figure 4.9, from top to bottom, cross sections are shown of apparent bathymetry. Travel times are converted to distances along the water bottom assuming that reflections originate at the water bottom. In the screenshots, “apparent” and not the real bathymetry is plotted. Processing is needed to determine real bathymetry by inclusion of directional information. For swath bathymetry sonar, the apparent angle of a target point is obtained from the phase difference measured between two close receiving arrays.

Before passage (Figure 4.9, top panel), we observe that the slope of the waterway at the left side is detected well. At the right side, the more or less flat top of the mud is also detected. For distances more than 50 m from the survey vessel, the top of the mud seems to undulate. This is due to noise. With increasing distance from the survey vessel, the amount of noise increases. This is a general effect of multibeam data. In this example, the water bottom seems to be oblique. Apparently, the instrument was attached to the vessel at an angle instead of perfectly horizontally. The Hydrochart was not calibrated because we decided not to pursue with Hydrochart data at this stage of the project. Although a patch test for calibration was performed, the data were not processed and analysed.

From the analysis of the backscatter intensity in Figure 4.8 we infer that during passage of the vessel, part of the reflections originated from the vessel and its bow wave. These reflections do not contain information on the water bottom. In the middle panel of Figure 4.9, the location

of the vessel is indicated. All signals to the right of the arrow are contaminated by the vessel and echoes. Part of the signal just left of the arrow is “contaminated” with the bow wave.

After passage of the vessel (bottom panel in Figure 4.9), the amount of noise is still substantial, containing bow wave and propulsion bubbles.

Quantitative information might be inferred from the travel times in the bathymetric image. Due to the noise of the vessel as explained in Figure 4.8, however, we do not expect to be able to derive sensible bathymetric information without dedicated processing. In standard multibeam or swath bathymetry sonar processing, the measured travel times are averaged in grid cells based on coordinates. In this experiment, all data would plot in one or a few grid cells (because of the stationary measurements), whereas changes in time for the fixed coordinates are required for internal wave interpretation. For that, the raw Hydrochart data need to be “tricked”, e.g. by adding artificial coordinates that reflect time. Additionally, the noise (vessel reflection, bow wave, echoes, and bubble screen) needs to be recognised and – if possible – removed from the raw data in order to interpret the possible signal from internal waves. The distinction between signal and noise can be done using directional information (using phase differences) and the reflection coefficient (if available in raw data). At this stage of the project, however, such dedicated processing has not been performed. Due to limited time and budget, we decided to focus our efforts on the measurements that showed promising raw data, such as SILAS. This decision was taken in consultation with RWS (Gert Brand).

In summary, the SSS images show that the acoustic signal is contaminated by noise from the vessel, its bow wave, echoes and propulsion bubbles. Therefore, no sensible bathymetric information during and after the passage of vessel can be derived from the Hydrochart data at this stage.

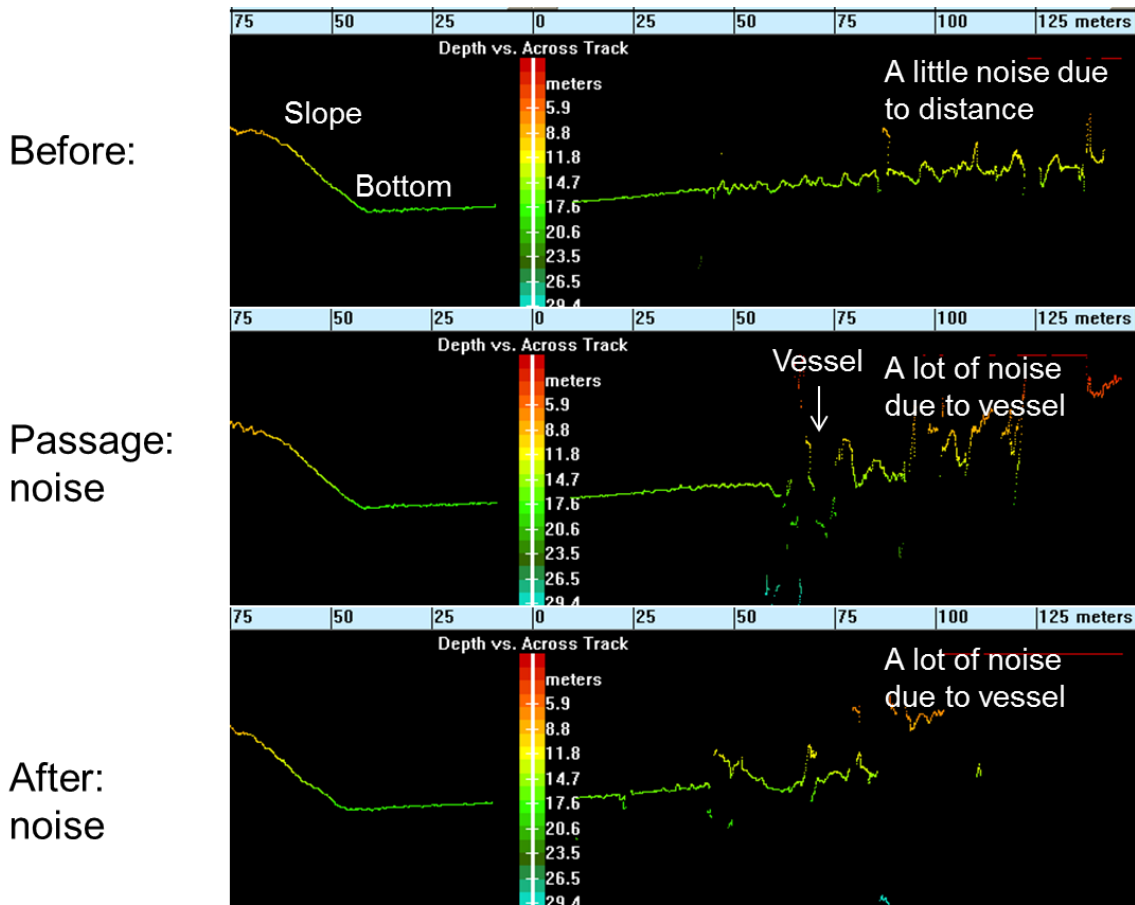


Figure 4.9 Hydrochart bathymetric image of vessel 6. Snapshots in time indicating the distance travelled by the acoustic signal perpendicular to the survey vessel. From top to bottom: before, during and after passage of vessel 6. In general, travel times and distances are converted to a spatial map of bathymetry. In this case, however, part of the reflections originate at the vessel, bow wave and propulsion bubbles, hampering the derivation of a bathymetric map.

4.7 Point measurements of density

During the survey RWS performed the regular point measurements of density using Navitracker. RWS interpolated the 1.2 kg/L level on those points to a grid of mud thickness (Figure 4.10).

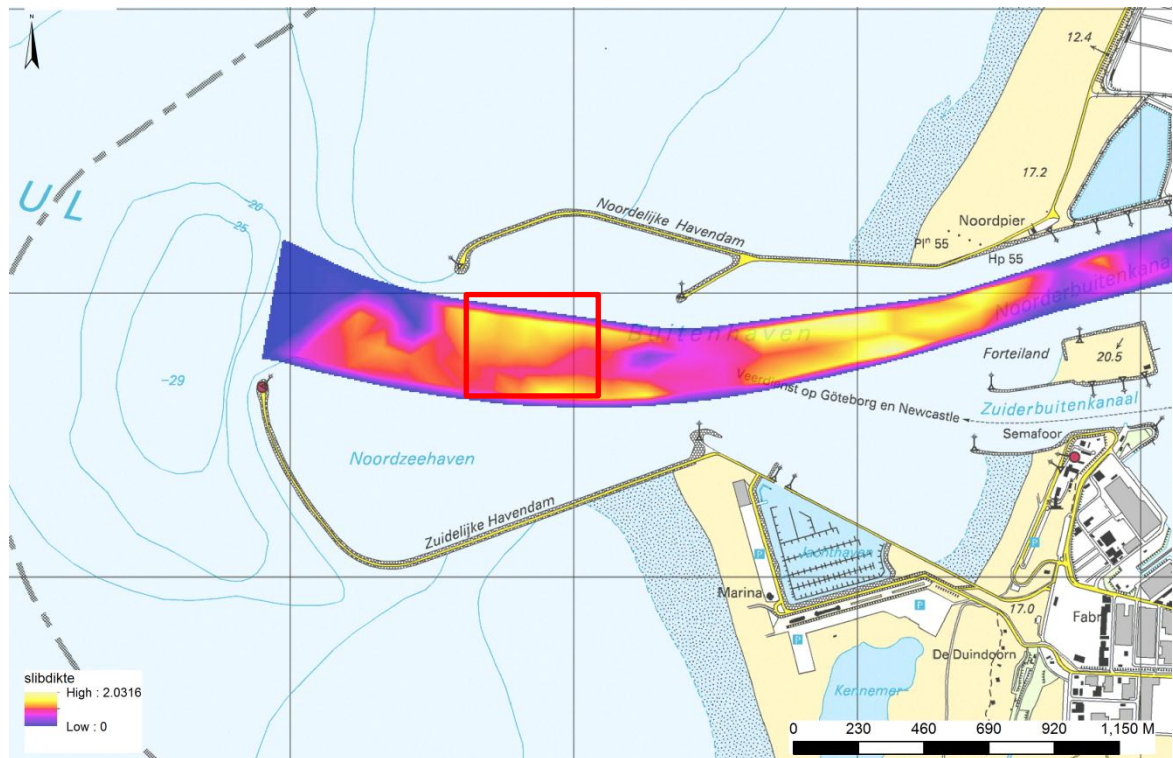


Figure 4.10 RWS map of mud thickness in the survey area (9-10 December 2013). The survey area for the internal wave experiment is indicated by the red square.

Additionally, when time and ship traffic permitted, point measurements were performed before and after passage of the vessel on one location at the expected route of the vessel. An example of the measurements before and after passage of vessel 18 is shown in Figure 4.11, left panel. The density profile seems to recover, in this case measured 20 minutes after passage.

Since acoustic measurements directly beneath the SILAS are to be used in interpretation, the density profiles at Ms. Zirfaea location are relevant as well. In general, Ms. Zirfaea was positioned between monitoring points. Therefore, the profiles at the nearest points near Ms. Zirfaea are shown in Figure 4.11, right panel.

In the week preceding the survey, there was a storm at the North Sea, providing the harbour of IJmuiden with fresh mud. The vertical distribution of the mud is a fresh, unconsolidated mud layer on top of an older, more consolidated layer.

All density profiles at or near the route of the vessel before and after passage and density profiles near Ms. Zirfaea locations are included in Appendix E. All density profiles in the survey area are included in Appendix F.

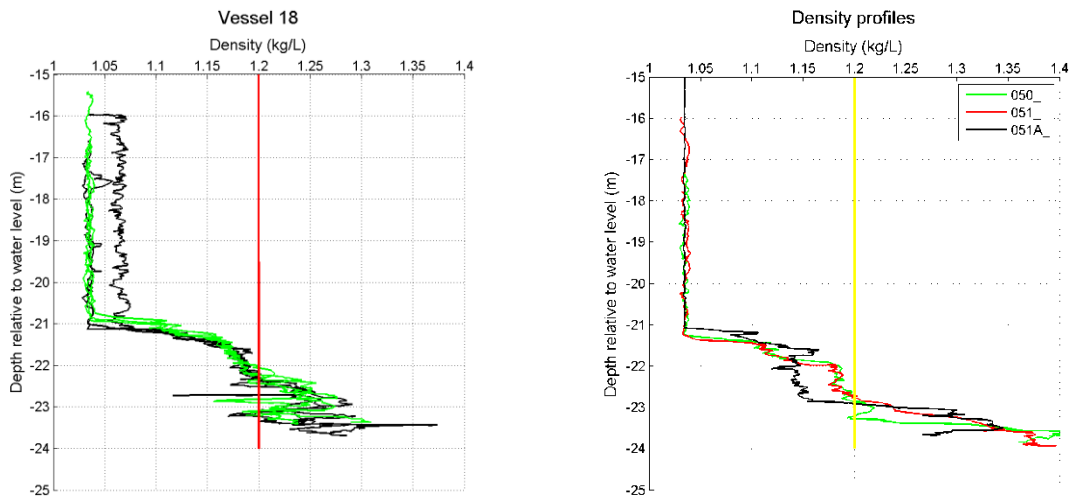


Figure 4.11 Example of point measurements of density using Navitracker. Left: before (green) and after (black) passage of vessel 18 approximately on its route, corrected for tide difference. One of the measurements after shows a shift in density (black line at 1.07 kg/L instead of 1.03 kg/L in the water column). Right: near Ms. Zirfaea, regular monitoring points no. 50, 51 and 51A.

5 Interpretation

5.1 Internal waves at the water/ mud interface

The objective of the current research was to determine whether internal waves, induced by ships sailing over soft mud layers, would be measurable with sufficient accuracy for quantification. Such internal waves are expected to be generated at the water/mud interface.

In the present results, such internal waves have not been observed. Beneath and close to the passing vessel, the Hydrochart data seem to be too noisy (on first glance). Beneath Ms. Zirfaea, at a considerable distance from the passing vessel, the top of the mud seems to be stationary based on the combined analysis of GPS and SILAS/X-star data. This lack of observation may be due to one of the following causes, or a combination:

1. No internal waves have been generated, either because the mud was too stiff, or because the “experimental set-up” was not suitable, i.e. the combination of mud properties, ship draught and velocity did not collaborate to induce such waves.
2. Internal waves were generated directly beneath the passing vessel, but were not detected. This can be either due to unsuitable instruments (or not sufficiently processed) or the dissipation of internal waves before they could be detected at Ms. Zirfaea.

The raw Hydrochart data probably contain useful information on the bathymetry directly beneath and close to the passing vessel. This information, however, is well hidden, because of the strong reflections from the vessel and bow wave. These interfering reflections could be recognised by amplitude and direction. Directional data could be derived from the phase of the acoustic signal. It is recommended to perform a more in-depth processing of the raw Hydrochart data to try to recover bathymetry information. This will require dedicated specific processing, rather than standard processing of bathymetry data.

5.2 Interpretation of reflections in SILAS

Since the Hydrochart data are not analysed any further in this phase of the study, the focus will be on the data acquired from directly beneath the survey vessel Ms. Zirfaea, using the SILAS data. Acoustic reflections occur at changes in acoustic impedance, which is the product of density and sound velocity. The calibration of the SILAS system with point measurements of density is based on this principle. In the validation study of SILAS (Diaferia, 2013), it was shown that for the Maasmond the SILAS system can track density levels of 1.16 to 1.25 kg/L with the same level of accuracy as the individual point measurement used for the calibration.

For this study, it was attempted to calibrate SILAS. It might be instructive to study the behaviour of different density levels before, during and after passage of a vessel. However, calibration of the standard 1.2 kg/L level failed. Because of this, no attempts were made to calibrate other density levels. The calibration of SILAS is described in Appendix D.

In the SILAS images, we observe reflections from within the mud. Moreover, these reflections vary in time and seem to be related to the passage of the vessel. Qualitatively, we observe:

- Several reflections within the mud, at stationary levels before passage.
- Disturbance of reflections within the mud during passage.

- Some time after passage of the vessel, the reflections within the mud are (nearly) the same as before passage.

We interpret the reflections before and after passage as layering in the mud. An attempt is made to link the reflections to the density profile measured by Navitracker. An example is shown in Figure 5.1 for vessel 15. The SILAS data show two clear reflections in the mud. The density profiles of near point locations 50, 51 and 51A show profiles with various jumps. The depth of the jump from appr. 1.2 to 1.3-1.4 kg/L seems to correlate with the deepest reflector. The jump from appr. 1.1 kg/L to 1.2 kg/L seems to be at shallower depths in the Navitracker profiles (0.5 m below top of the mud) than in the SILAS image (1.2 m below top of the mud). For other vessels, the relation between reflections in the SILAS data and the corresponding Navitracker profiles is not unambiguous as well. The Navitracker density profiles of all point measurements in the survey area are shown in Appendix F. The plots of SILAS and nearby Navitracker point measurements are included in Appendix G.

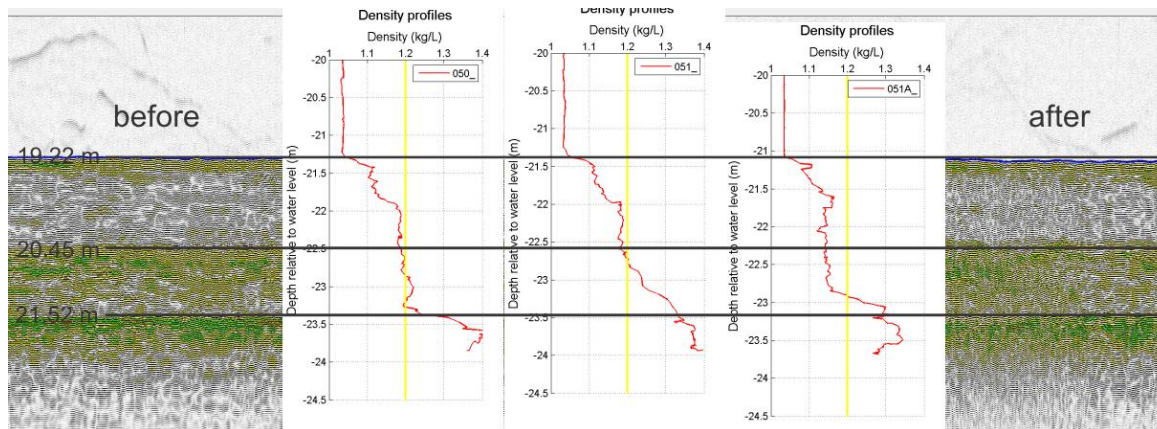


Figure 5.1 SILAS reflections and Navitracker profiles near SILAS location for vessel 15. The top jumps in density at the water to mud interface in the Navitracker profiles are aligned with the SILAS top reflection and shown on the same vertical scale. For comparison, the level of the clear reflections in SILAS data are shown as black lines and plotted on top of the Navitracker profiles.

Although the relation between reflections and densities is not entirely clear, the reflections somehow reflect the internal structure of the mud.

In order to characterise an internal wave, information is needed on its amplitude, wave length, velocity and attenuation. These data cannot be derived at or very close to the route of passage of the vessel. However, in the SILAS data, at some distance from the passing vessel, we observe disturbances in the reflections. In this section we try to characterise the observations in the SILAS data in terms of amplitude and the duration of the disturbance.

The disturbances of the reflections in the SILAS data seem to have wave like patterns. There are three possible explanations for the disturbances in the reflections:

1. They are manifestations of internal waves caused by passing vessels.
2. They reflect mud flow within the fluid mud layer.
3. They are due to the fact that the survey vessel Ms. Zirfaea was not completely stationary during passage of a vessel, but moved over some distance.

From the modelling of the internal wave (Kruiver et al, 2013a) it appeared that the extent of the internal wave at the top of the mud underneath and to the side of the passing vessel is limited to several tens of meters. Although the model was not calibrated, we might expect that

the internal wave at the water/fluid mud interface has dissipated before it reaches the position of Ms. Zirfaea. Indeed, from the analysis of the water level and the apparent top of the mud in section 4.1 it appears that there is no internal wave at the water/fluid mud interface beneath Ms. Zirfaea during passage of vessels.

The amplitude of an internal wave is reciprocal of the difference in density. This means that less energy is required to induce an internal wave for smaller density differences. For vessel 15, the density jumps near Ms. Zirfaea (Figure 5.1) are from 1.05 to approx. 1.11 kg/L (water-fluid mud) and 1.11 to 1.18 kg/L (within the mud). The jumps are in the same order of magnitude. Since we did not observe an internal wave at the water to fluid mud interface beneath Ms. Zirfaea, it is not expected that internal waves will occur within the mud at the second jump in density. At other locations (Appendix F), however, the density profiles have different characteristics (smaller jumps, gradual increase). The occurrence of internal waves within the mud might be possible at other locations.

The second explanation considers mud flow. From the ADCP measurements it appears that the entire water column flows at passage of the vessels. Water flow over a sandy bottom shows a logarithmic velocity profile because of friction at the bottom. In this case however, the mud might be mobile as well. As the upper part of the mud is very soft, the upper part of the mud layer may have been affected by the water displacement of the passing vessel. The fact that the entire water column shows quite uniform flow velocity during passage suggests that flow within the mud might be happening.

The third explanation of changing reflections during passage of the vessel is that Ms. Zirfaea was not completely stationary during passage. When operating SILAS in the usual way, by sailing a line, the reflectors vary over a distance of a couple of meters. We observed that behaviour during the survey as well. In that case, however, the depth of all reflectors varies over distances of 5 to 10 m. The amount of movement during passage was monitored and is displayed in Appendix G. Except for vessel 3, the movement of Ms. Zirfaea is 2 to 10 m at most. During passage, however, not all reflectors seem to vary with depth. The bottom reflector appears at the same depth (corrected for the vertical movement as explained in section 4.1), while the other internal reflectors get disturbed. From this, we conclude that there is an effect of movement, but it seems to be limited.

Since we cannot attribute the disturbances of the reflectors in the mud to one cause, we cannot derive "internal wave parameters" or "parameters linked to flow". Moreover, we cannot be certain that we follow one and the same reflection in time. Reflections of different layers seem to interfere in a complex pattern. Therefore, we will interpret the SILAS data in terms of "observation parameters".

5.3 Derivation of observation parameters for vessel 6a

Figure 5.2 illustrates the derivation of parameters for vessel 6a. This figure, together with navigation plots to check movement during passage and the figures for the other vessels are included in Appendix G. Before conducting the internal wave experiment, 4 internal wave parameters would be derived from the data: amplitude, period, wavelength and attenuation. Since we are not sure that the disturbances are caused by internal waves, flow and/or movement, we will derive the amplitude and the duration of the disturbance only.

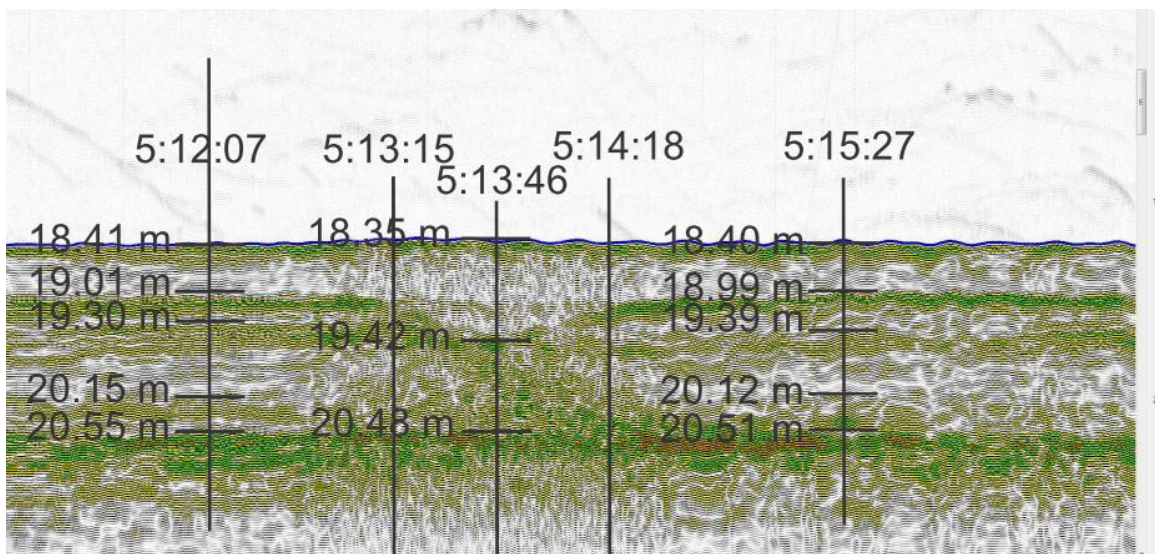


Figure 5.2 Example of derivation of observation parameters for vessel 6a from the SILAS record.

Amplitude of disturbance

The level of various reflectors is shown in Figure 5.2 relative NAP. During passage, the first two reflectors seem to merge, or the first reflector dips and the second disappears. Because of the lowering of Ms. Zirfaea during passage of vessel 6a (as explained in section 4.1), all levels need to be corrected for the apparent top of the mud. Before passage, the top of the first reflector is at $18.41 - 19.01 = 0.6$ m below the top of the mud. During passage, the first reflector is lowered to $18.35 - 19.42 = 1.07$ m below the top of the mud. This results in a dip of the first reflector of $1.07 - 0.6 = 0.47$ m. Therefore, the amplitude of the disturbance is approximately 0.47 m for vessel 6a.

Duration of disturbance

The duration can be determined by the difference in time between the start and the end of the disturbance of the reflectors. For vessel 6a, the constant structure of the mud starts to change at 5:13:15. At 5:14:18, the wave like structure in the reflection ends. This means that the duration of the disturbance is 1 minute and 3 seconds for vessel 6a.

Period

Periods apply to oscillations. In some of the SILAS data, there might be one or two oscillation-like patterns present. However, due to the movement of Ms. Zirfaea and the fact that the disturbance might be caused by flow rather than (internal) waves, the oscillation-like patterns might not reflect true oscillations. Therefore, we decide not to convert durations to periods.

Wavelength

In theory, the wavelength is the product of velocity and period. Assuming that the internal wave is tied to the passing vessel, the velocity can be approximated by the velocity of the vessel. We did not determine the period from the SILAS data. Therefore, we do not derive wavelengths of the disturbances as well.

Attenuation of disturbances – recovery of the original reflections

Some measure of attenuation of disturbances can be derived from the SILAS data from the time it takes for the reflectors to recover to what they were before passage. In some cases, like for vessel 15, the reflectors are the same as before immediately after the last signs of

disturbance of the reflectors. In other cases, e.g. for vessel 6 and 6b it takes 1 to 2 minutes to recover.

5.4 Derivation of observation parameters for all vessels

The plots and numbers of levels of reflectors and times used in the derivation are shown in Appendix G. The parameters derived from that are summarised in Table 5.1. No parameters were derived for vessel 3, because Ms. Zirfaea moved more than 60 m during passage of vessel 3. During later measurements, movement was between 2 and 10 m.

During passage of vessel 18, Ms. Zirfaea had to move aside on request of the Harbour authorities. The second half of the SILAS data is not useful, because of this movement.

In general, the first reflector is displaced over a vertical distance of 1 to 6 decimetres. In one case, for vessel 15, the second reflector also shows a clear disturbance, with slightly less amplitude than the first. The duration of the disturbance varies between 1 and 2.5 minutes. For vessels 6a and 6, it takes 1 to 2 minutes extra for the original mud profile (reflected in the reflectors) to recover.

It is expected that the disturbance is larger and takes longer when the passing vessel is closer by, has a higher speed and a deeper draught. For the limited amount of vessels analysed here, we plot the various vessel parameters versus the duration of the disturbance and the vertical movement of the reflector in the SILAS data in Figure 5.3. For a range of vertical displacement values, e.g. 0.14 – 0.26 m for the first reflector of vessel 15, the average value is plotted in the graphs.

Table 5.1 Observation parameters for all analysed vessels derived from SILAS data. Note that the time in SILAS files is “approximately” UTC, since the SILAS software uses computer time rather than GPS time (synchronised at start of experiment, but computer clocks tend to get out of sync).

Id.	Undisturbed depth of reflector relative to top of the mud (m)	Vertical displacement reflector (m)	Time start disturbances (UTC)	Time end disturbances (UTC)	Total duration disturbance (m:ss)	Time of recovery of original reflector positions (UTC)	Attenuation	Vessel speed (m/s)	Estimated duration of passage (length / vessel speed) (m:ss)	Duration passage vessel from SSS (m:ss)	Remark
3	n.a.	n.a.	n.a.	n.a.	n.a.	n.a.	n.a.	6.07	0:48	n.a.	Ms. Zirfaea moved too much to derive parameters
6a	0.62	0.42	05:13:15	05:14:18	1:03	05:14:18	fast	3.65	0:50	0:43	
6	0.55	0.55	05:31:21	05:33:15	1:54	05:35:38	approx. 2 minutes	2.00	2:25	2:19	
6b	0.55	0.14	05:44:34	05:46:06	1:32	05:47:16	approx. 1 minute	4.63	0:40	0:34	
15	1.21	0.14-0.26	09:19:17	09:21:53	2:36	09:21:53	fast	5.00	0:37	0:30	First reflector
15	2.29	0.10-0.20	09:19:17	09:21:53	2:36	09:21:53	fast	5.00	0:37	0:30	Second reflector also shows disturbance
18	1.42	0.45	19:02:45	19:04:06	1:21	n.a.	n.a.	2.52	1:55	1:47	Move away during measurement passage
20	0.98	0.09-0.16	10:10:31	10:12:09	1:38	10:12:09	fast	5.76	0:43	0:26	

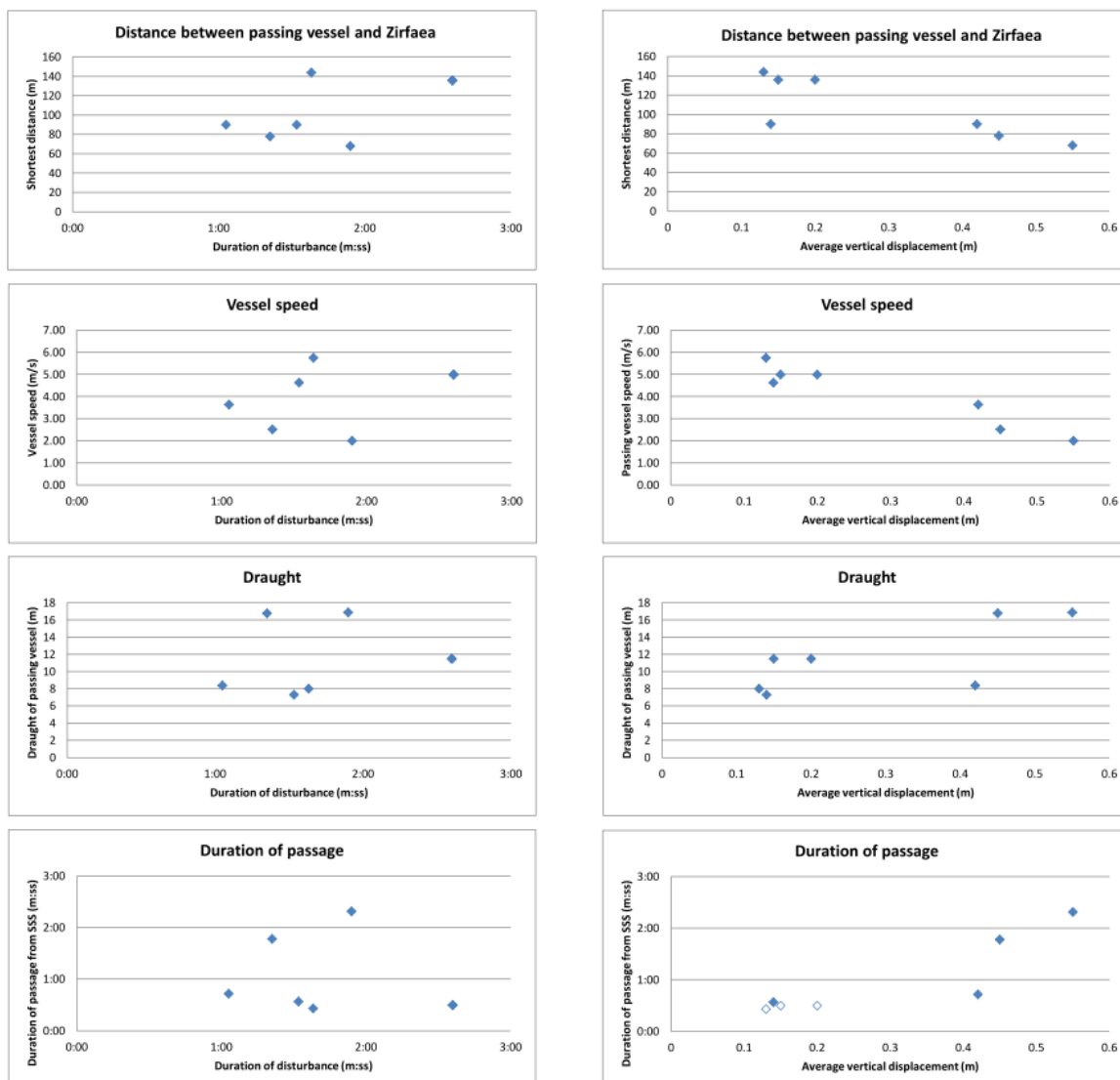


Figure 5.3 Vessel parameters plotted versus SILAS duration of disturbance (left) and average vertical displacement (right). From top to bottom: Distance between the passing vessel and the survey vessel Ms. Zirfaea, speed of the passing vessel, draught of the passing vessel and duration of passage (from Side Scan Sonar data). In the bottom right panel, the open symbols denote durations of passage for vessels that were on the outer range of the SSS image. The exact start and end time of the passage could not be determined for these vessels (15 and 20). The time indicated here is the minimum duration for those passages.

From Figure 5.3, left panels, it appears that the duration of the disturbance is uncorrelated to the speed and the size of the passing vessel. The amplitude of the disturbance (Figure 5.3, right panel), however, seems to be linearly related the draught of the vessel and the duration of passage and inversely related of distance and vessel speed. This last observation seems odd: one would expect a larger influence from a faster vessel, but the opposite seems to be the case here. Perhaps the influence of the distance is larger than that of the vessel speed.

5.5 Accuracy

Acoustic measurements (e.g. multibeam) in general have an accuracy in height of approx. 5 cm. This is the accumulated error of factors such as positioning errors, errors in sound velocity, errors in movement of the survey vessel (heave, pitch, roll). During SILAS measurements, no true heave correction was applied. Heave was corrected by filtering during processing. Therefore, the level of accuracy for these SILAS measurements are slightly worse than for e.g. multibeam. For this survey, we estimate that the levels of reflections from the top of the mud and in the mud can be determined with an accuracy of 5 to 10 cm.

The timing of start of disturbances of the reflections is generally quite clear and can be achieved with an accuracy of several seconds. The interpretation of the end of the disturbance is much less clear. Therefore, we estimate that the duration can be determined with an accuracy of approximately 10 seconds.

6 Conclusions

RWS and Deltares performed a pilot survey in the harbour of IJmuiden, the Netherlands, in December 2013. The pilot was set up to observe internal waves in the fluid mud, caused by the passage of deep draught vessels. The goal was to detect internal waves during vessel passages and describe them in terms of amplitude, wavelength, velocity and attenuation, with sufficient accuracy. The background question is the derivation of properties of fluid mud that are linked to the navigability of this mud. For this, the dynamic behaviour of the fluid mud needs to be determined.

During the five-day survey, the passage of 23 vessels with a variety of vessel speeds and draughts was measured with a combination of different acoustic instruments. Data was acquired of the flow of the water column (ADCP), the water/ fluid mud interface (multibeam and swath bathymetry sonar) and the internal structures of the mud (SILAS and subbottom profiler). Additionally, point measurements of density were acquired by Navitracker.

Due to the limited time and budget, a selection of vessel passages to be analysed was made based on vessel speed and draught. Seven out of 23 vessels were analysed.

Observations beneath and close to the passing vessel were made by swath bathymetry sonar. In the initial interpretation of the data, the reflections from the passing vessel (hull, bow wave, bubbles from propulsion) obscure the bathymetry of the water/fluid mud interface beneath and close to the passing vessel. In the raw data, indications of changes in the bathymetry before and after the passing of the vessel are present. More thorough analysis of the raw swath bathymetry sonar data is needed and might render valuable information on internal waves at the water/fluid mud interface near the passing vessel. Due to limited time and budget it was decided to focus at this stage of the project on the measurements at the location of the survey vessel Ms. Zirfaea, that showed more promising raw data, such as SILAS. This decision was taken in consultation with RWS.

Because of the shift in focus, the original goal of characterising internal waves at the interface of the water and fluid mud beneath and close to the passing vessel was not achieved. Instead, a new goal was formulated: to analyse and describe the dynamic behaviour of the fluid mud at the location of the survey vessel as a result of the passing vessel at a distance.

Beneath the survey vessel, penetrating acoustic instruments (SILAS, 33 kHz echosounder and X-star subbottom profiler) showed disturbances of the internal structure of the mud during passage of a vessel at distance. The disturbances can be manifestations of internal waves from the passing vessel, fluid mud flow and/or slight horizontal movement of the survey vessel during passage. Based on the current dataset and the current level of processing and interpretation, no distinction between these causes can be made. ADCP measurements suggest that the entire water column flows during passage of a vessel, which supports a process within the mud layer. The ADCP signal, however, does not penetrate the mud and provides flow velocities of the water layer only.

If we assume that the observed disturbances are real (or influenced by survey vessel movement to a limited extent), we can interpret the observed disturbances in internal mud structure in terms of vertical displacement, duration and recovery of the original structure. During passage of a vessel, the first reflector in the SILAS data is displaced over a vertical

distance of 1 to 6 decimetres. The duration of the disturbance varies between 1 and 2.5 minutes. For 5 vessels, the internal structure is recovered immediately after the end of the disturbance. For 2 vessels, it takes 1 to 2 minutes extra for the original mud profile (reflected in the reflectors) to recover. The amplitude of the disturbance seems to be related to the speed and draught of the passing vessel, the distance between Ms. Zirfaea and the passing vessel and the duration of passage. The duration of the disturbance seems to be uncorrelated to these vessel and geometry parameters. These relations are based on 7 observations only.

Although our initial processing and interpretation does not show internal waves at the water/mud interface below the passing vessel, the experiment delivered useful information about the fluid mud in terms of navigability, which is the background question of the pilot. Combining all observations, it is likely that the top part of the mud layer is mobile, to be set in motion by waves or flow. If the observed disturbances are no artefact of survey vessel movement, the motion of the fluid mud is related to the properties of the mud. The fact that the top layer of 0.6 to 1.4 m thickness shows dynamic behaviour could be an indicator that the top part of the mud will be navigable.

For either wave or flow, it needs to be determined if the apparent disturbances in the mud are no artefact of movement of the survey vessel. For this, additional measurements are required. If the observed patterns are real, discrimination between the different hypotheses explaining the observed dynamics needs to be made. This is important for the model to link the observations to the mud properties. The model can be based on (internal) waves and/or flow. This points to possibilities for an operational system based on fluid dynamics.

Beforehand, the survey set up had been designed to be able to detect changes underneath a passing vessel. Through this pilot, we now have better insight in factors to be considered. For example, the X-star and SILAS results indicate that disturbances in the mud can be measured at considerable distance from the passing vessel. Apparent disturbances in the mud are visible for distances up to 140 m from the passing vessel (maximum range of SSS and noted vessels in the log). This is favourable for the design of an operational system and possibilities of establishing a system in the harbour of IJmuiden or Maasmond (Kruiver, 2013c).

From the data, it is indicated that not only the very large bulk cargo carriers (draught 17 m) cause disturbances, but also much smaller vessels (e.g. draught of 7 m). This means that if the detected dynamics are real and can be used as indicator for the navigability, this mud information can be collected much more often than twice a week (passage of large bulk carriers). In this case, there are opportunities for data acquisition several times a day.

The main objective of this study was to detect internal waves in fluid mud. If these waves can be detected, they could yield a new method for the determination of navigability of shipping lanes in which fluid mud is present. The executed survey should be seen as a 'proof of concept' focusing on the detection of fluid mud dynamics below and next to passing ships. Part of the data indicates that the passing of ships yields dynamics in part of the fluid mud layer. Other parts of the data need to be analysed to further extent to determine if these are in conjunction with observed dynamics. The first results are promising and show potential for this concept.

7 Recommendations

This first pilot survey provided a wealth of information on the behaviour of fluid mud upon ship traffic in a harbour with soft water bottom, in this case IJmuiden, the Netherlands. Within the limited time and budget, choices had to be made regarding acquisition, processing and interpretation. The preliminary results are such promising, that we recommend to continue this line of research on navigable water depth. The recommendations are grouped in processing, acquisition/experiments and modelling issues.

Processing:

1. The raw data of the swath bathymetry sonar (Hydrochart) probably contain information on the water/fluid mud interface beneath and close to the passing vessel. In the current data, this information is obscured by noise from the vessel's hull, bow wave and propulsion bubbles. Dedicated processing (noise removal from raw data) will allow recovery of more information on bathymetry near the passing vessel than currently available, as noise from the vessel can be recognised by its amplitude and direction (derived from phase information).
2. Analysis of all 23 vessels instead of only 7. The analysis of 7 selected vessels gave valuable, but partially ambiguous data with regard to the mechanism (wave, flow, movement). The additional data might point to one of the factors more clearly. The apparent relations between the size of the disturbance and vessel parameters will also be better constrained by adding data from more vessels.
3. The Graviprobe data have not been included in the analysis. Since they describe the mud in terms of density (indicative) and dynamic undrained shear strength, analysis of profiles before and after the passage of large vessels will be valuable.

Acquisition/experiments:

4. In this survey, the acoustic data were collected on a survey vessel. The vessel moved over a horizontal distance during the passage of a vessel and thus during the measurements. To exclude the effect of movement, it is recommended to acquire data from a fixed platform. This can be e.g. a post equipped with suitable acoustic instruments or a newly to be designed setup with streamer and off-the-shelf transducers. Moreover, the current results show that the distance between the measuring platform and the passing vessel can be large (e.g. up to 140 m) for detectable effects. This makes the fixed platform more feasible than anticipated before the experiment. Moreover, this experiment is useful for determining proof of concept/feasibility for future a 'low' cost operational system.
5. To be able to distinguish between waves and flow within the mud, collection of flow measurements within the mud are recommended. This flow can be measured using electromagnetic devices (P-EMS) that can be placed in the mud. Additionally, water flow measurements need to be collected by ADCP to retrieve the flow over the entire water-mud column. Optimal ADCP frequency and height above the water bottom need to be decided.

Modelling:

6. Calculations on the expected dissipation of internal waves by linear wave theory in the situation of IJmuiden. The resulting estimation of the order of magnitude of dissipation can be used to distinguish between waves and flow at the location of the survey vessel. The linear wave theory has been developed to establish wave

dissipation over a muddy coast, and implemented in SWAN-mud, a special of the wave-propagation model SWAN (Winterwerp et al., 2007, Kranenburg et al, 2011).

7. Numerical modelling of behaviour of the mud for the IJmuiden basin configuration, the distribution of mud and movement of a vessel. This model can be used to verify the hypothesis of flow of fluid mud. The objective of this recommendation is to study the flow of a thin layer of fluid mud in response to the passage of a vessel, as anticipated from the data analysis. This would imply numerical modelling of the entire IJmuiden basin, with the actual bathymetry and a thin layer of fluid mud on top. A sailing vessel can be implemented in Delft3D by a moving pressure field. The return flow induced by a sailing vessel can then be calculated.

A References

P.P. Kruiver, B.F. Paap, V. Hopman, J.C. Winterwerp, J.G.S. Pennekamp, A.A. van Rooijen (2013a). Navigable waterdepth in waterways with muddy water bottoms - Parameters, models and measurement techniques, September 2013, Deltares rapport 1205981-004-VEB-0008-v4.

R.J. Versteeg, P.P. Kruiver (2013). Proof of concept Internal wave for mud properties - Survey plan. Deltares rapport, 27 November 2013, Deltares rapport 1207934-001-VEB-0001-v4.

W.M. Kranenburg, J.C. Winterwerp, G.J. de Boer, J.M. Cornelisse, M. Zijlema (2013). SWAN-mud, an engineering model for mud-induced wave-damping. ASCE, Journal of Hydraulic Engineering, Vol. 137, Nr. 9, pp 959-976, doi: 10.1061/1/(ASCE)HY.1943-7900.0000370.

P.P. Kruiver (2013b). Stappenplan Implementatie Interne Golf concept - zaaknummer 31085444, 18 December 2013. Deltares memo 1208767-000-BGS-000s-v4-m.

P.P. Kruiver (2013c). Inventarisatie mogelijkheden voor implementatie van Interne Golf concept - zaaknummer 31085444, 18 December 2013. Deltares memo 1208767-000-BGS-003-v2-m.

P.P. Kruiver (2013d) Verslag survey interne golf, 17 December 2013, Deltares memo 1207934-001-VEB-0005.

G. Diaferia, P.P. Kruiver, T. Vermaas (2013). Validation study of SILAS - Study area: Maasmond (The Netherlands), July 2013, Deltares report 1207624-000-BGS-0006-v6.

J. van Roeyen (2013). Karakterisatie van slibgolven aan de hand van de Graviprobe, 18 December 2013, DotOcean report.

J.C. Winterwerp, R.F. de Graaff, J. Groeneweg, A. Luyendijk (2007). Modeling of wave damping at Guyana mud coast. Coastal Engineering, Vol 54, pp 249-261.

B Short survey report

Memo

Aan
Gert Brand;Rijkswaterstaat Centrale Informatievoorziening

Datum	Kenmerk	Aantal pagina's
17 december 2013	1207934-001-VEB-0005	6
Van	Doorkiesnummer	E-mail
Pauline Kruiver	+31 (0)88 33 57 859	pauline.kruiver@deltares.nl

Onderwerp
Verslag survey interne golf

Survey ten behoeve van detectie interne golf in het slib

Periode: 9 tot en met 13 december 2013

Locatie: IJmuiden

Survey schip: Zirfaea (RWS)

Personele bezetting:

- Kapitein RWS: Peter Jongejan
- Meetleider RWS: Bert van Angeren
- Projectleider RWS: Gert Brand
- Surveyors Deltares: Ane Wiersma (ma-vr), Pauline Kruiver (ma-woe) en Chris Mesdag (do-vr)

Gebruikte apparatuur:

- Multibeam (RWS)
- ADCP (RWS)
- SILAS (RWS)
- Navitracker (RWS)
- Positionering: RTK-GPS (RWS)
- Graviprobe (DotOcean, di-woe)
- Bathymetrische side scan sonar Hydrochart Klein 5000 (Deltares), incl motion sensor CODA
- Subbottom profiler X-star chirper (Deltares)

Hierna volgt een korte samenvatting van de uitgevoerde werkzaamheden per dag. Enkele foto's zijn opgenomen in bijlage 1. De logboeken van RWS en Deltares zijn opgenomen in de bijlage 2 en 3.

Vrijdag 6 december 2013:

- Opbouw apparatuur op Zirfaea in Scheveningen.

Maandag 9 december 2013:

- Afronden opbouw apparaten op Zirfaea in Scheveningen.
- Inmeten relatieve offsets tussen diverse apparaten t.o.v. centre of gravity ten behoeve van coördinaten.
- Varen van Scheveningen naar IJmuiden.
- Uitvoeren reguliere puntmetingen (RWS).
- Uitvoeren Sound Velocity meting
- Test interferentie akoestische apparaten. Resultaat: geen interferentie tussen Multibeam, 33kHz echolood, ADCP en Hydrochart.
- Meten met MB, ADCP, 33 kHz en Hydrochart aan (1).
- Navitracker metingen bij (1).

Dinsdag 10 december 2013:

- Uitvoeren reguliere puntmetingen (RWS).
- Uitvoeren Sound Velocity meting
- Uitvoeren van Graviprobe metingen (op punten van RWS reguliere metingen en bij schepen).
- Meten met ADCP aan (2)
- Meten met MB, ADCP, 33 kHz en Hydrochart aan (3) en (5)
- Meten met MB, ADCP, 33 kHz en Hydrochart op de lichtenlijn (4)
- Navitracker metingen en Graviprobe metingen voor en na passage (3)
- Meten SILAS calibratielijnen

Woensdag 11 december 2013:

- Uitvoeren reguliere puntmetingen (RWS), vandaag afgerond.
- Uitvoeren Sound Velocity meting
- Uitvoeren van Graviprobe metingen (op punten van RWS reguliere metingen en bij schepen).
- Meten met MB, ADCP, 33 kHz en Hydrochart aan (6), meevarend (10) en (12)
- Bi (6) komt eerst (6a) langs, dan (6) en tenslotte (6b)
- Navitracker metingen en Graviprobe metingen voor en na passage (6) en (10).
- Meten met Hydrochart bij (7), (9) en (11), tijdens reguliere metingen van RWS.
- Meten met Hydrochart en ADCP bij (8), tijdens reguliere metingen van RWS.
- Graviprobe metingen na passage (12).
- Installeren van X-star: geen interferentie met andere akoestische instrumenten. Meegemeten met een aantal schepen (middag).
- Meten SILAS calibratielijnen
- Patch test tbv Hydrochart (alle akoestische instrumenten aan). Mislukt voor Hydrochart ivm uitvallen van de navigatie (alleen bij Hydrochart)

Donderdag 12 december 2013:

- Herhalen patch test tbv Hydrochart (alle akoestische instrumenten aan, behalve ADCP)
- Uitvoeren Sound Velocity meting
- Meten met MB, ADCP, 33 kHz, X-star en Hydrochart bij (13), (14), (15), (17), (18).
- Meten met MB, ADCP, 33 kHz, X-star bij (16). Hydrochart uitgevallen.
- Navitracker metingen voor en na passage (14) en (18).

Datum
17 december 2013

Ons kenmerk
1207934-001-VEB-0005

Pagina
3/6

- Inmeten slibgebied met alle akoestische instrumenten (behalve ADCP): lengte en dwarsraaien.

Vrijdag 13 december 2013:

- Aantal extra Navitracker metingen.
- Meten met MB, ADCP, 33 kHz, X-star en Hydrochart bij (19), (20)
- Navitracker metingen na passage (20)
- Meten met alle akoestische instrumenten (behalve ADCP): dwarsraai
- Terugvaren van IJmuiden naar Scheveningen
- Afbouwen in Scheveningen

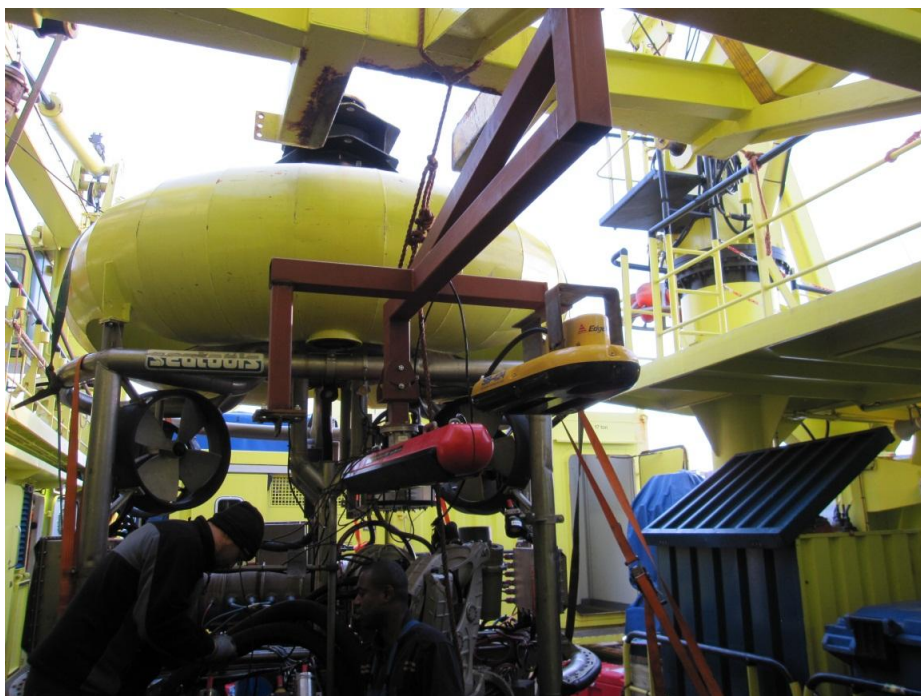
Bijlage(n)

- 1. Foto's survey (adjusted to exclude vessel names)**
- 2. Logboeken RWS (not included because of vessel names)**
- 3. Logboeken Deltares(not included because of vessel names)**

Bijlage 1 – Foto's survey



Surveyschip Ms. Zirfaea



Bevestiging van Hydrochart (rood) en X-star (geel) aan moonpool-frame



ADCP aan moonpool-frame



Motionsensor CODA tbv Hydrochart op het dak van de laboratorium-keet



Control-unit (gele box) en monitoren van Hydrochart

C Instruments

The instruments X-star, Hydrochart and ADCP were attached to a frame to be lowered through the moonpool (see pictures in Appendix B). Ms. Zirfaea is equipped with hull mounted Multibeam and hull mounted 33 kHz transducer for SILAS.

Since these systems all are acoustic, but operating at different frequencies, interference between instruments is possible. We checked for interference by switching the instruments on and off in all combinations. No interference was detected. Therefore, all acoustic instruments could be operated simultaneously.

Additionally, coordinates were registered by RTK-GPS (2 antennae on Ms. Zirfaea). During the survey, vessel traffic was monitored by live AIS.

C.1 ADCP

The ADCP was provided and installed by RWS. It consisted of a Teledyne 600 kHz instrument. Typical data during surveying are in Figure C.1.

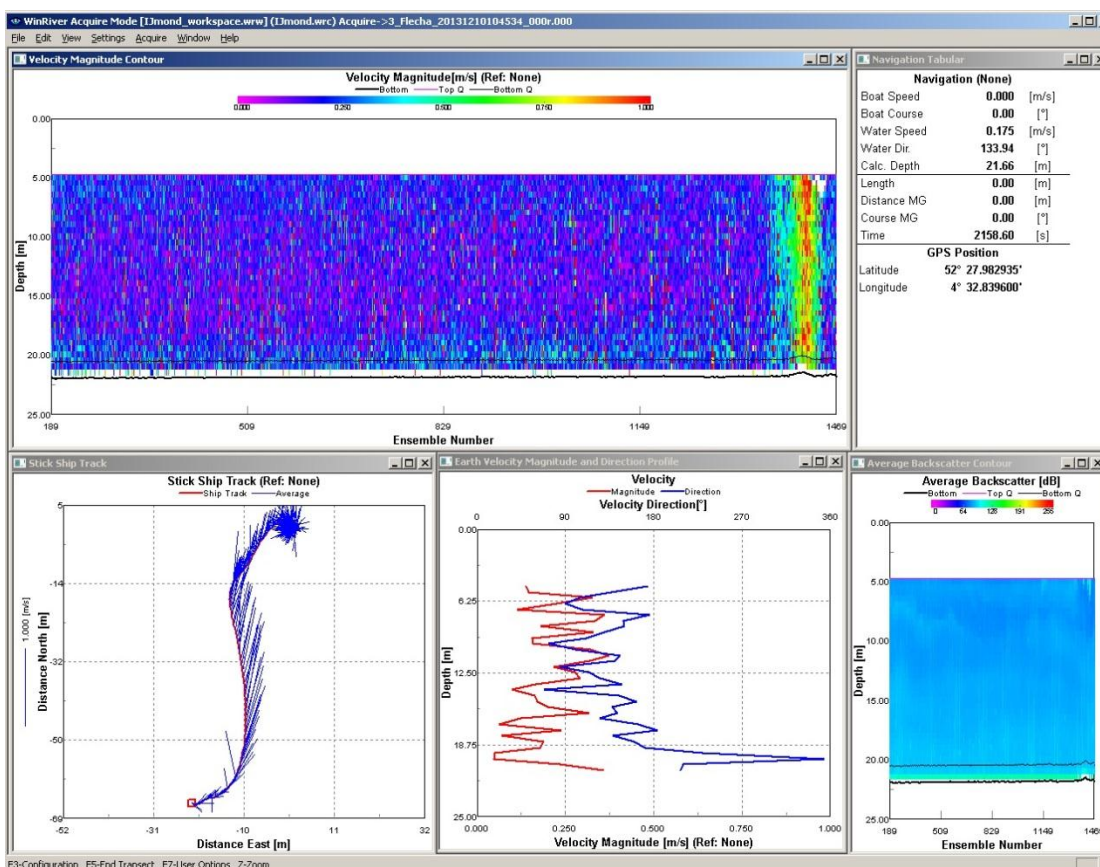


Figure C.1 Typical ADCP data during acquisition, Teledyne 600 kHz ADCP.

C.2 Hydrochart

The HydroChart 5000 is a system that combines both Side Scan Sonar and bathymetry measurements (Figure C.2). A chirp signal is emitted at 455 kHz with a maximum pulse length of 16 ms. For bathymetry, the maximum swath is 10 to 12 times the water depth. For Side Scan Sonar, the swath range is 250 m to both sides in reconnaissance mode, achieved by 5 beams to each side. The along track resolution depends linearly on the water depth and ranges from 10 cm at 38 m to 61 cm at 250 m water depth.

For swath bathymetry, the movements of the vessel (heave, pitch, roll) need to be accounted for. A motion sensor registers the heave, pitch and roll during Hydrochart measurements.



Figure C.2 HydroChart 5000 swath bathymetry sonar system

In the original survey plan, it was suggested to mount the Hydrochart instrument at an angle, to increase the swath (Versteeg and Kruiver, 2013). During installation, the Hydrochart was attached approximately horizontal. When necessary, the orientation could be adjusted during the survey. The swath, however, was sufficient. No adjustments were applied.

In Side Scan Sonar (SSS) images, the backscatter intensity is plotted on a grey (or sepia) scale. During standard SSS data acquisition, the x-axis shows the distance from the vessel, to the left and right of the vessel. On the y-axis, the distance in the direction of movement of the vessel is shown. An example of a SSS image, showing a ship wreck is shown in Figure C.3, left panel.

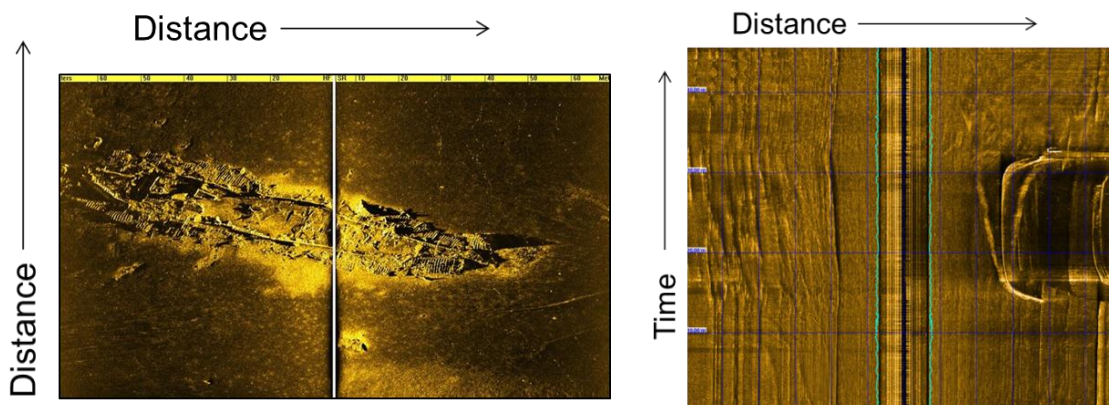


Figure C.3 Left: Example of regular SSS image, showing a ship wreck with usual distance- distance. Right: example of SSS image in internal wave experiment, with distance on x-axis and time on y-axis.

In the internal wave experiment, measurements are acquired in a stationary position. This means that the y-axis represents time rather than distance. Time progresses from the bottom to the top of the image. The x-axis still shows the distance from the vessel, to the left and right of the vessel. An example of a SSS in the internal wave experiment is shown in Figure C.3, right panel. On the left side, the slope of the water way is visible. On the right side, the reflection of a passing vessel and its bow wave are discerned.

C.3 Multibeam RWS

During (almost) all measurements, the standard hull mounted Multibeam of Ms. Zirfaea acquired data as well. The instrument consists of a Kongsberg EM3002, with 293, 300 and 307 kHz frequencies, single head. Standard settings were used, including registration of heave, pitch and roll by a motion sensor. The maximum angular coverage for a single sonar head is 130 degrees. In water depths of approx. 20 m, the swath is expected to be approx. 40 m. Therefore, the RWS multibeam is not able to detect the water bottom underneath a passing vessel that will be located at at least 50 m from Ms. Zirfaea.

RWS Multibeam data were acquired, but not analysed in this study. During the first days of the survey, a small survey vessel performed a multibeam survey for bathymetry for RWS West Nederland Noord. RWS provided the resulting bathymetry grid to Deltares.

C.4 X-star (subbottom profiler)

The Chirp Sub Bottom Profiler (X-star) is a Triton Seismic System consisting of tow fish, manufactured by Edgetech, a deck unit that controls the fish and a top side PC with software for visualization and interpretation. The system emits a signal of finite time duration (e.g. 5 ms) within which the frequency increases linearly. The signal is generated by a piëzo-electric transducer and is received by short hydrophone arrays in the tow fish. The received signal is transmitted to a computer system that processes and stores the data. Computer processing involves compression of the sweep to a short pulse. The result of the processed data is a profile that resembles a well penetrating echo sounder, but with a minimum of noise.

The X-star type SB512i has a penetration depth varying from 5 to 20 m, which depends on the type of sediment and the frequency band. In soft clay, the penetration depth can be up to 20 m, while in sand it can be limited to 5 m. The frequency band varies from 0.5 - 4.5 kHz to 2 - 12 kHz, corresponding to minimum and maximum penetration depth.

The X-star type SB424 has a maximum penetration depth up to 5 m. The frequency ranges from 2 to 24 kHz. Because of the higher frequency relative to SB512i, the vertical resolution is better, but the penetration depth is less than for SB512i.

In the internal wave experiment, the X-star SB424 was used. It was set to perform a sweep from 4 to 24 kHz with record length of 50 ms and shooting rate of 501 ms.

During standard X-star surveys, the y-axis shows two way travel time (TWT) of the compressed acoustic signal. During processing, TWT can be converted to vertical distance using the velocity of the acoustic signal through mud/sediment. On the horizontal axis, the intensity of the individual traces is plotted in a grey scale. Usually, when sailing during data

acquisition, each trace represents a different location, thus showing distance on the x-axis. An example of a typical X-star result is shown in Figure C.4, left panel.

In the internal wave experiment, measurements are acquired in a stationary position. This means that the y-axis represents time rather than distance. The y-axis still shows TWT. An example of an X-star result acquired during passage of a vessel is shown in Figure C.4, right panel. The top of the mud shows as a faint reflection. The bottom of the mud is a much clearer reflection (darker line). Between the top and the bottom of the mud, reflections from within the mud are visible.

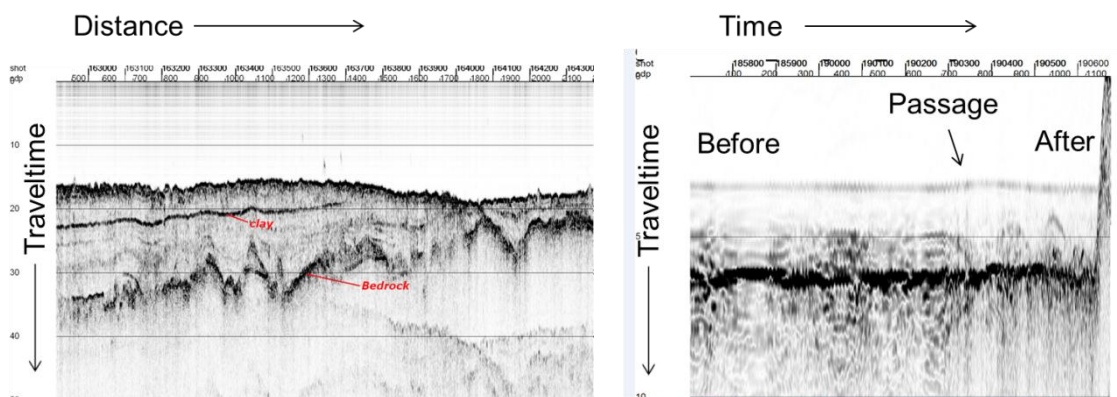


Figure C.4 Left: typical X-star result showing distance on the x-axis and two way travel time on the y-axis. Reflections show up as dark lines. Right: Example of X-star result of the internal wave experiment with measurements in stationary position, showing time on the x-axis and two way travel time on the y-axis. The top of the mud shows as a faint reflection, the bottom of the mud as a much darker line. Between those, reflections from within the mud are visible.

C.5 SILAS

Ms. Zirfaea is equipped with a hull mounted 33 kHz transducer connected to a SILAS acquisition system. During (almost) all measurements, SILAS acquired data as well. Standard settings were used. True heave was not included in the SILAS measurements, because there was no physical connection between the motion sensor and the SILAS acquisition computer.

As with X-star measurements, during standard SILAS data acquisition, the x-axis represents distance. The SILAS software automatically converts TWT to distance using the sound velocity in water and mud. Heave is corrected for by filtering and tide corrections are applied. Therefore, the y-axis shows the distance relative to NAP. An example of a standard SILAS result is shown in Figure C.5. The top of the mud is represented by the blue line, the interpreted 1.2 kg/L level (obtained by calibration with point measurements of density) is shown in orange.

In the internal wave experiment, measurements are acquired in a stationary position. This means that the y-axis represents time instead of distance. The y-axis still shows depth relative to NAP. An example of a SILAS image for the internal wave experiment is shown in Figure C.6. The top of the mud is represented by the blue line. In this case, calibration of the SILAS system was not successful (see Appendix D). Therefore, no density level is shown in the image. We use the 33 kHz as a relatively high frequency subbottom profiler. The bottom of the mud shows as a clear reflection. Between the top and the bottom of the mud, reflections can be observed with the mud.

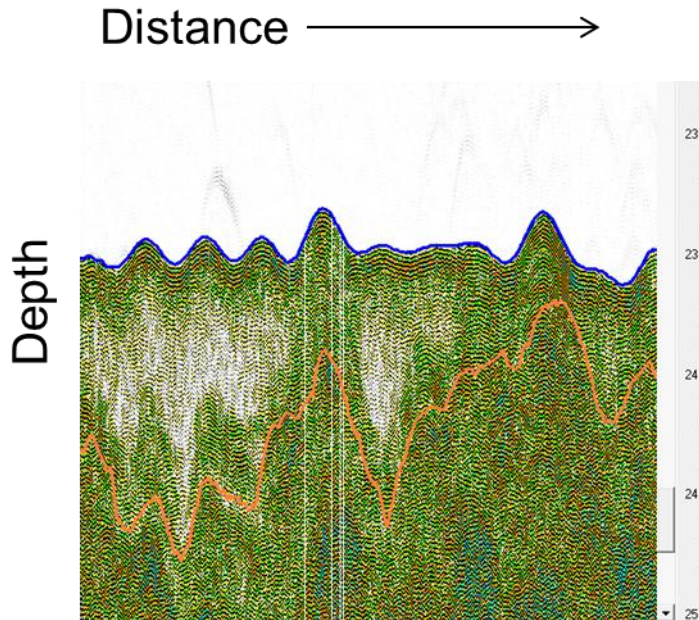


Figure C.5 Example of regular SILAS measurement, showing top of the mud in blue and predefined density level (1.2 kg/L in this case) in orange. The x-axis represents horizontal distance, the y-axis depth relative to NAP.

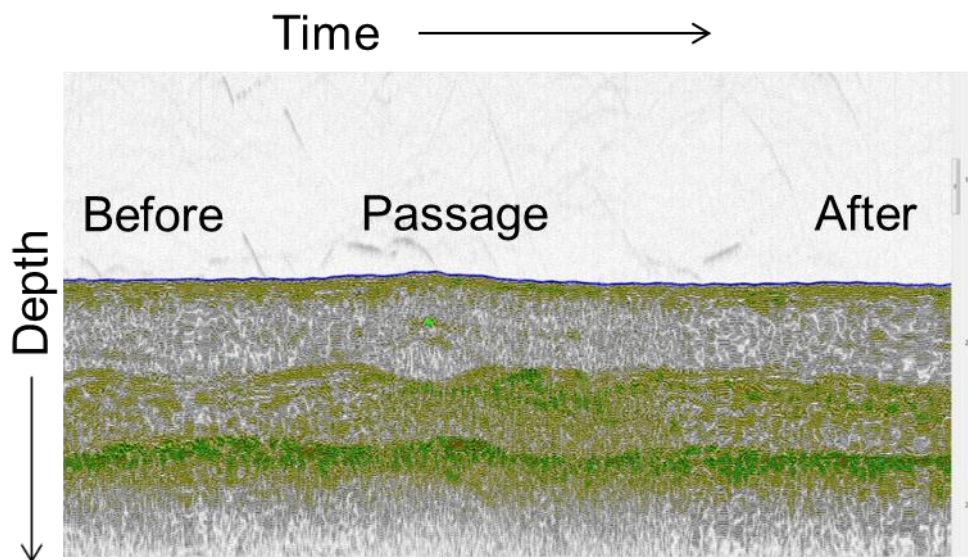


Figure C.6 Example of SILAS measurement in this experiment, measured in stationary position. The x-axis represents time, the y-axis depth relative to NAP. The top of the mud is represented by the blue line. No density levels were interpreted.

D Summary processing

Processing of SILAS data consists of various steps, described in section D.2. For the other acoustic techniques, processing was either (i) rather simple, (ii) not performed because of limited time and budget and related choices or (iii) not performed by Deltares (section D.1).

D.1 Simple processing

Processing of the various acoustic techniques is summarised below:

- ADCP: correction for (slight) movement of survey vessel.
- Hydrochart:
 - Bathymetry: not processed, because of too much noise.
 - SSS: plot with SonarPro (acquisition software) and Delph (interpretation software).
- Multibeam: standard multibeam processing for bathymetry performed by RWS, otherwise not used.
- X-star: plotting results in grey scale.

Dedicated processing of the Hydrochart data will probably give useful information on the water/fluid mud interface near the vessel. More complex processing than standard is required for that.

D.2 SILAS processing

In order to interpret a user defined density level (e.g. 1.2 kg/L), the SILAS data need to be calibrated using point measurements. Before calibration, pre-processing consists of several steps (see also Diaferia, 2013):

- Define sound velocity to allow for conversion of TWT to depth.
- Define top of the mud by autotracing.
- Apply heave correction, in this case filtering because no true heave was measured.
- Apply tide correction to obtain depths relative to NAP.

For calibration purposes, a SILAS line was measured straight after performance of a series of Navitracker measurements. Three calibration lines were acquired:

1. cal-67-75 SILAS, over point measurements 67 through 75 (10 December 2013)
2. cal17-29 SILAS over point measurements 17 through 29 (11 December 2013)
3. cal35-44 SILAS over point measurements 35 through 44 (11 December 2013)

In the calibration procedure, the “arrival power” of the system is determined. This value facilitates the conversion between seismic traces and the density level chosen for that calibration.

During calibration, several settings need to be defined:

- The maximum allowable distance between a point measurement and the nearest SILAS line used in calibration. In this case, the threshold value is set to 10 m. In total, 31 Navitracker profiles were measured on or near the calibration lines. 28 of them fall within the 10 m threshold.
- Definition of the density level. We defined the density level of interest as 1.2 kg/L (standard definition of nautical depth)
- Choice of calibration model: cumulative model with or without vertical corrections. We use the Cumulative model without vertical corrections.

Using these setting, the calibration results in an arrival power of 956.69. The standard deviation of the vertical error, however, is huge: 109 cm. This means that the calibration is not reliable at all.

In order to understand the large standard deviation, we performed calibrations for each of the calibration lines separately. The results are summarised in Table D.1. The resulting arrival powers vary a lot. Moreover, the standard deviations of the vertical errors are large. The best option is to use the calibration of cal67-75, because that data set results in the smallest standard deviation, which is also is an acceptable value. The varying arrival powers, however, suggest that calibration for this dataset is rather tricky.

Table D.1 Results of various calibration attempts for SILAS in IJmuiden during internal wave experiment. Distance threshold of 10 m, target density 1.2 kg/L.

	Arrival power (Ainv)	Density error (g/cm ³)	Standard deviation vertical error (cm)
calibration_1200_10_cum (all three lines)	956.69	-33	109
20121210 – cal-67-75	522.73	-8	17
20121211 - cal-17-29	867.38	1	61
20121211 - cal-35-44	2101.76	5	40

The calibration file (based on cal67-75) was applied to all data. The 1.2 kg/L level for the cal67-75 line is shown in Figure D.1. From this figure, it appears that the level roughly follows the mud thickness.

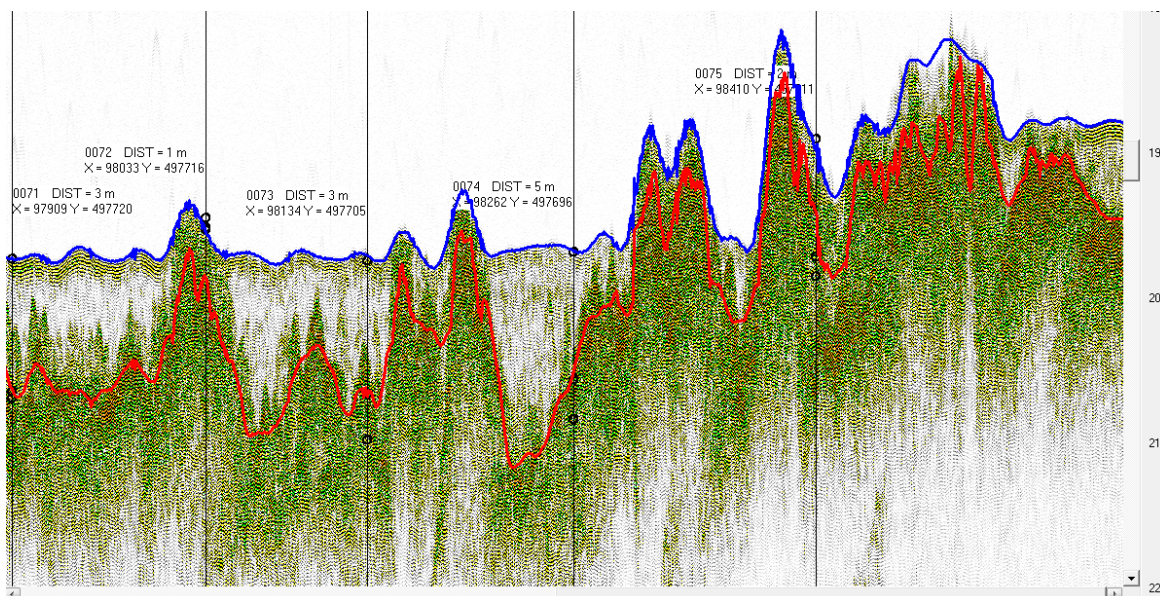


Figure D.1 1.2 kg/L level for the calibration line cal-67-75. The blue line shows the top of the mud. The red line represents the 1.2 kg/L level as determined by SILAS software, based on using cal67-75 and corresponding Navitracker profiles as input for calibration. The point measurements used for calibration are shown by vertical lines and labels.

When the calibration is applied to SILAS files of passing vessels, however, the 1.2 kg/L level does not seem to make sense. An example is shown in Figure D.2. The red line does not seem to follow a certain reflection in a sensible way. We do not completely understand this behaviour. A possible explanation might be that the fluid mud does not react linearly (e.g. stress-strain relation is not linear). In that case, the concept of impedances, which forms the basis of the calibration, might not be applicable. Another explanation might be that the movement of the mud causes temporal gradual changes in density causing diffraction rather than reflection of the acoustic signal.

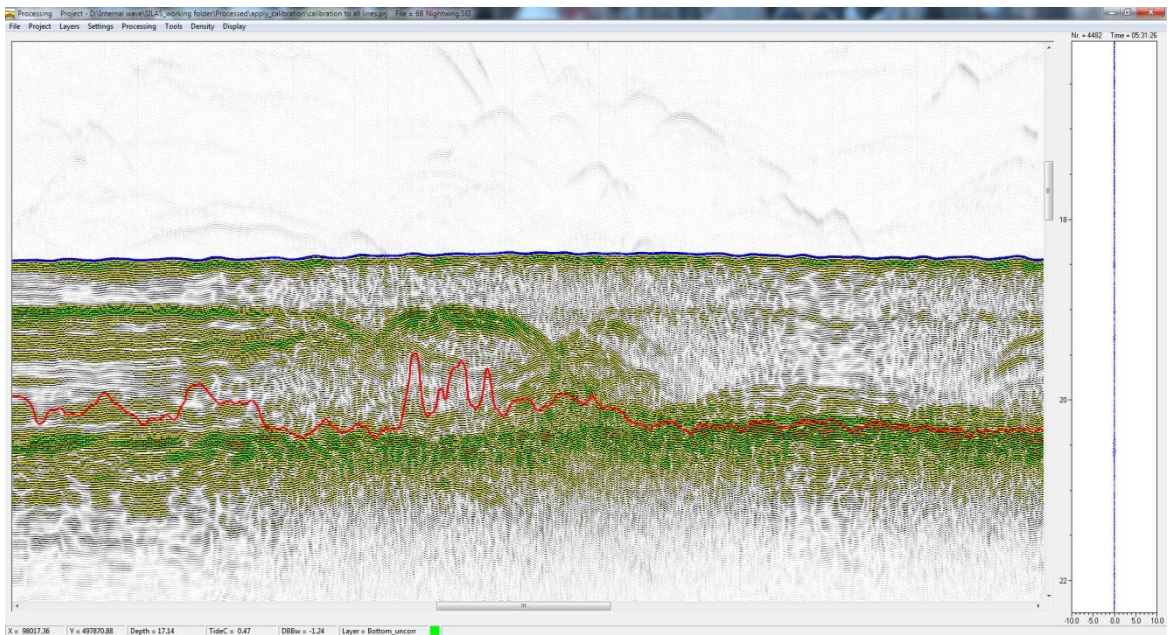


Figure D.2 Example of 1.2 kg/L level before, during and after passage of vessel xx. The blue line shows the top of the mud. The red line represents the 1.2 kg/L level.

E Screenshots of measurements of all selected vessels

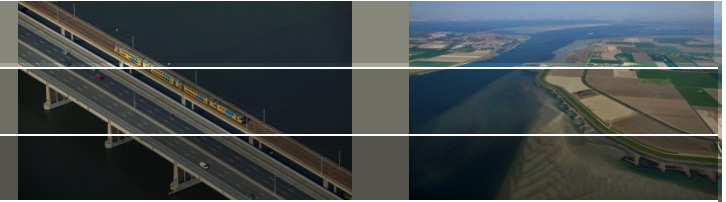


Screen.dumps processed vessels Internal wave experiment IJmuiden

Survey 9-13 December 2013

31 March 2014

Selection vessels

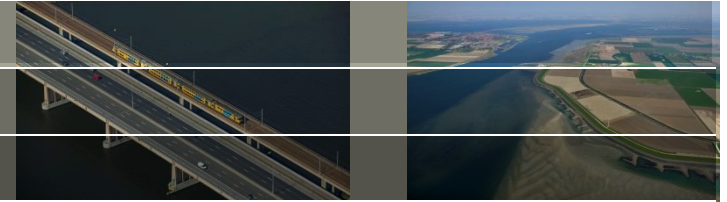


Date	Vessel number	Time from (UTC)	Time to (UTC)	Duration (minutes)	Time of passage (UTC)	Speed (knots)	Draught (m)	Shortest distance noted during survey (m)	Shortest distance according to SSS (m)	Stationary position	MB	ADCP	Hydrochart	SILAS	X-star	Point measurements before (Navi-tracker)	Point measurements after (Navi-tracker)
10-12-13	3	11:00	11:25	00:25	11:15-11:17	11.8	11.6	80	76	no	x	x	x	x		5	7
11-12-13	6a	05:08	05:20	00:12	05:12	7.1	8.4	65	90	yes	x	x	x	x		5	
11-12-13	6	05:15	05:48	00:33	5:31-5:33	3.8	16.9	75	68	yes	x	x	x	x			
11-12-13	6b	05:40	05:48	00:08	5:44-5:45	9	7.3	80	90	yes	x	x	x	x			5
12-12-13	15	09:15	09:26	00:11	09:20	9.7	11.5		136	yes	x	x	x	x	x	0	0
12-12-13	18	18:50	19:20	00:30	19:02	4.9	16.8	50	78	yes	x	x	x	x	x	3	3
13-12-13	20	10:04	10:17	00:13	10:10-10:12	11.2	8		144	yes	x	x	x	x	x	0	3

Based on height internal wave:

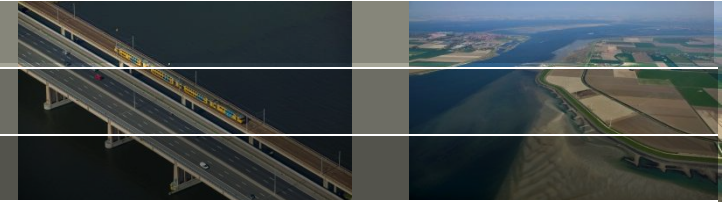
- 1) Proportional to square of speed
- 2) Proportional to reciprocal of exponential of keel clearance, but in this range more or less linear

Methods

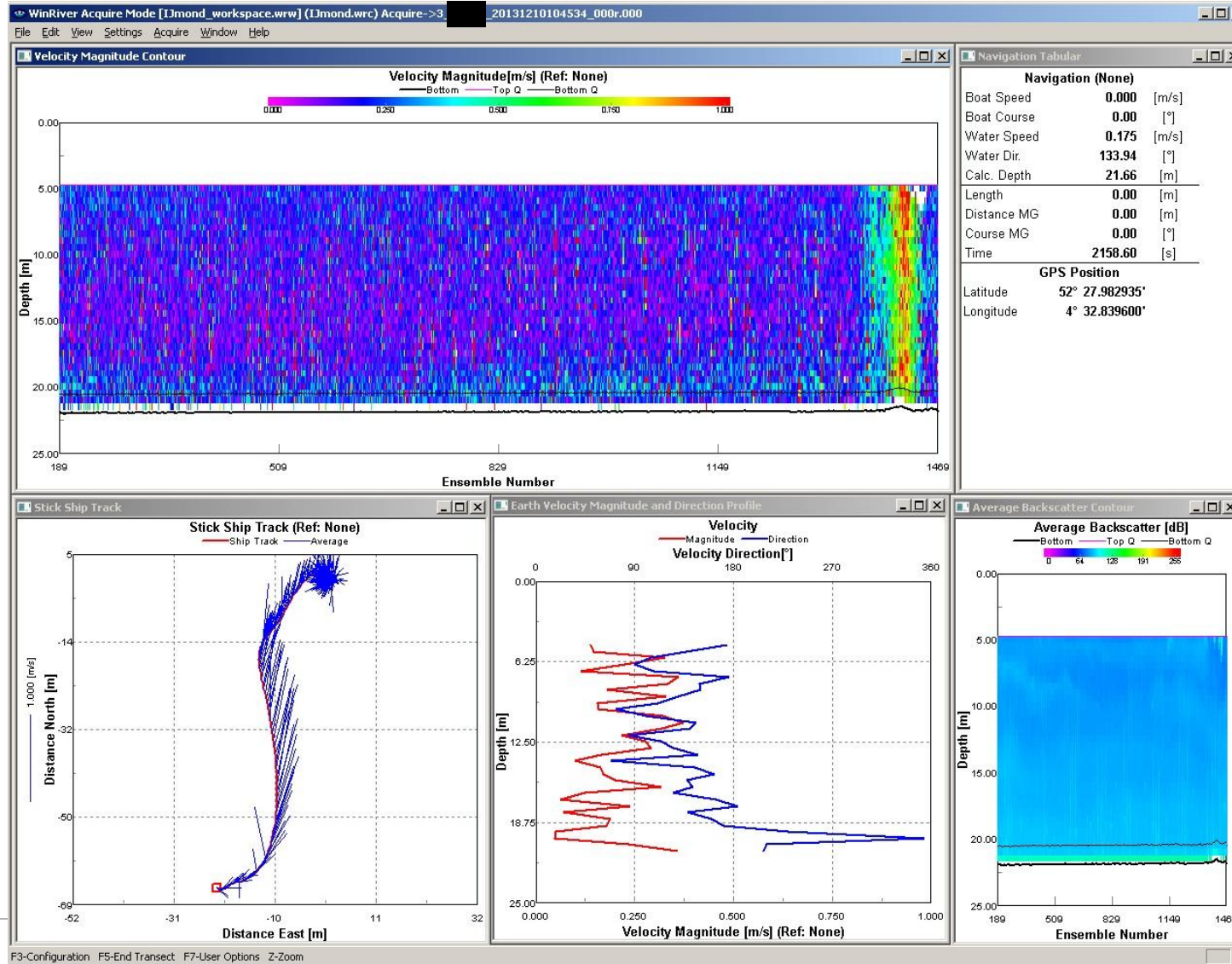


- Navitracker measurements:
 - Regular grid
 - Before and after passage (when possible)
- ADCP (RWS): not analysed now
- Multibeam (RWS): only for bathymetry (top of the mud)
- X-star: Subbottom profiler, for internal structure of mud
- SILAS: for internal structure of mud
- Hydrochart:
 - Side Scan Sonar: structures in top of the mud
 - Bathymetry: top of the mud, too much noise, not processed

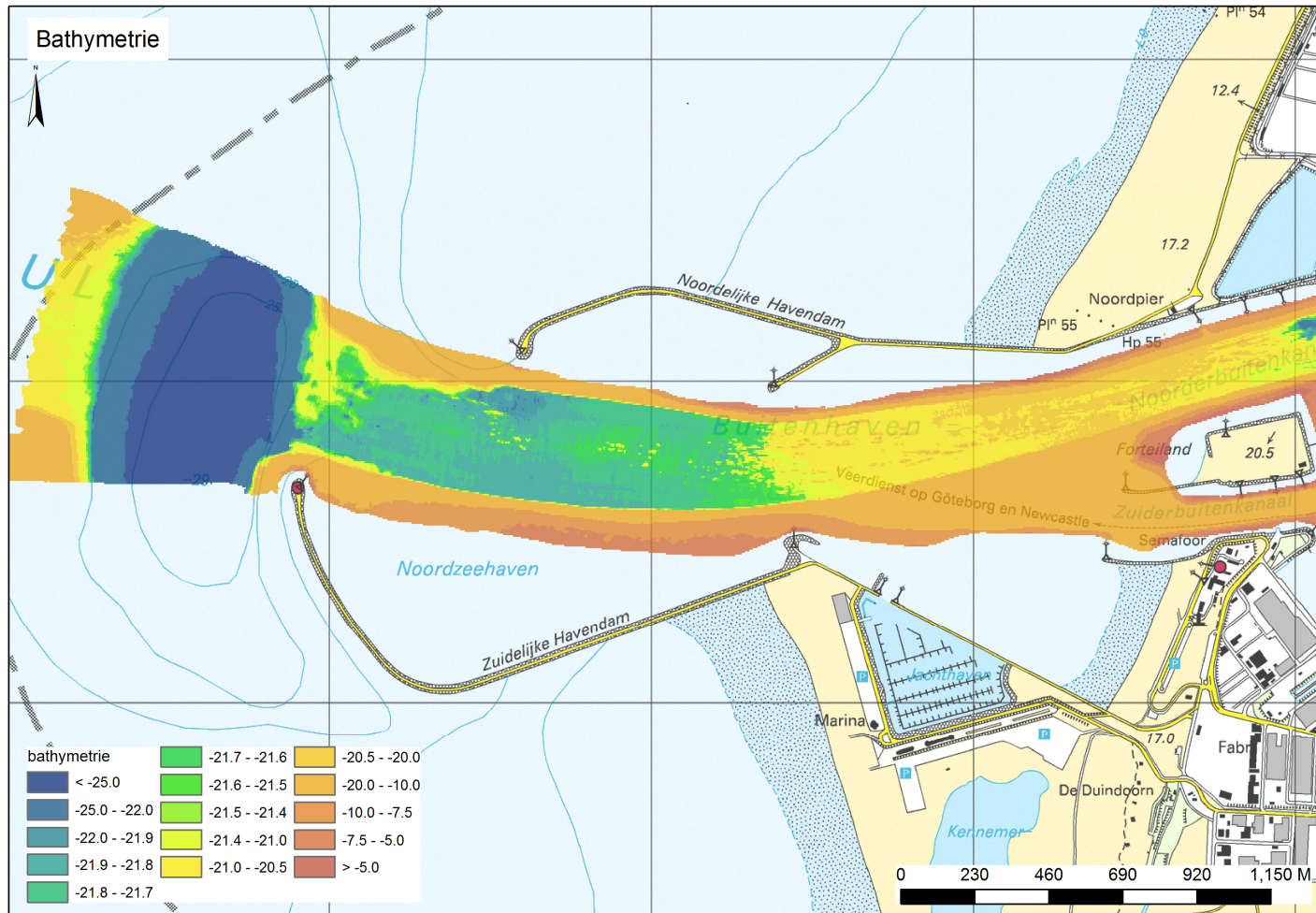
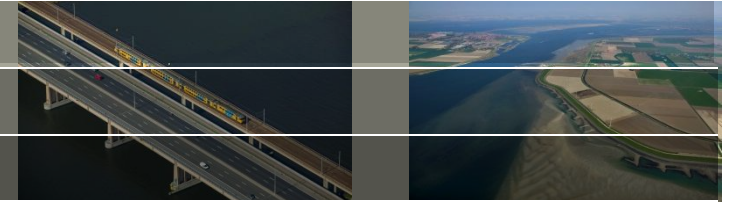
ACDP



Just one example of screendump

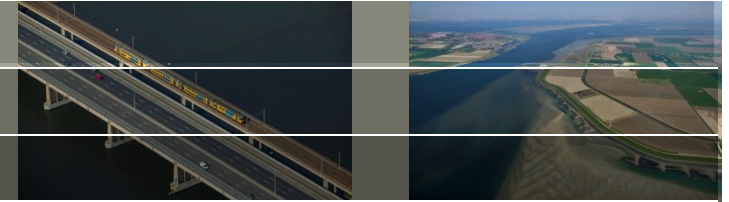


Multibeam – bathymetry



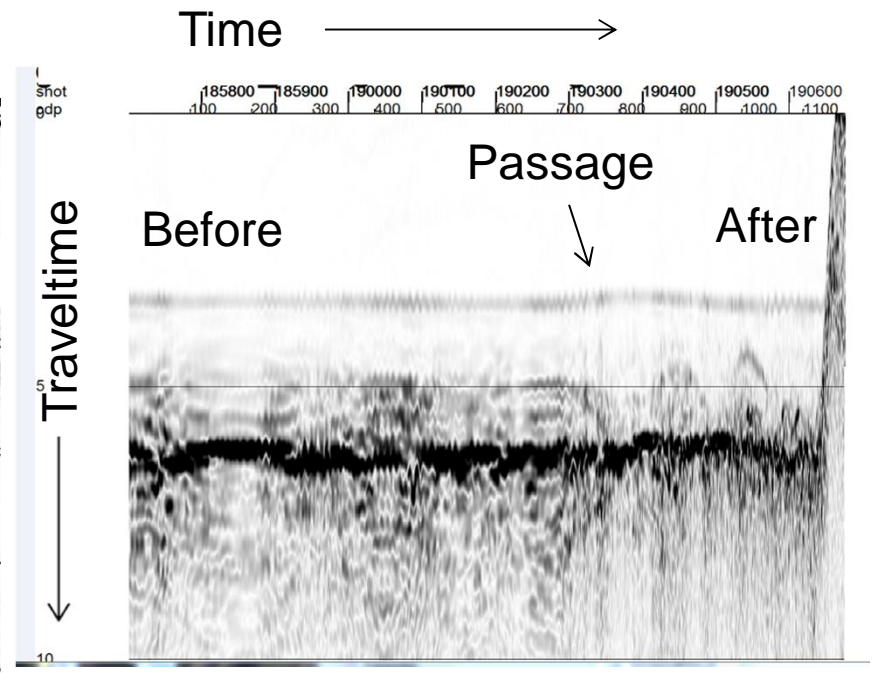
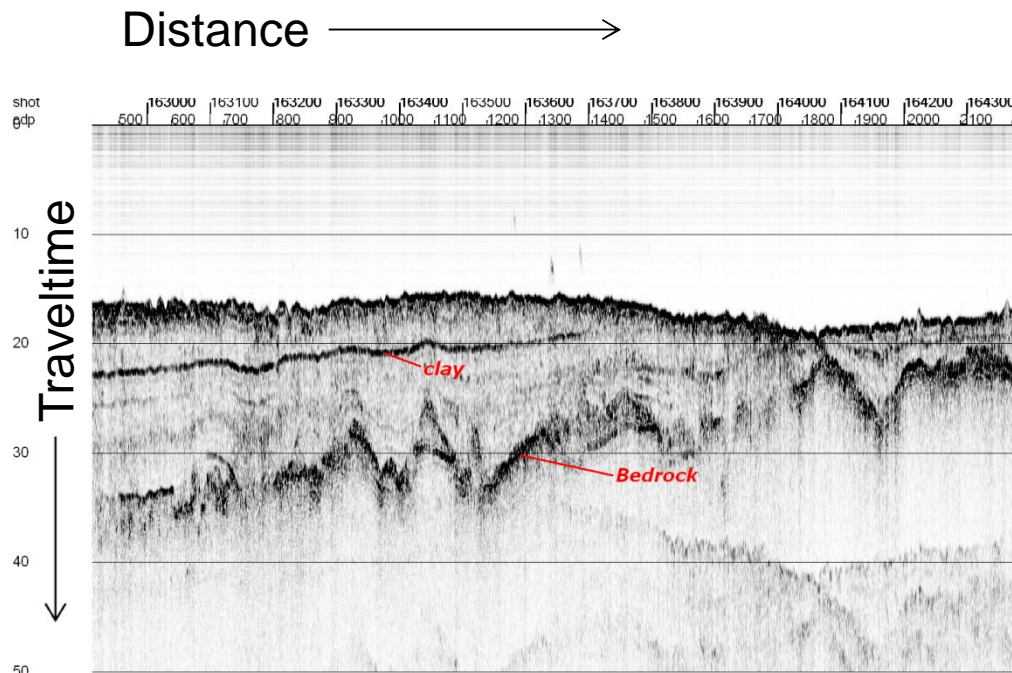
Provided by RWS West-Nederland Noord

X-star

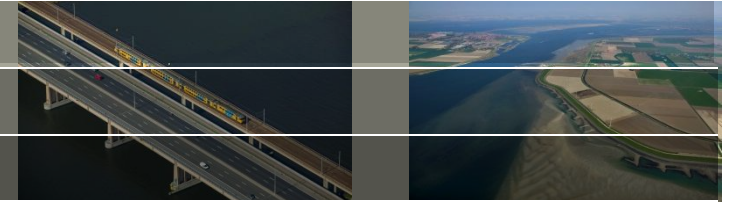


Normal:
Surveying when moving
horizontal is distance

Here:
Surveying in stationary position
horizontal is time

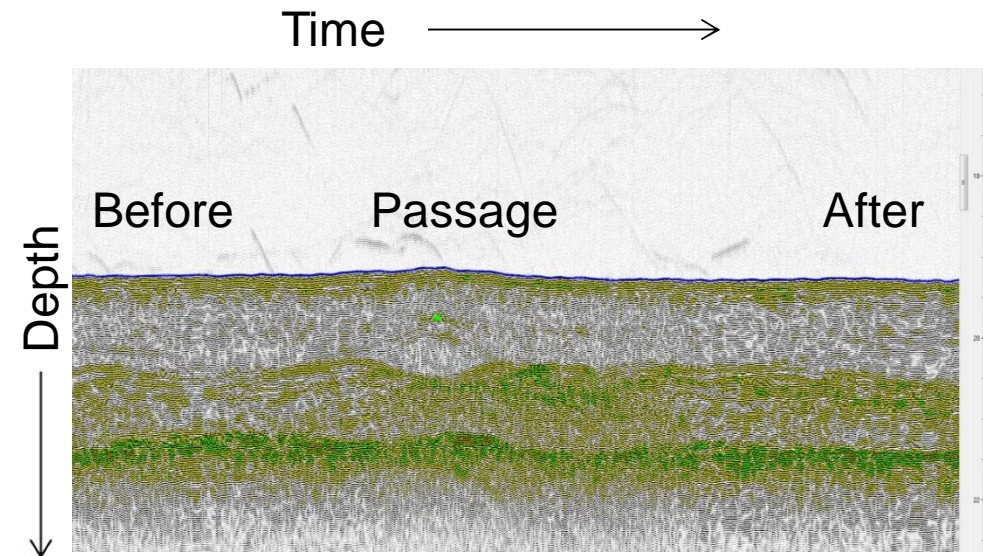
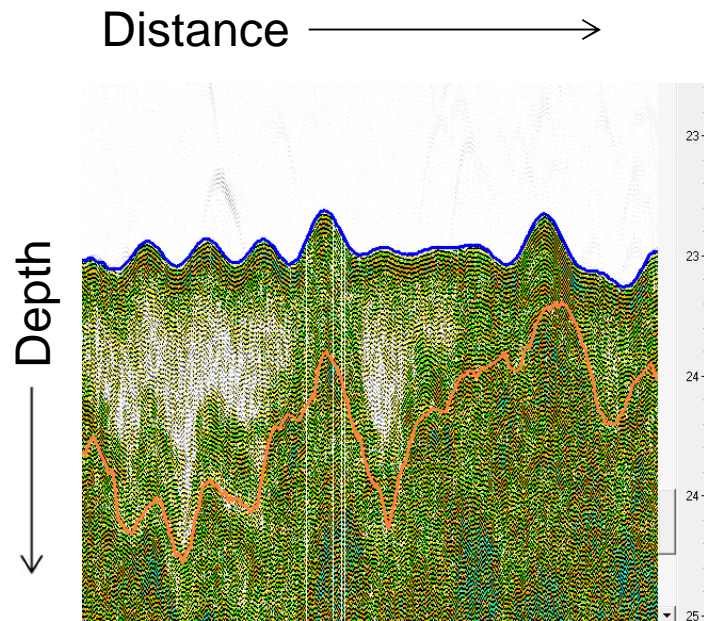


SILAS

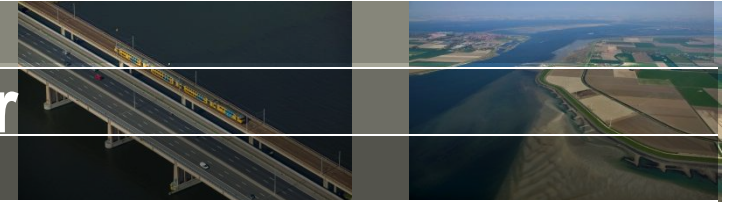


Normal:
Surveying when moving
horizontal is distance

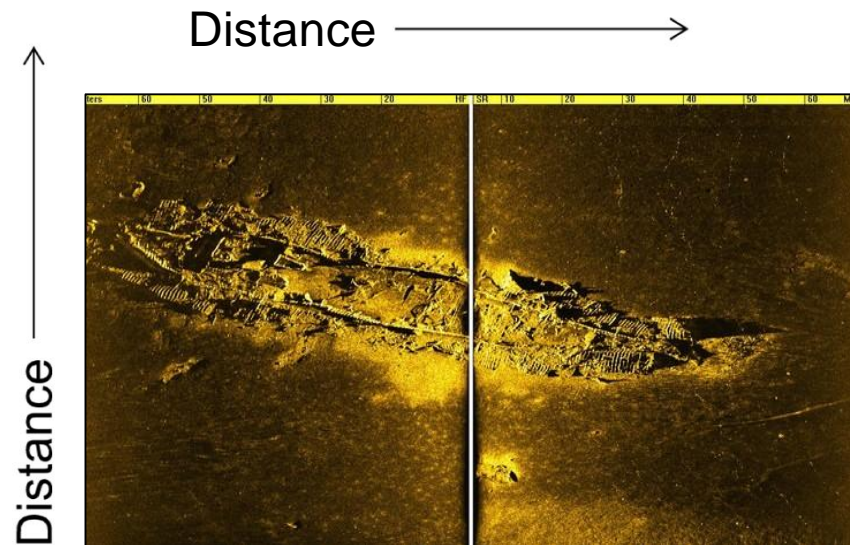
Here:
Surveying in stationary position
horizontal is time



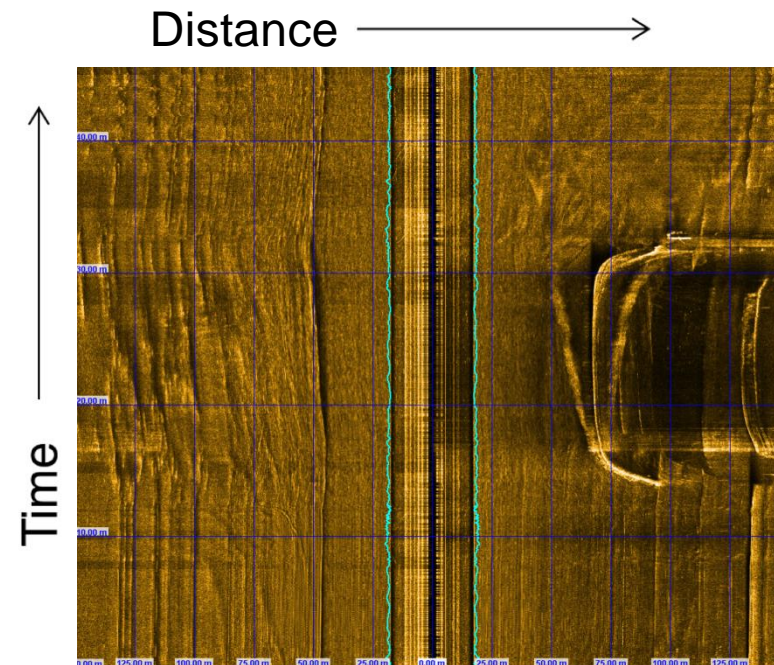
Hydrochart – Side Scan Sonar



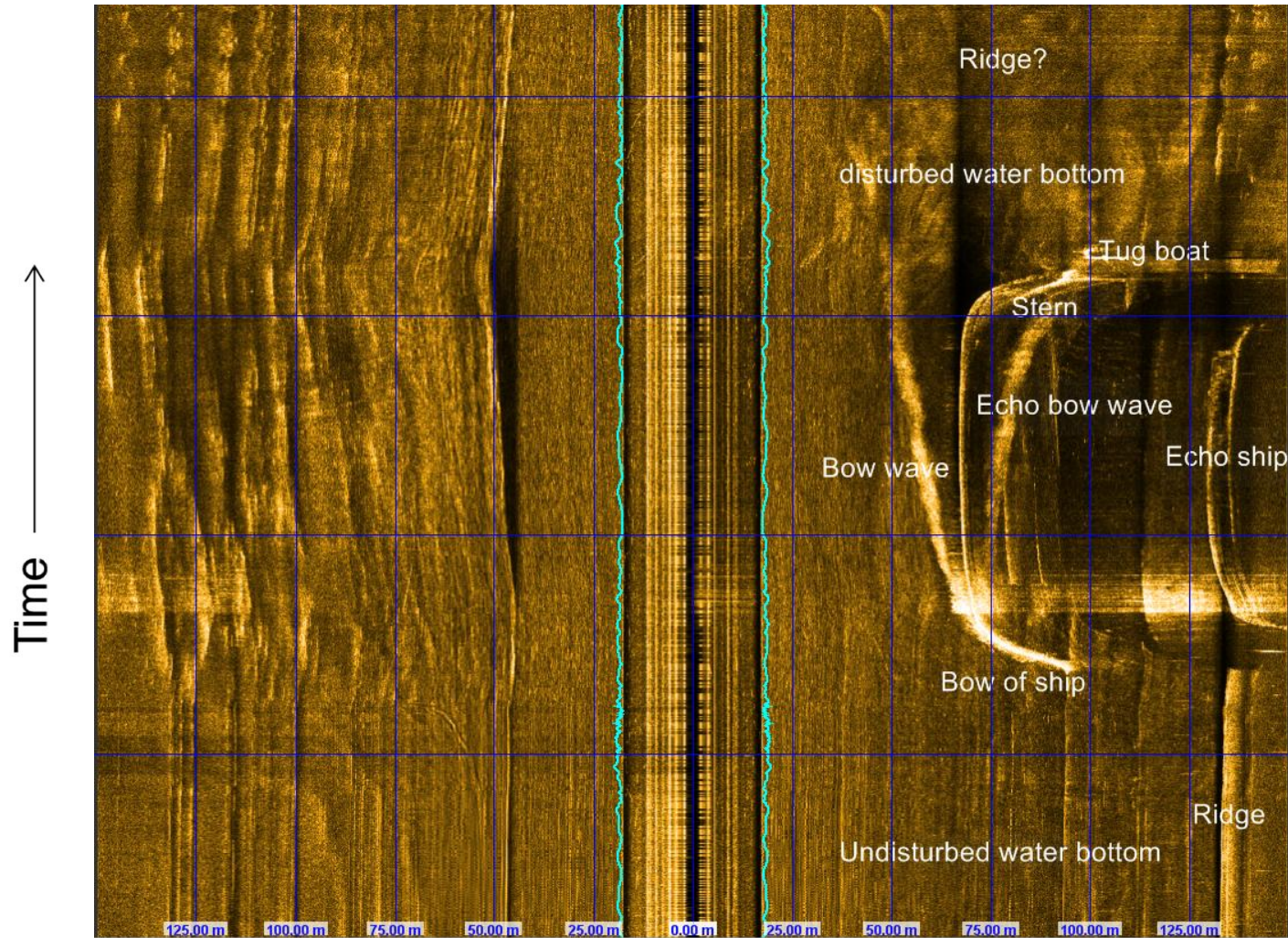
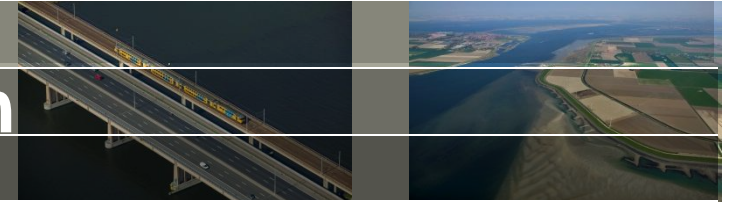
Normal:
Surveying when moving
vertical is distance
(SSS: horizontal is distance)



Here:
Surveying in stationary position
vertical is time
(SSS: horizontal is distance)

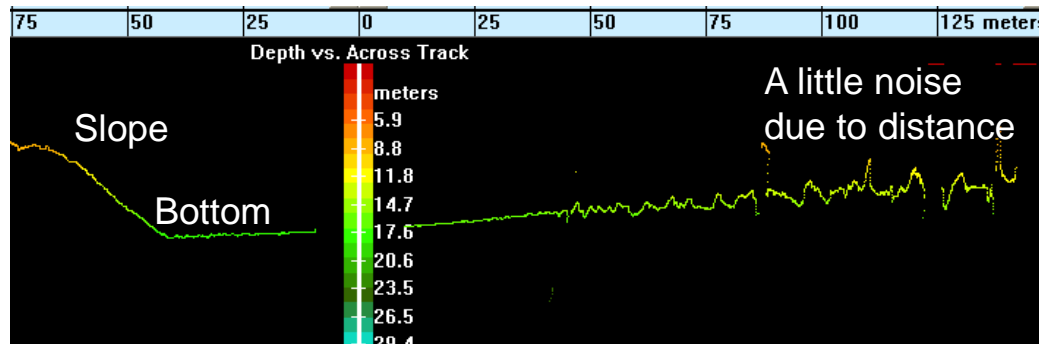


Hydrochart – SSS explanation

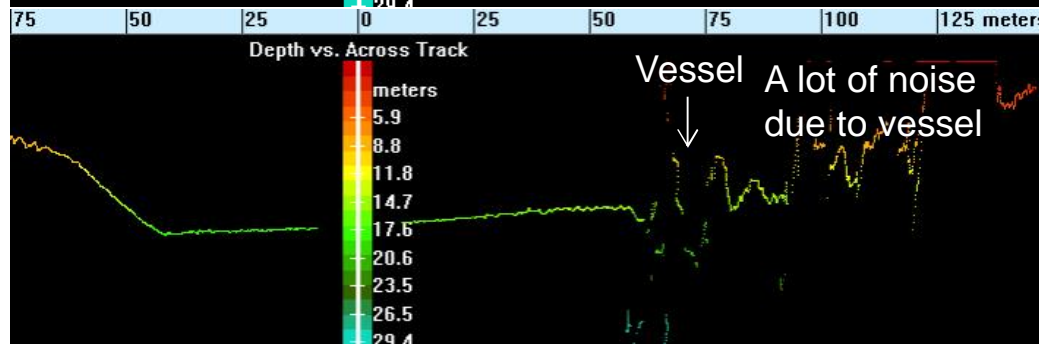


Hydrochart – Bathymetry snapshots in time

Before:



Passage:
noise

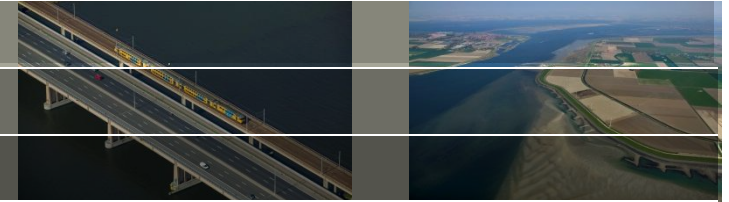


After:
noise



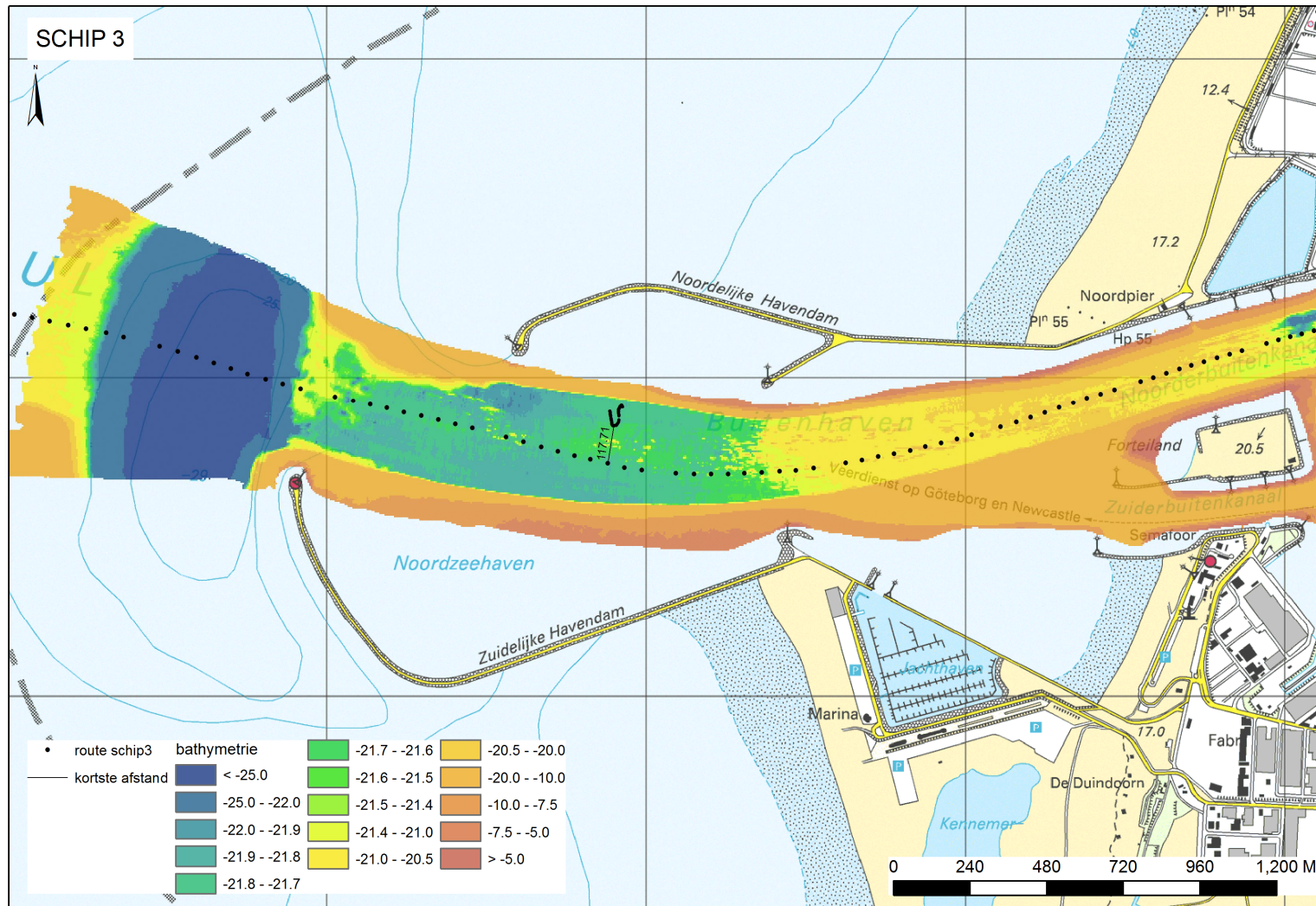
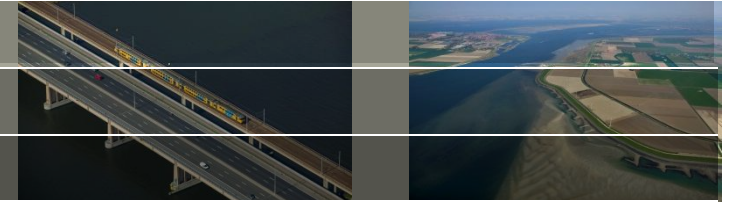
Conclusion: too much noise, dedicated processing required to distinguish signal from noise, not use Hydrochart data at this stage

For each vessel

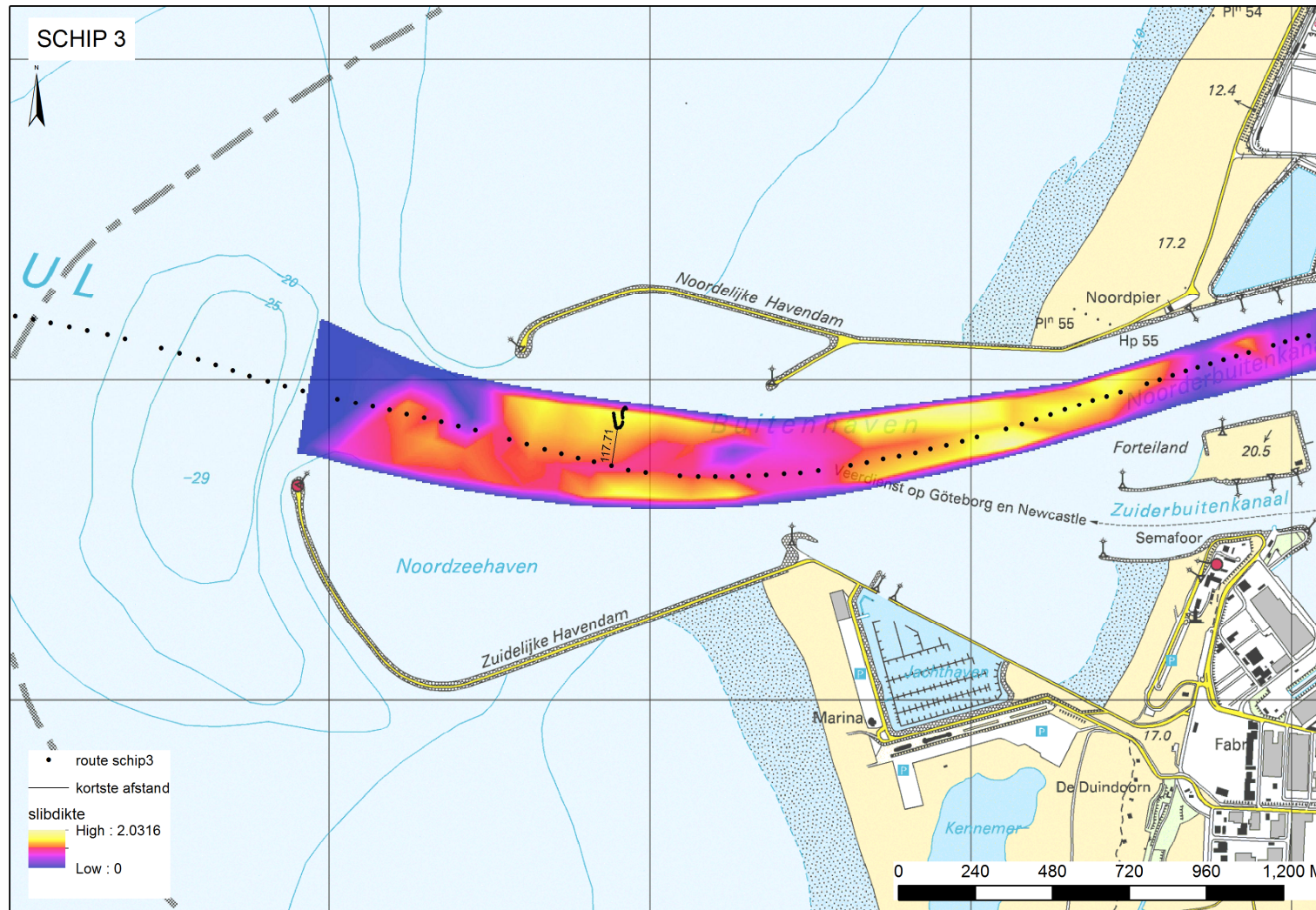
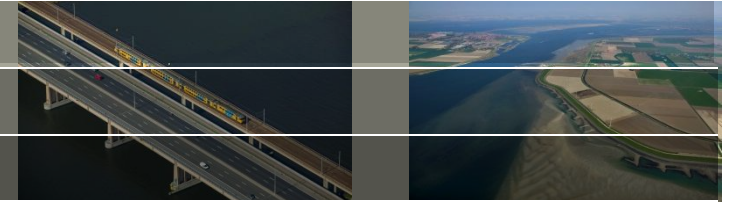


- Vessel track plotted on bathymetry
- Vessel track plotted on mud thickness (top mud – 1.2 kg/L level)
- Tide information
- GPS heights and apparent SILAS water bottom depth
- ADCP:
 - Magnitude and direction of flow
 - Backscatter intensity and motion sensor readings
 - Vertical velocity profiles
 - Coordinates from GPS and bottom tracking
- Hydrochart, SILAS, X-star:
 - Before
 - During
 - After passage
- Navitracker density profiles on line of passage vessel (if available)
- Navitracker density profiles near Ms. Zirfaea

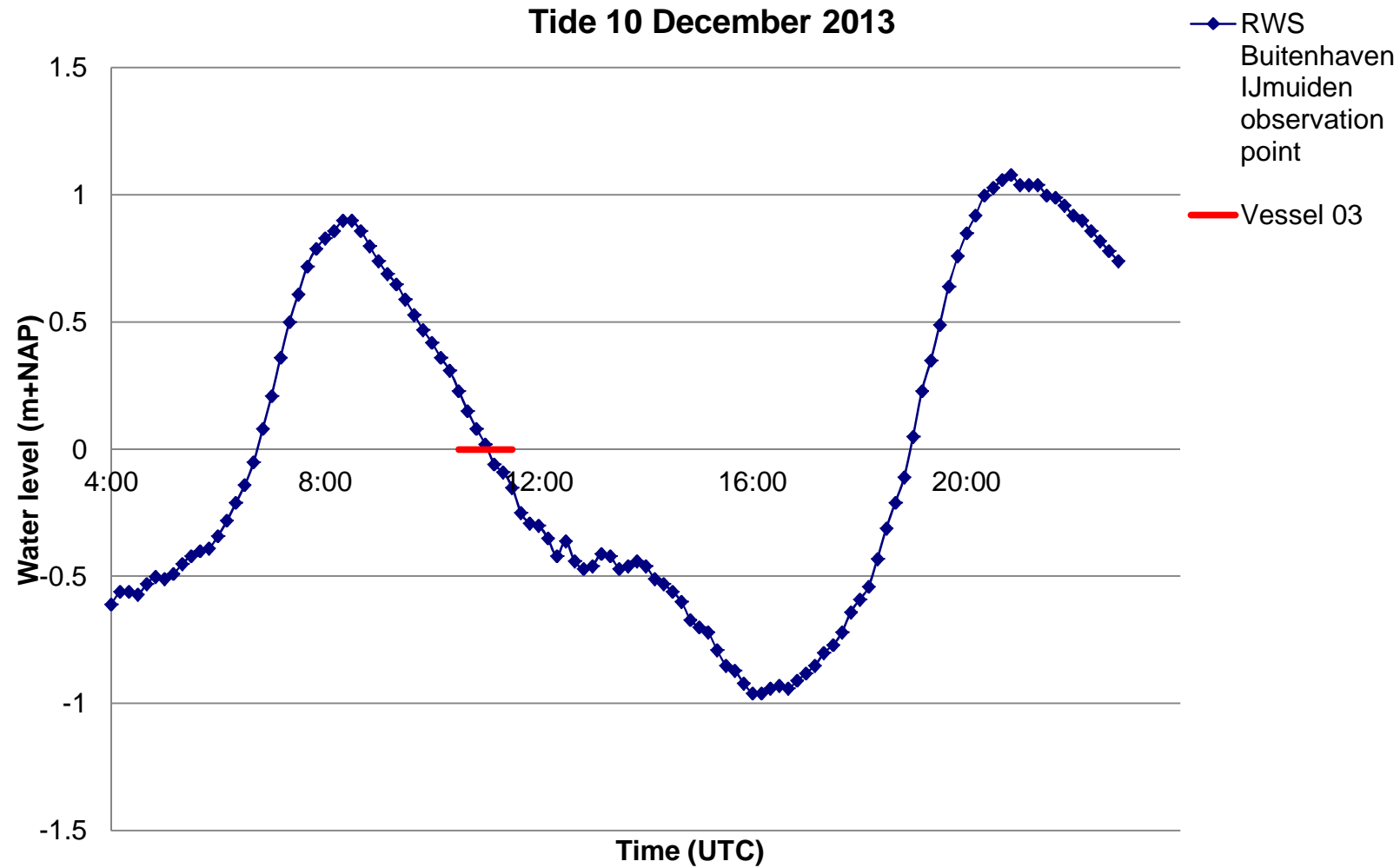
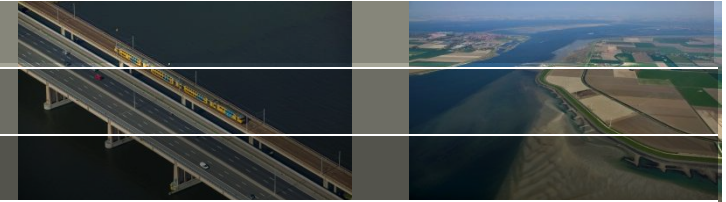
Vessel 3



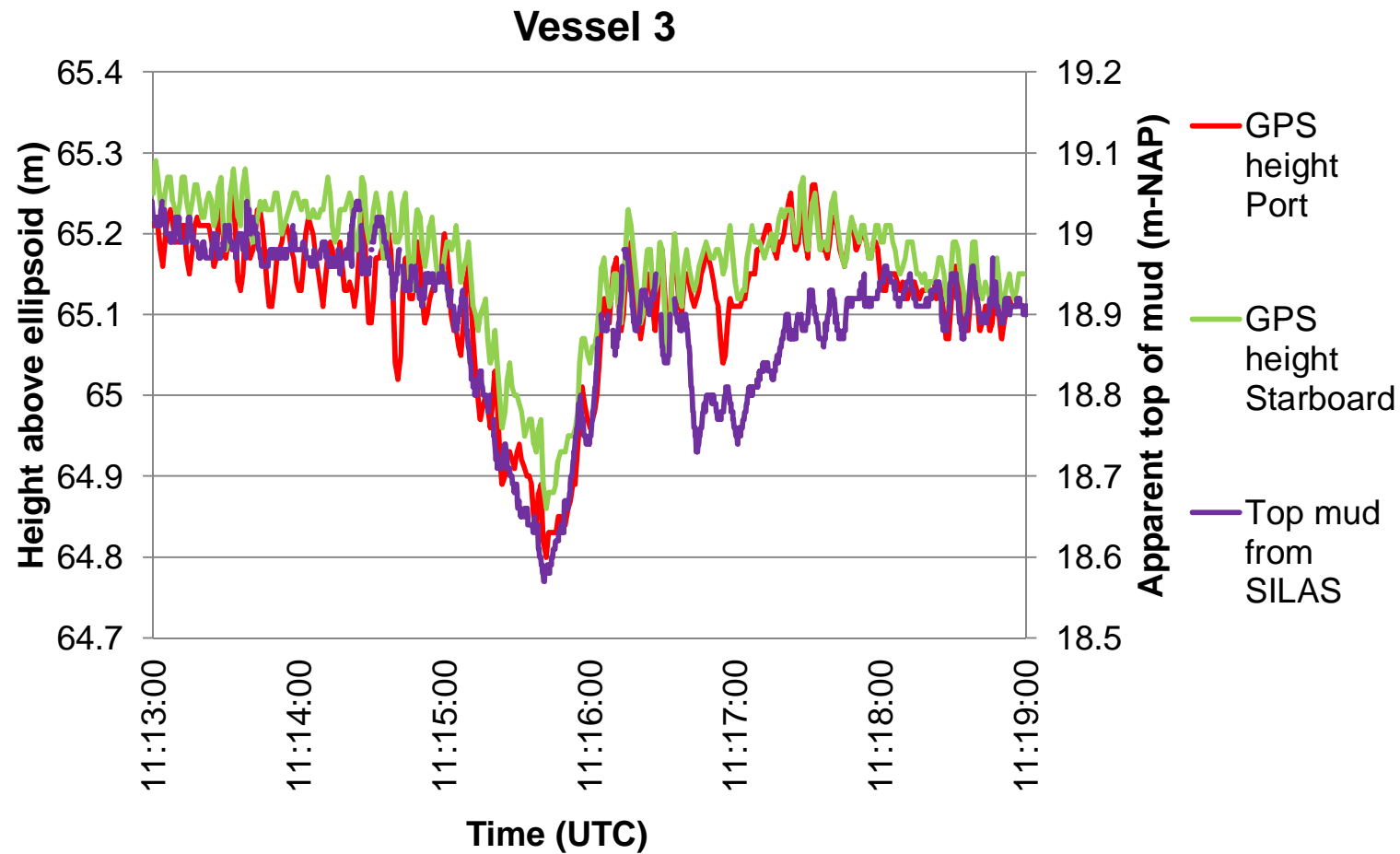
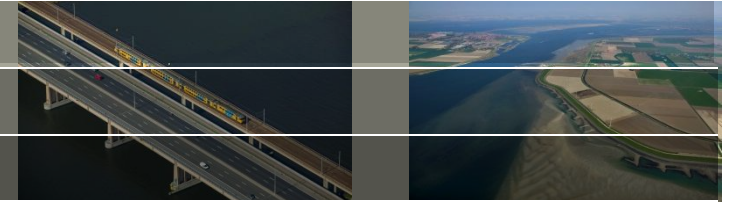
Vessel 3



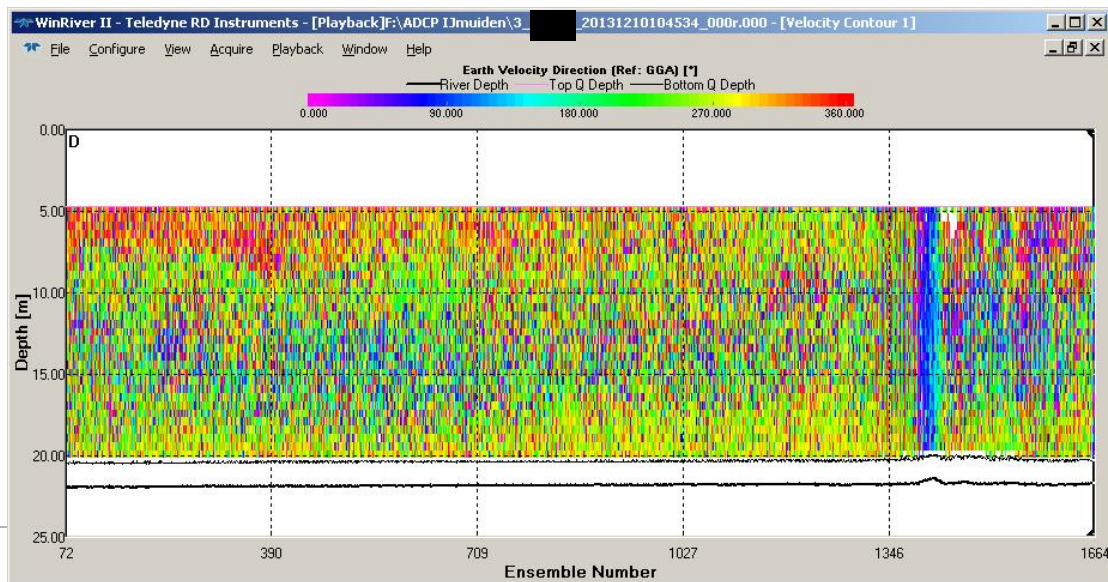
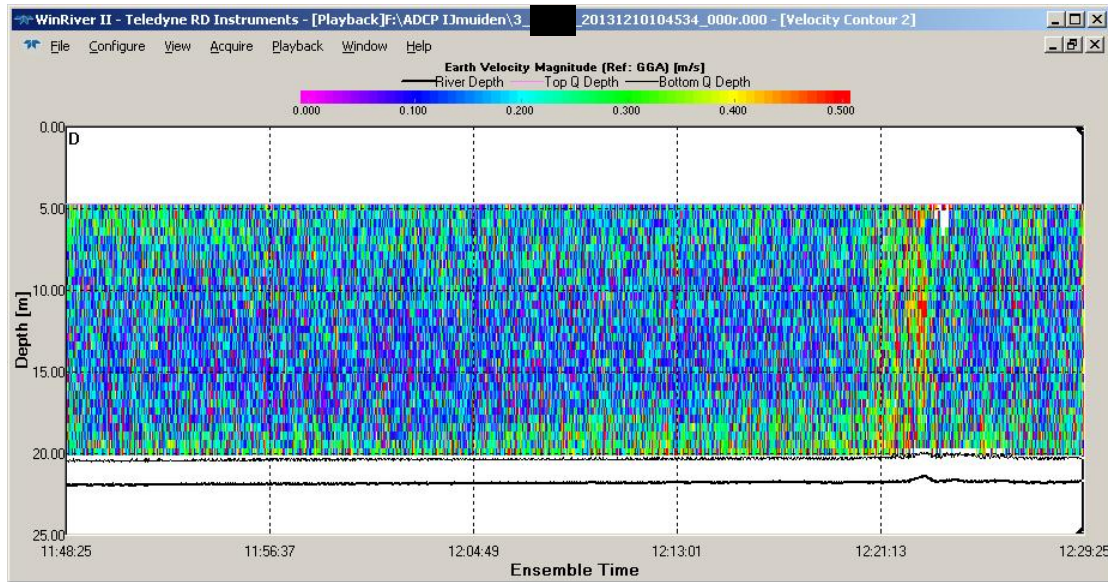
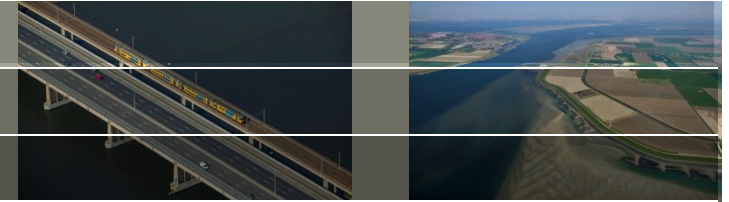
Vessel 3 - tide



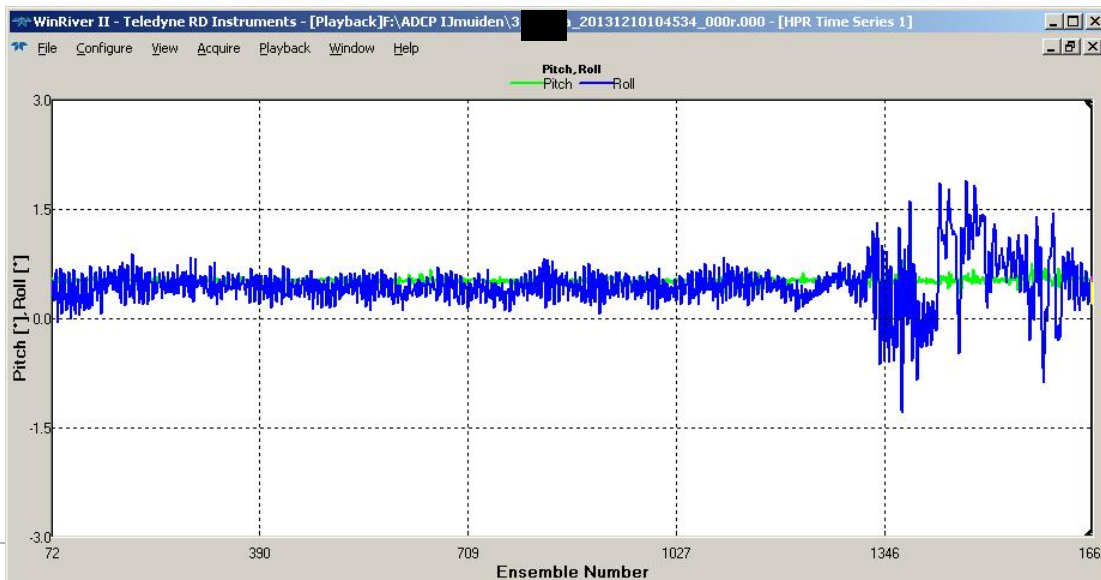
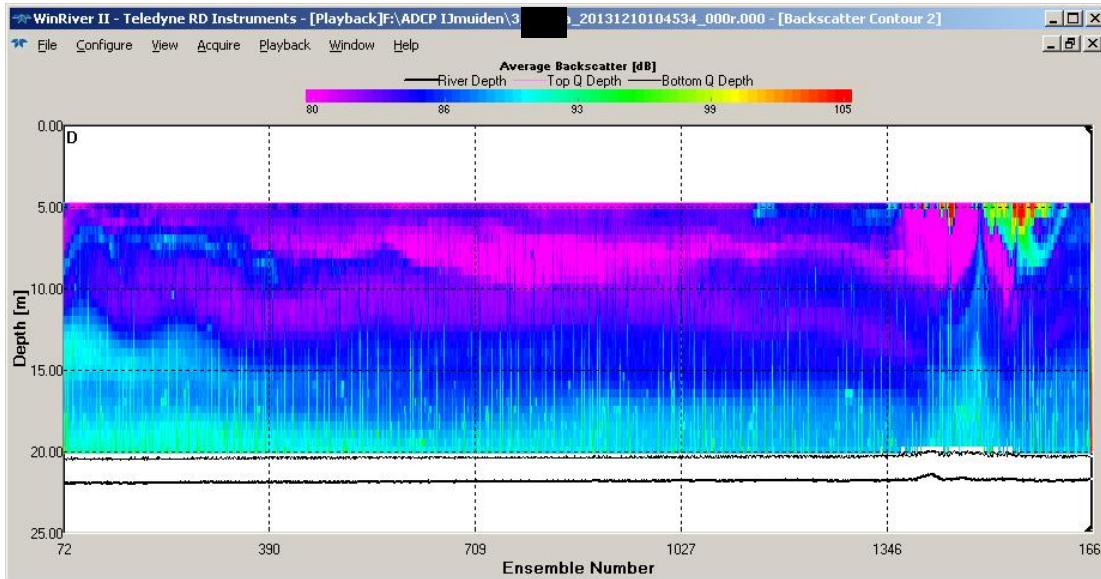
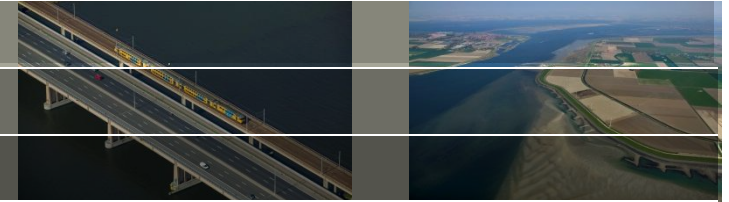
Vessel 3 – GPS Heights



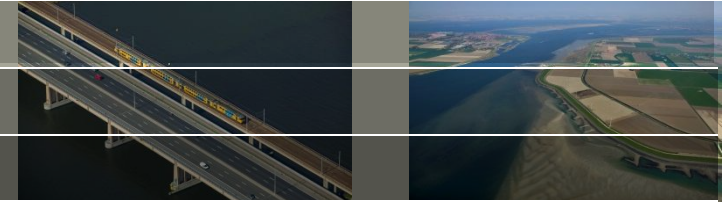
Vessel 3 – ADCP



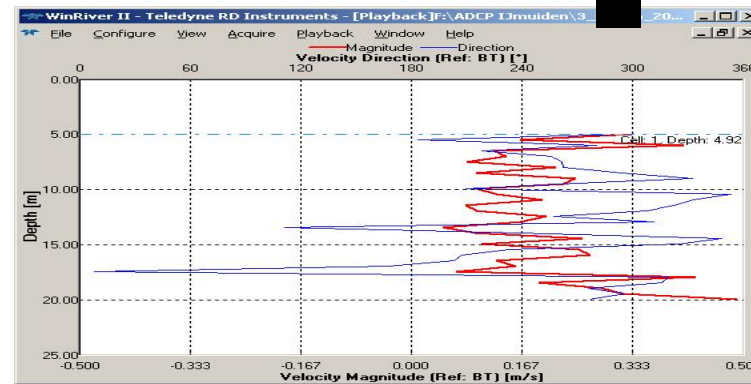
Vessel 3 – ADCP



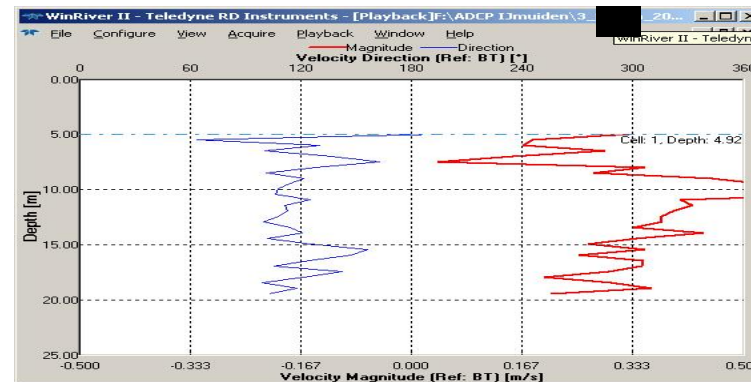
Vessel 3 – ADCP



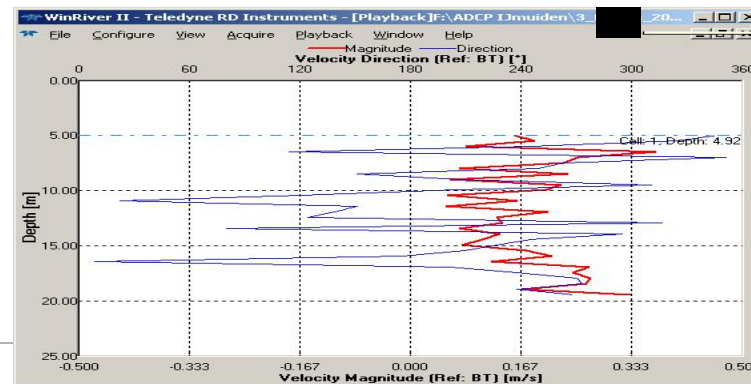
ensemble 1360



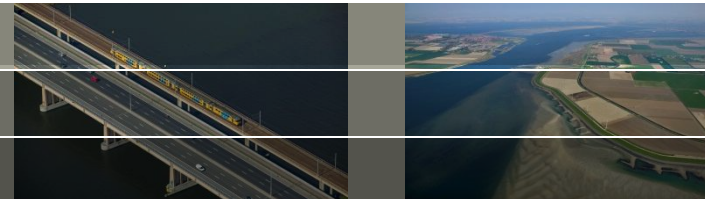
ensemble 1420



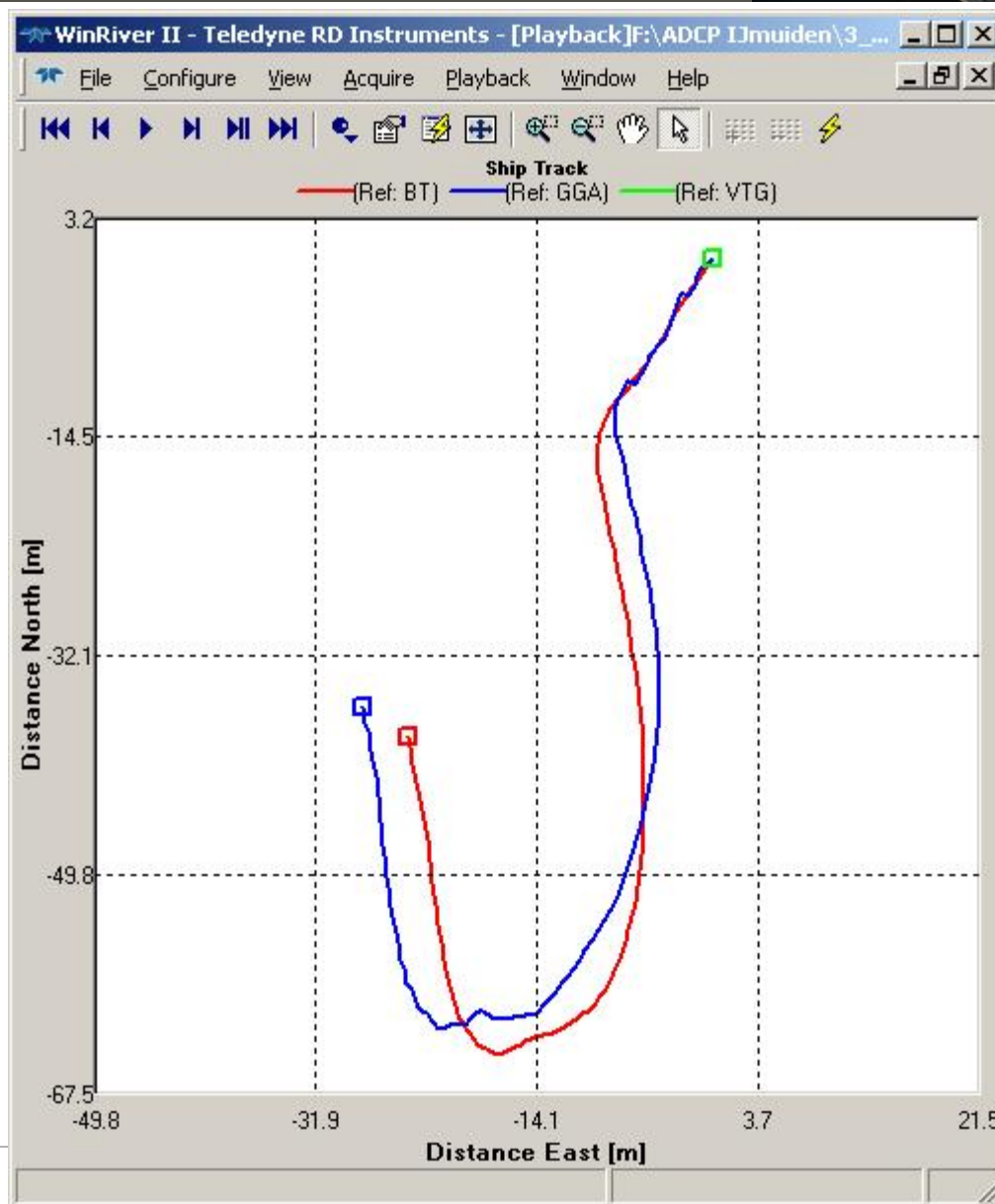
ensemble 1510



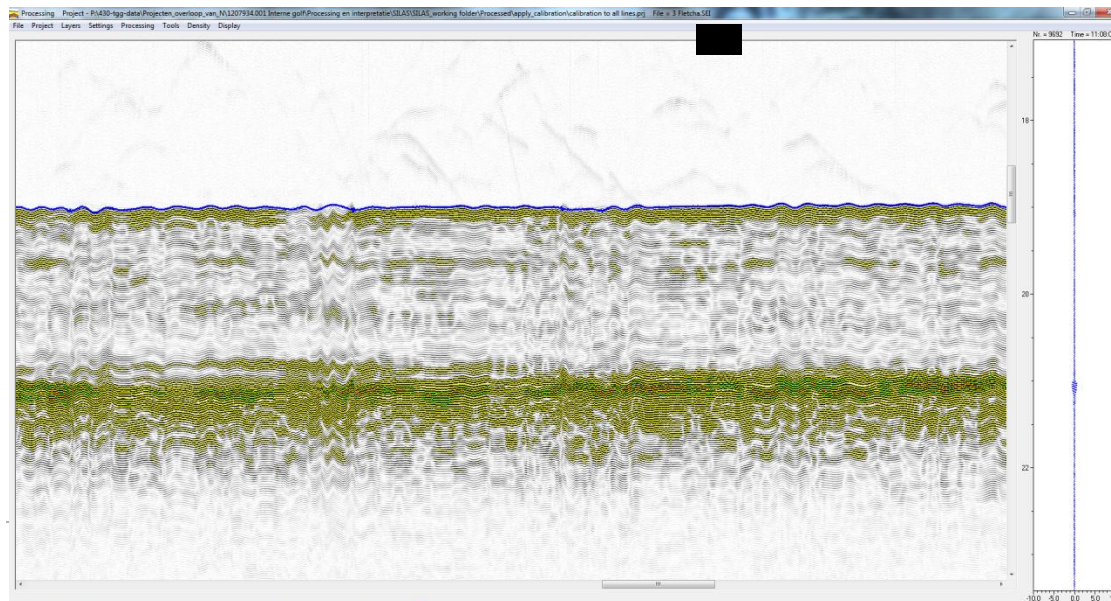
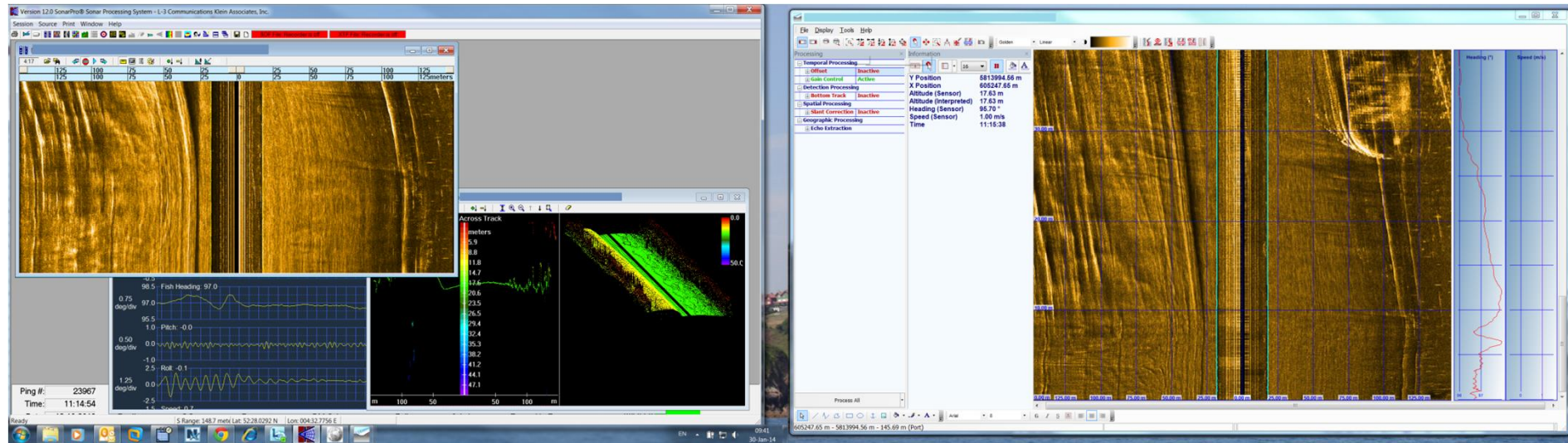
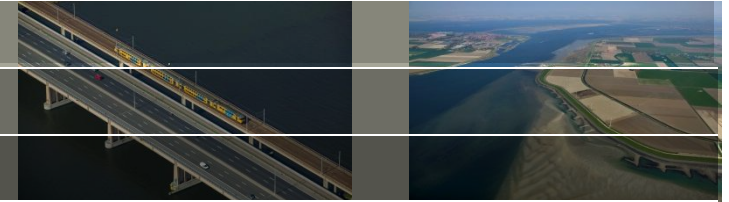
Vessel 3 – ADCP



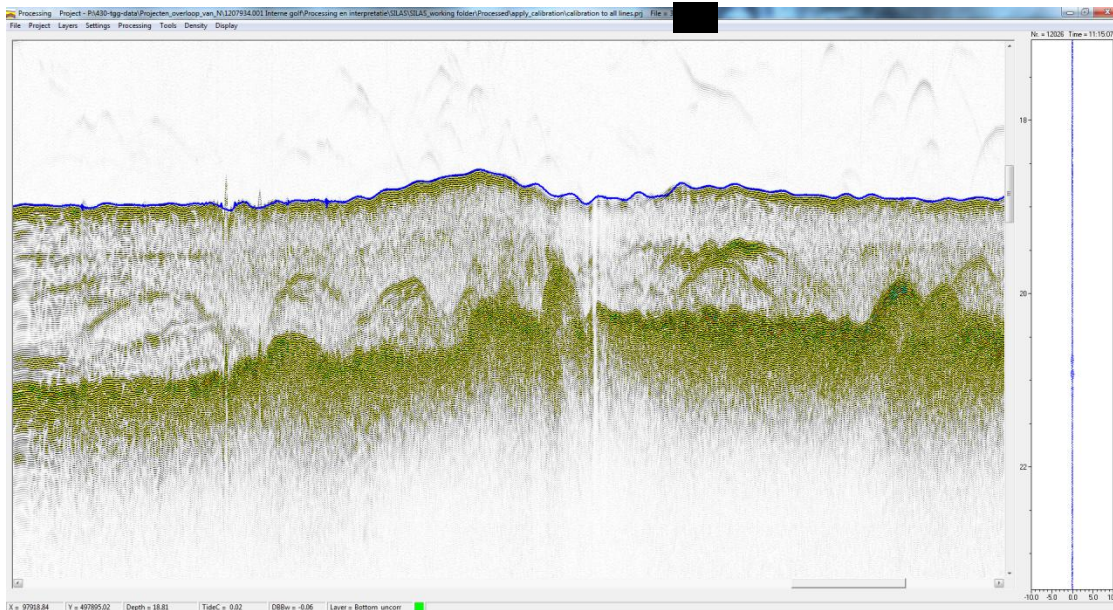
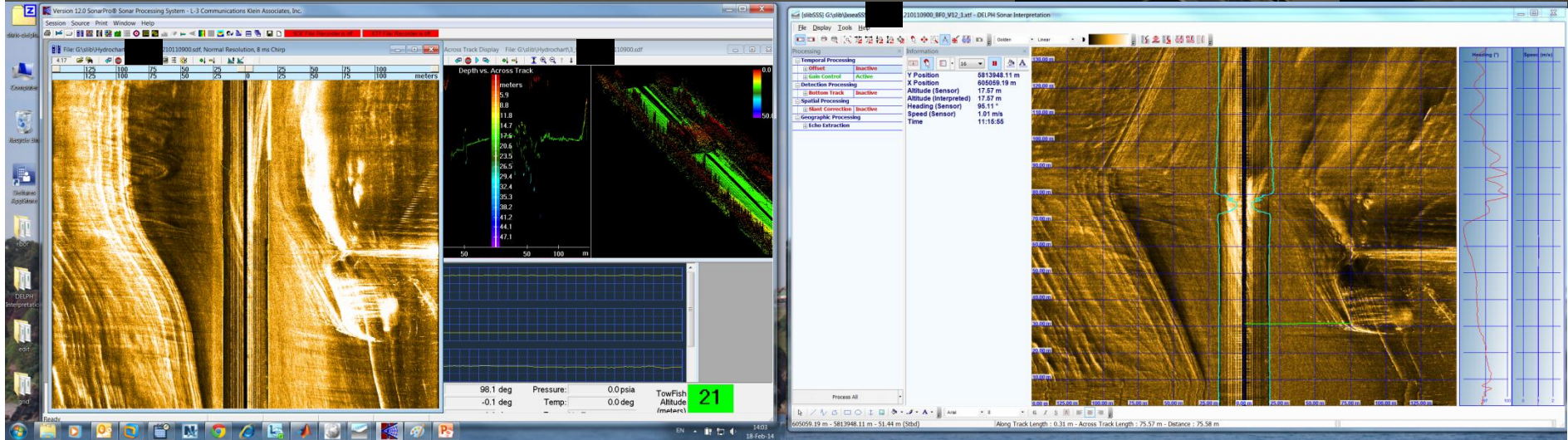
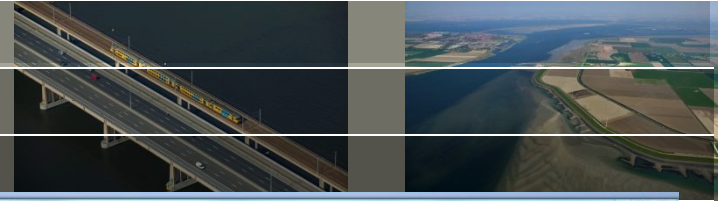
ensembles 1360 - 1510



Vessel 3 - Before

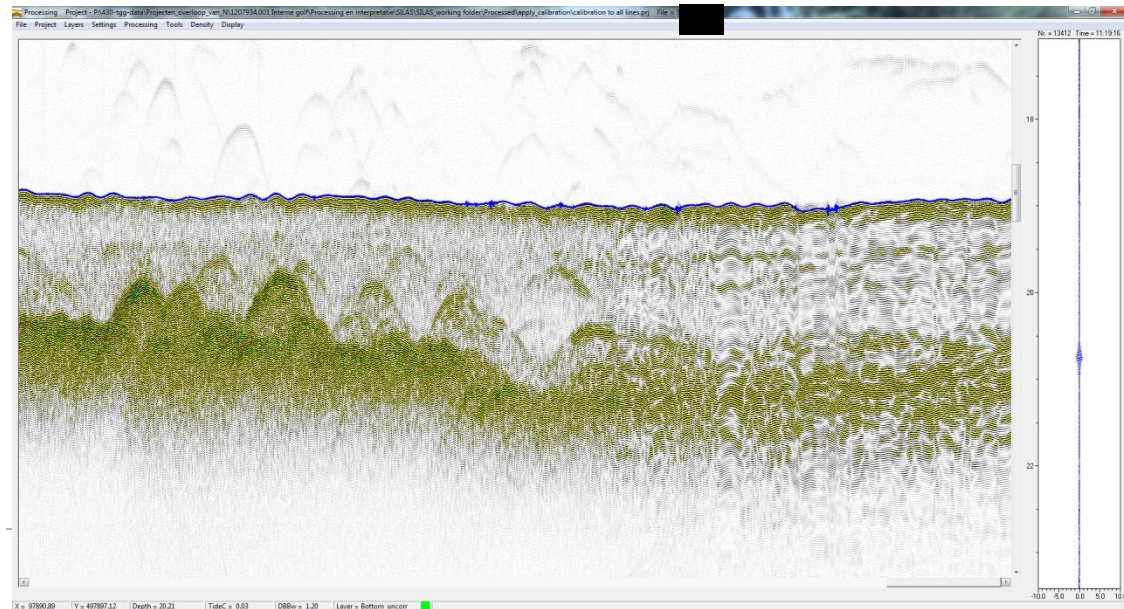
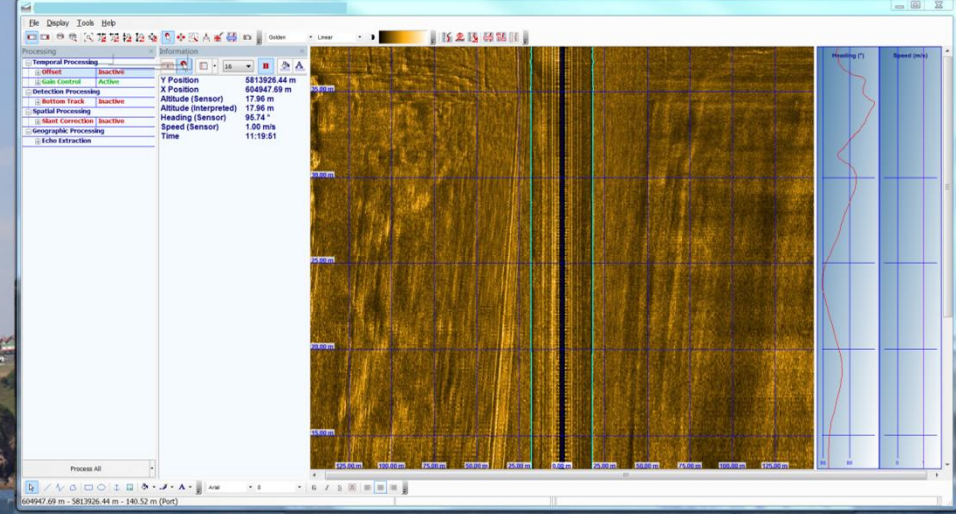
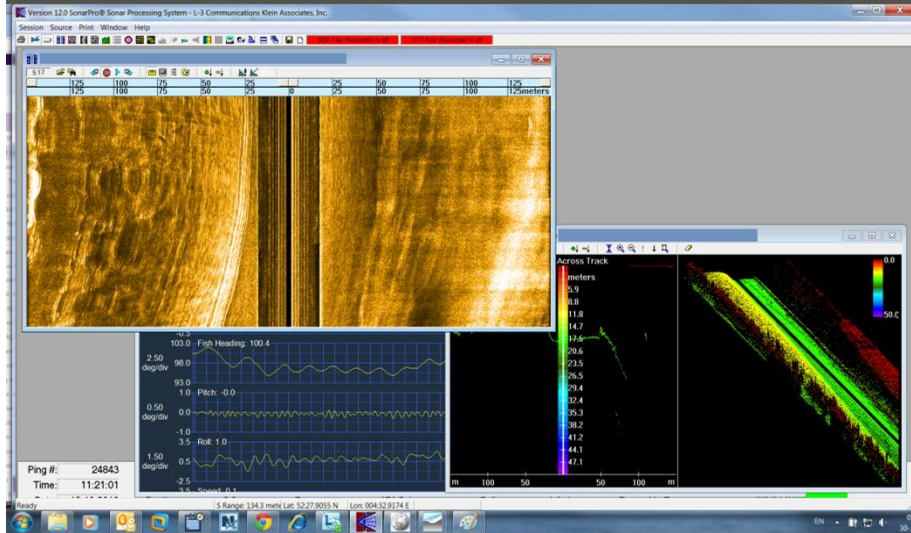
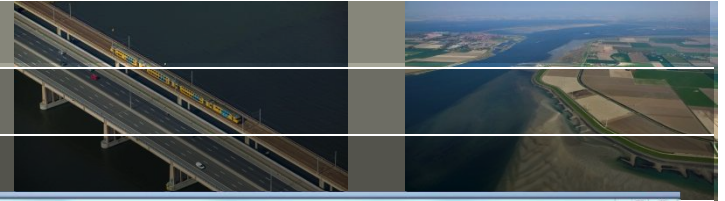


Vessel 3 - Passage



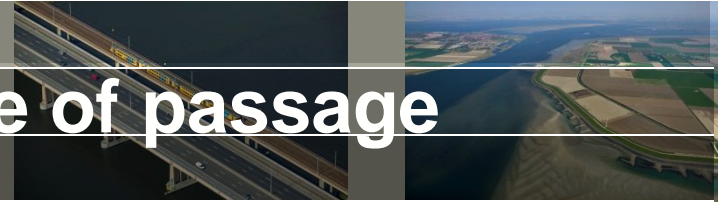
Deltares

Vessel 3 - After

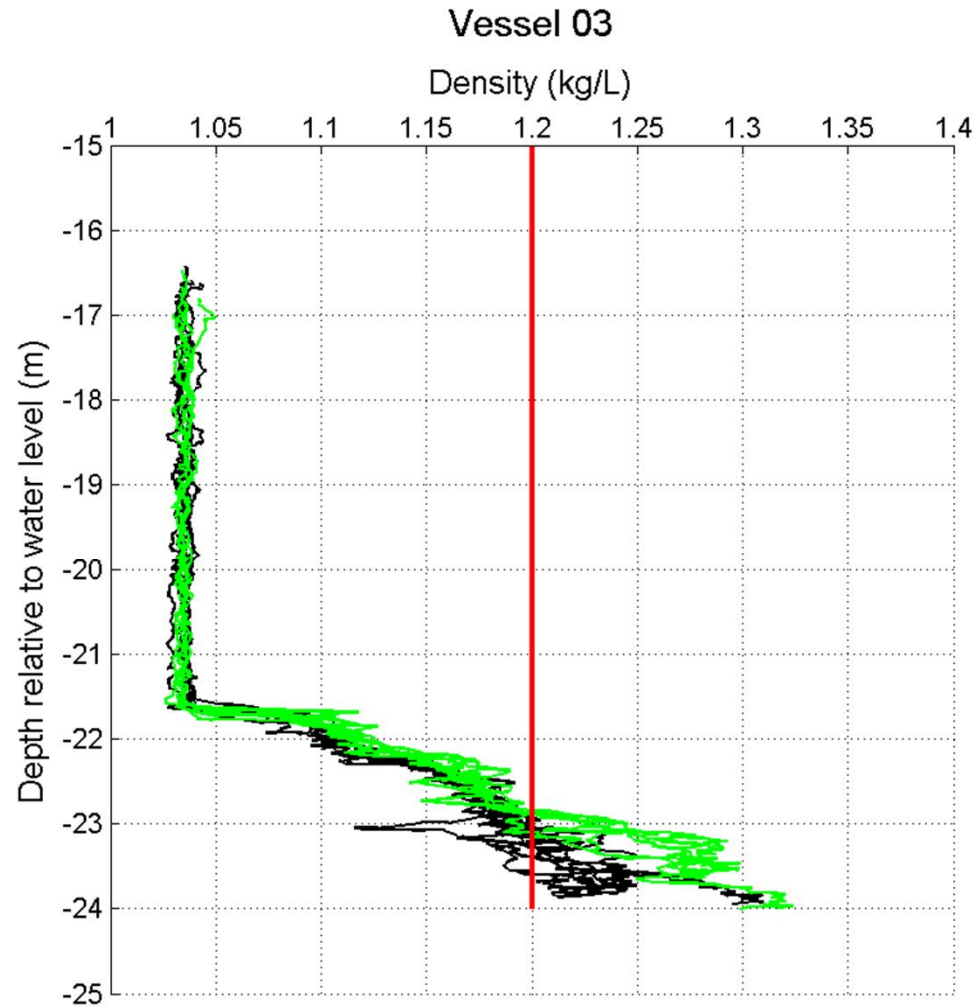


Deltares

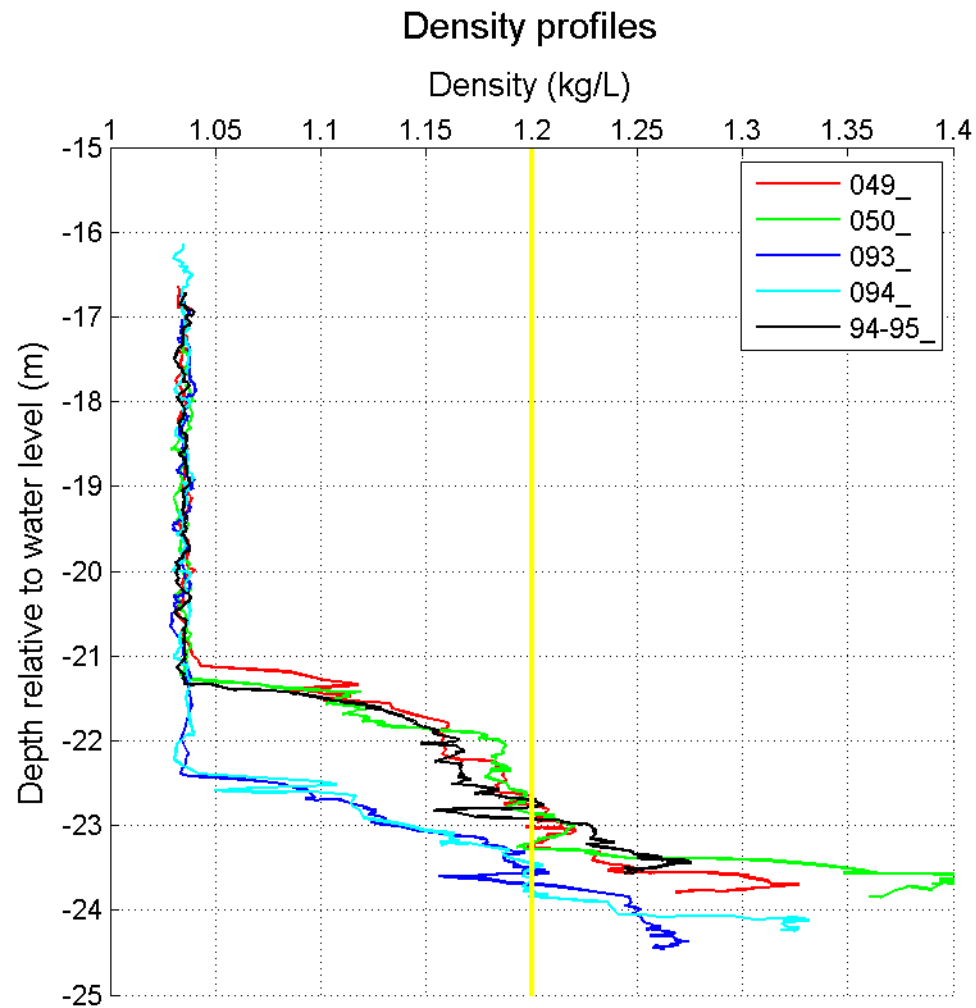
Vessel 3 – density profiles line of passage



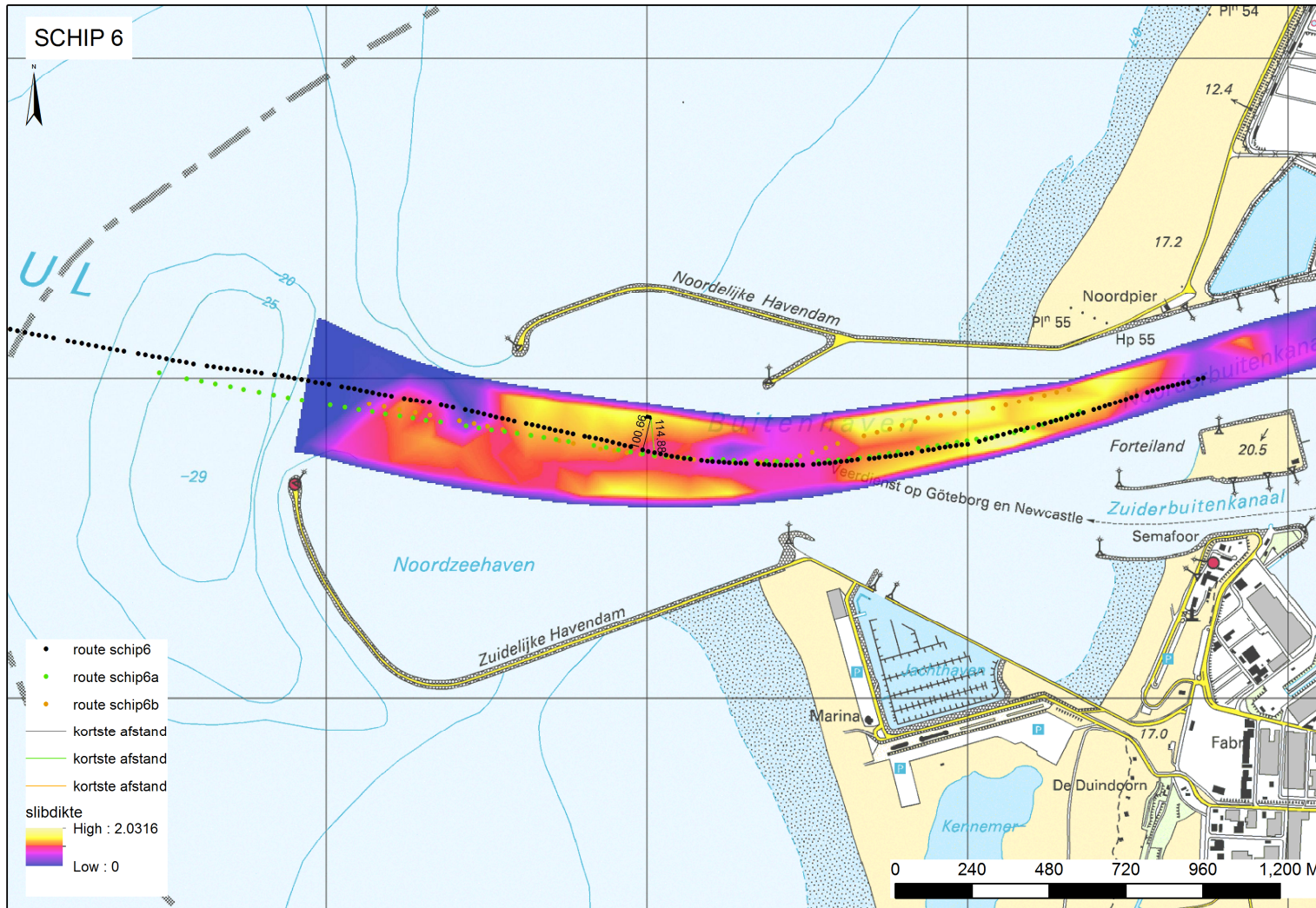
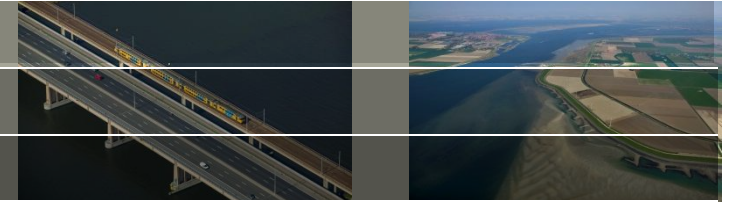
Green: before
Black: after
Corrected for tide
difference



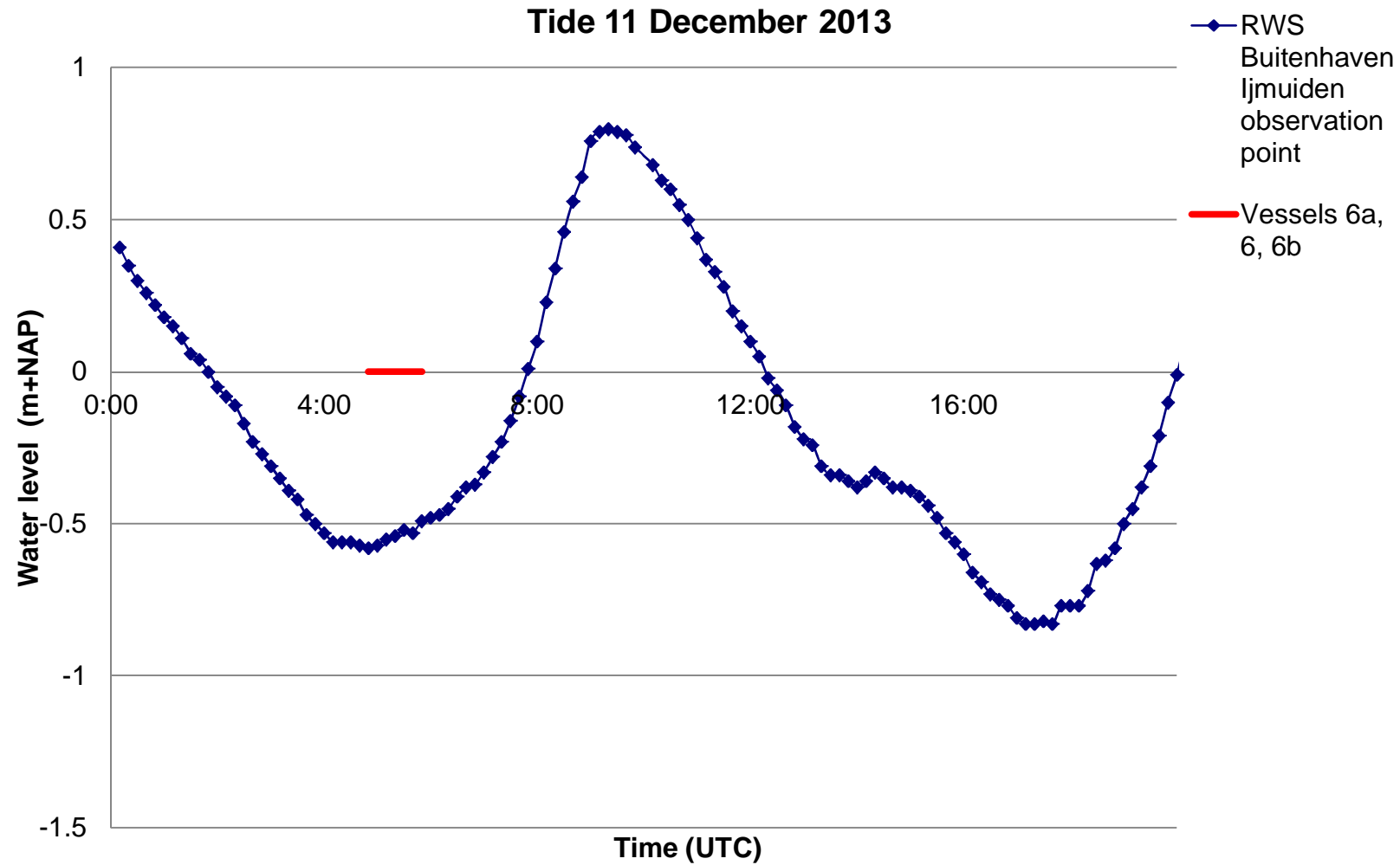
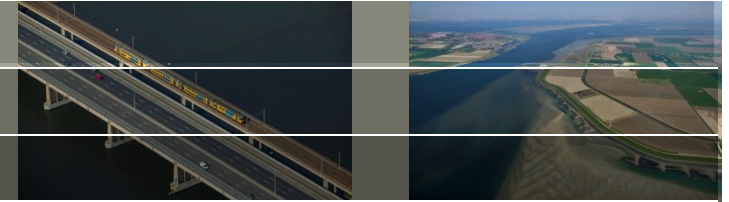
Vessel 3 – Density profiles near Zirfaea



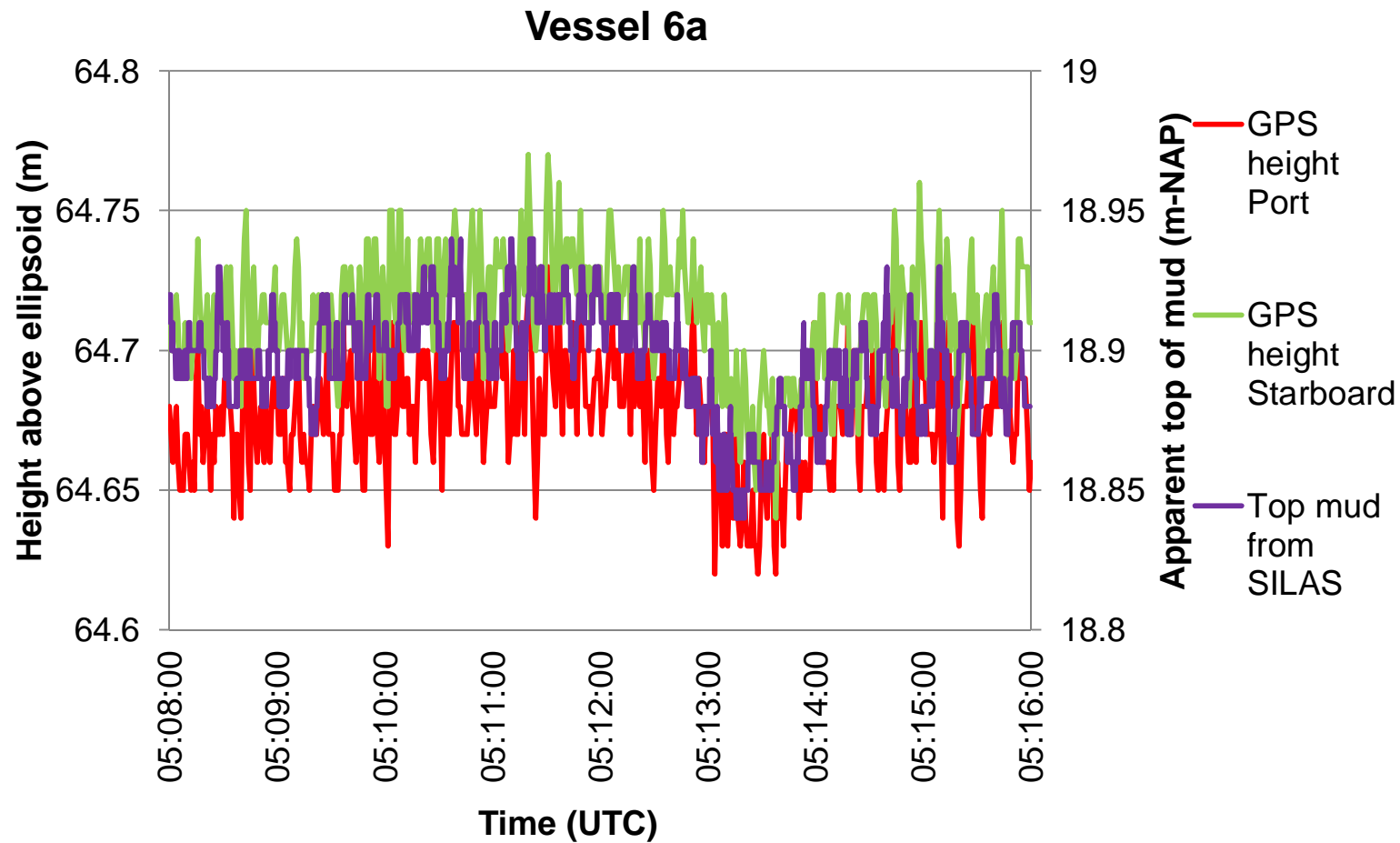
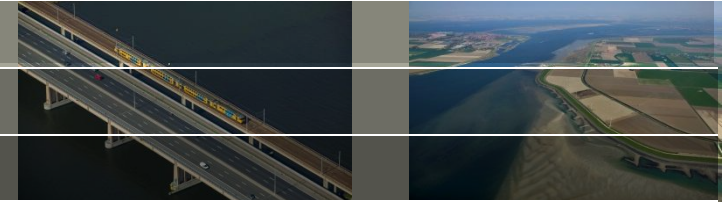
Vessels: 6a – 6 – 6b



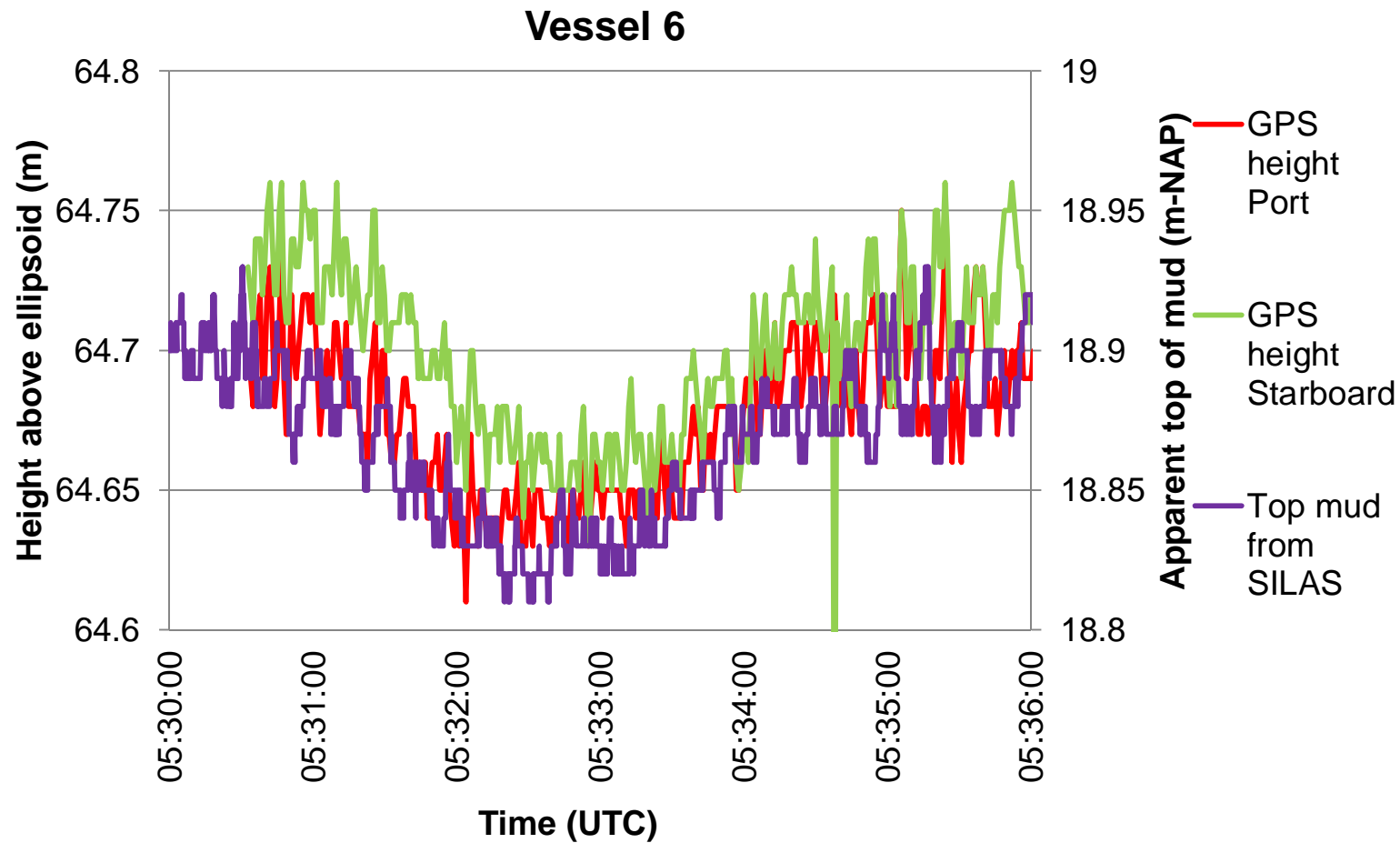
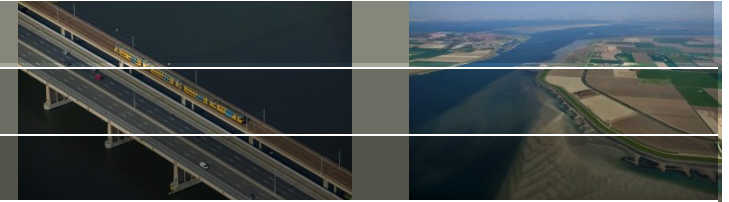
Vessels 6a, 6, 6b - Tide



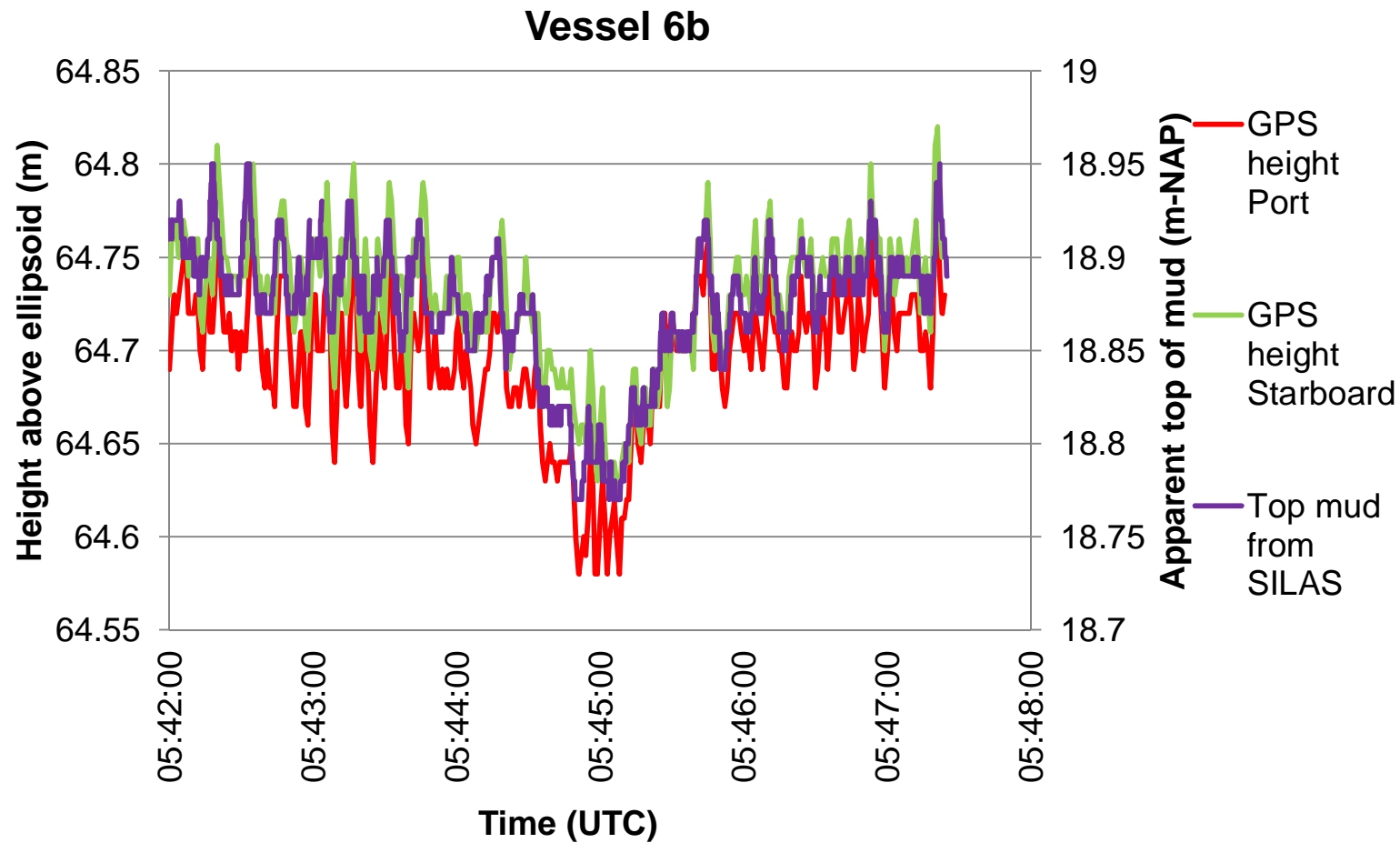
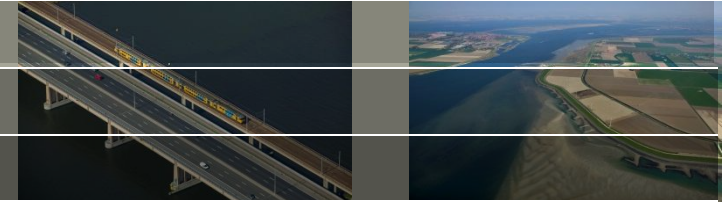
Vessel 6a – GPS Heights



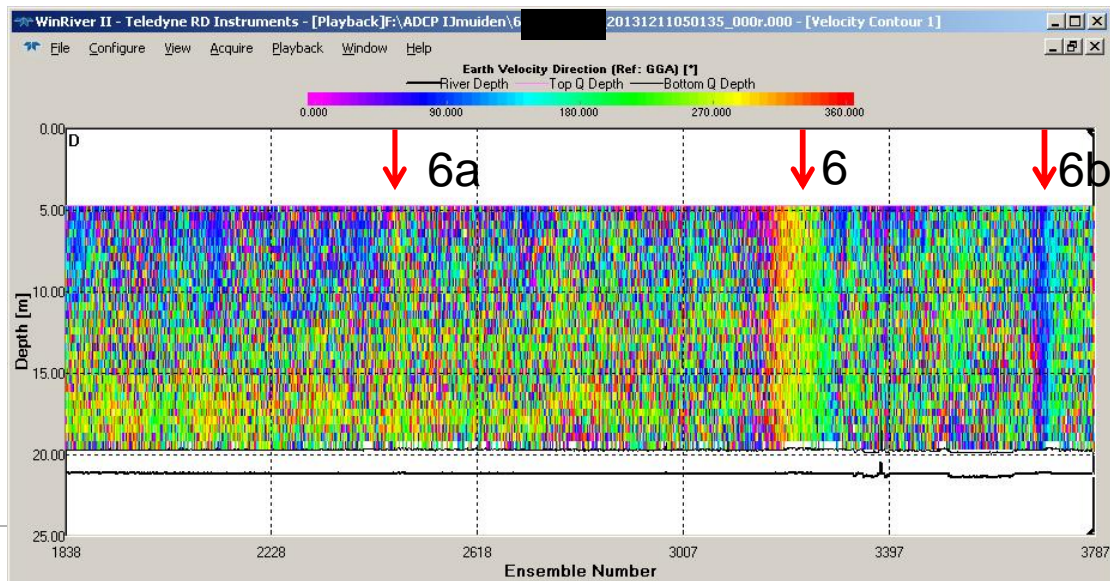
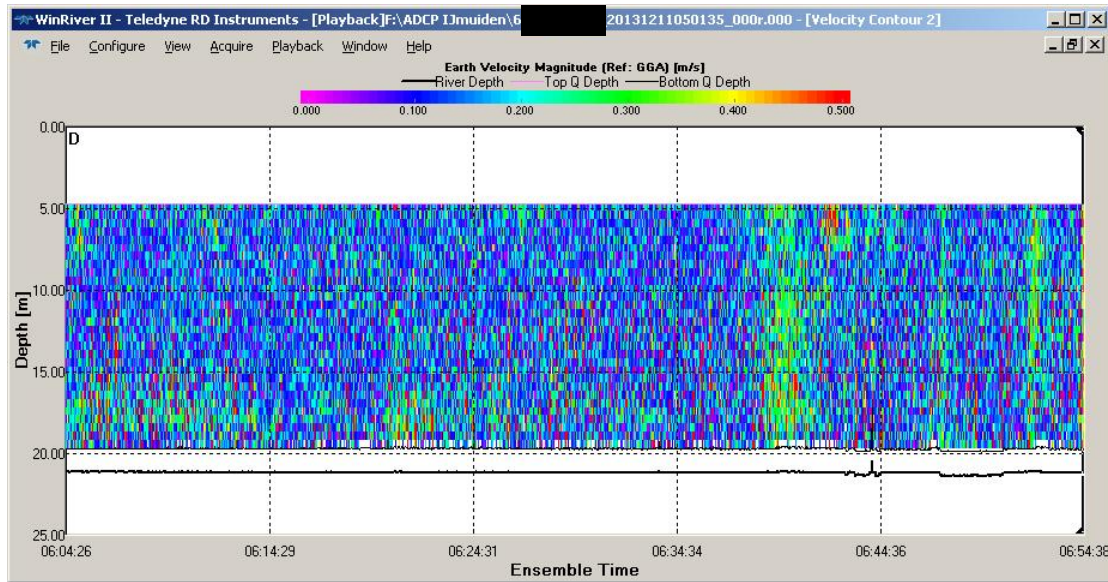
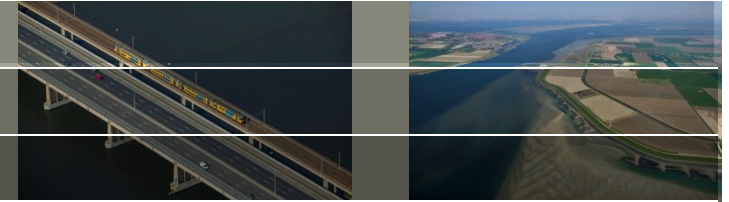
Vessel 6 – GPS Heights



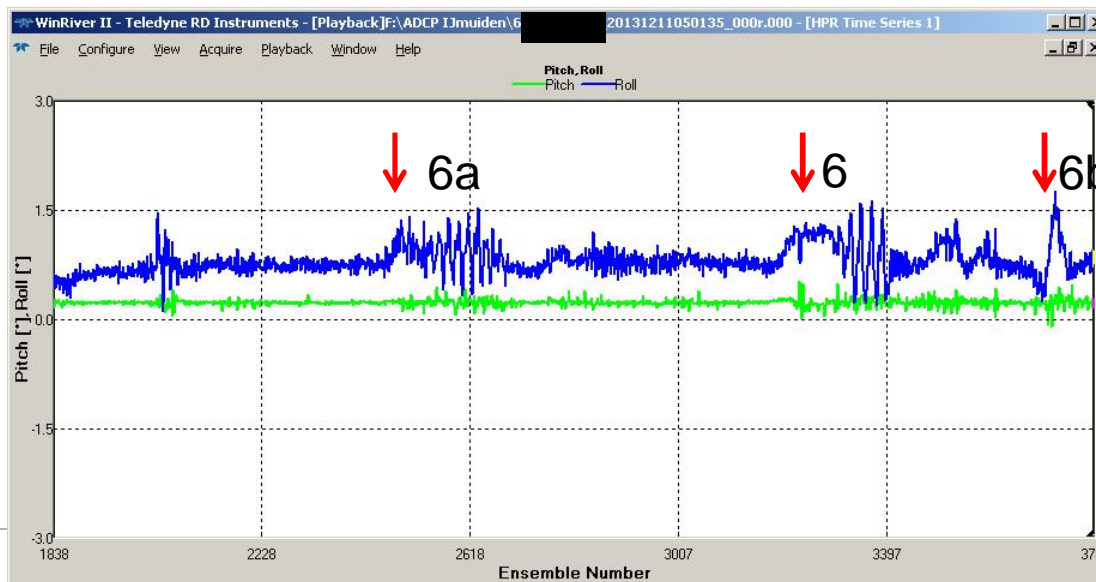
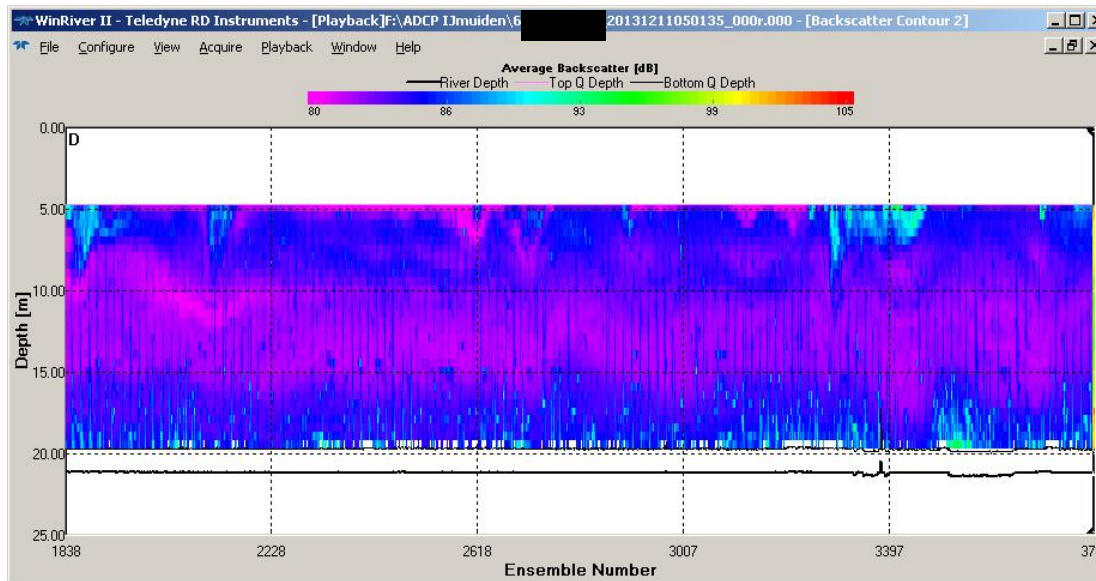
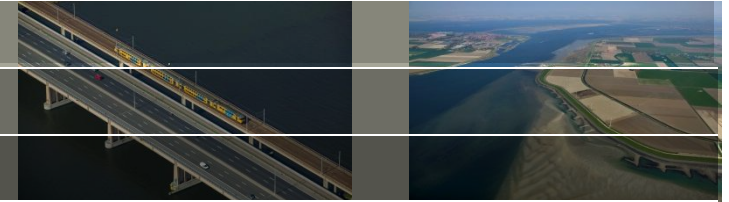
Vessel 6b – GPS Heights



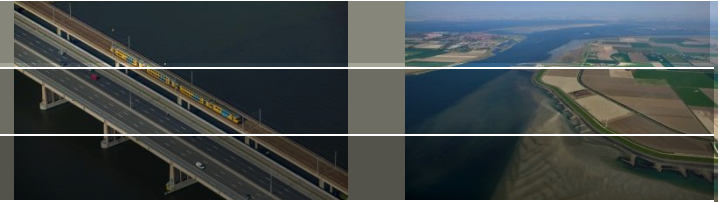
Vessel 6a – 6 – 6b – ADCP



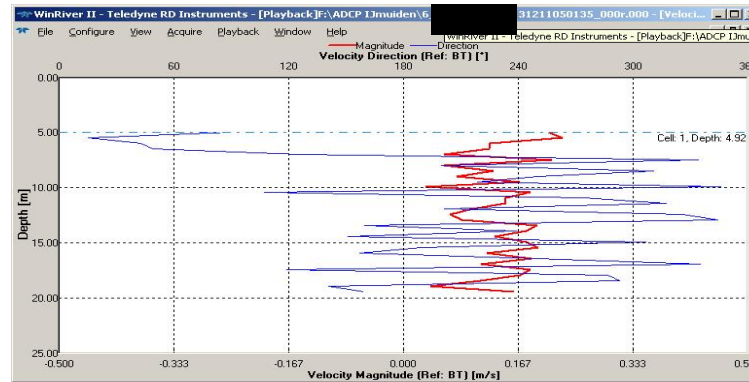
Vessel 6 – ADCP



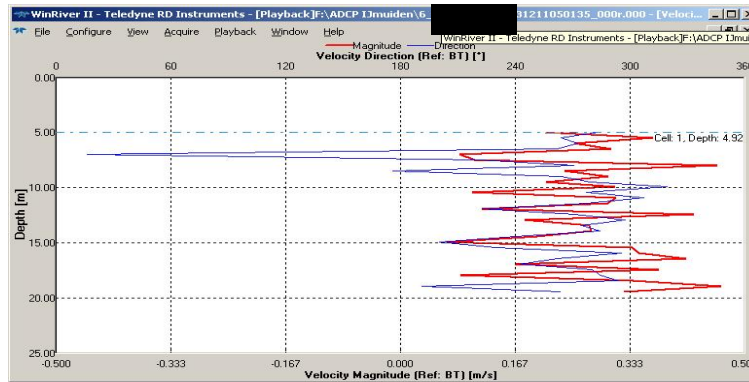
Vessel 6 – ADCP



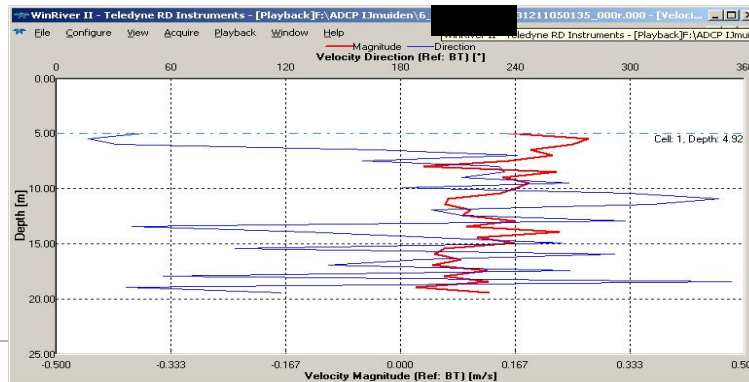
ensemble 3077



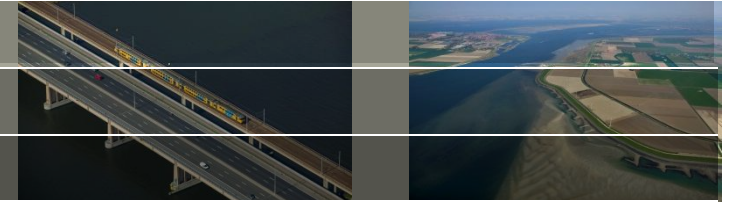
ensemble 3235



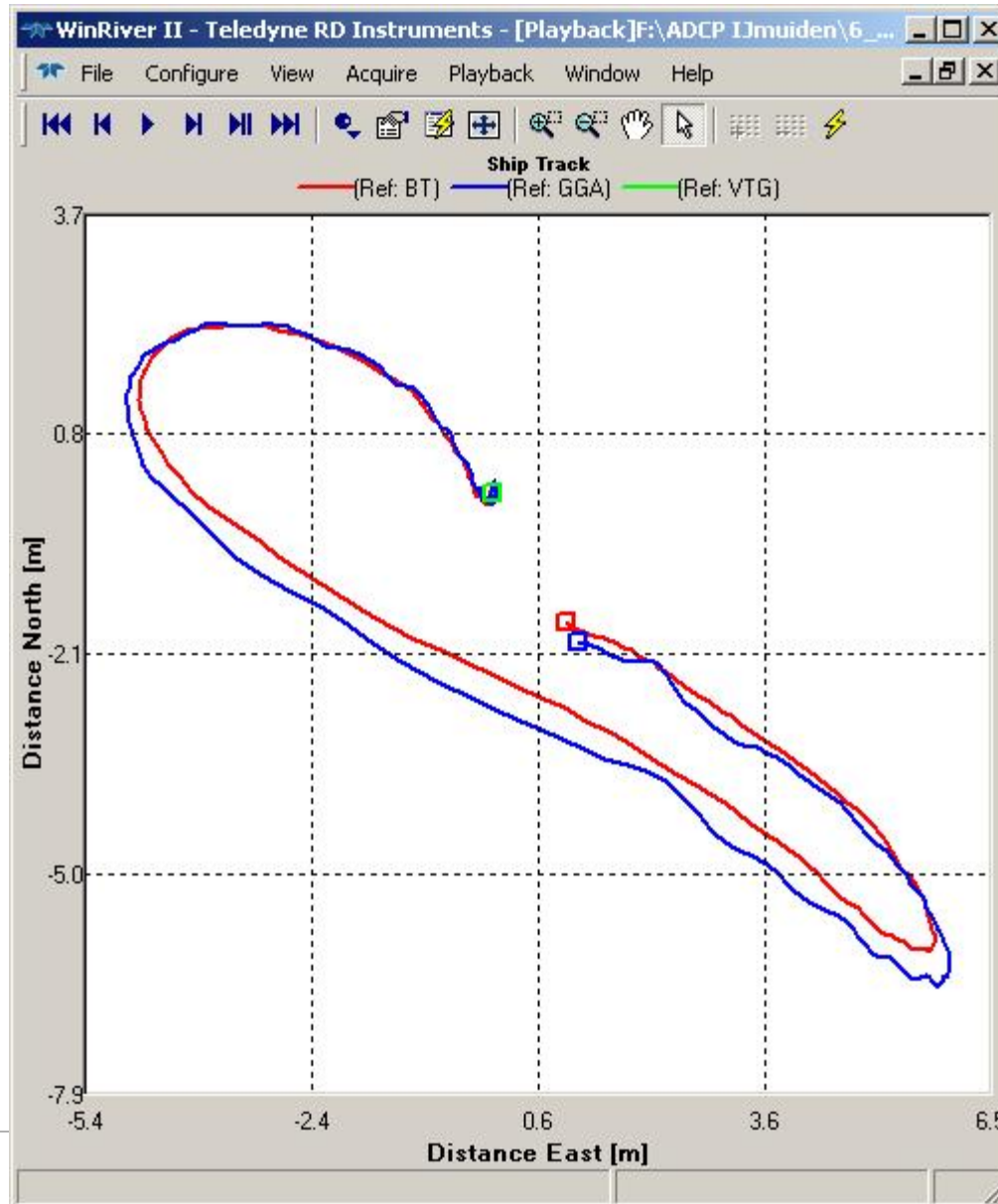
ensemble xxxx (after)



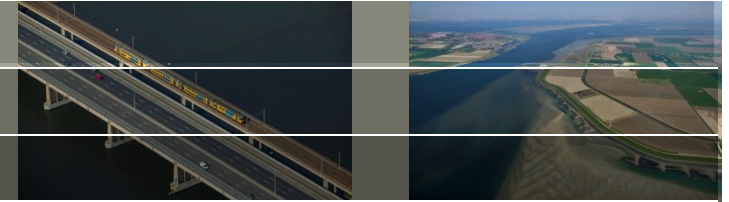
Vessel 6 – ADCP



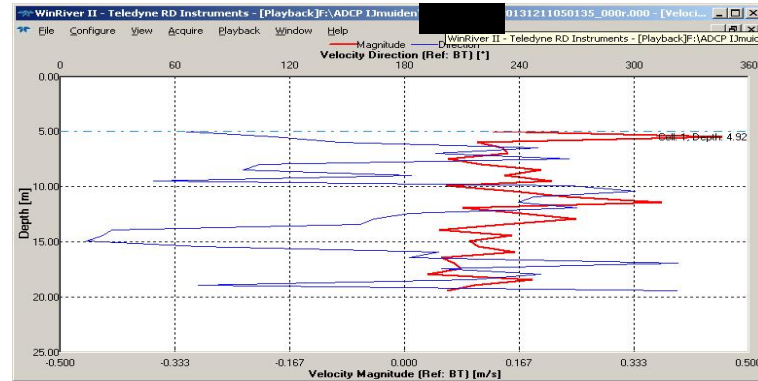
ensembles 3075 – 3325



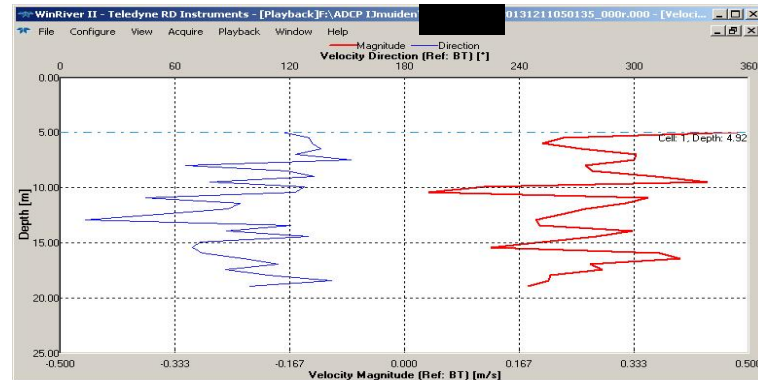
Vessel 6b – ADCP



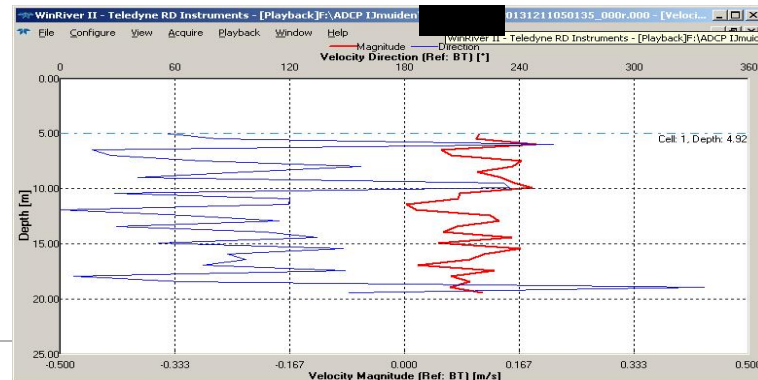
ensemble 3400



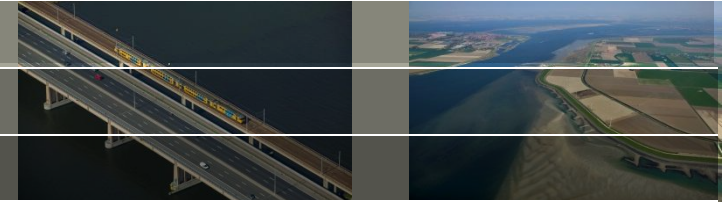
ensemble 3698



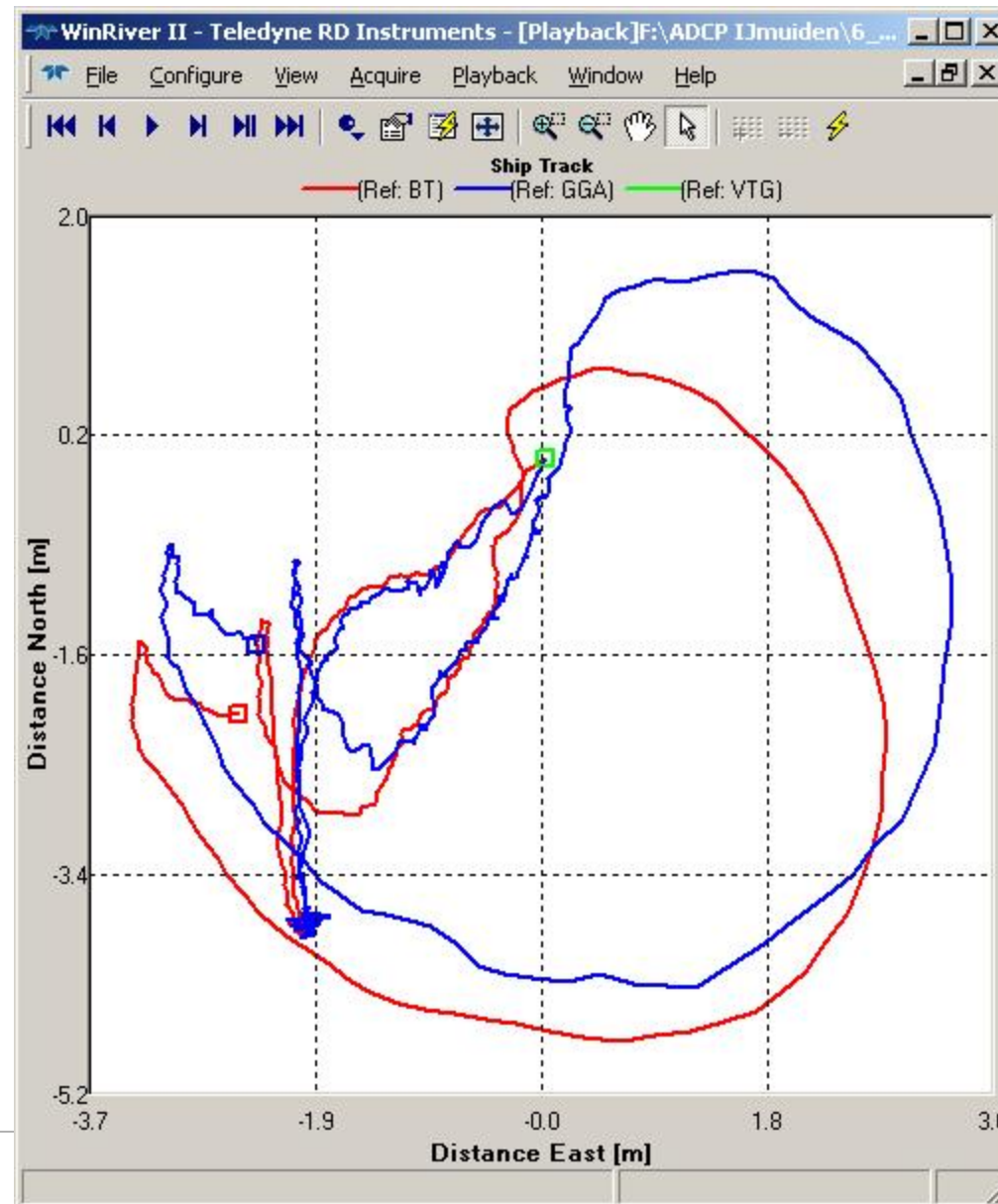
ensemble 3787



Vessel 6b – ADCP

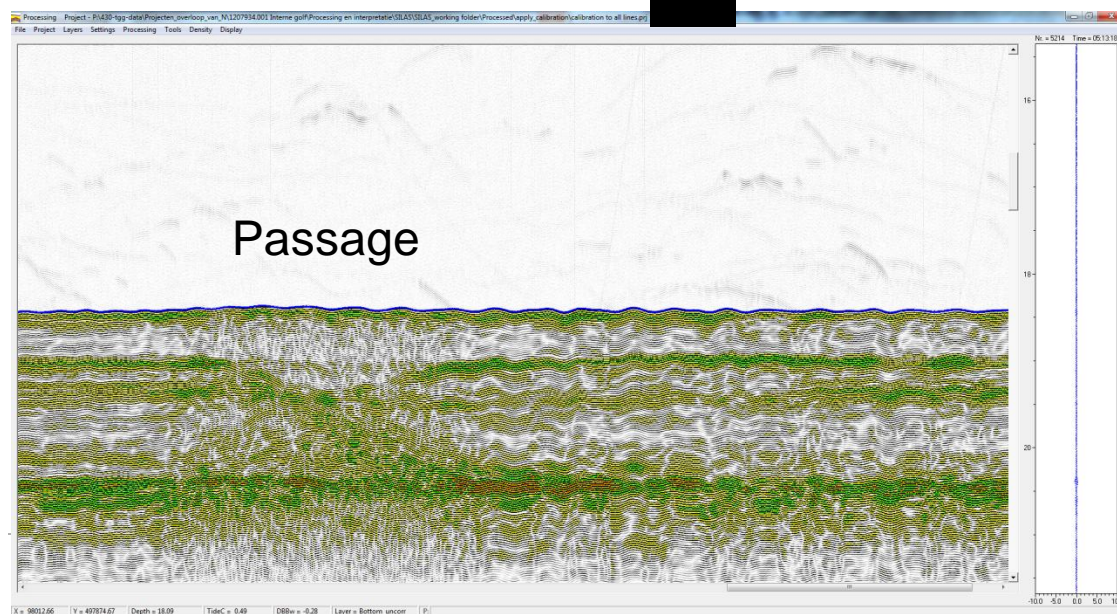
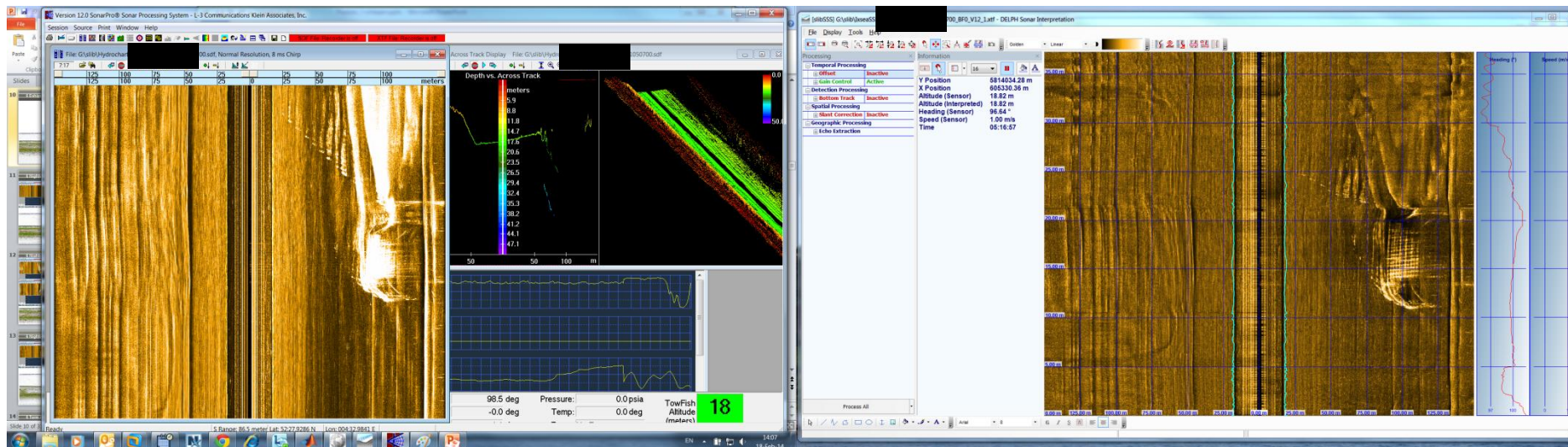
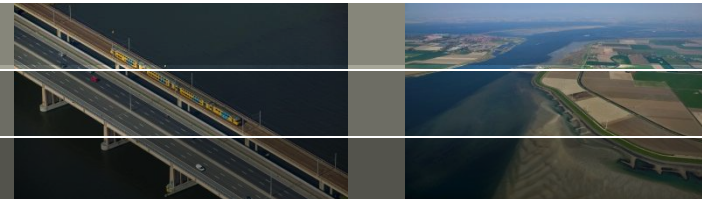


ensembles 3400 - 3787



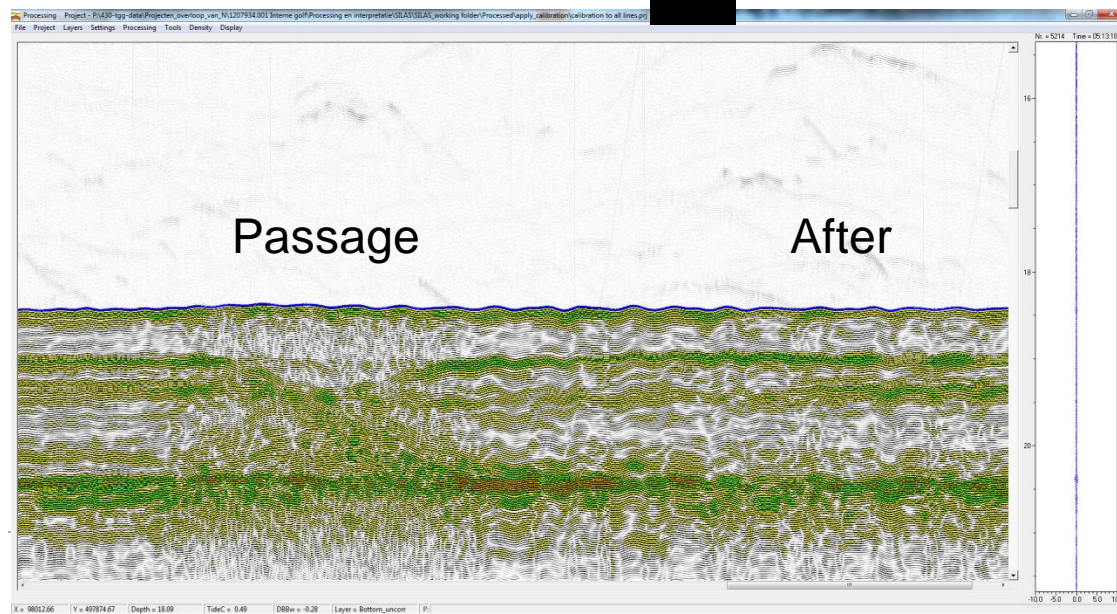
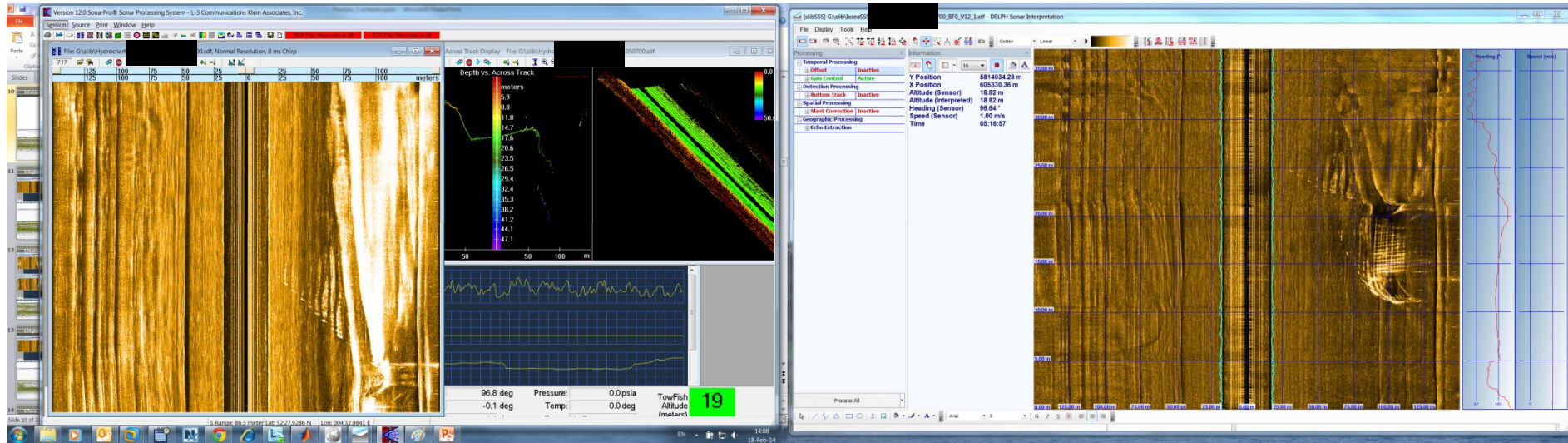
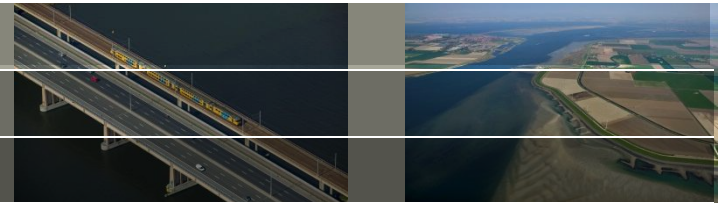
Deltares

Vessel 6a - passage



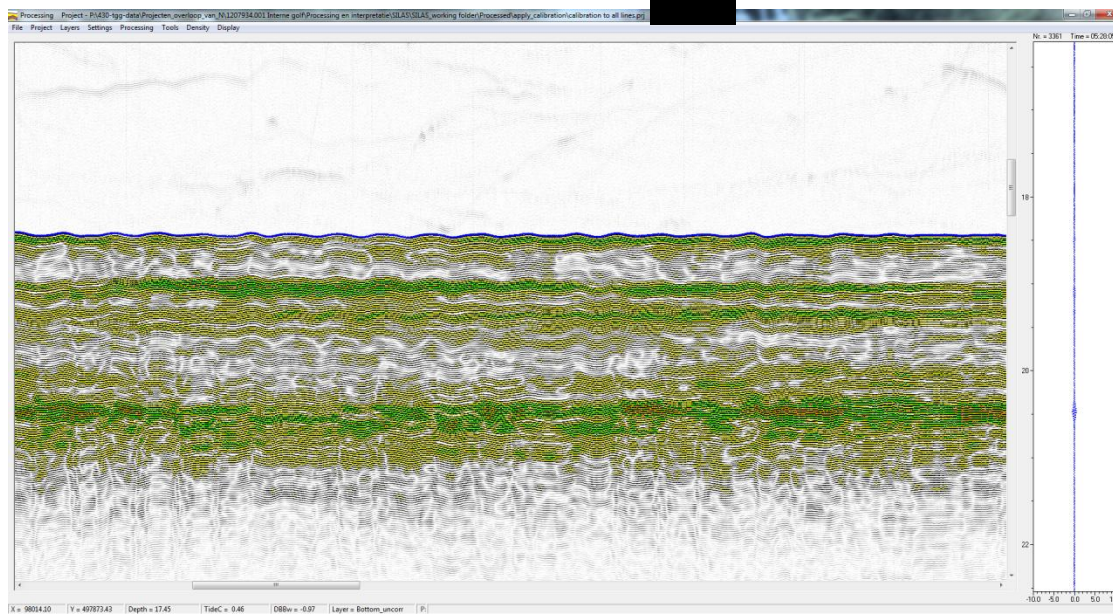
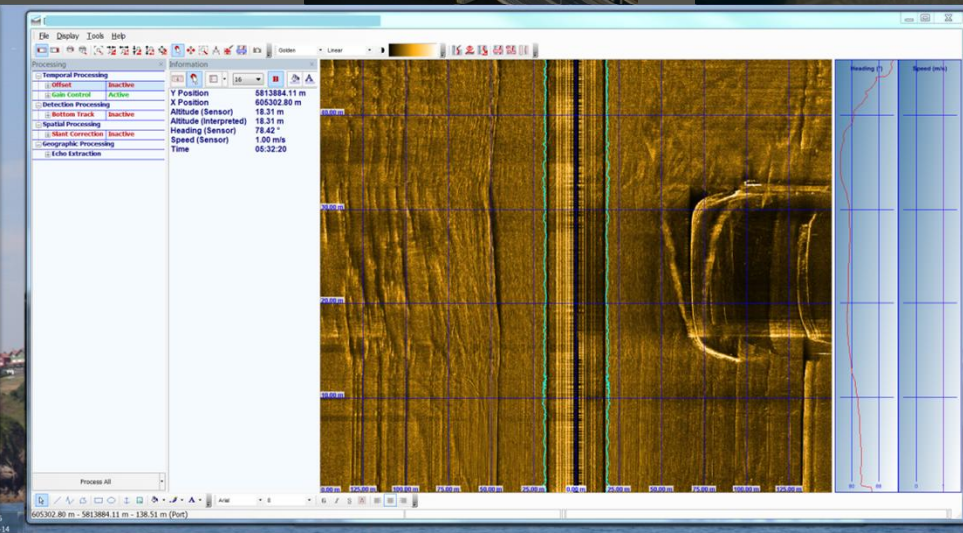
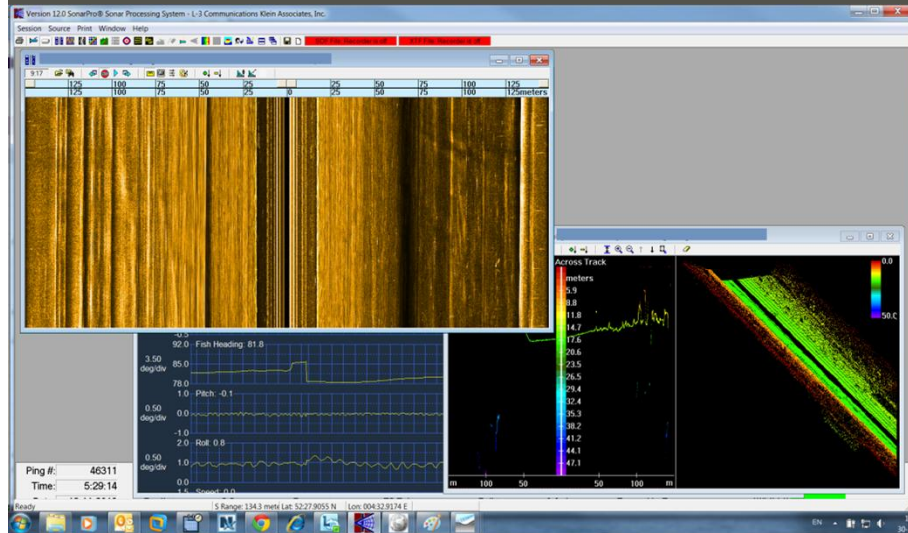
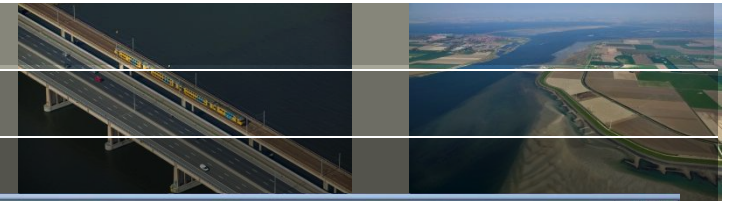
Deltares

Vessel 6a - after



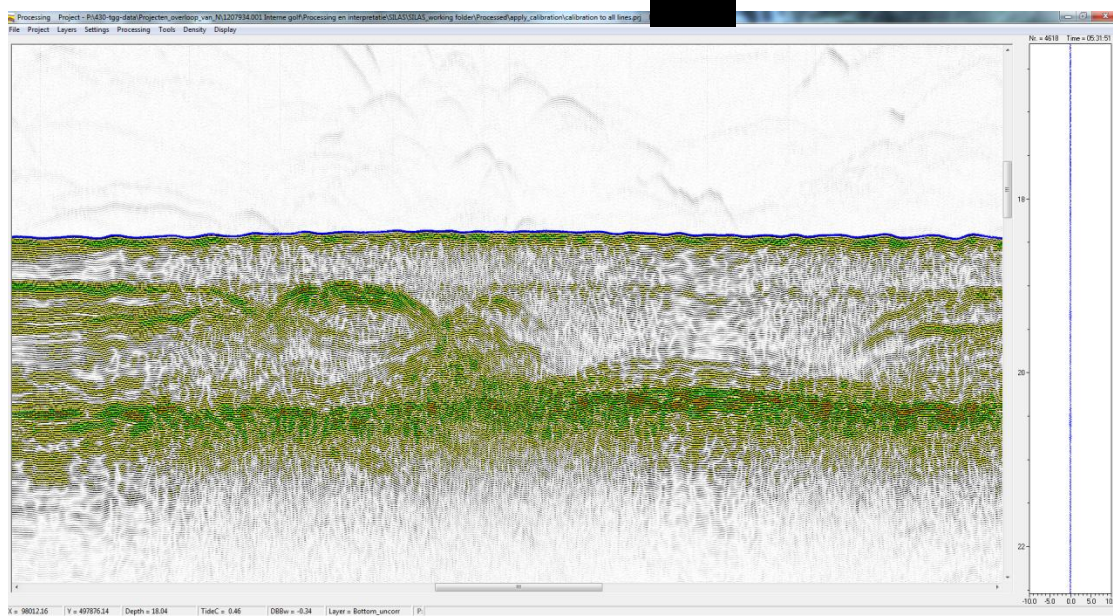
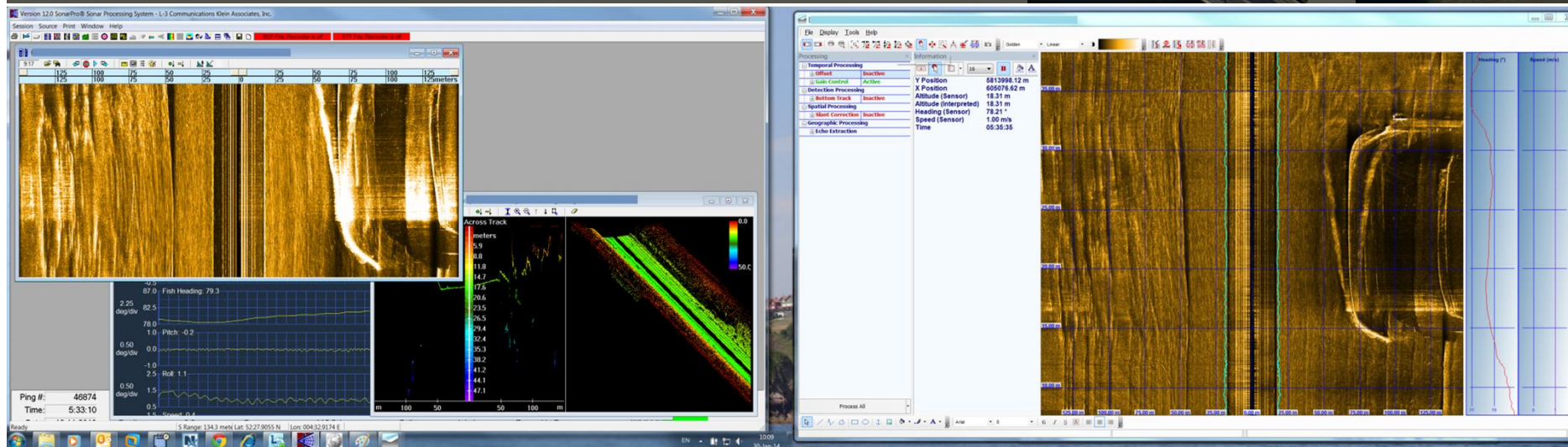
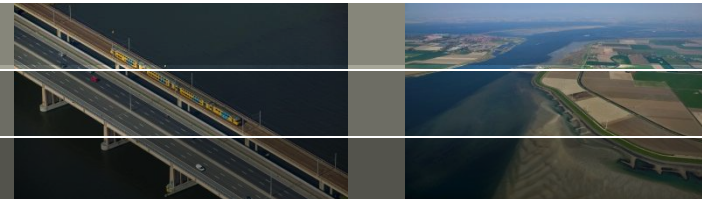
Deltares

Vessel 6 – before



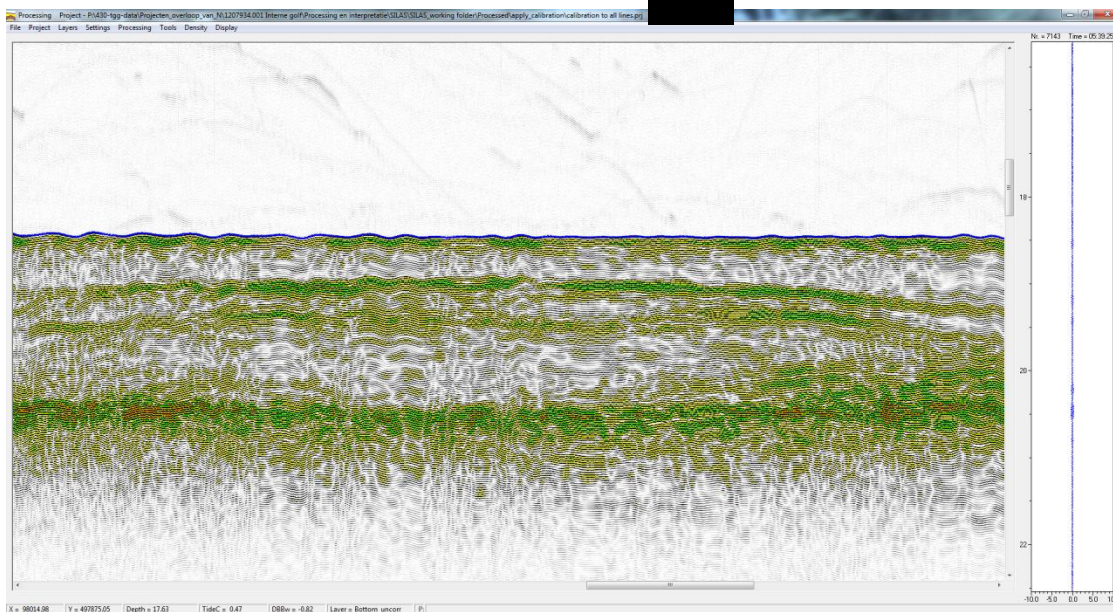
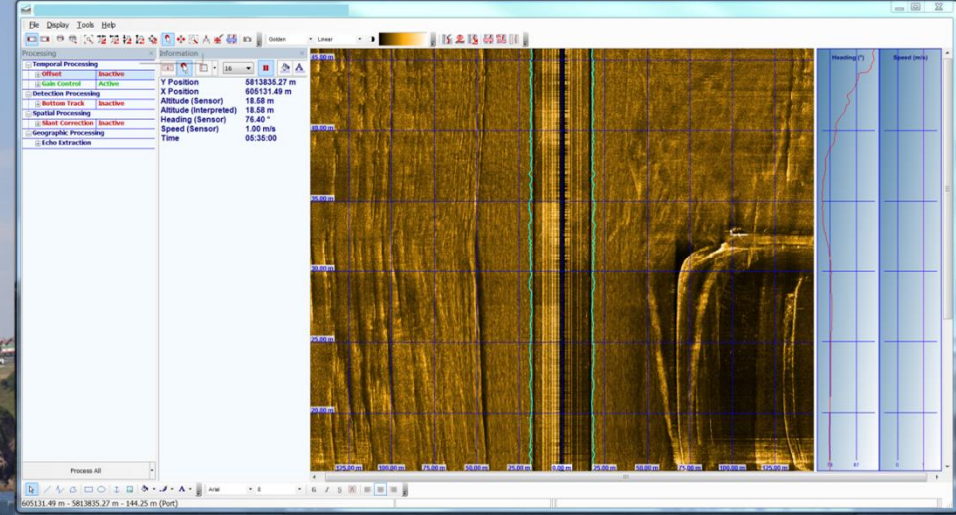
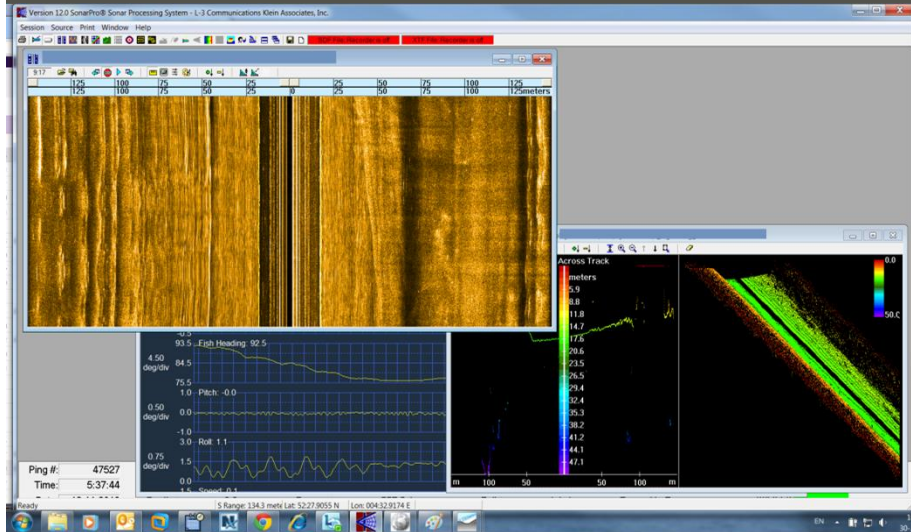
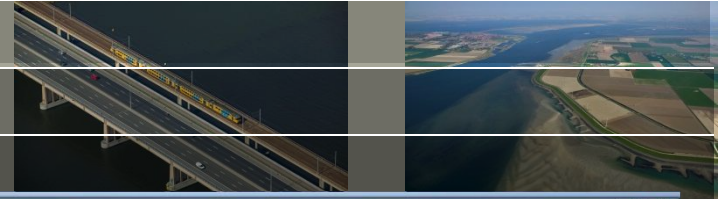
Deltares

Vessel 6 – passage



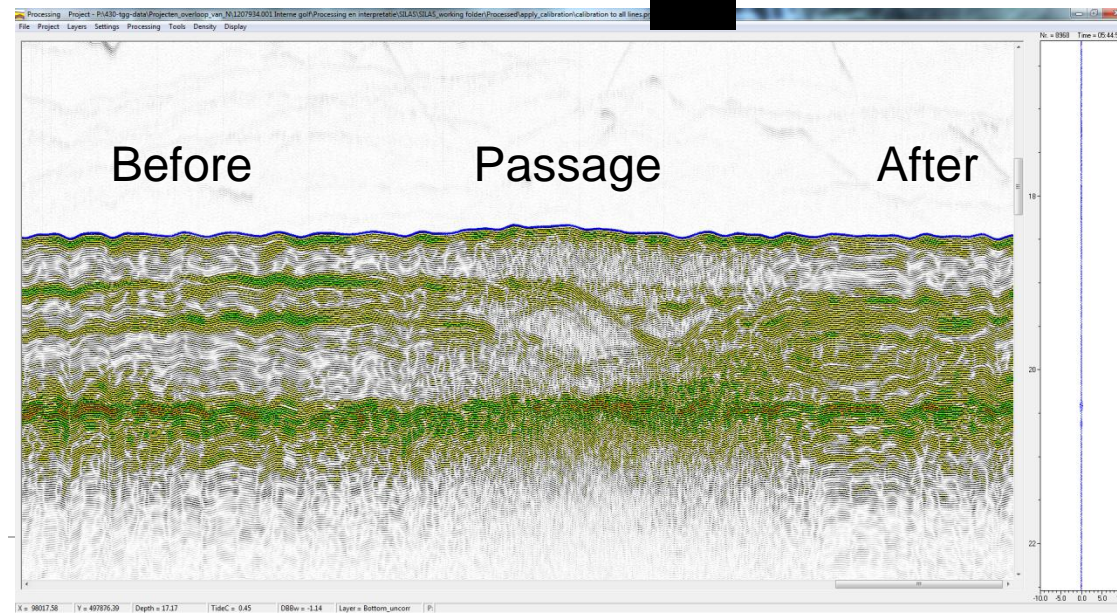
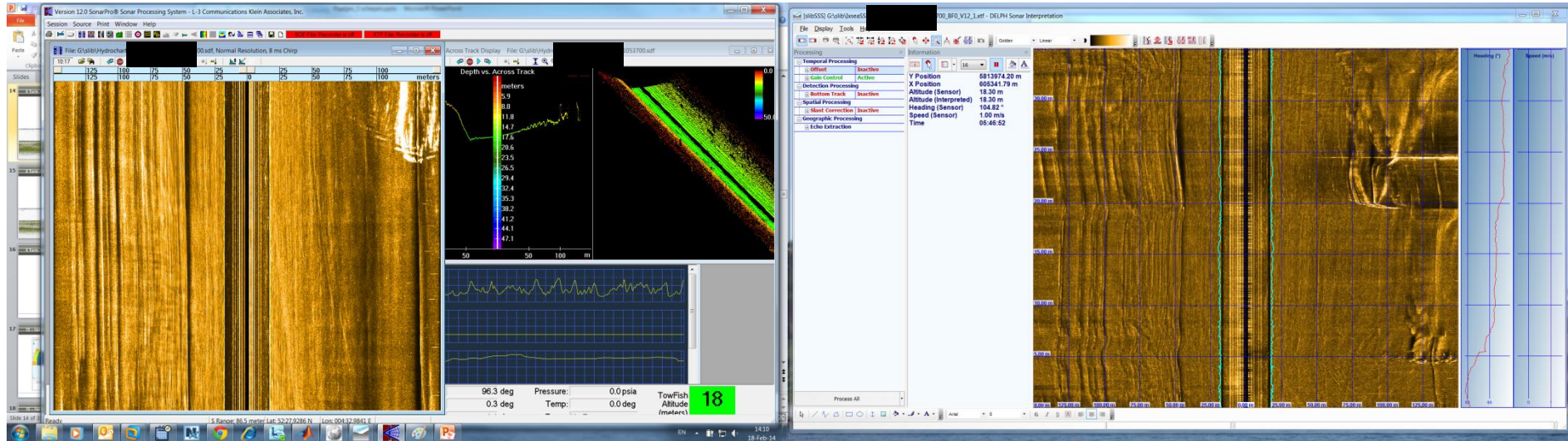
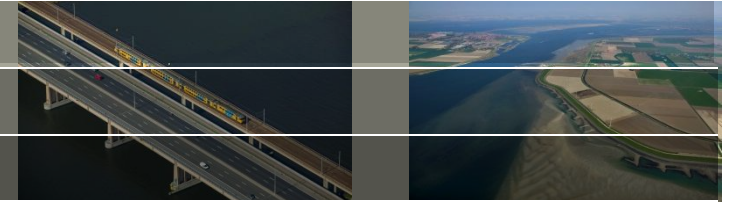
Deltares

Vessel 6 – after



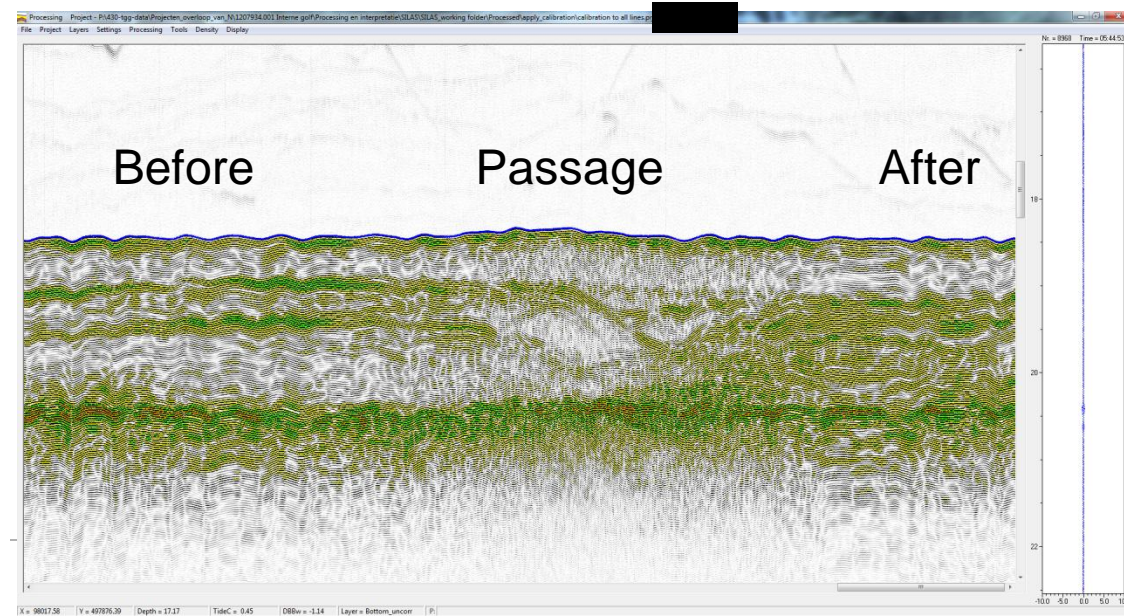
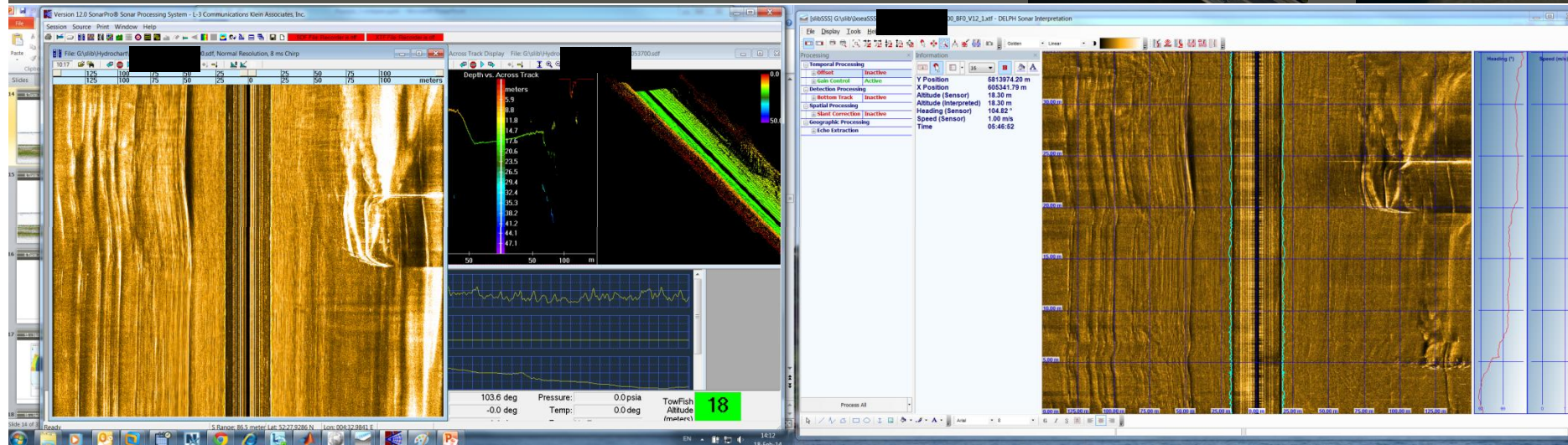
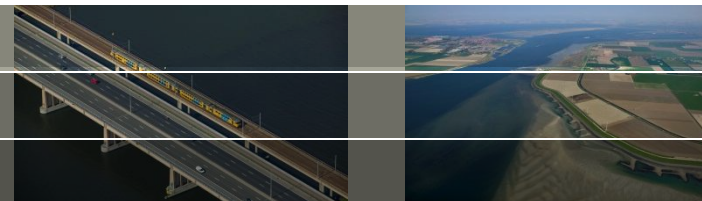
Deltares

Vessel 6b – before



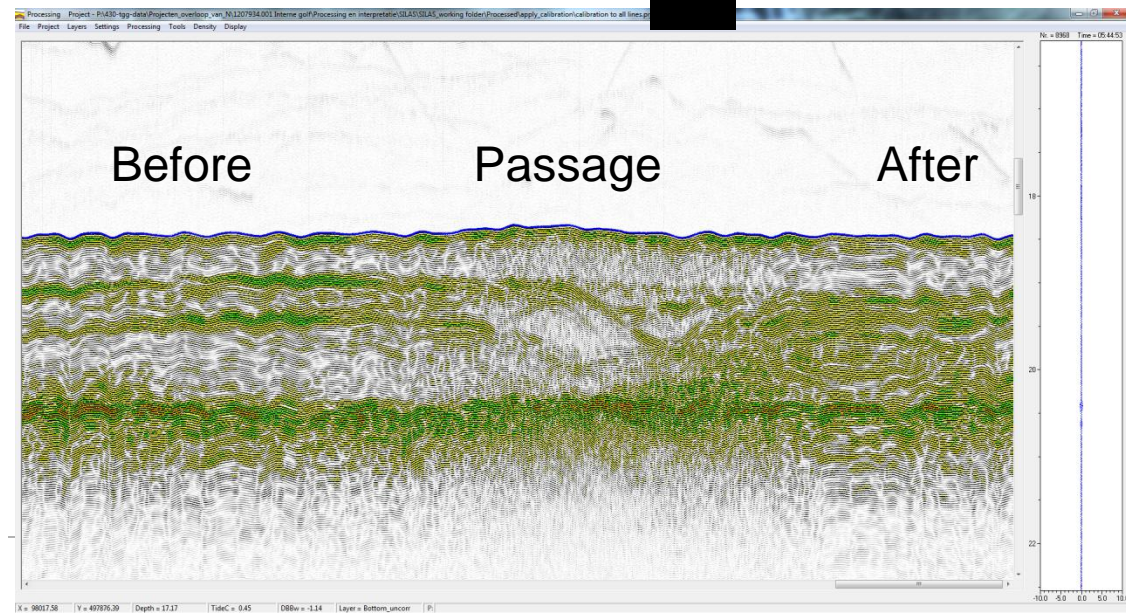
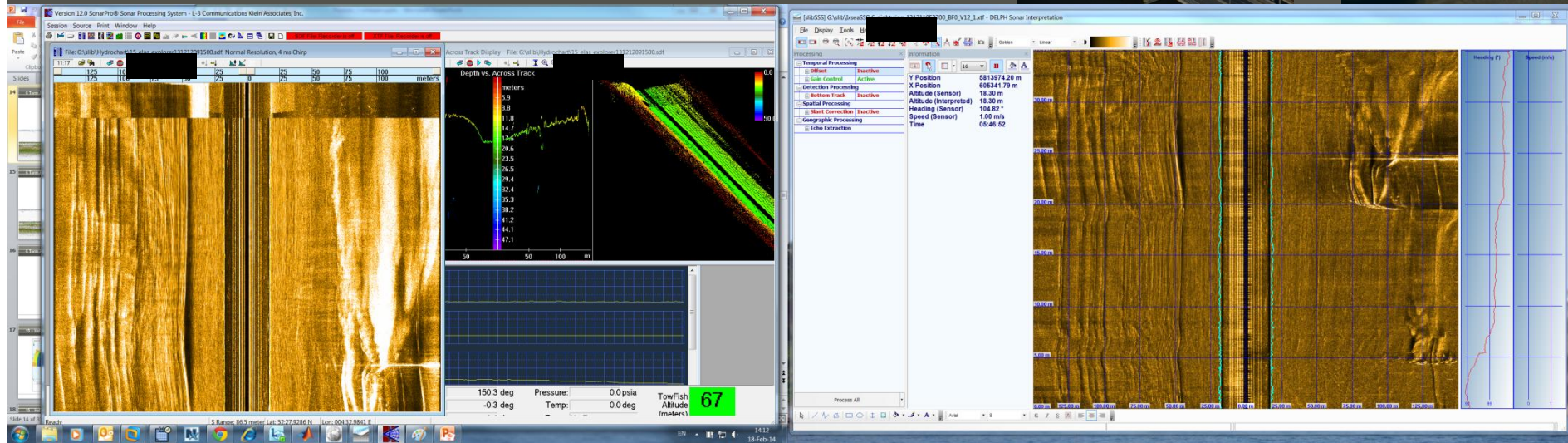
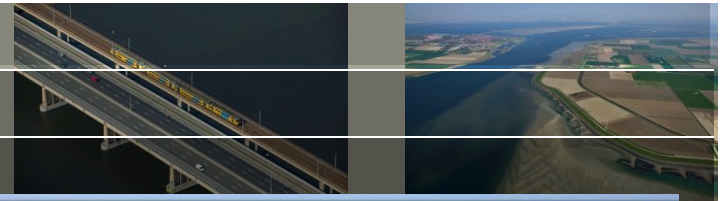
Deltares

Vessel 6b – passage



Deltares

Vessel 6b – after

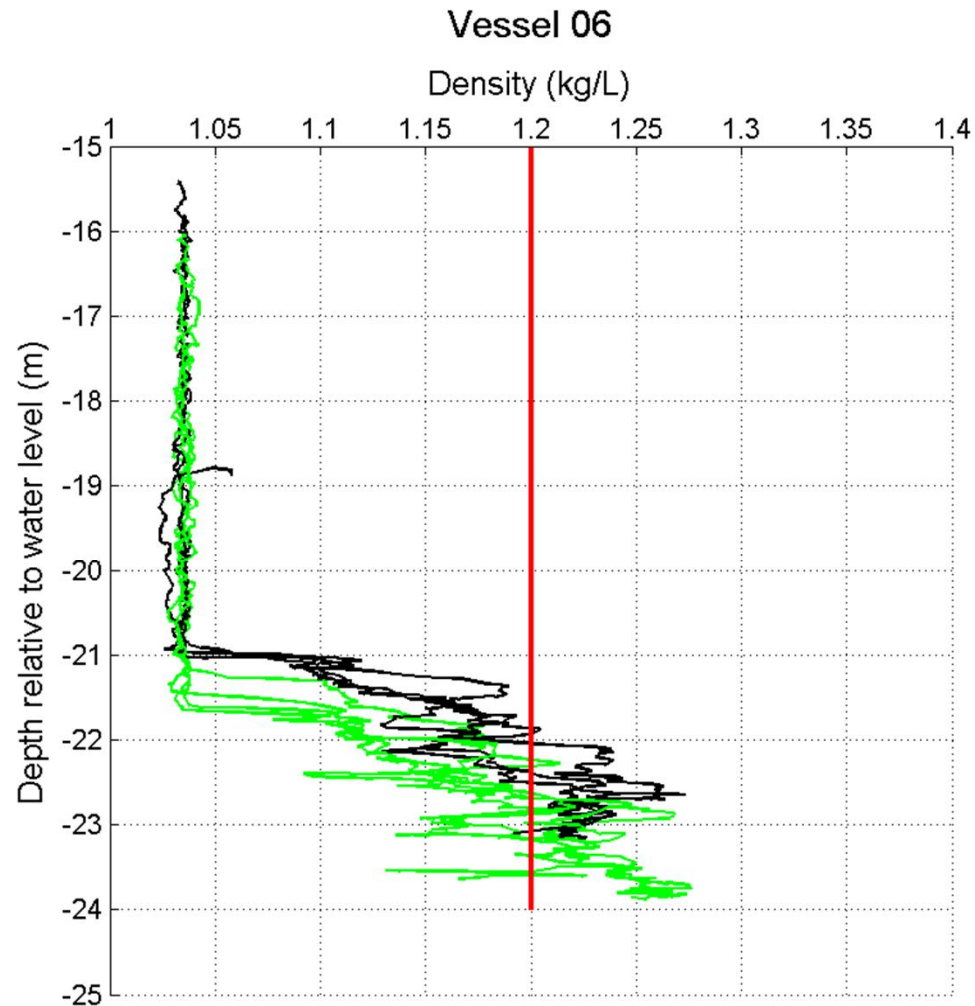


Deltares

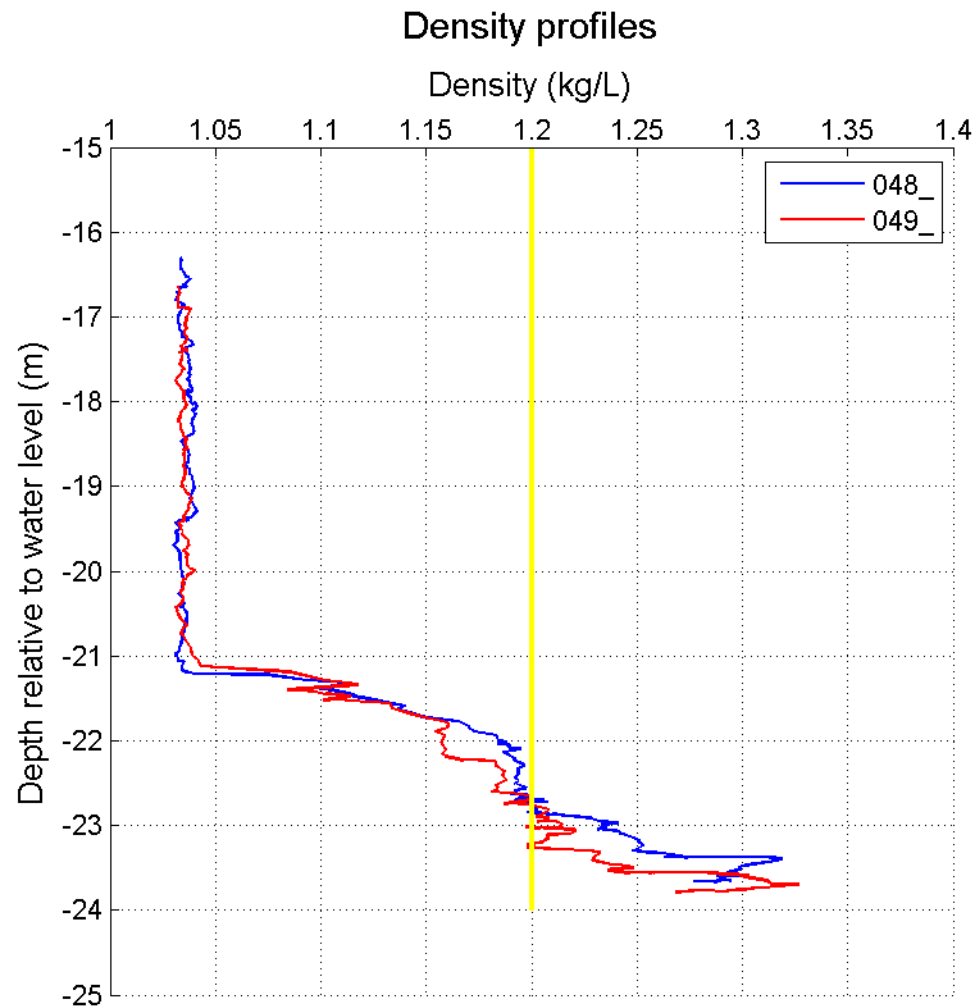
Vessel 6 – density profiles line of passage



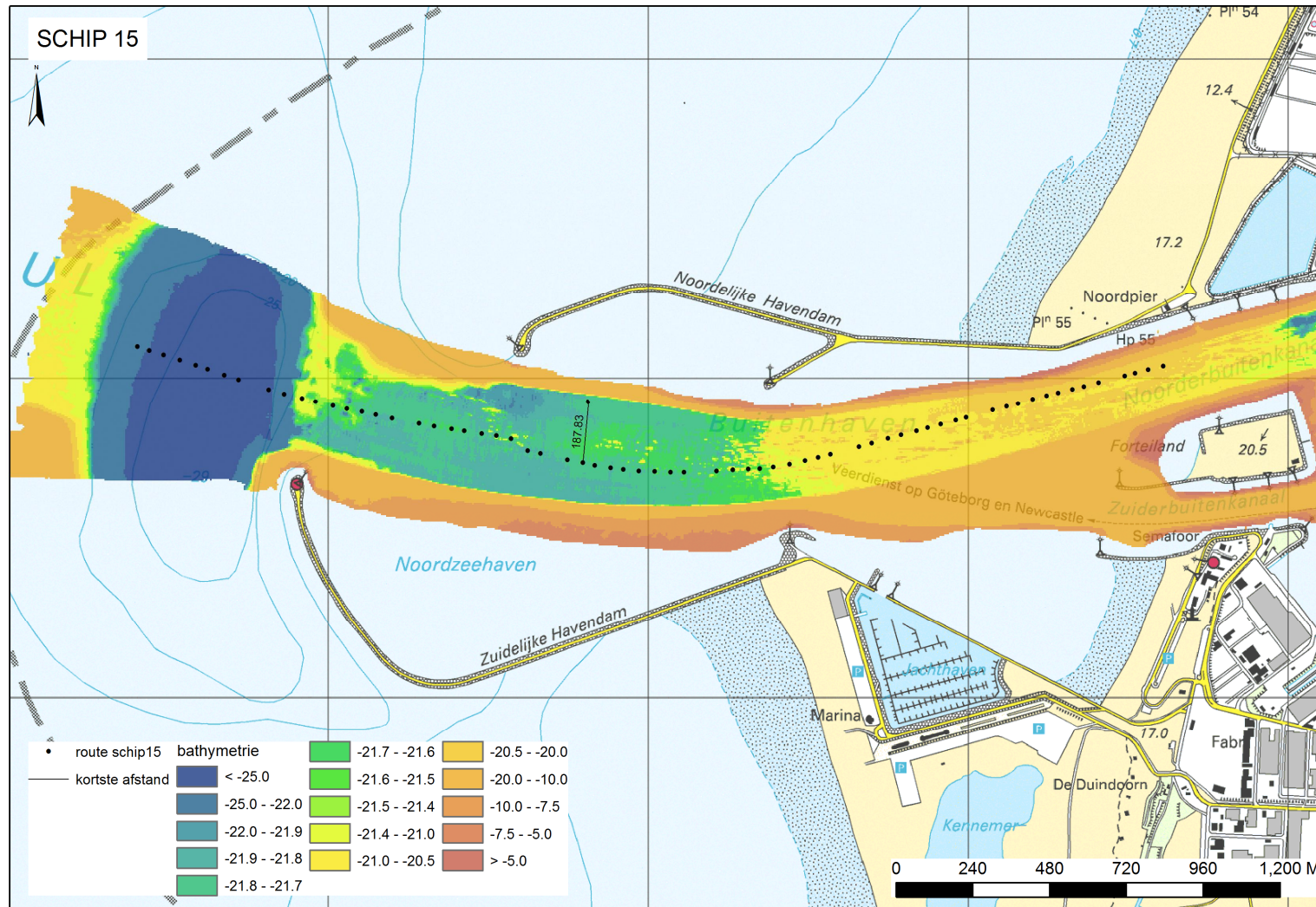
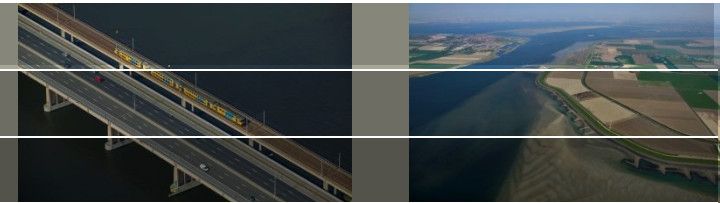
Green: before 6a
Black: after 6b
Corrected for tide
difference



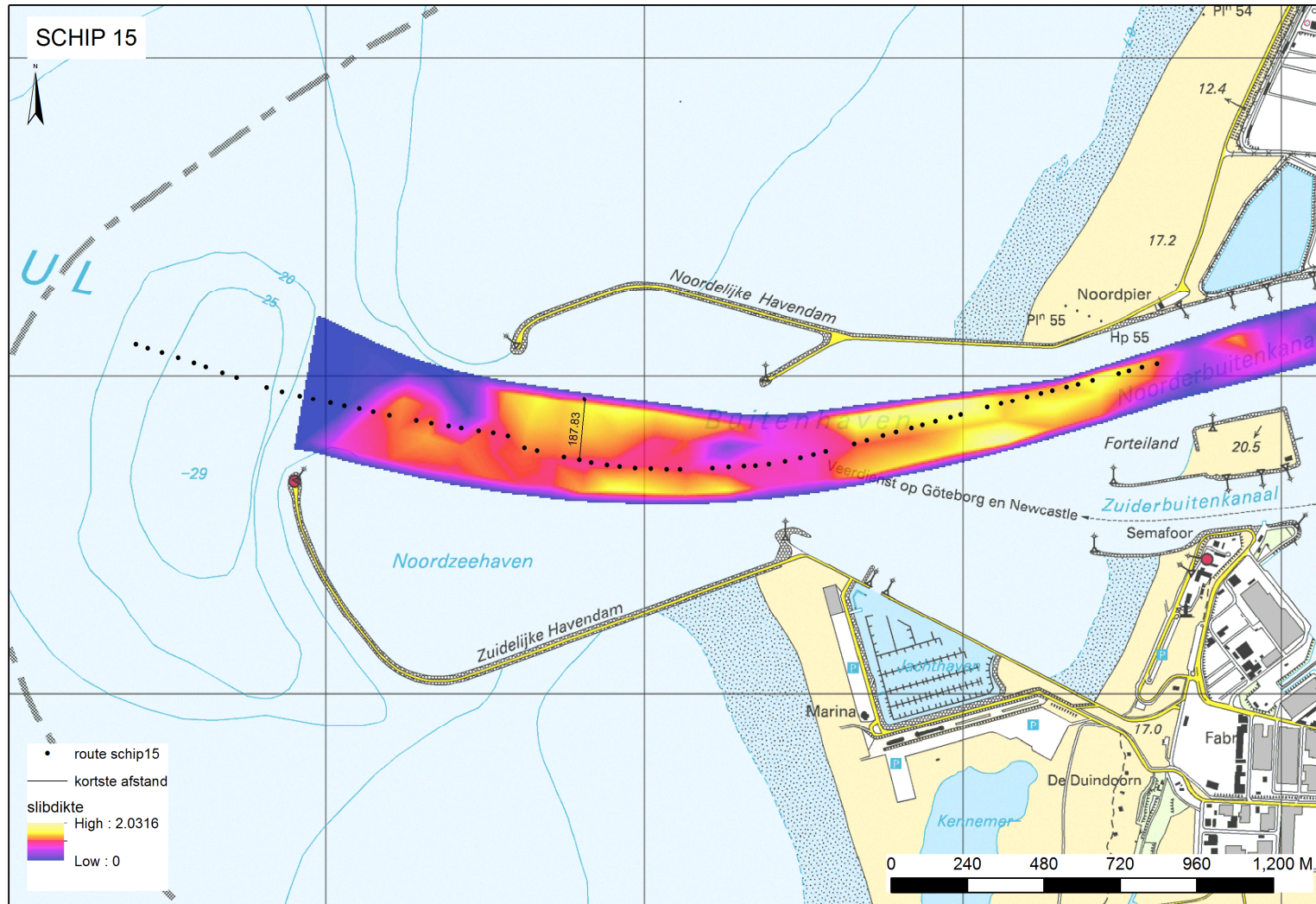
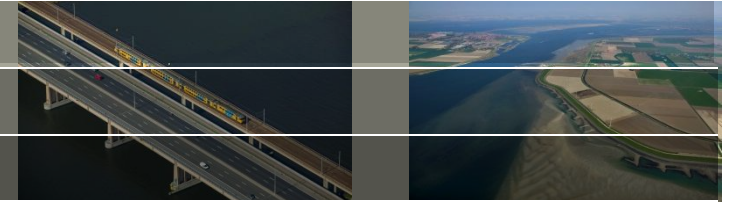
Vessel 6 – density profiles near Zirfaea



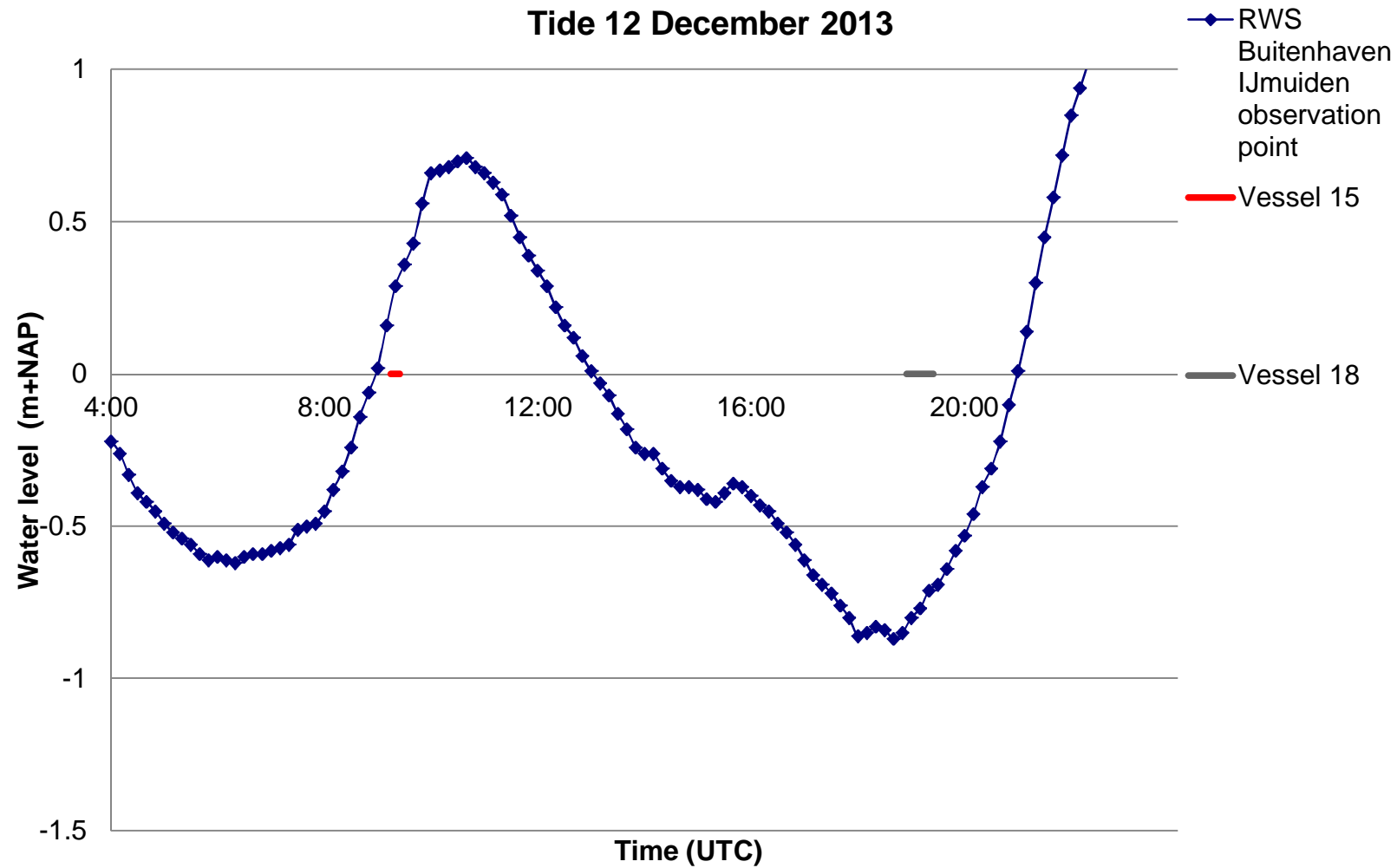
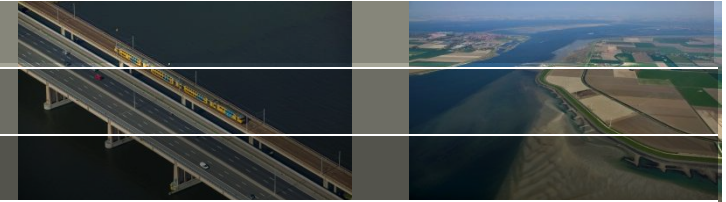
Vessel 15



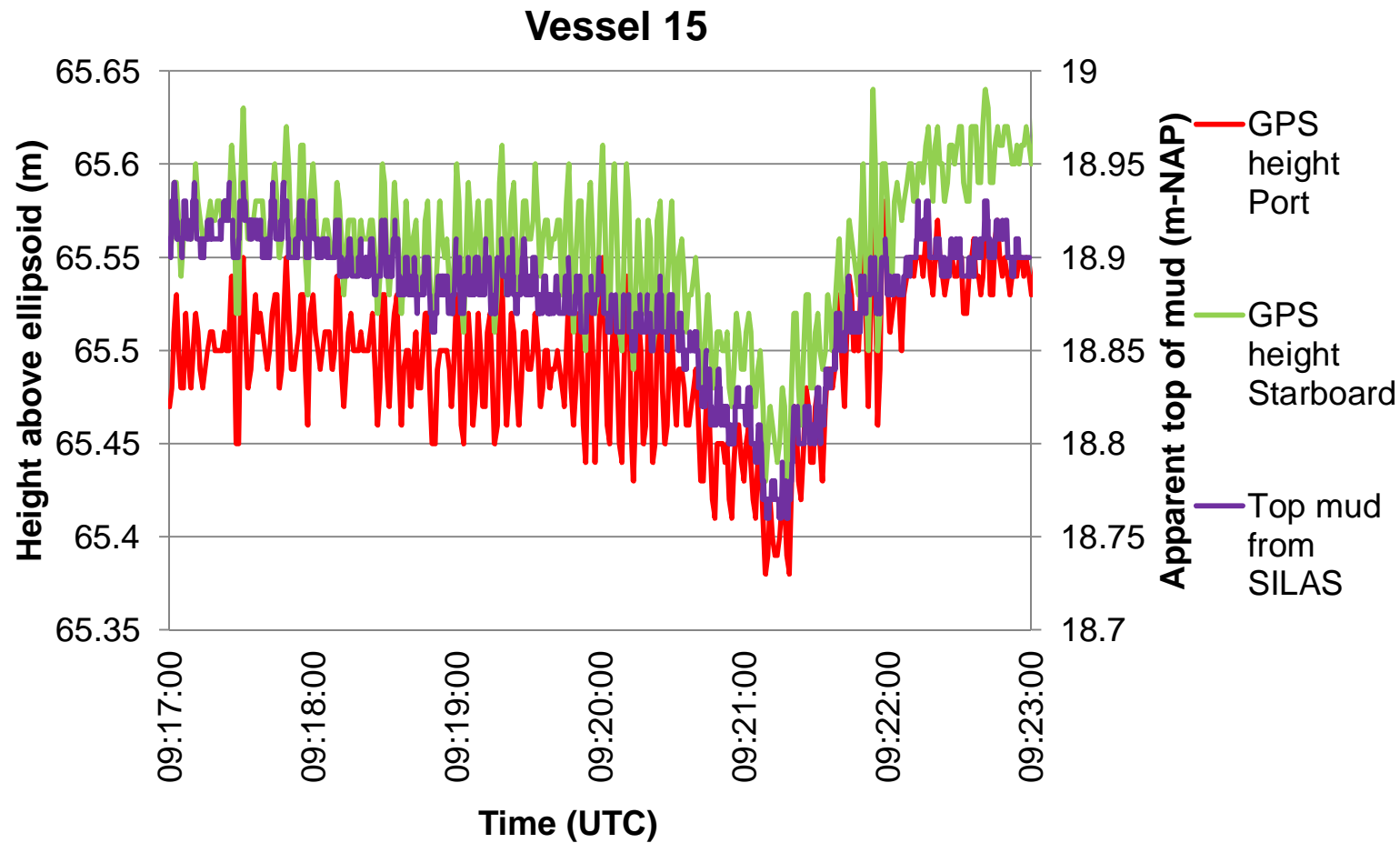
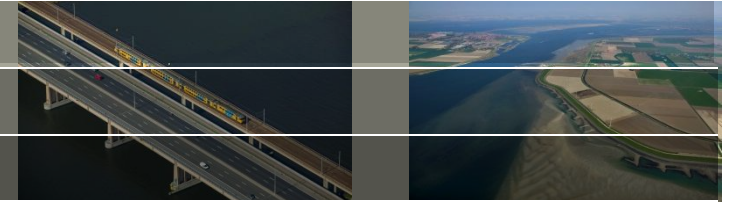
Vessel 15



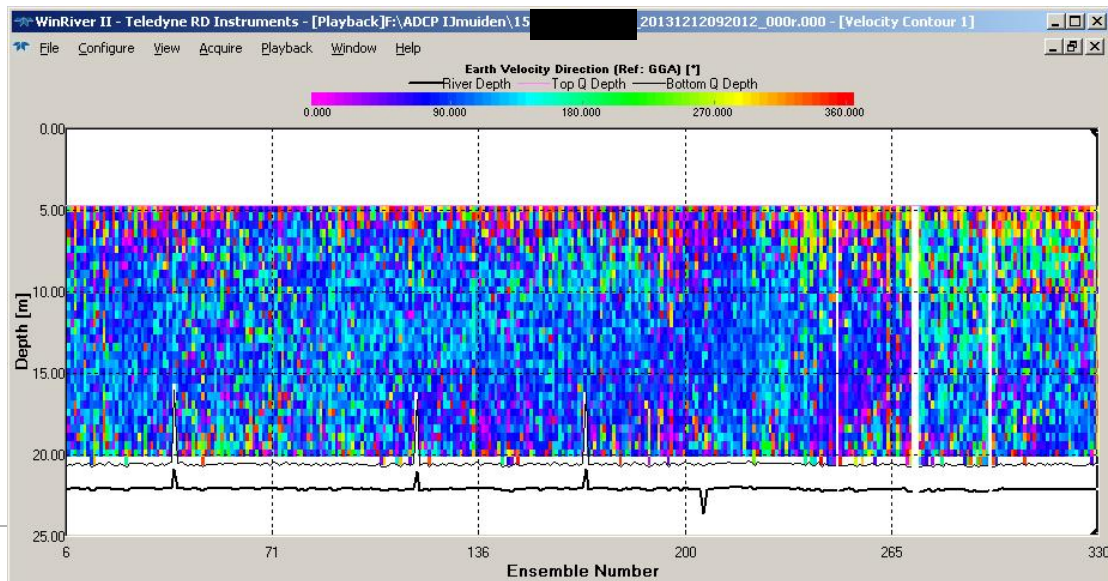
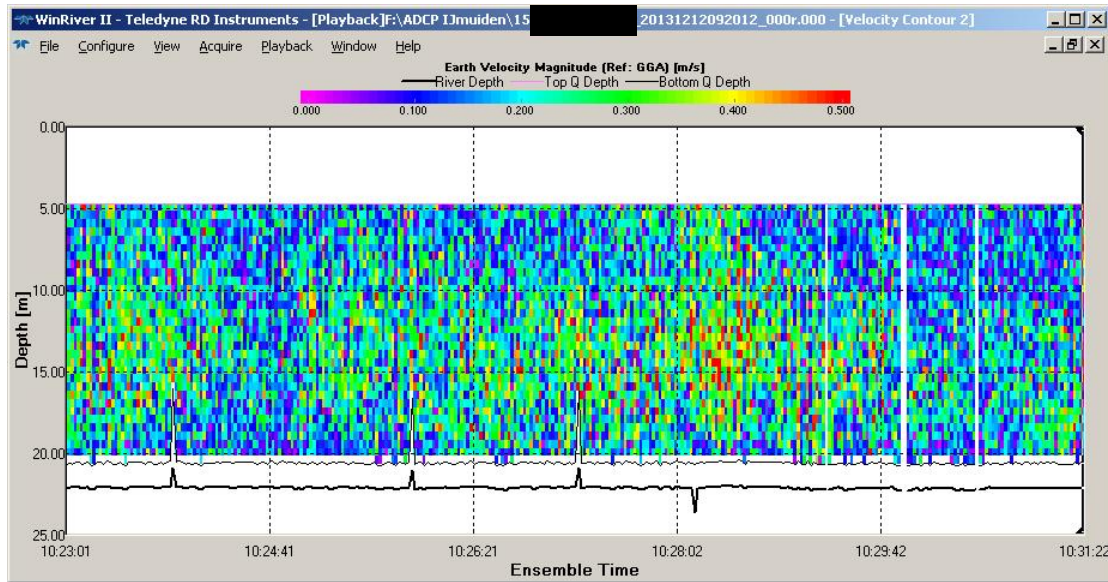
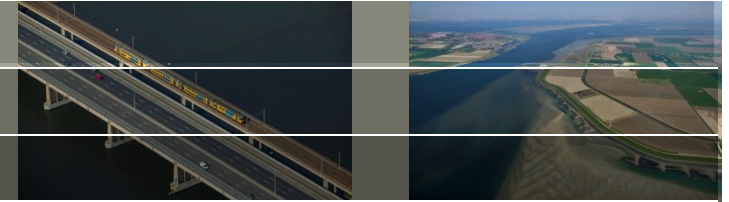
Vessel 15 - Tide



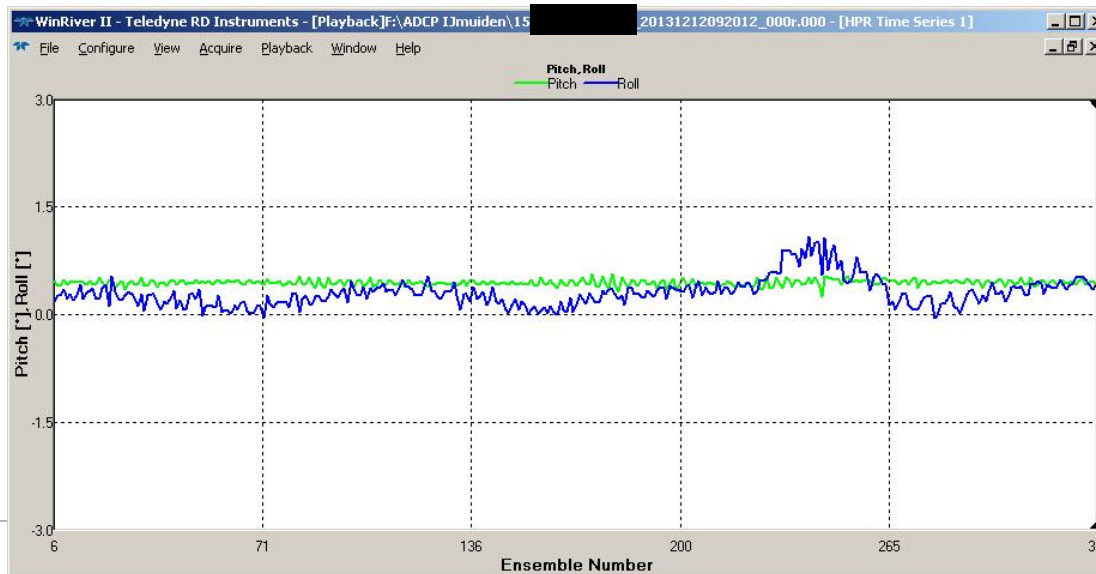
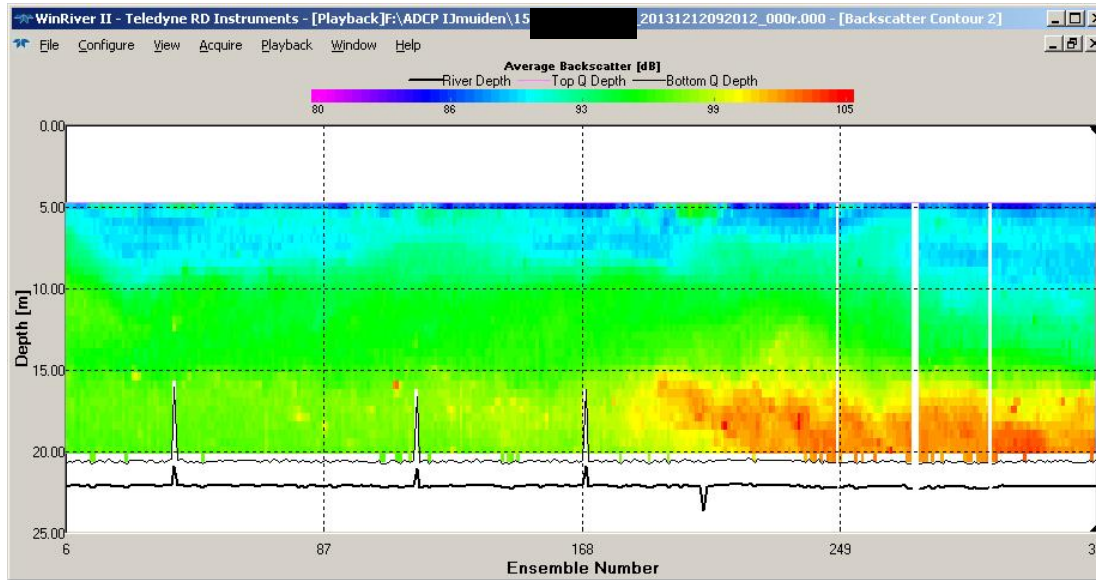
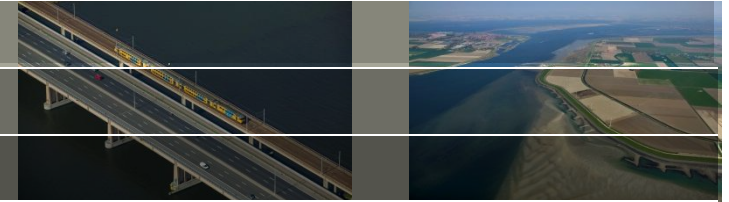
Vessel 15 – GPS Heights



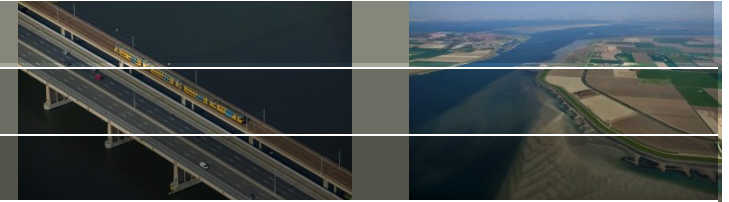
Vessel 15 – ADCP



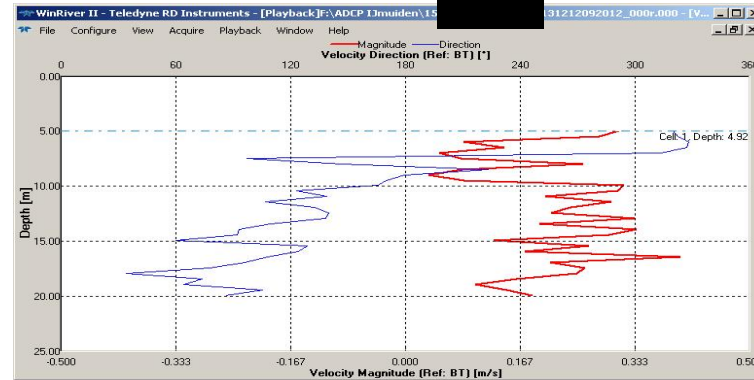
Vessel 15 – ADCP



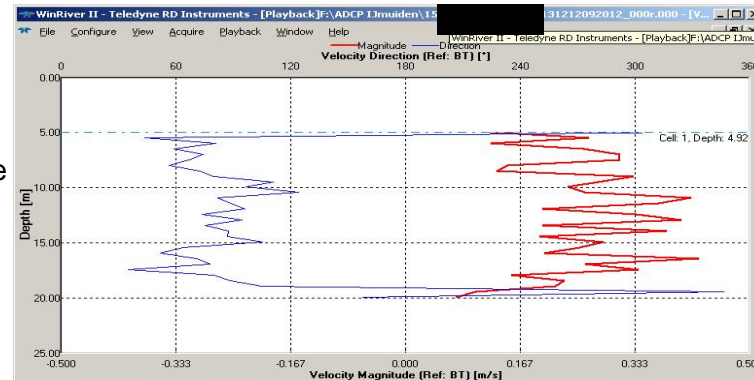
Vessel 15 – ADCP



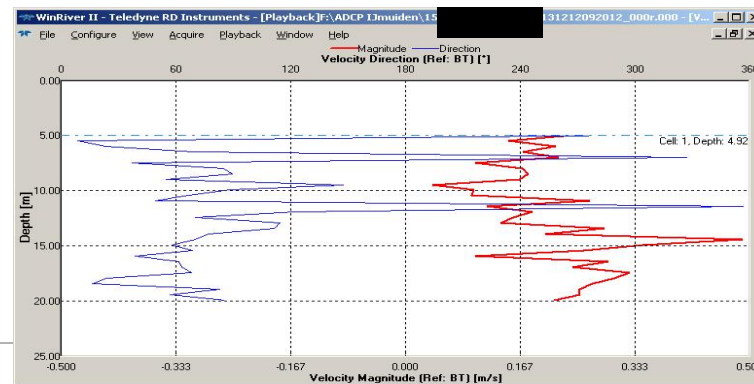
ensemble 170



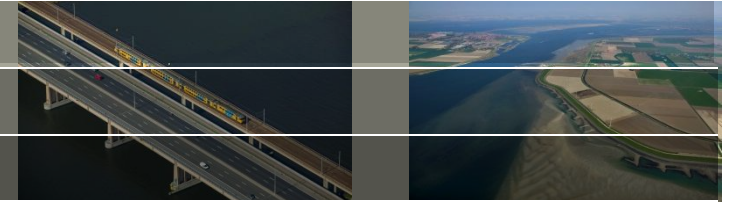
ensemble xxx, during passage



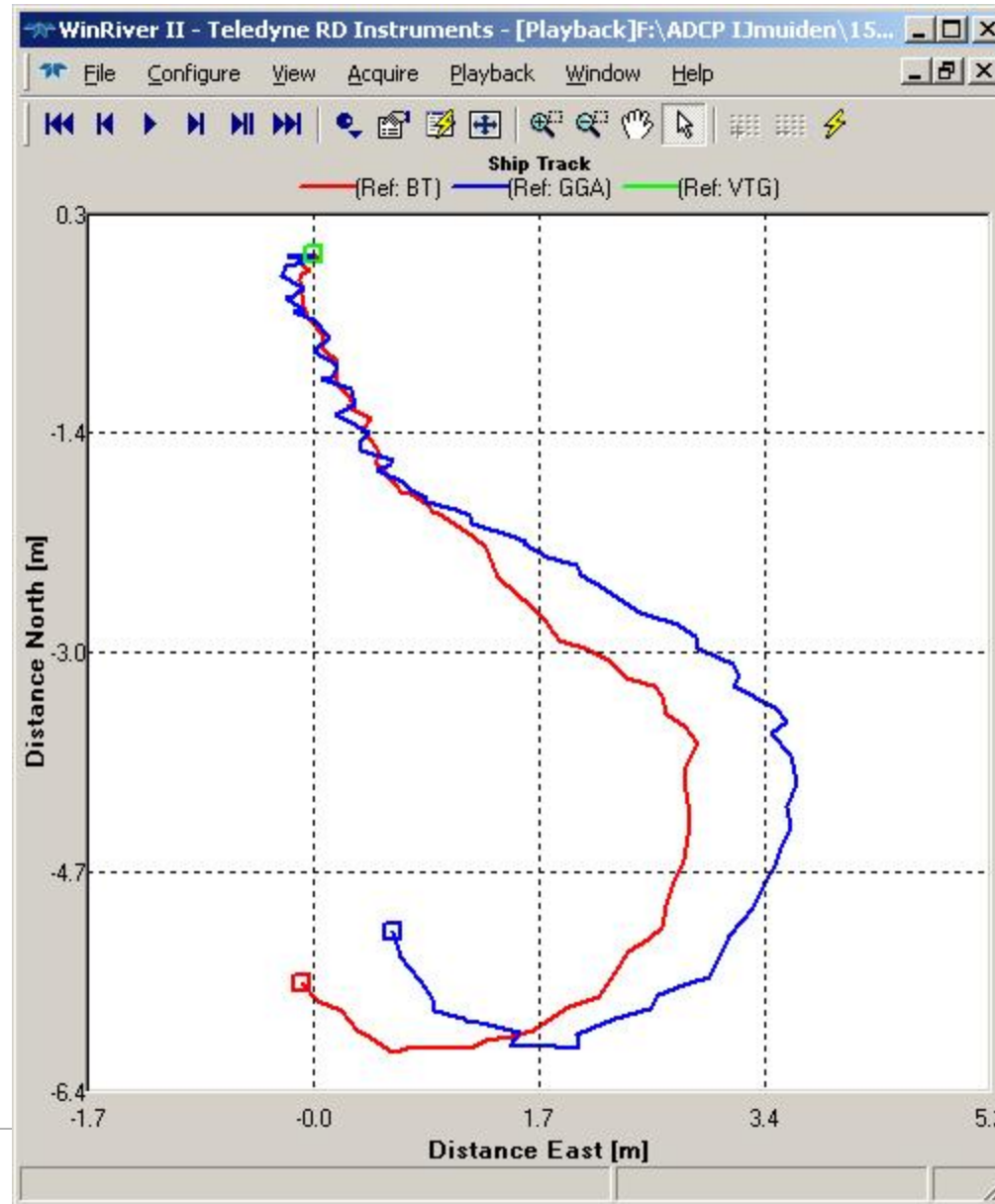
ensemble 250



Vessel 15 – ADCP

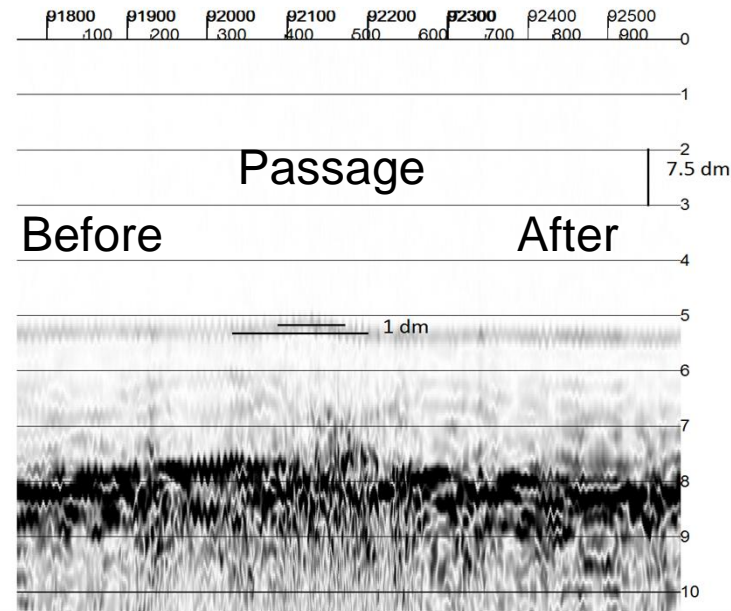
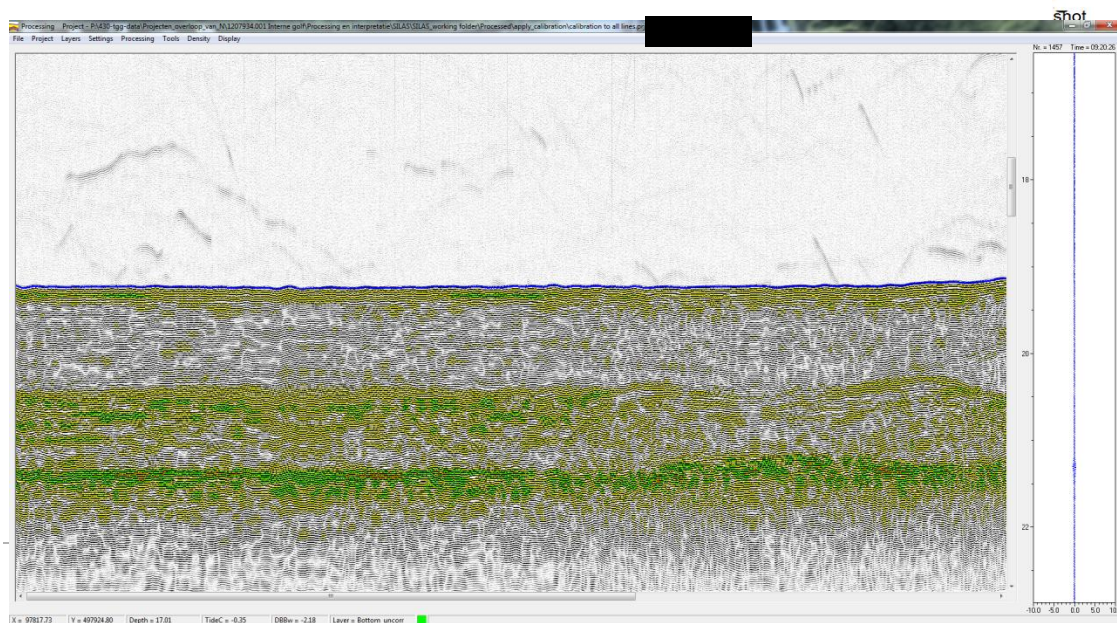
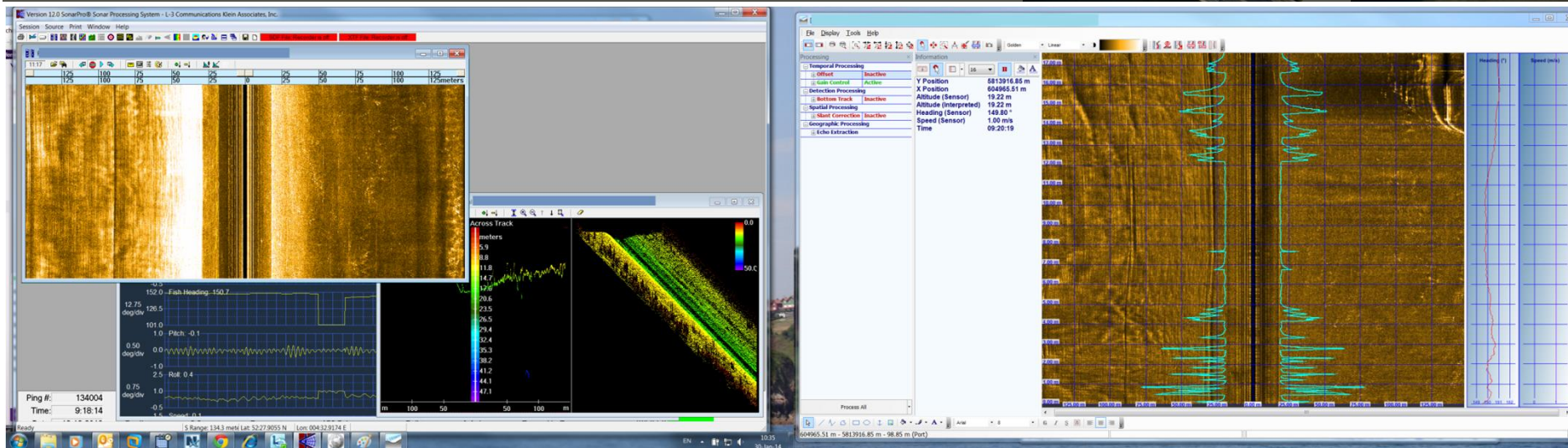
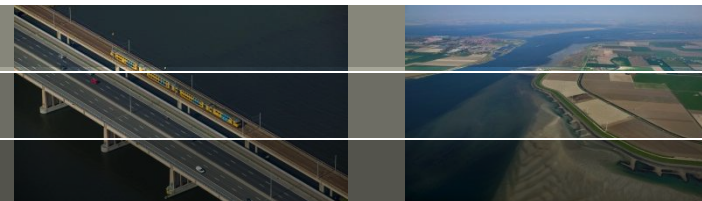


ensembles 170 - 250

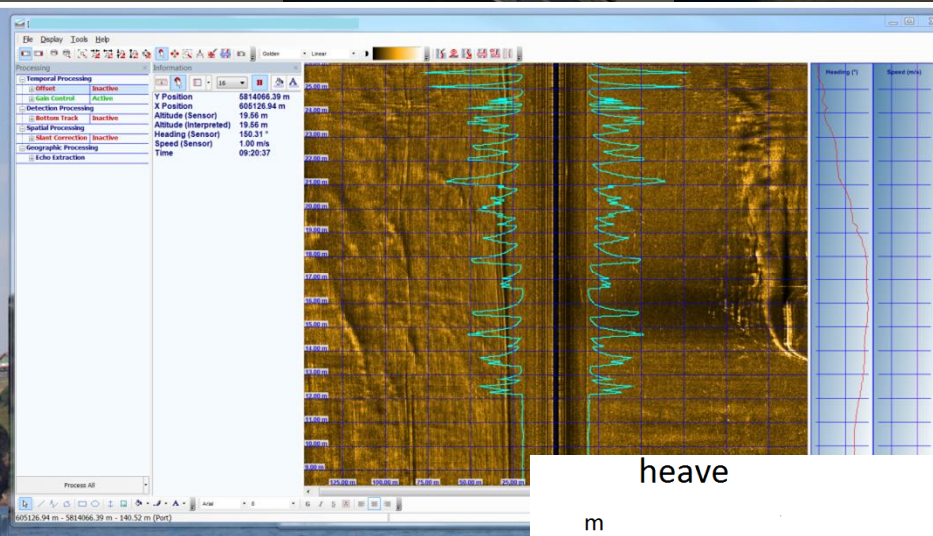
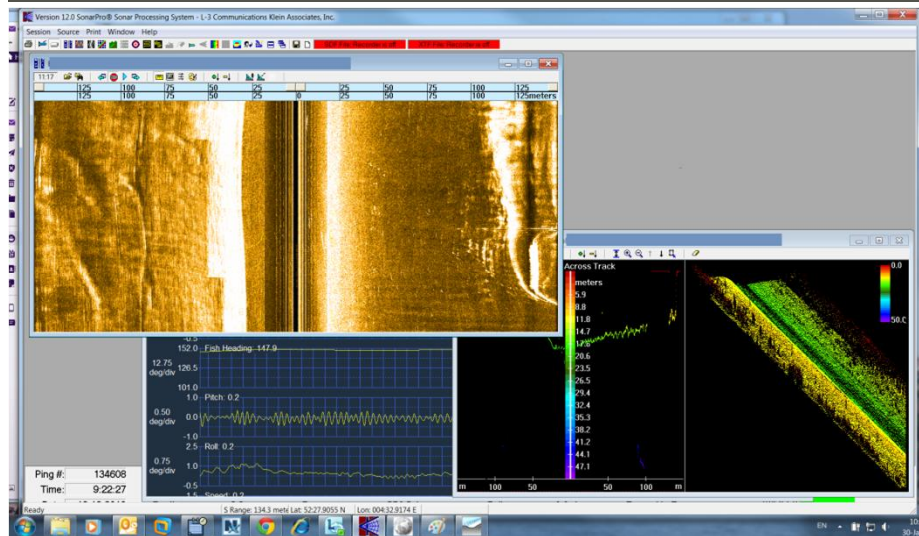
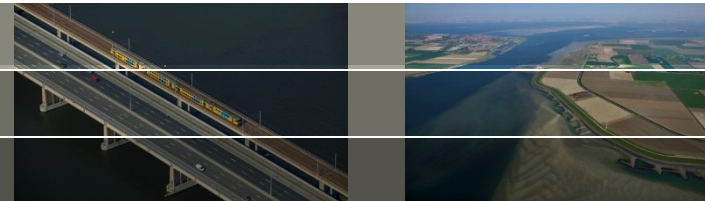


Deltares

Vessel 15 - before

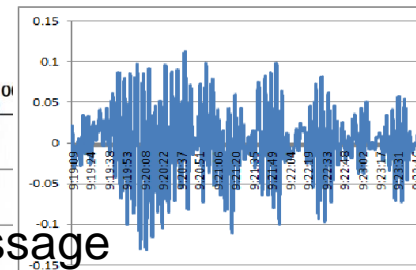


Vessel 15 - passage

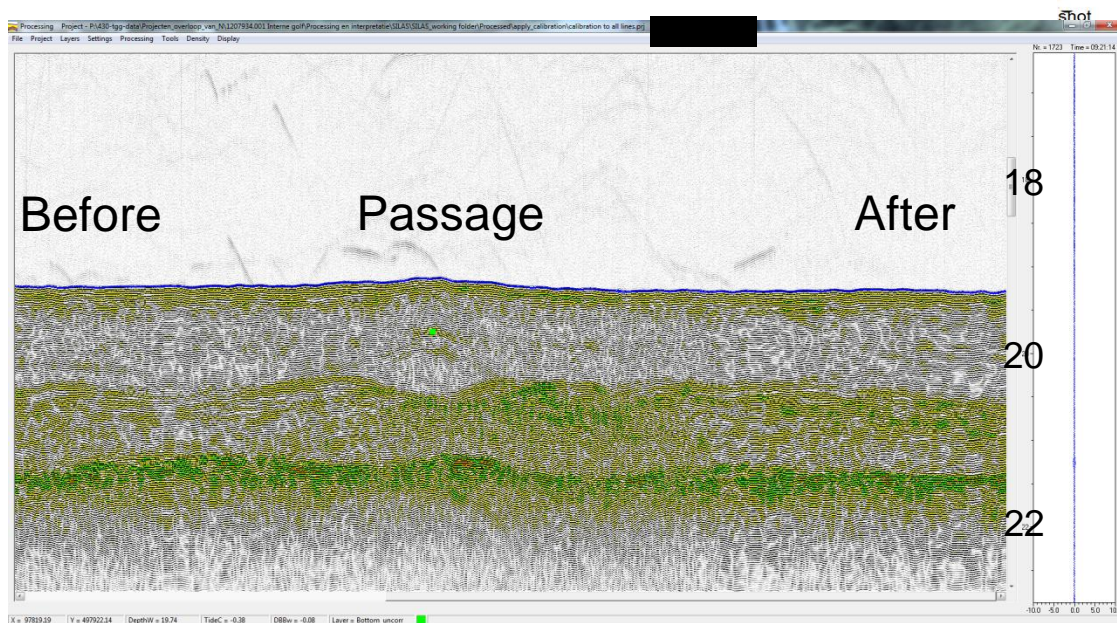


heave

m



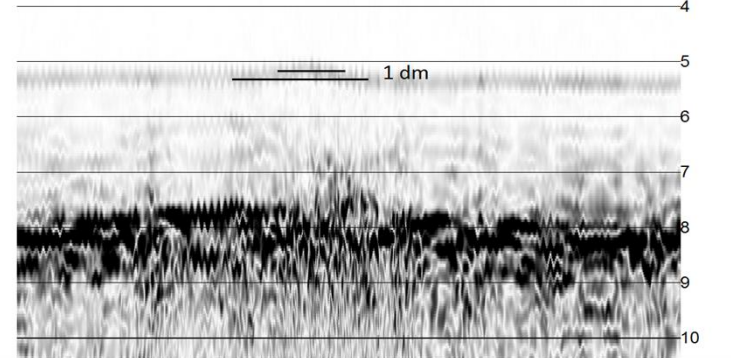
Passage



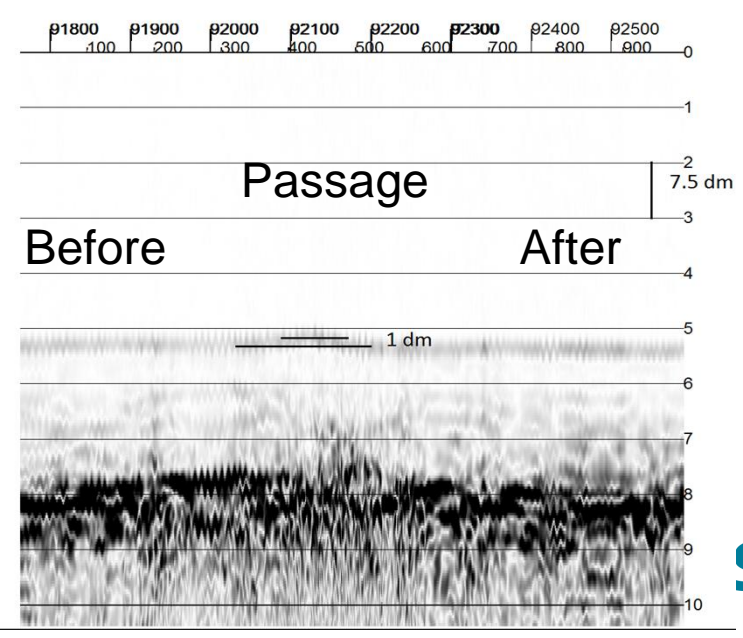
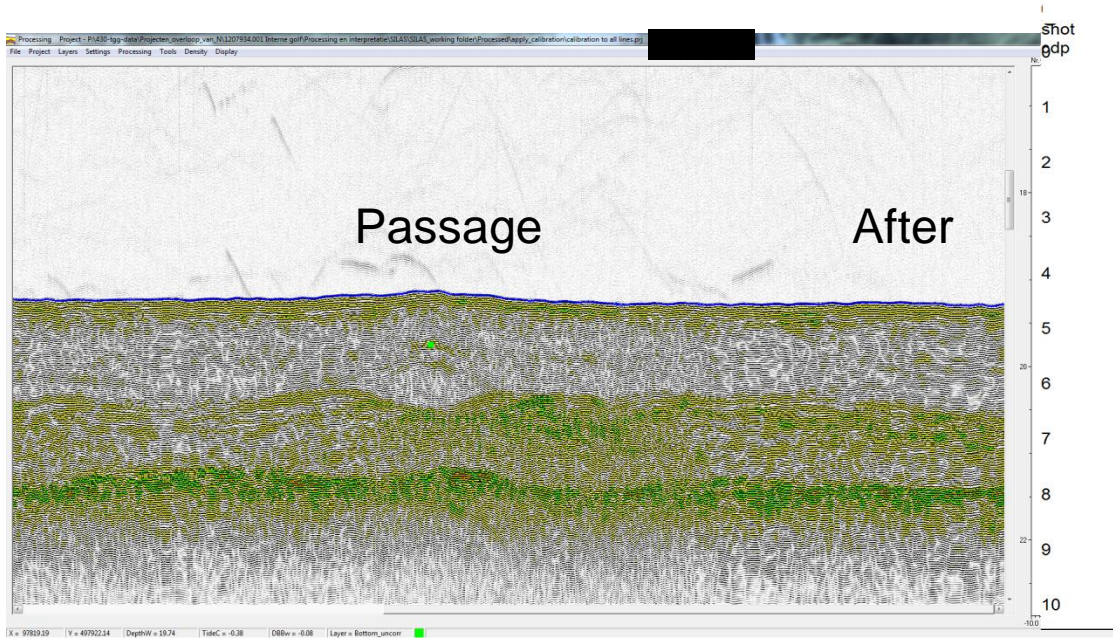
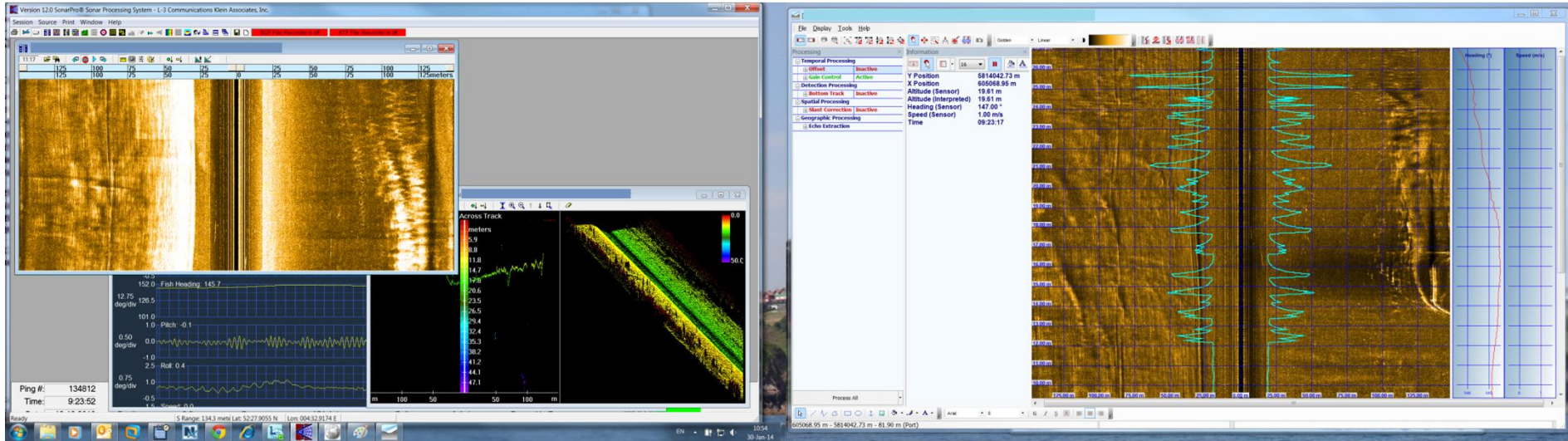
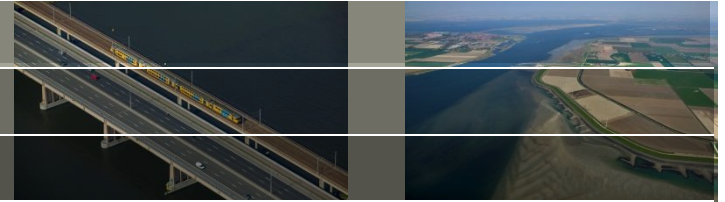
Before

After

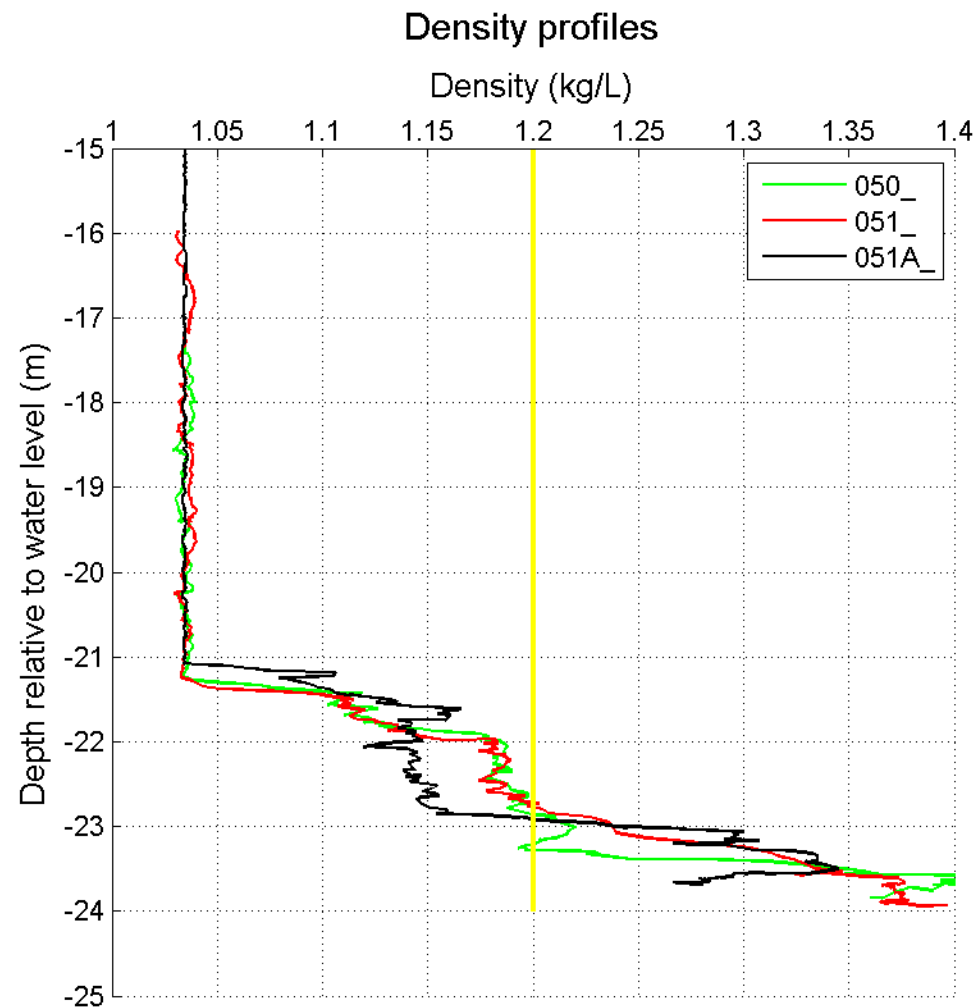
1 dm



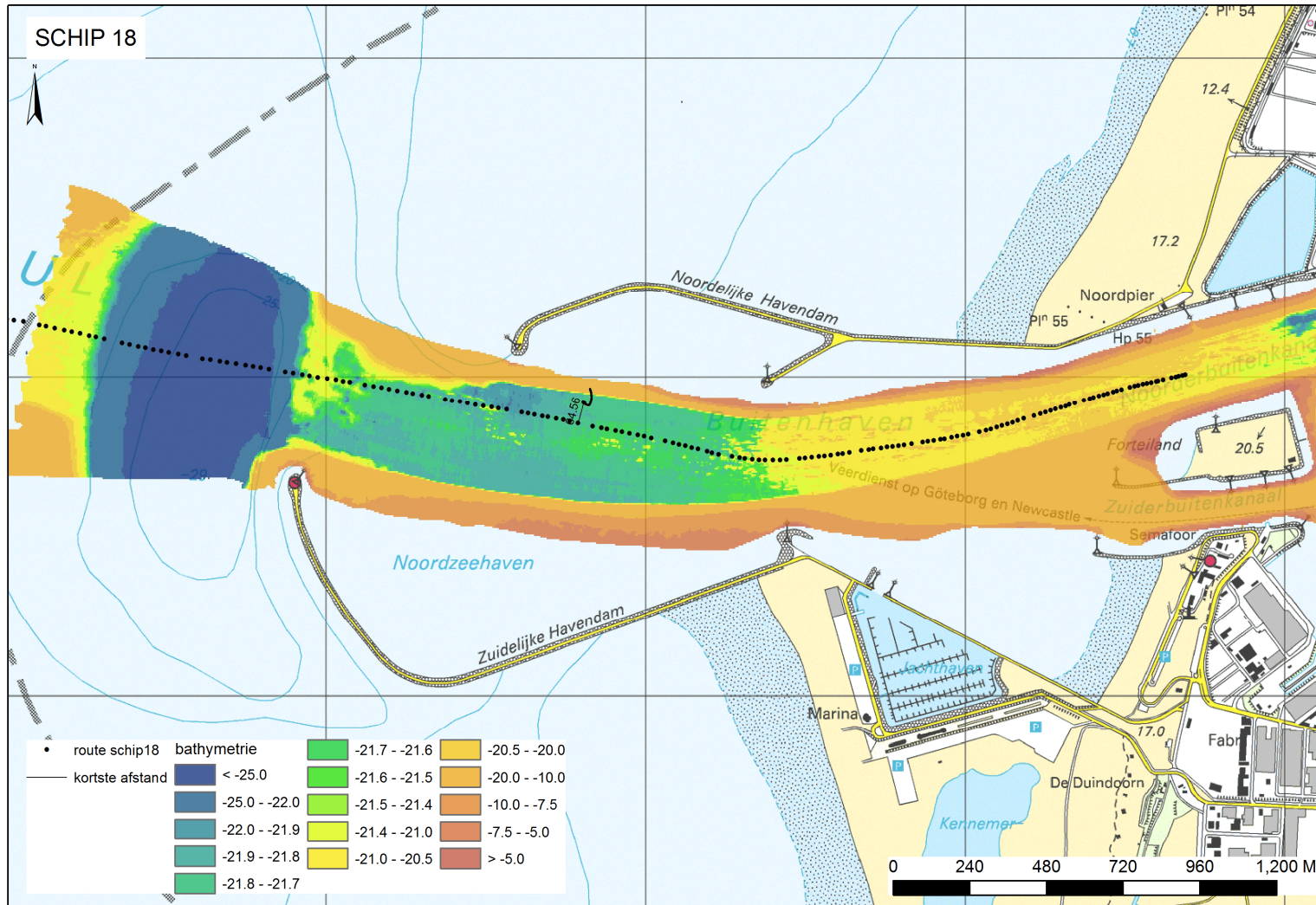
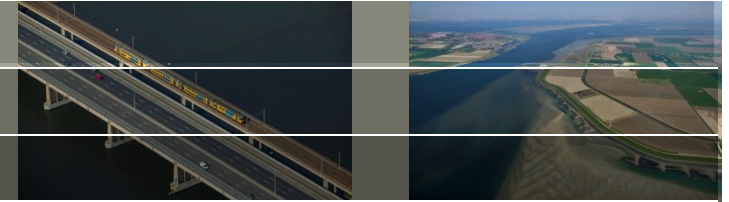
Vessel 15 - after



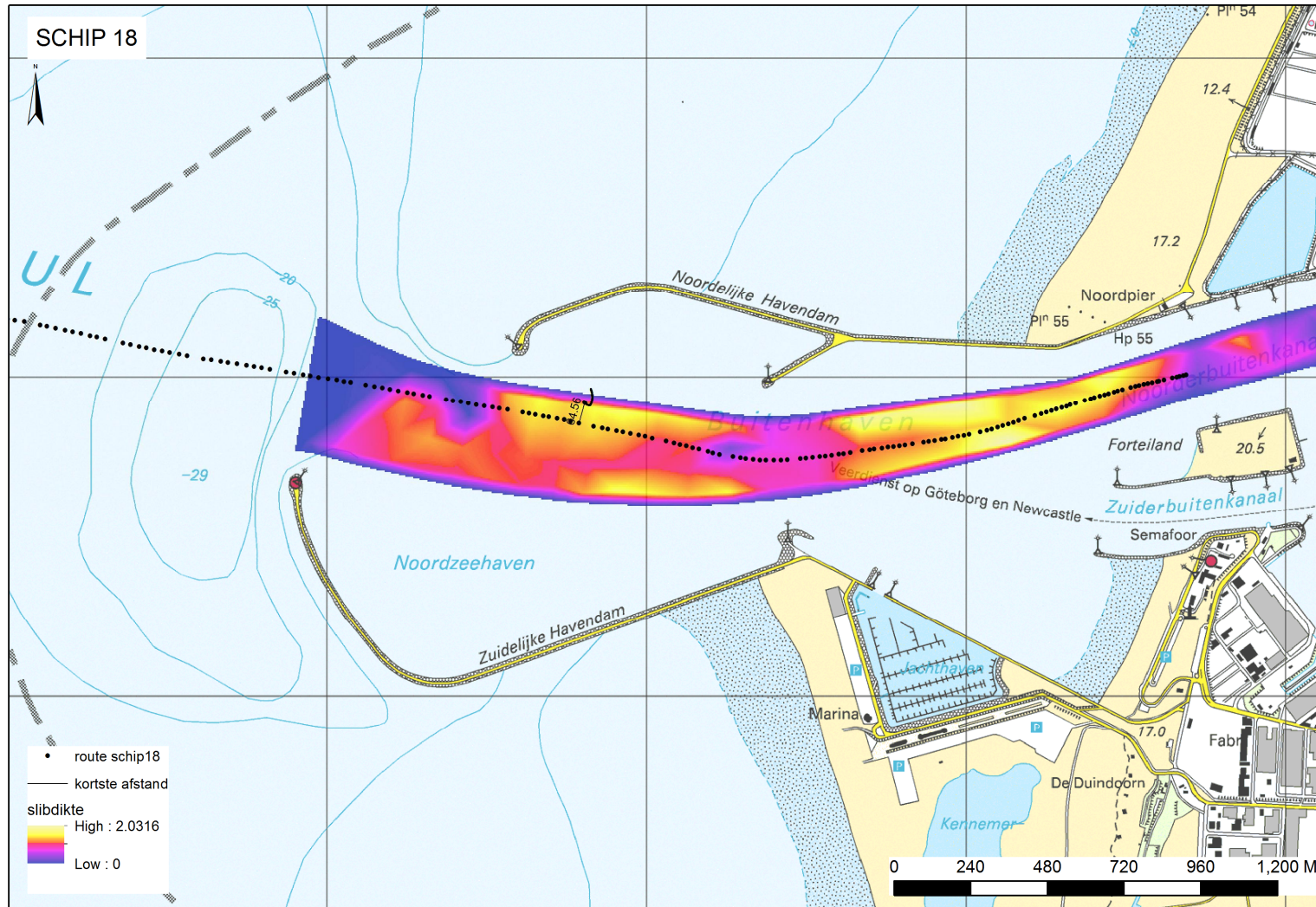
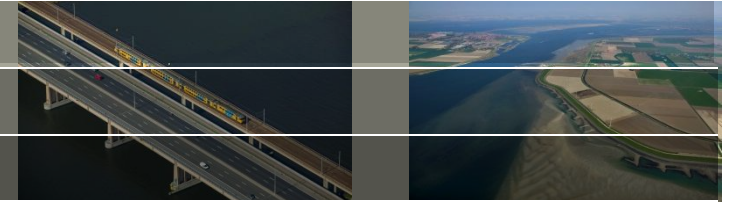
Vessel 15 – density profiles near Zirfaea



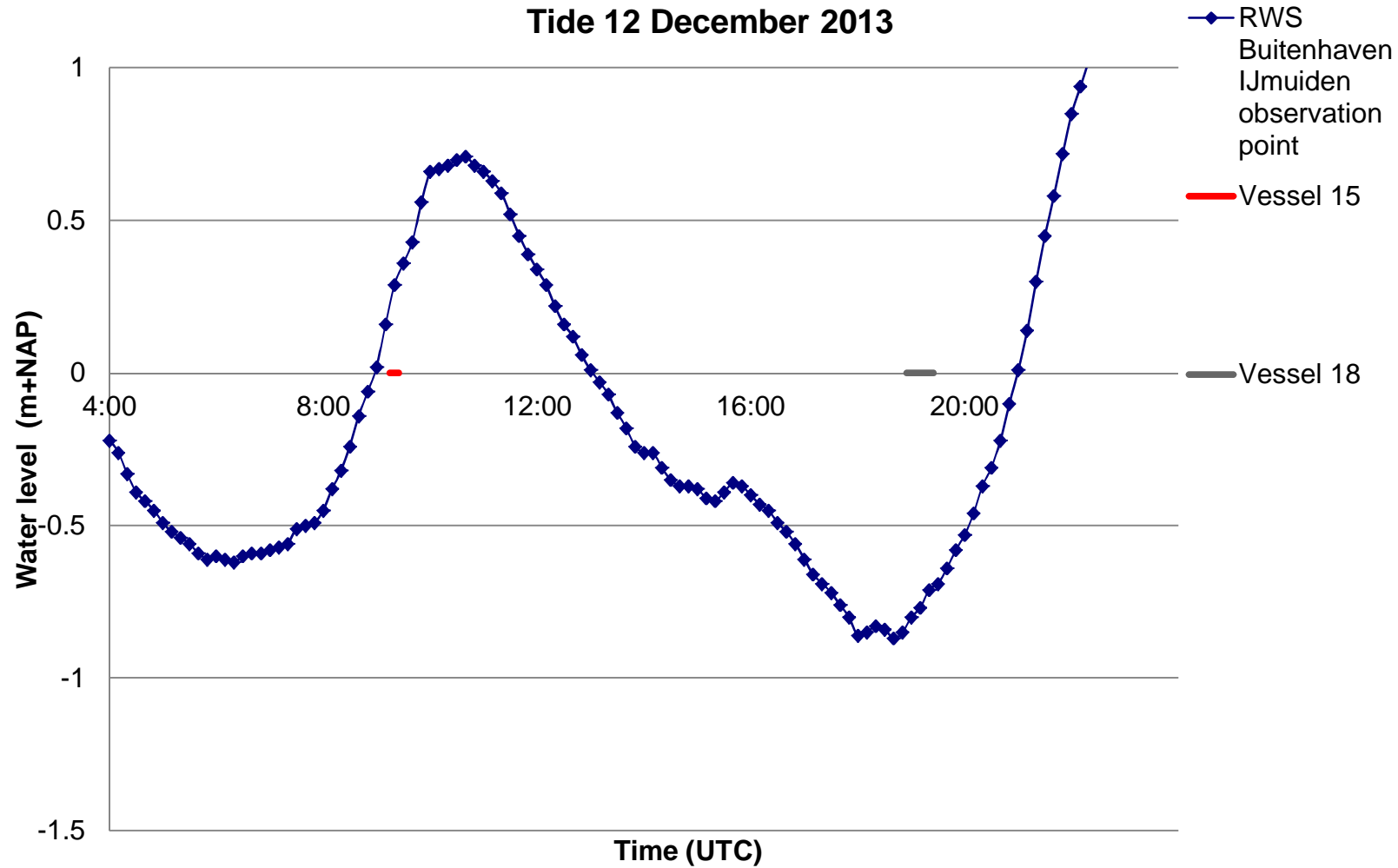
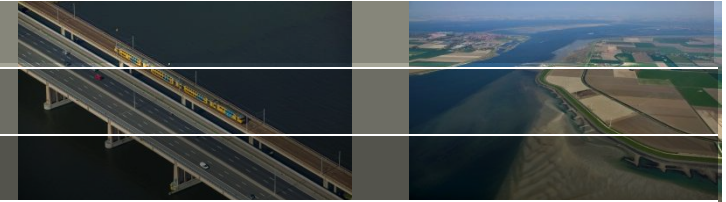
Vessel 18



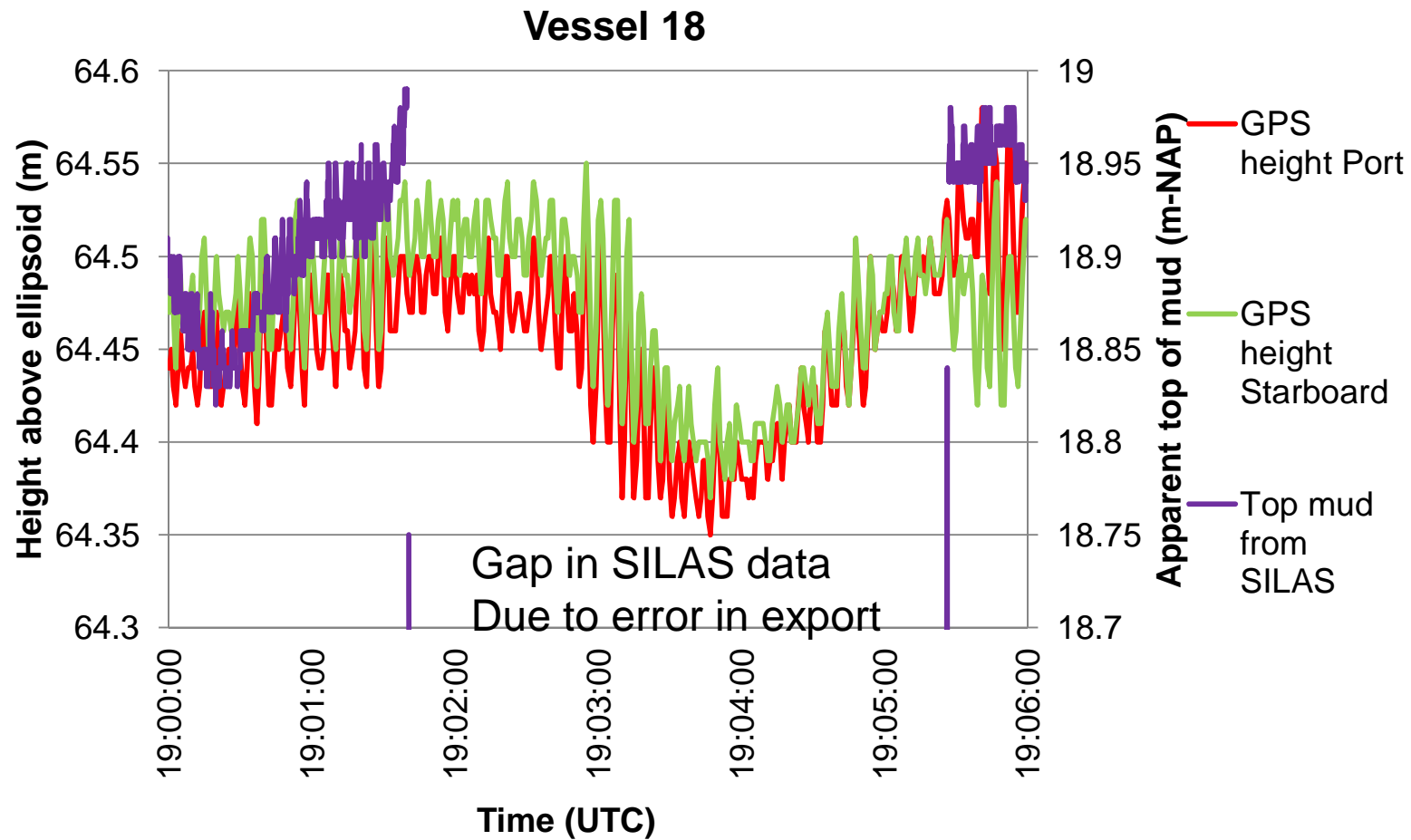
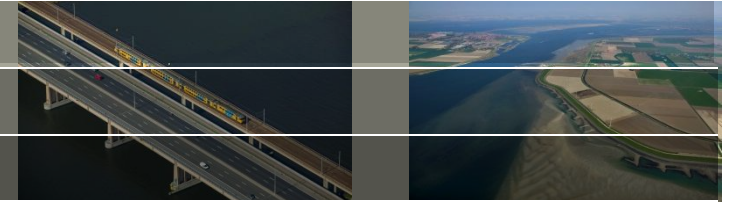
Vessel 18



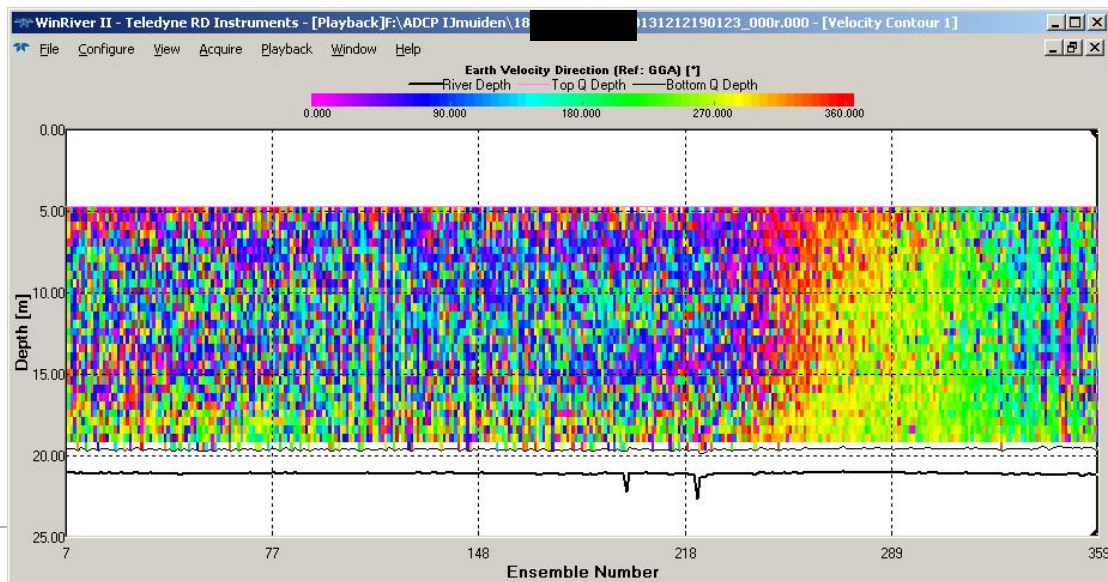
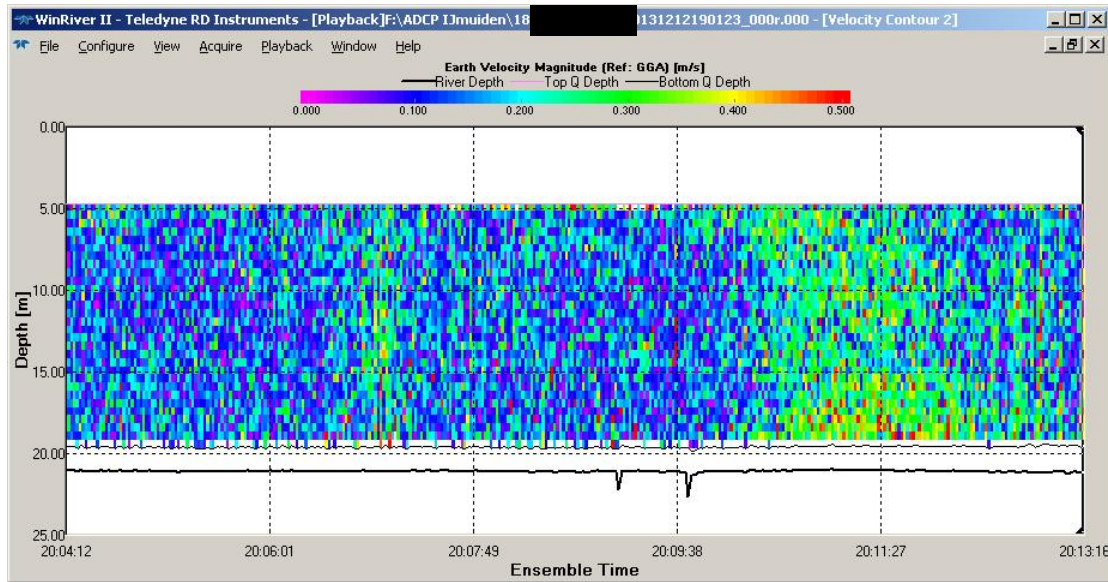
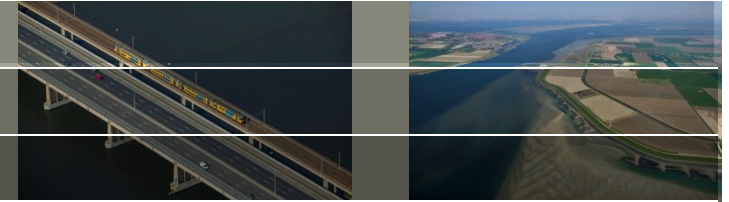
Vessel 18 - Tide



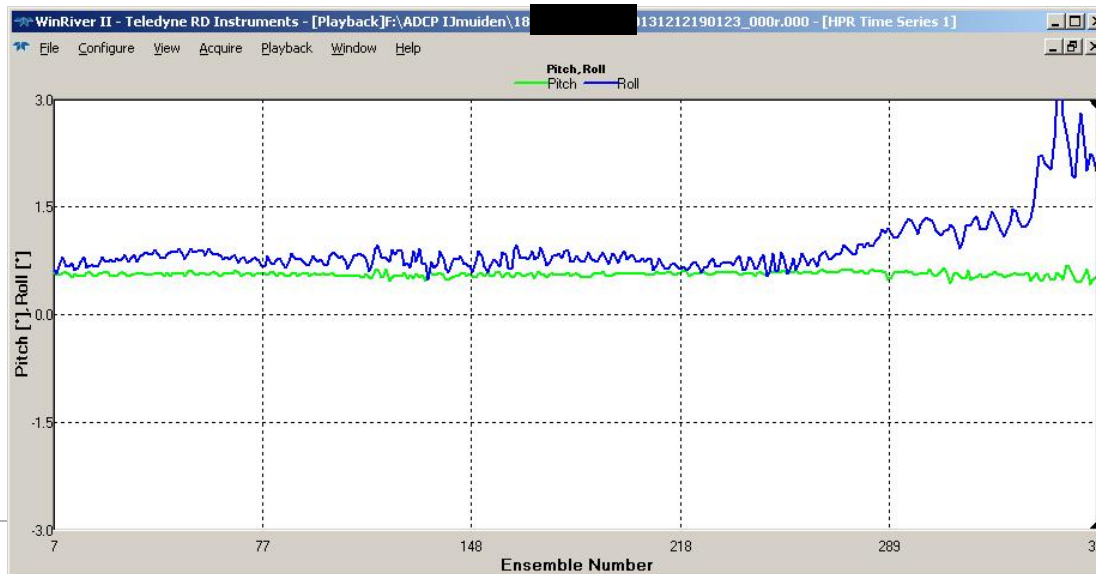
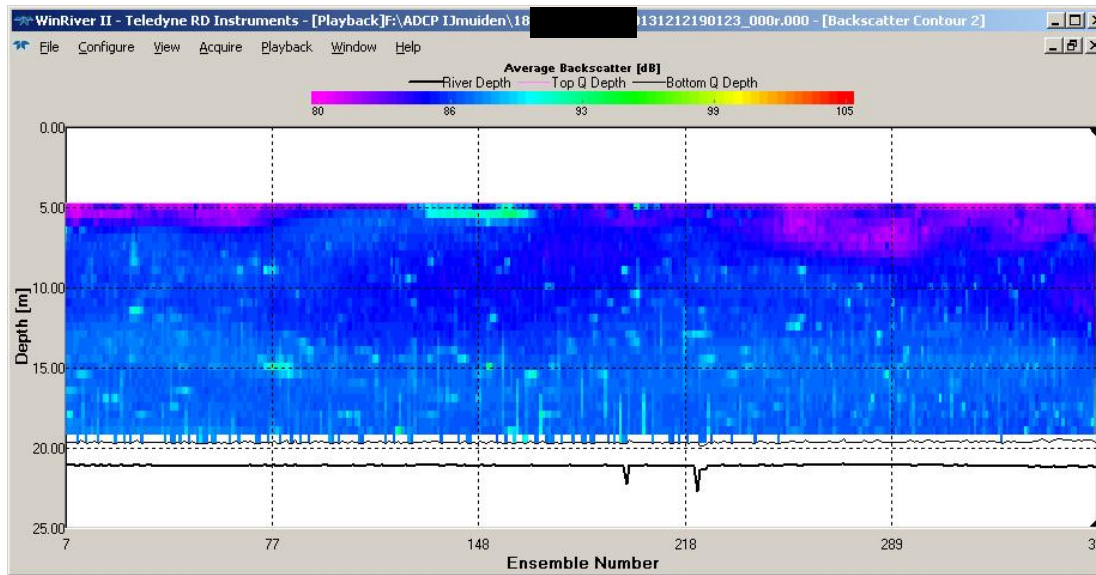
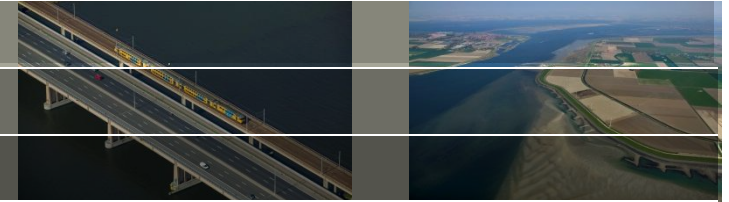
Vessel 18 – GPS Heights



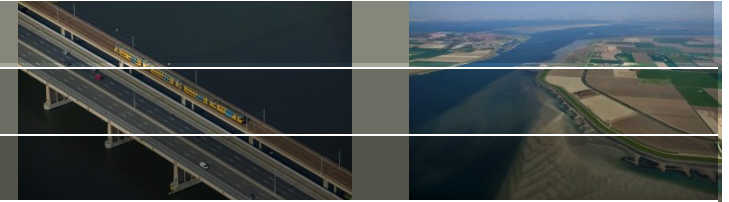
Vessel 18 – ADCP



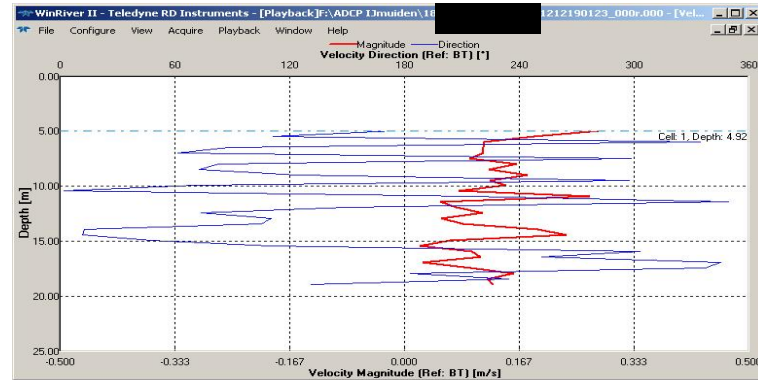
Vessel 18 – ADCP



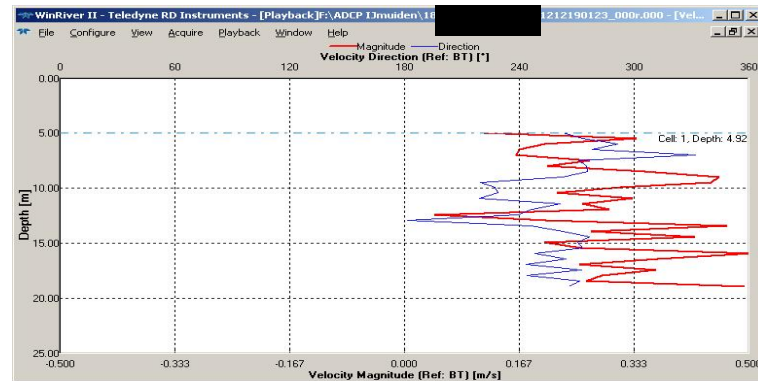
Vessel 18 – ADCP



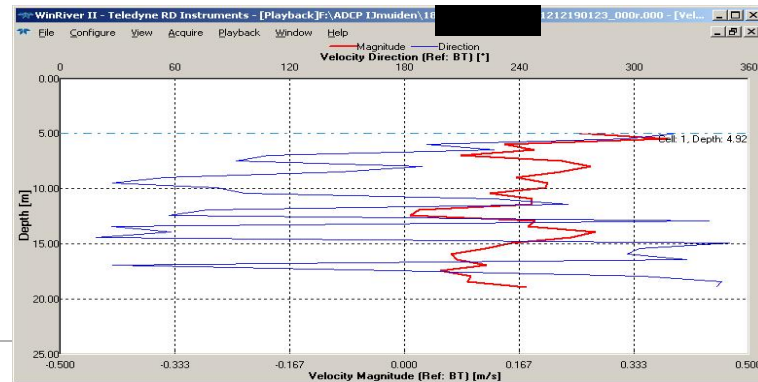
Ensemble 220



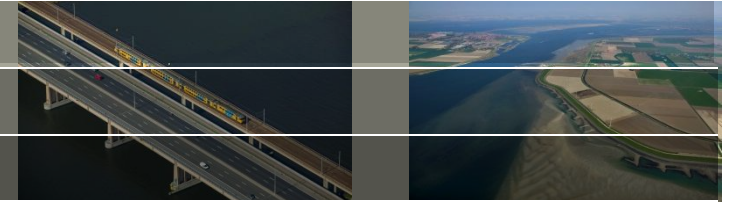
Ensemble 300



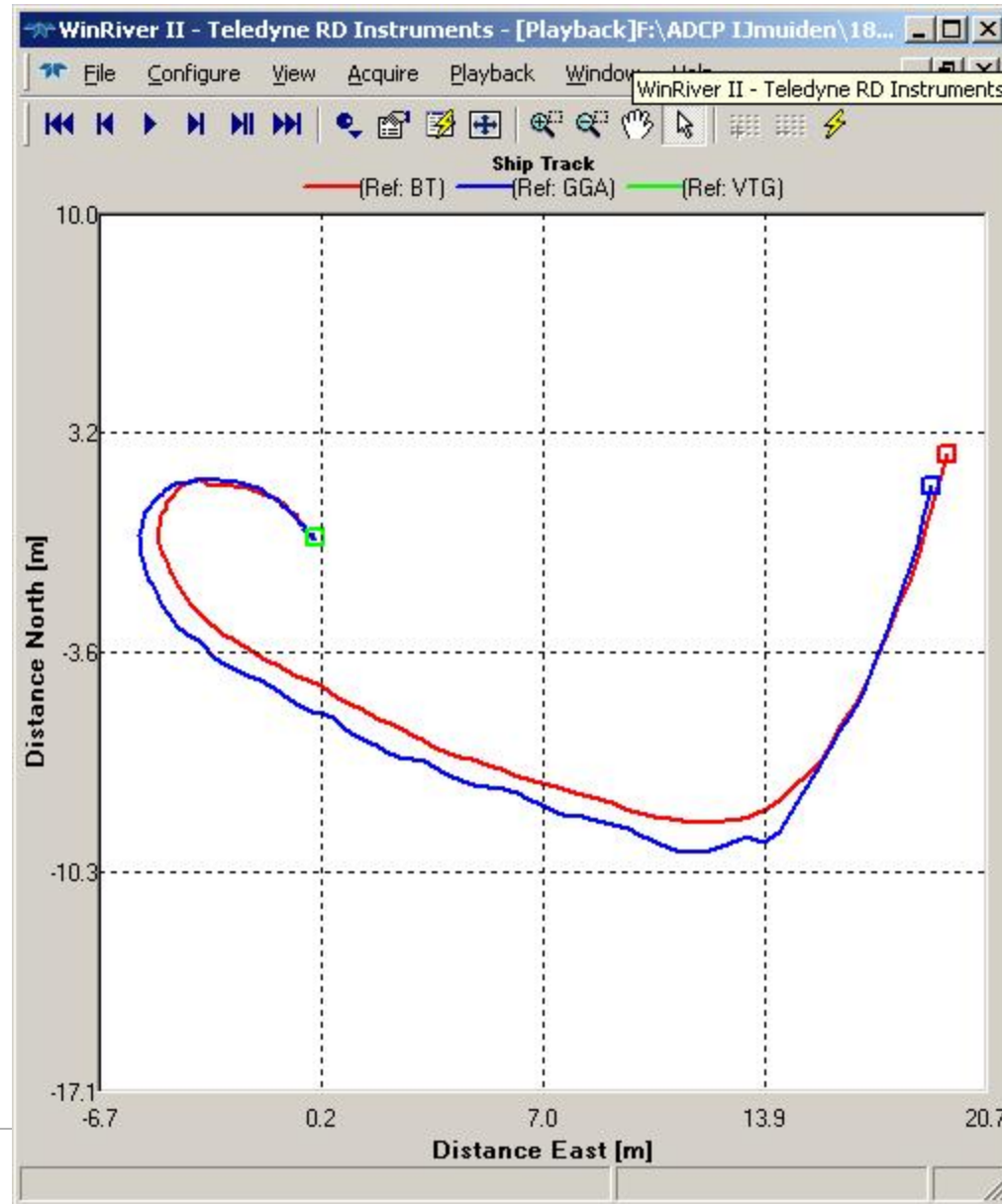
Ensemble 359



Vessel 18 – ADCP

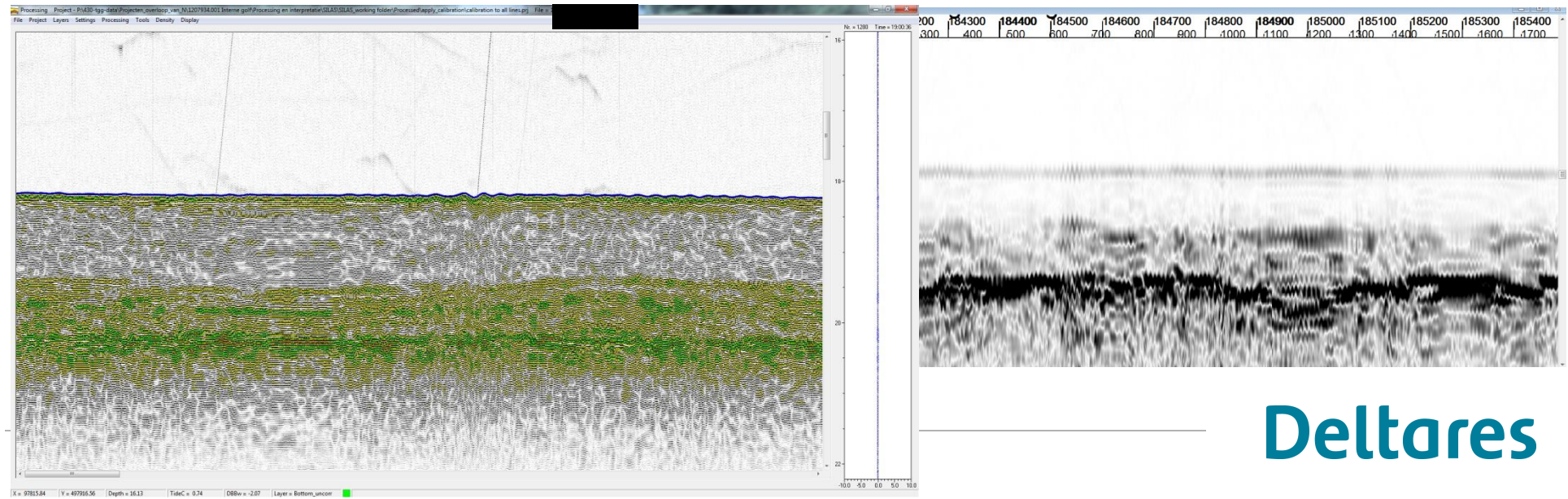
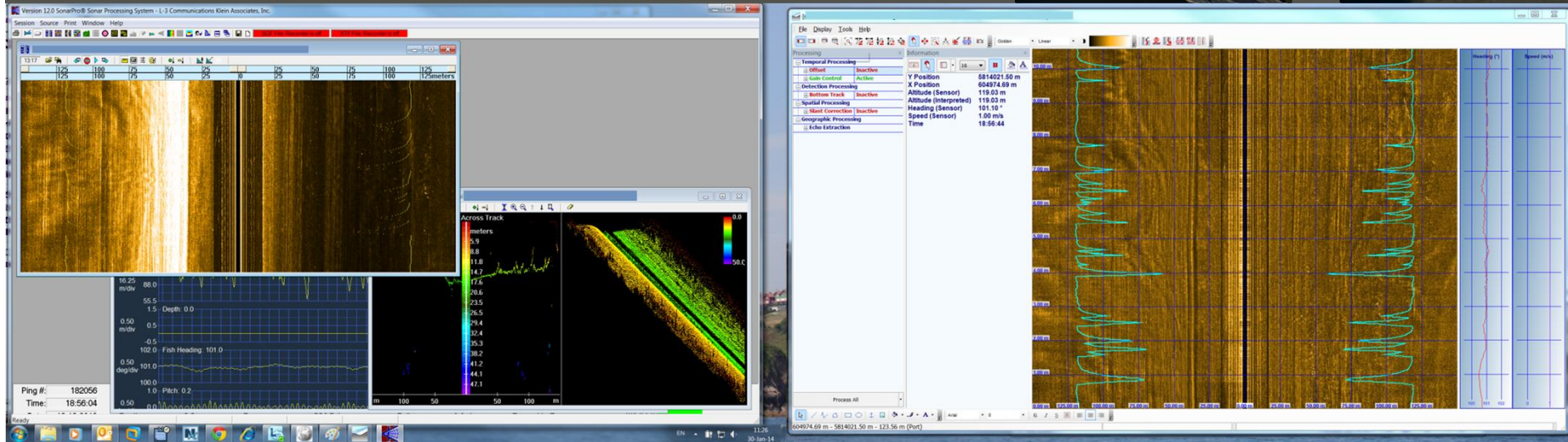
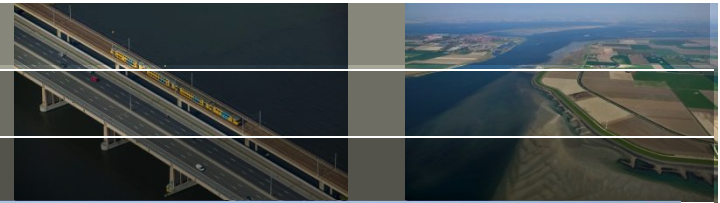


ensembles 220 – 359



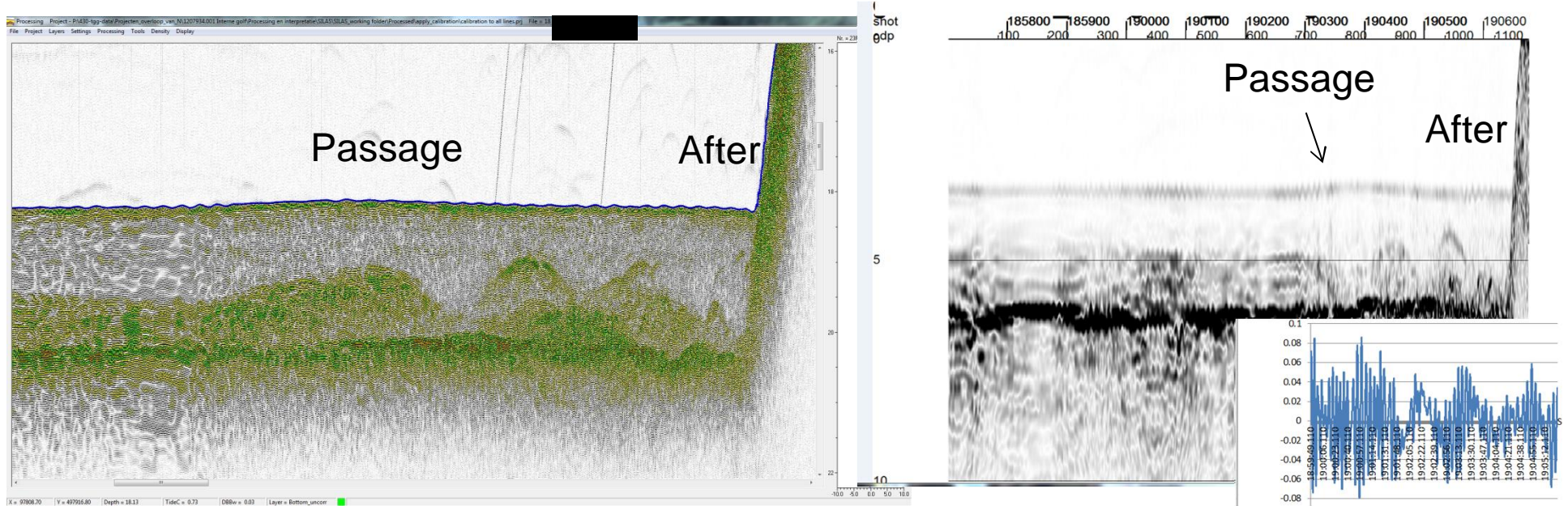
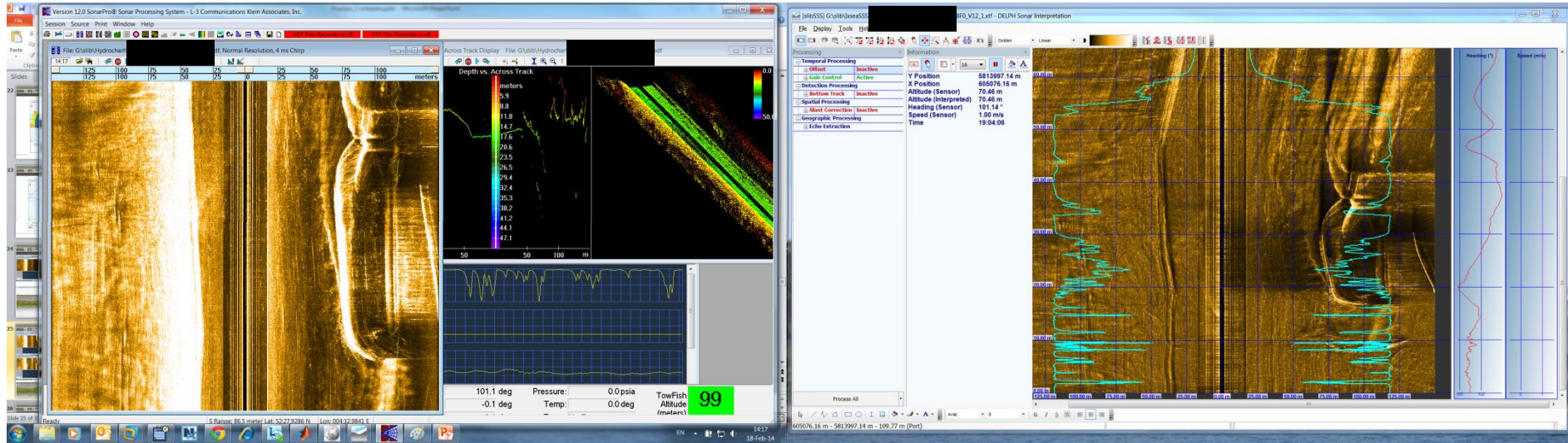
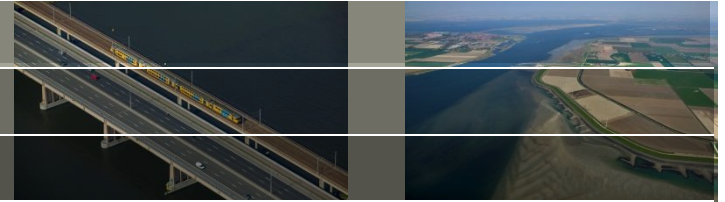
Deltares

Vessel 18 - before

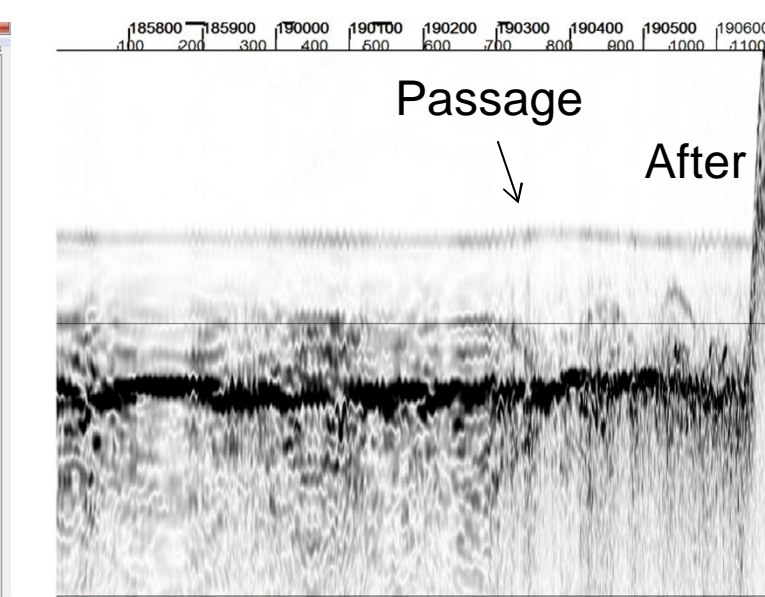
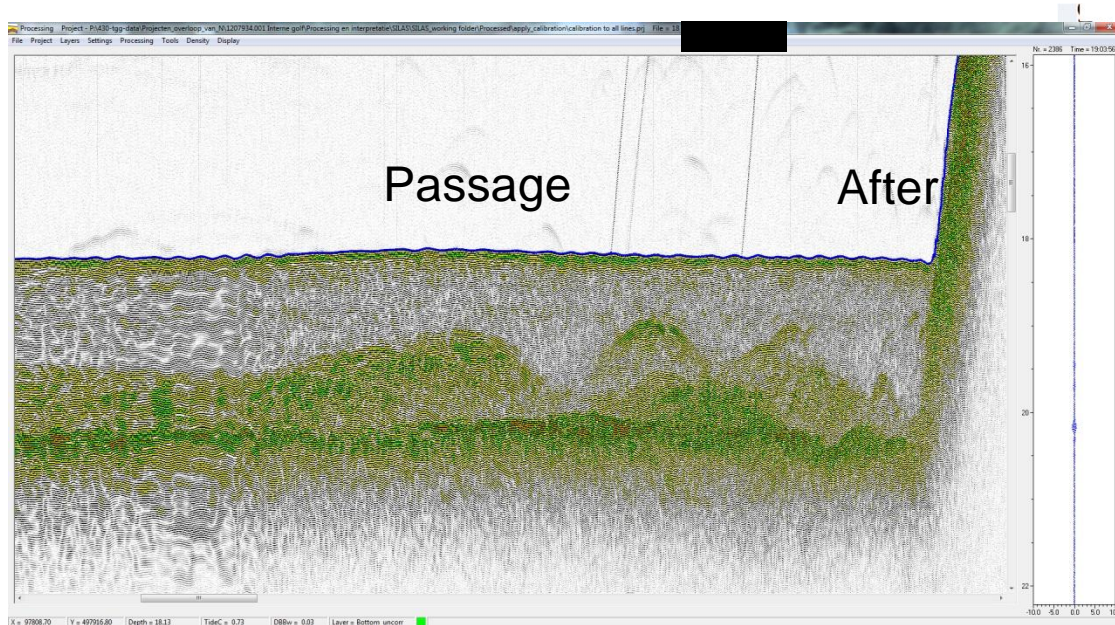
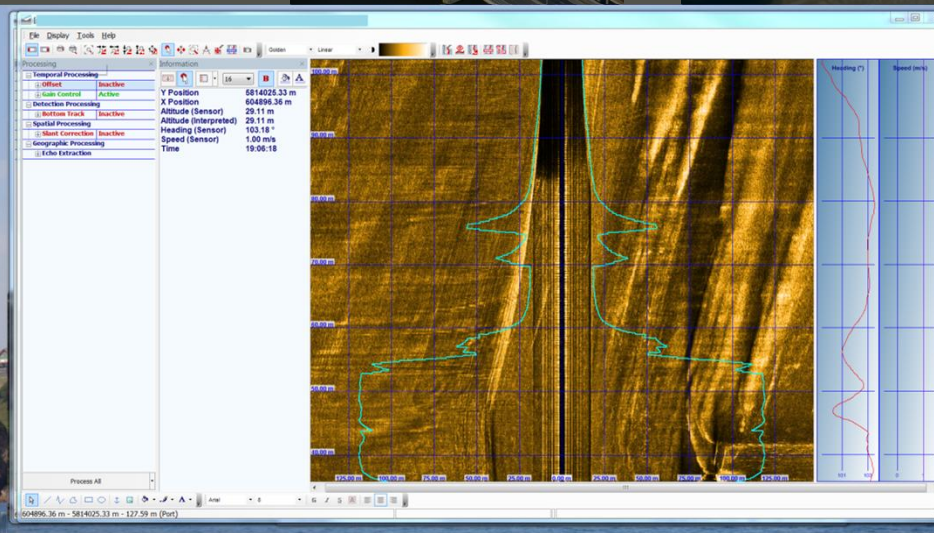
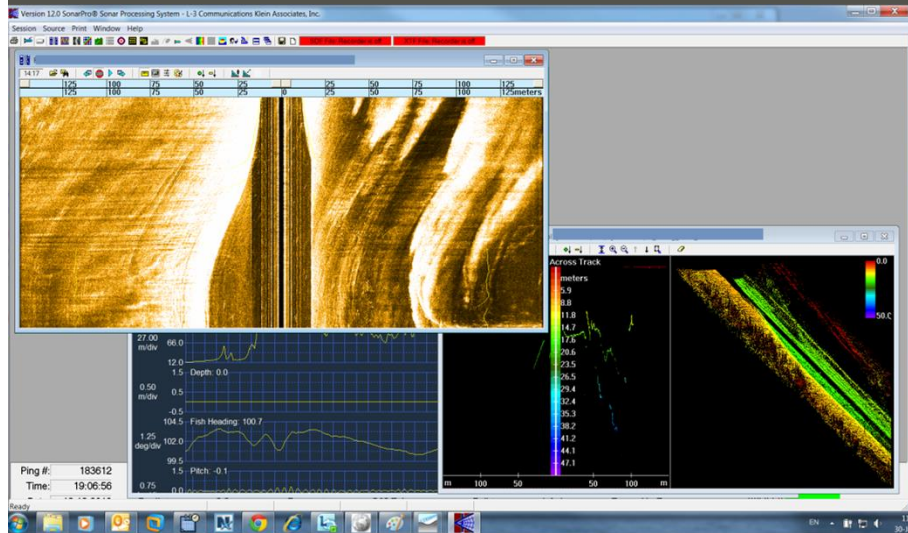
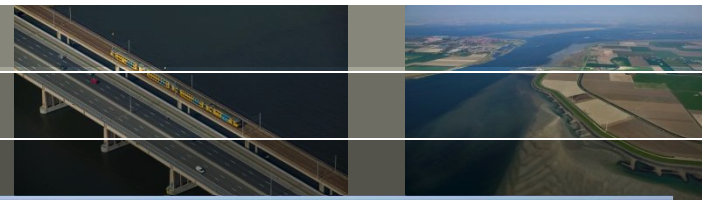


Deltares

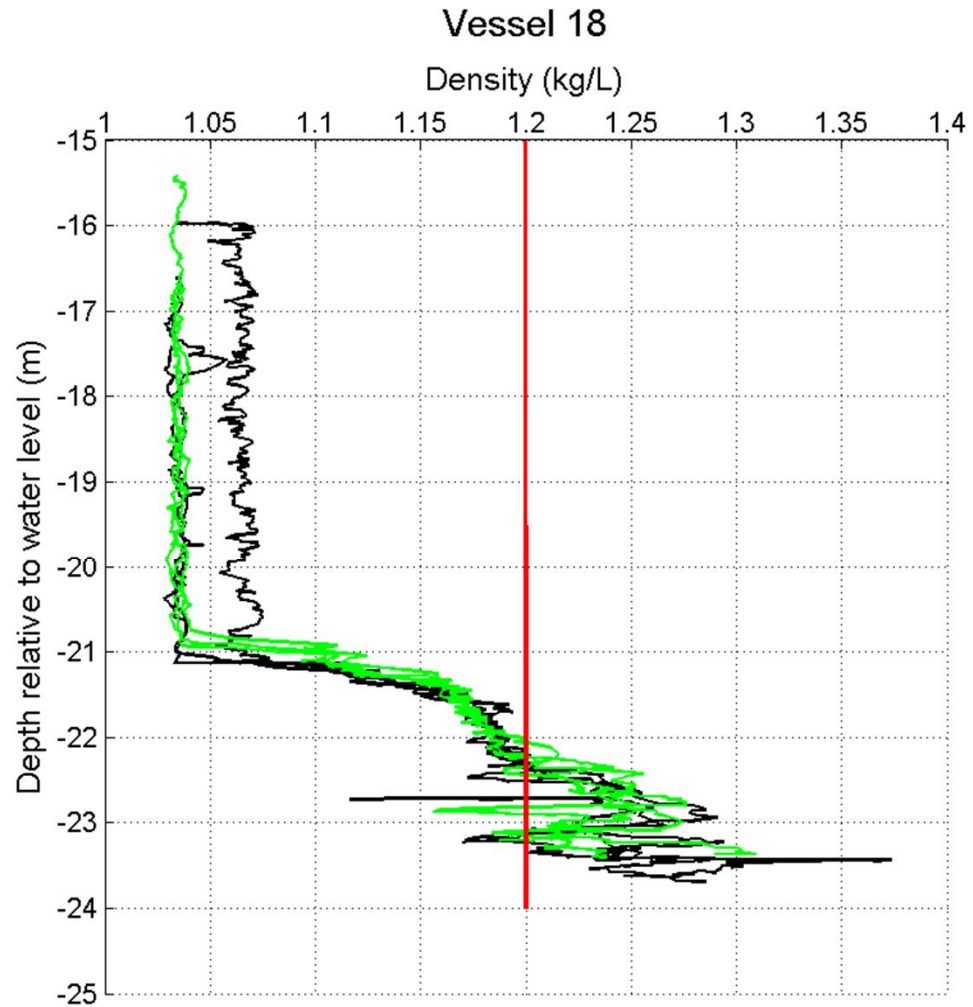
Vessel 18 - passage



Vessel 18 - after

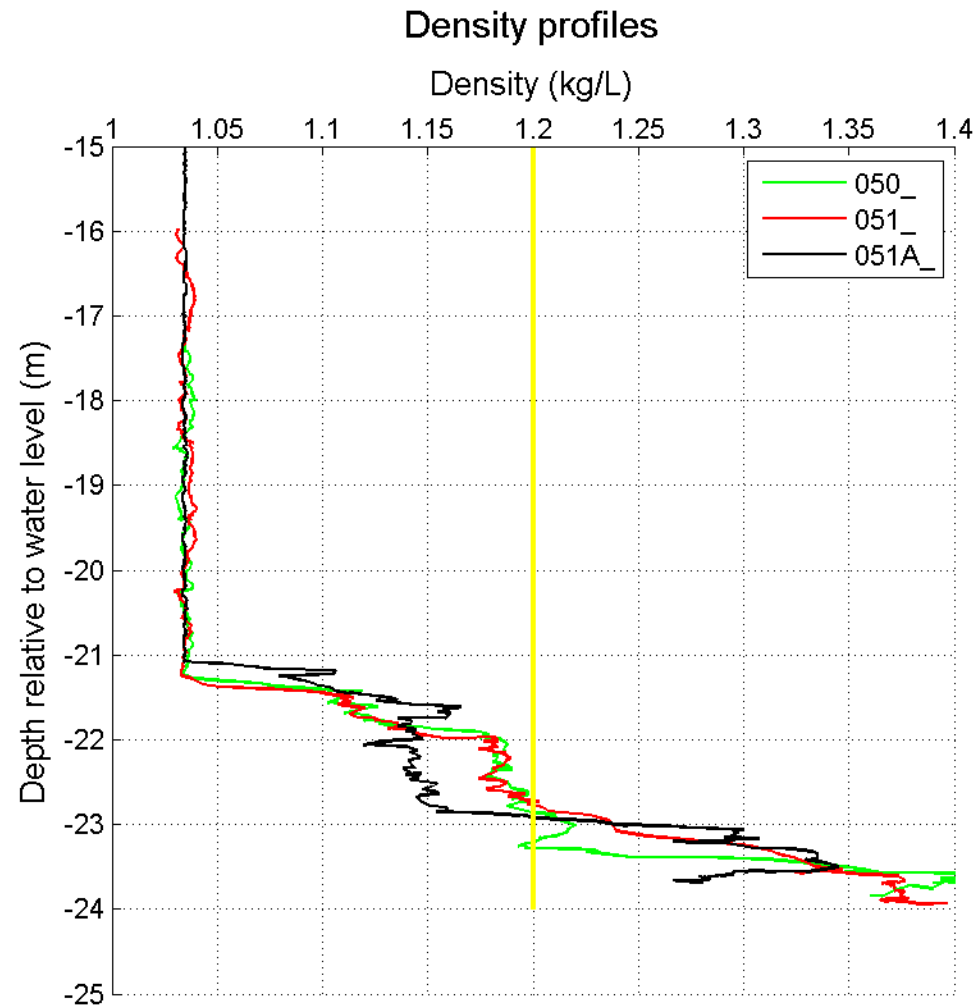


Vessel 18 – density profiles line of passage

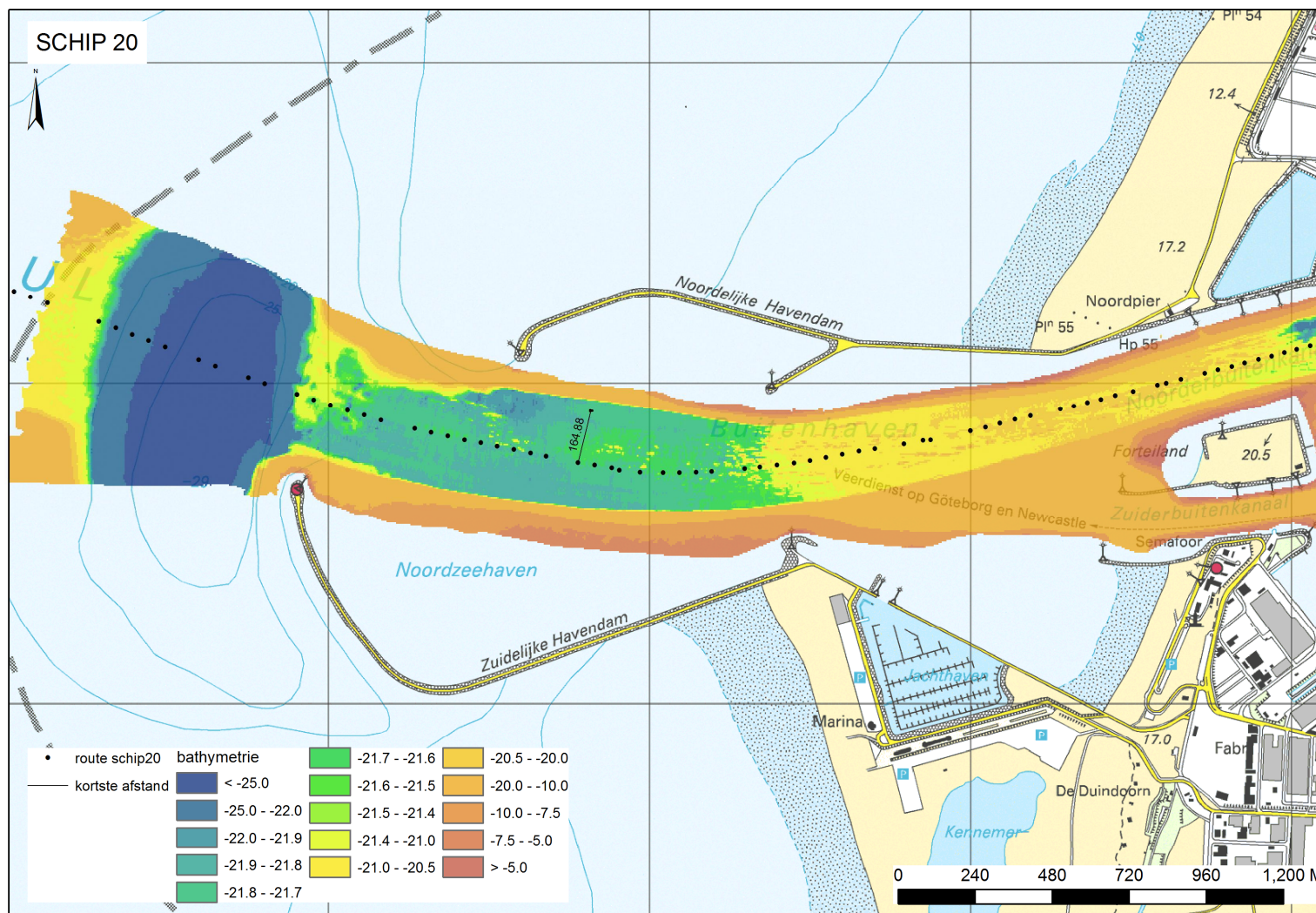
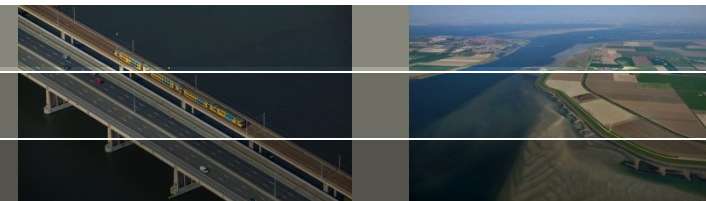


Green: before
Black: after
Corrected for tide
difference

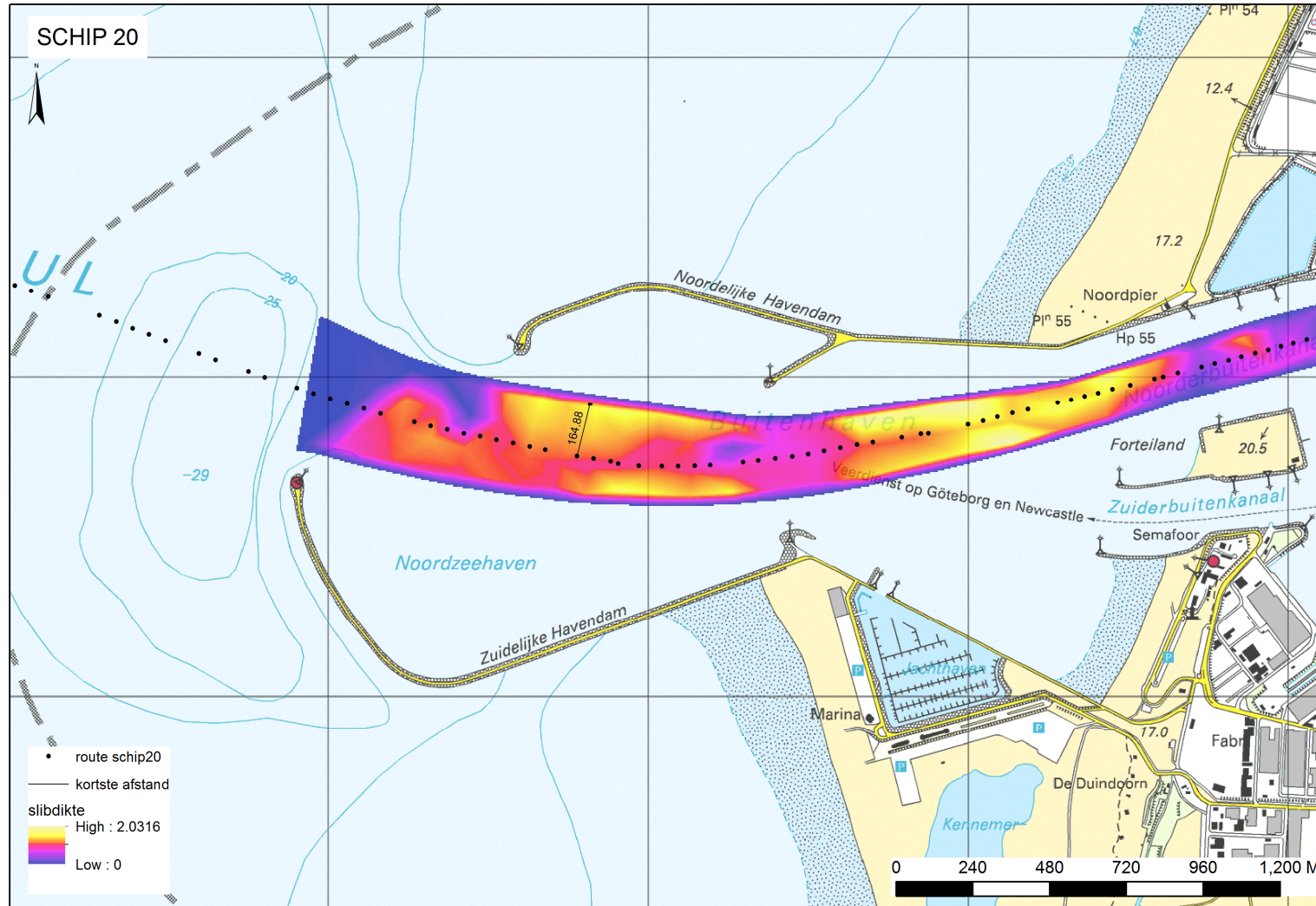
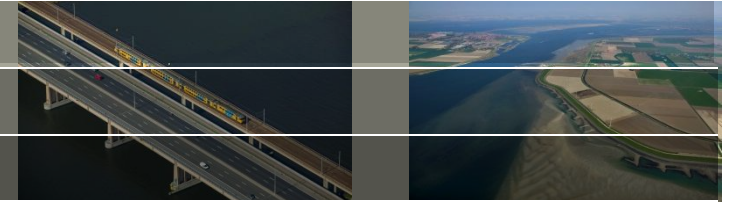
Vessel 18 – density profiles near Zirfaea



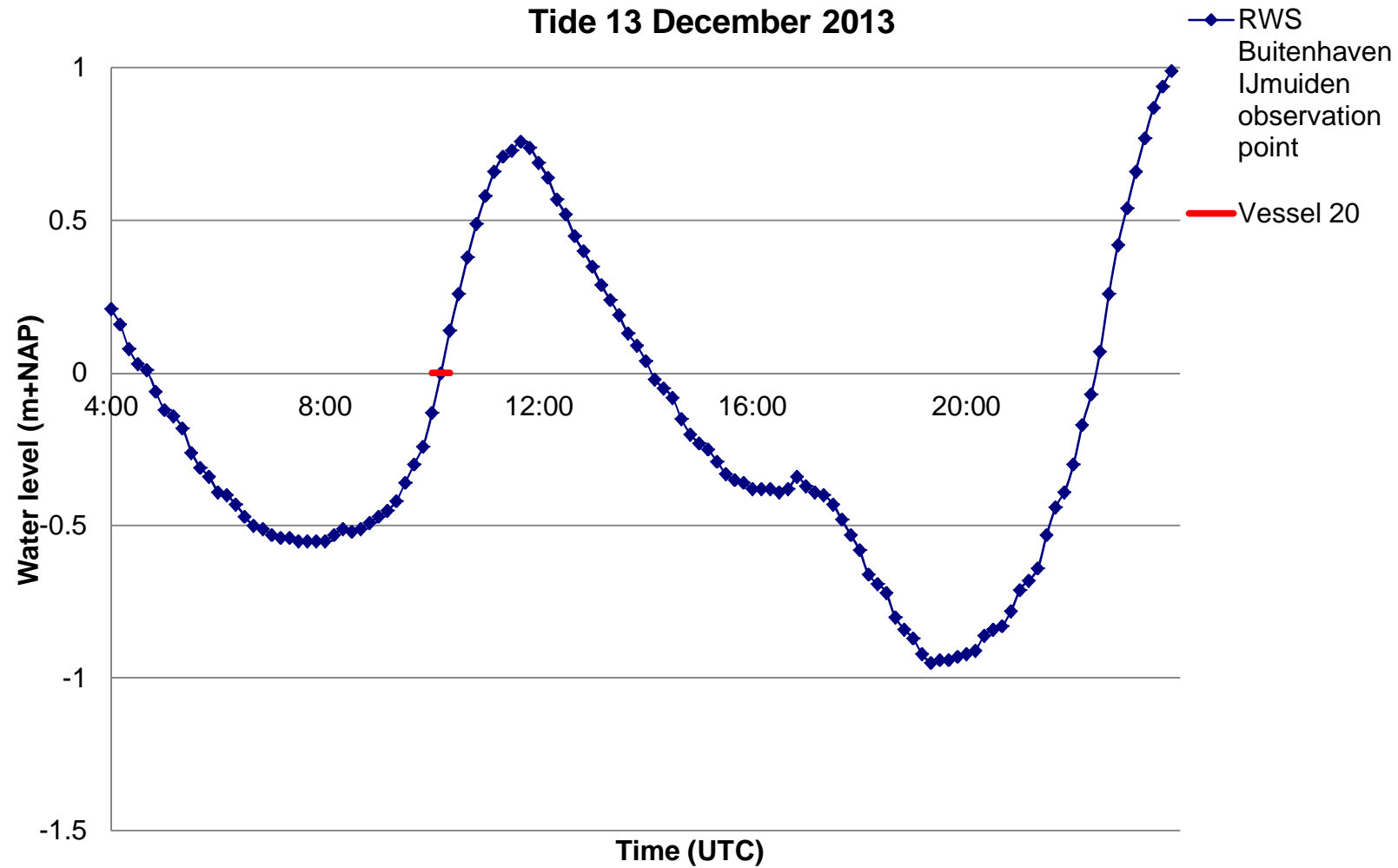
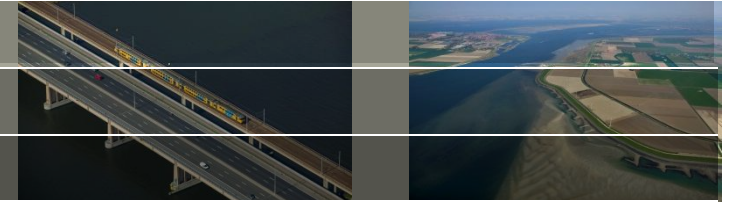
Vessel 20



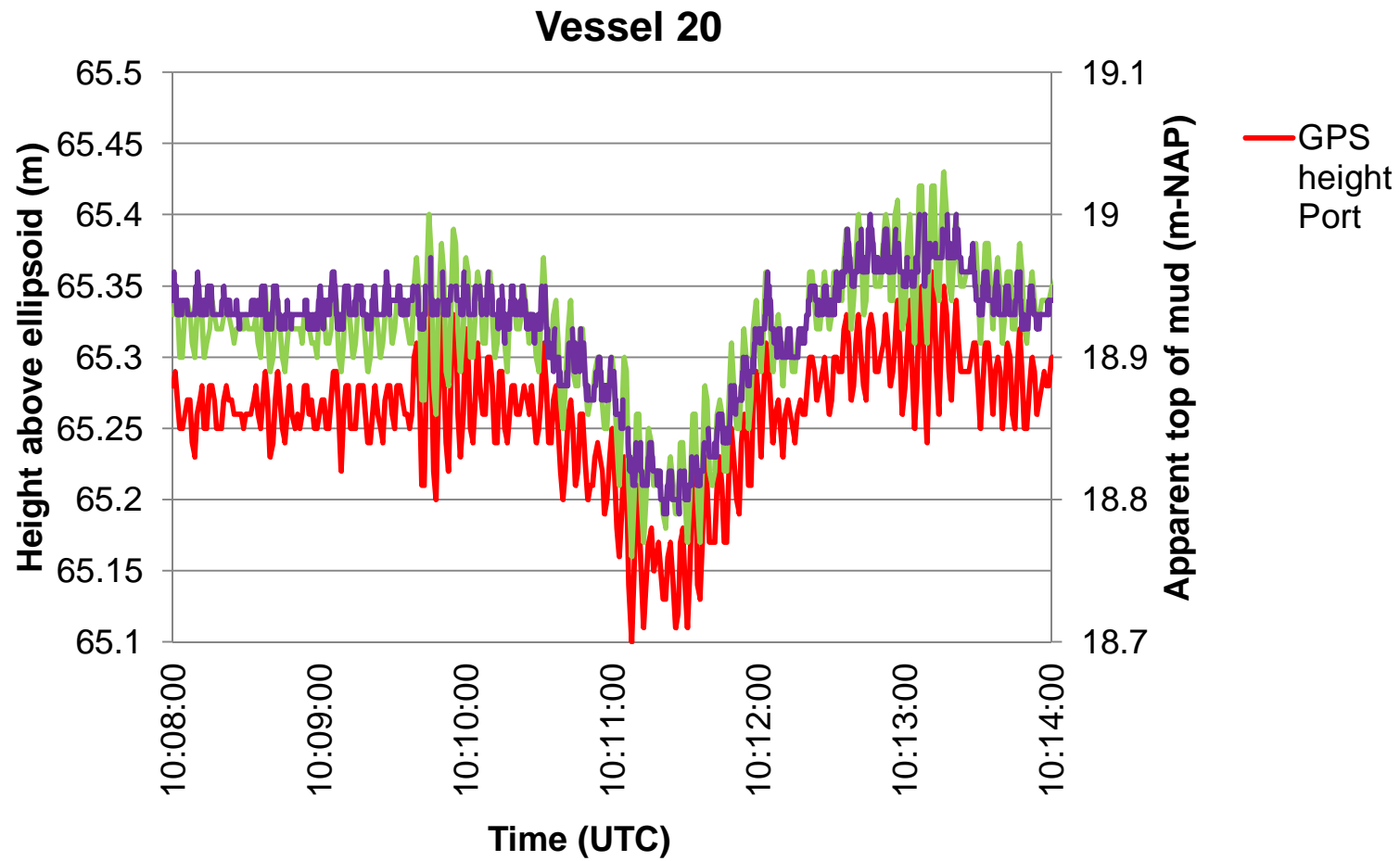
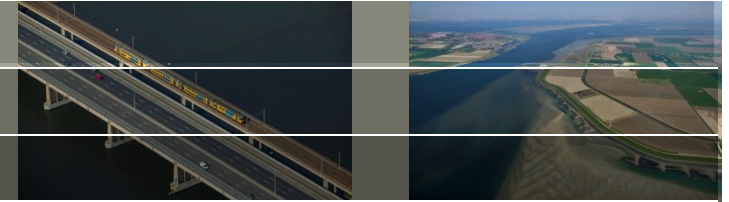
Vessel 20



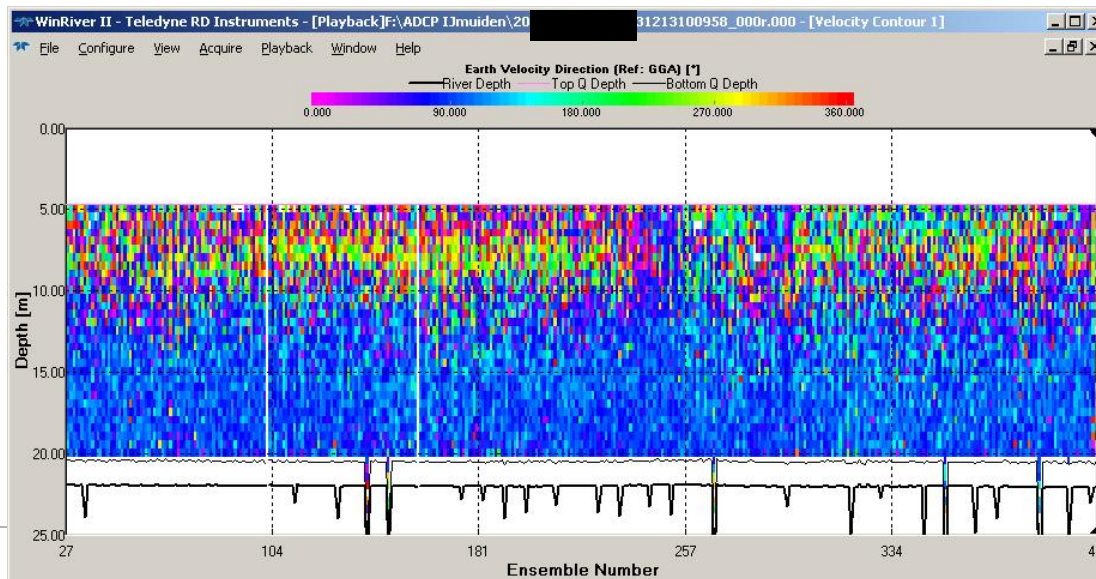
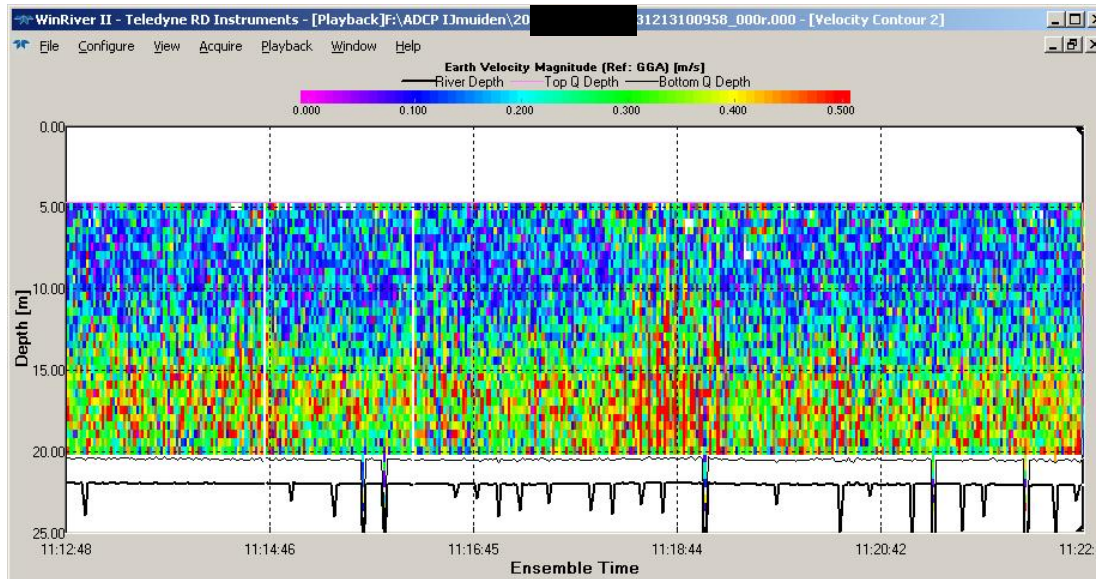
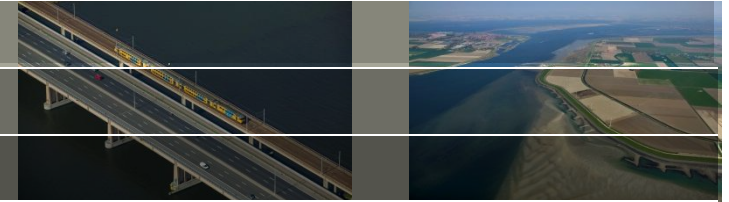
Vessel 20 - Tide



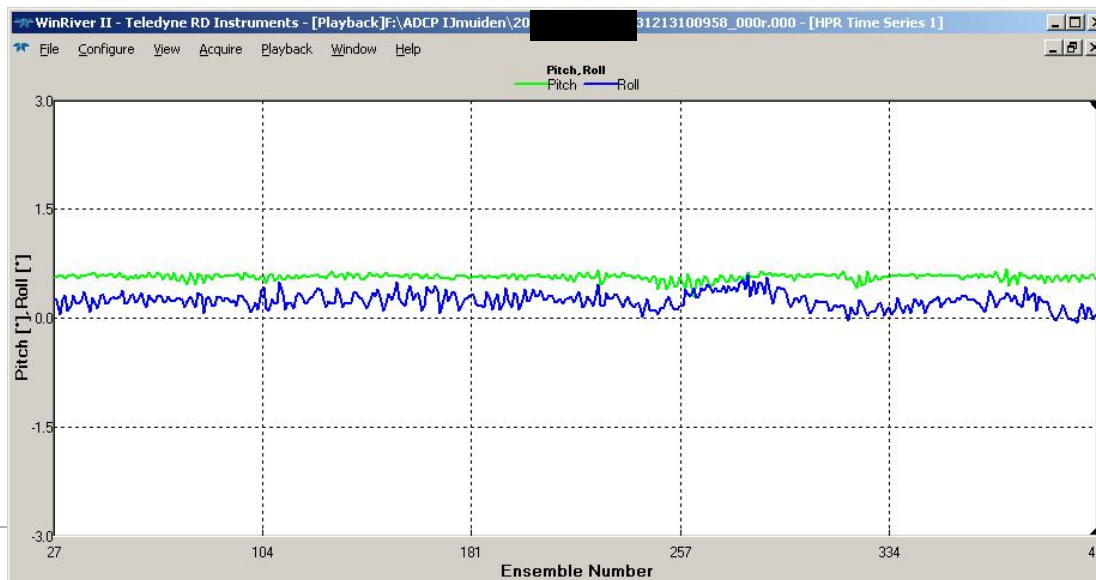
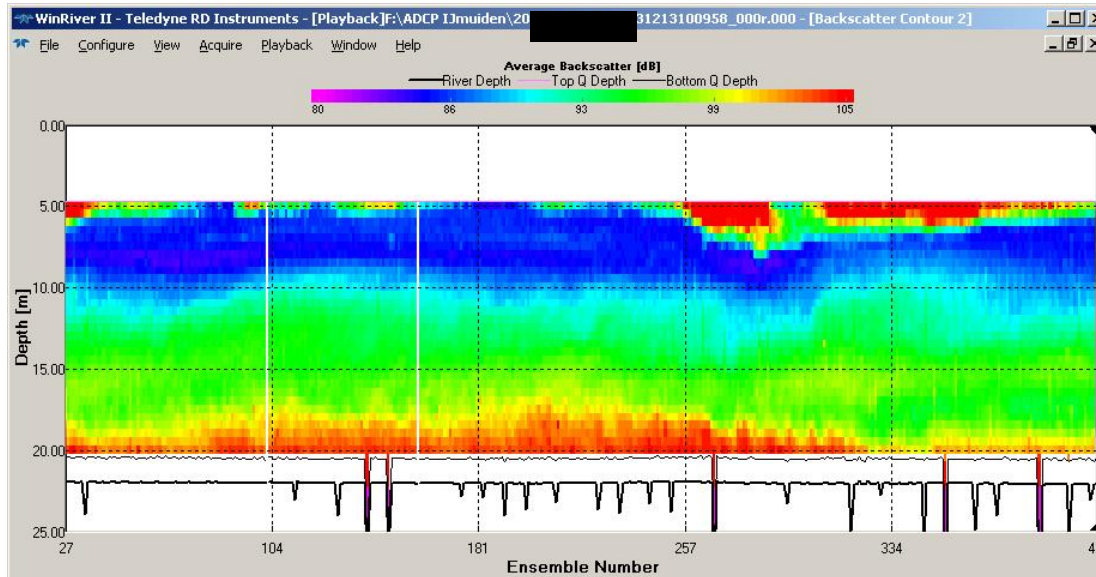
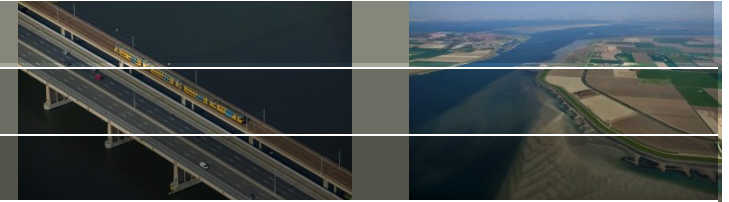
Vessel 20 – GPS Heights



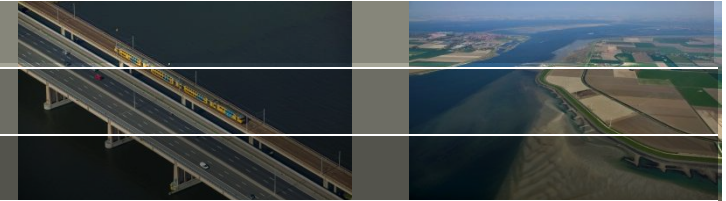
Vessel 20 – ADCP



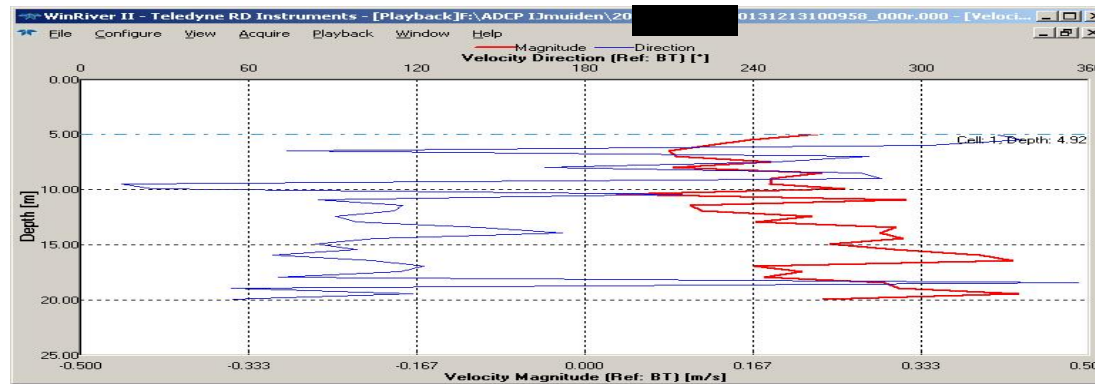
Vessel 20 – ADCP



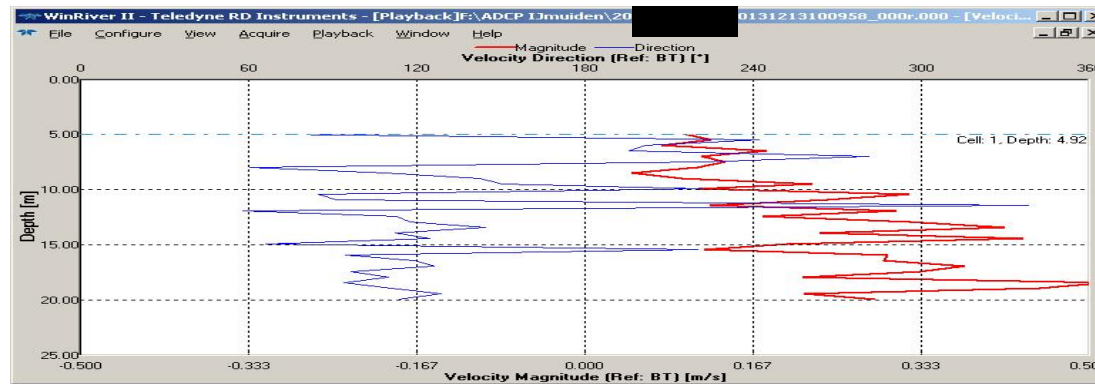
Vessel 20 – ADCP



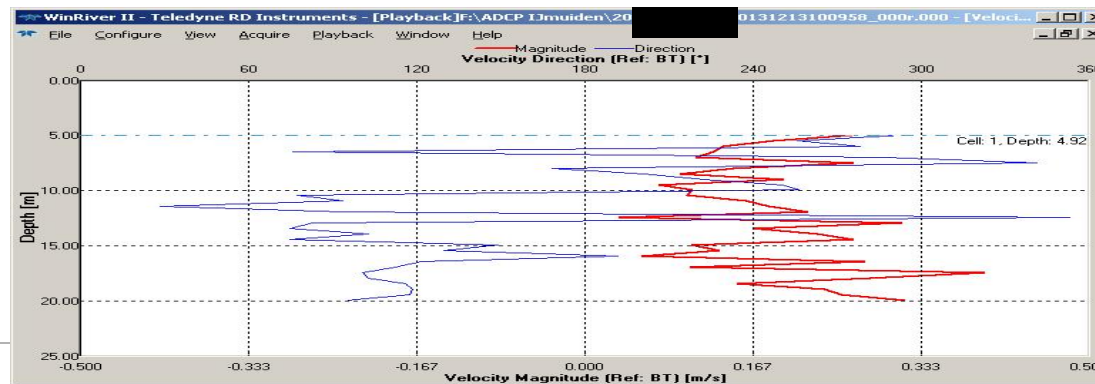
Ensemble 180



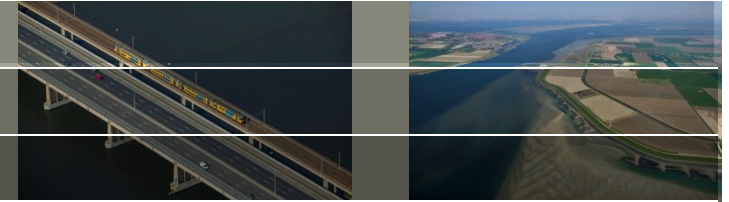
Ensemble 255



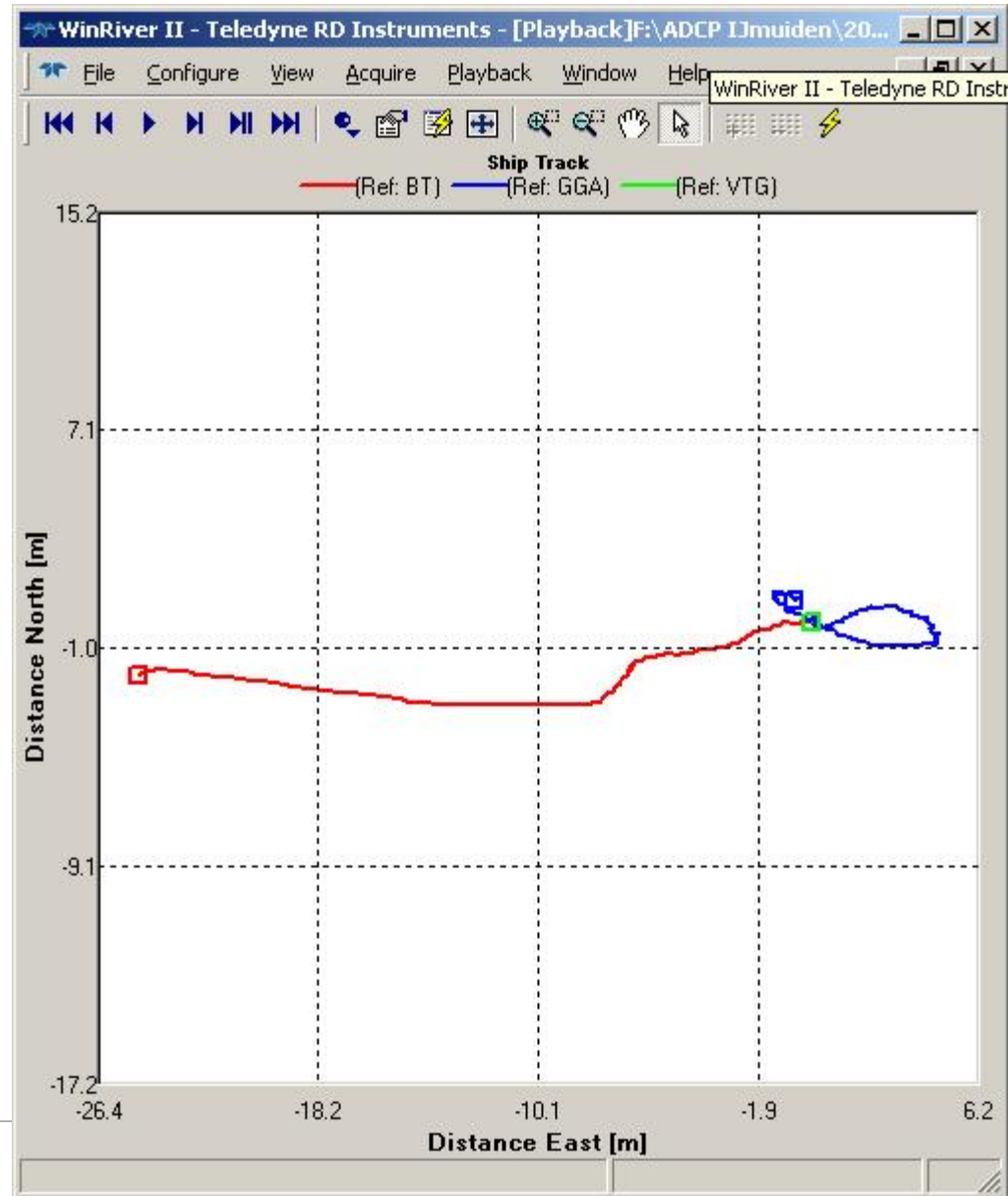
Ensemble 330



Vessel 20 – ADCP

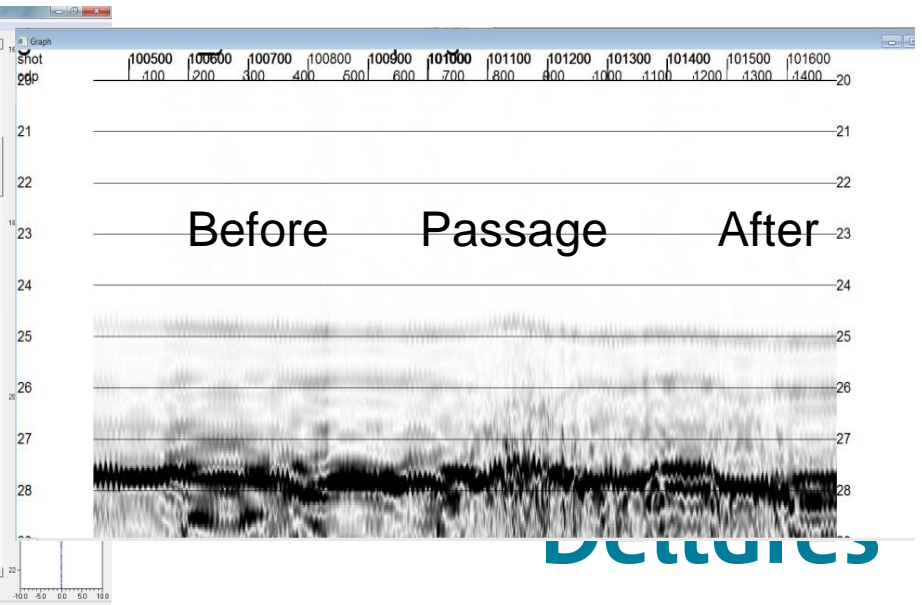
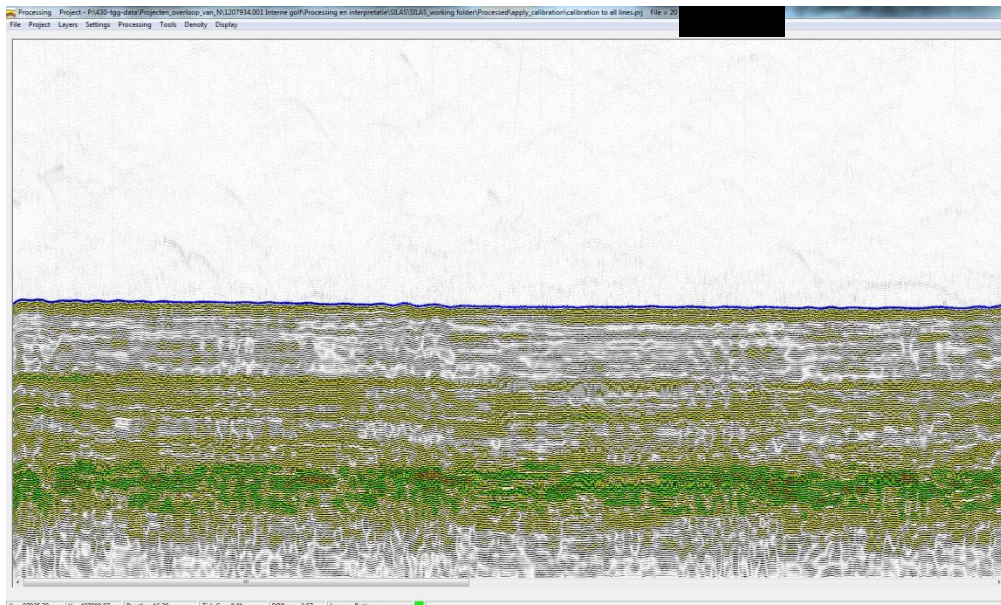
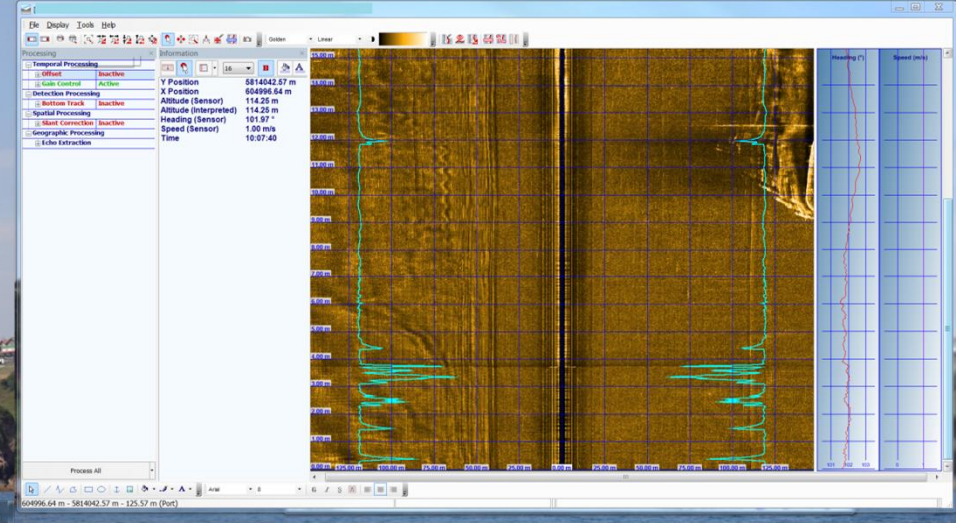
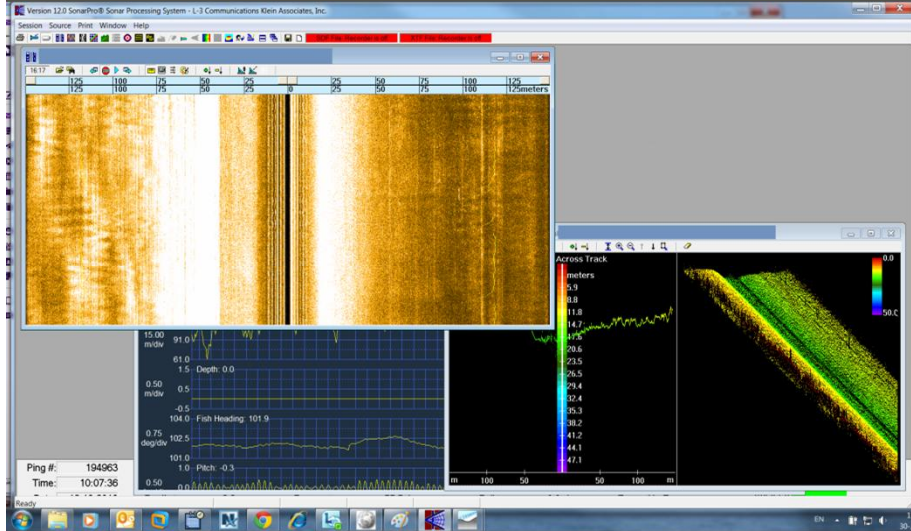
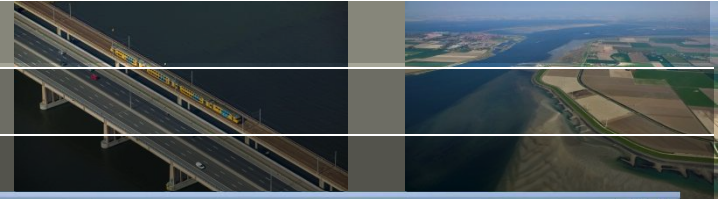


ensembles 180 - 330

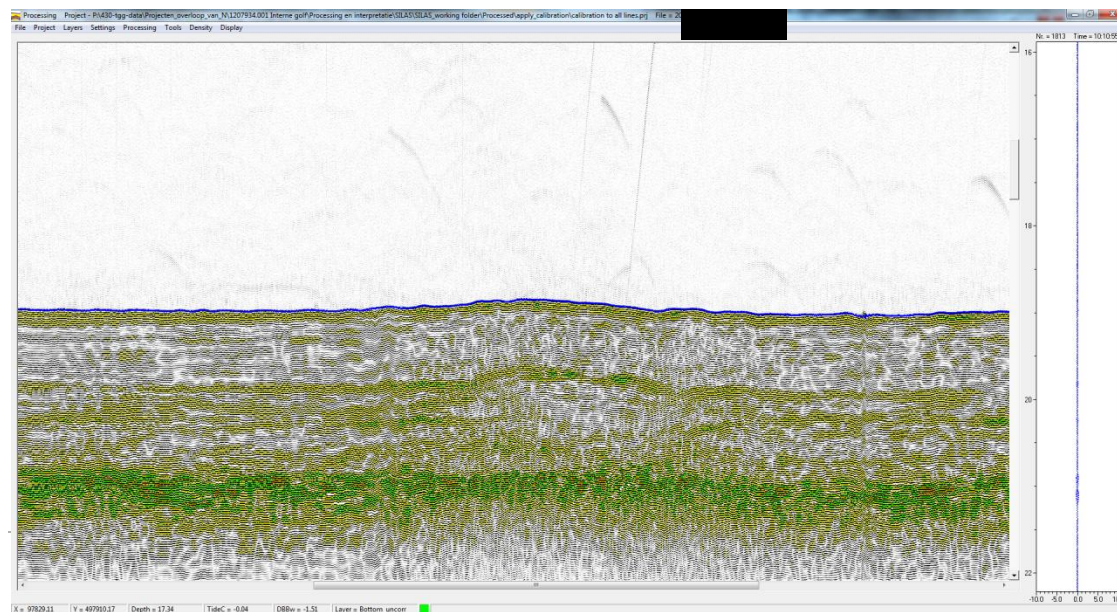
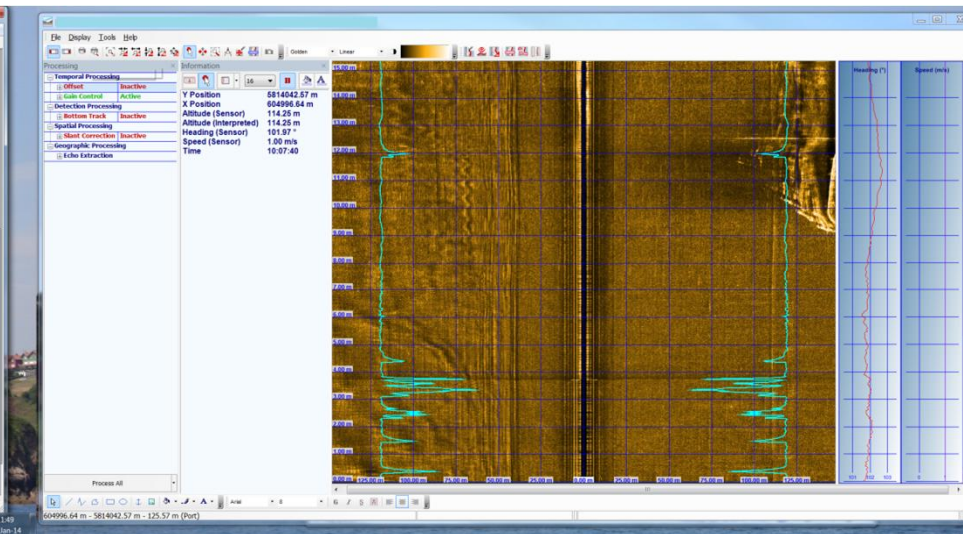
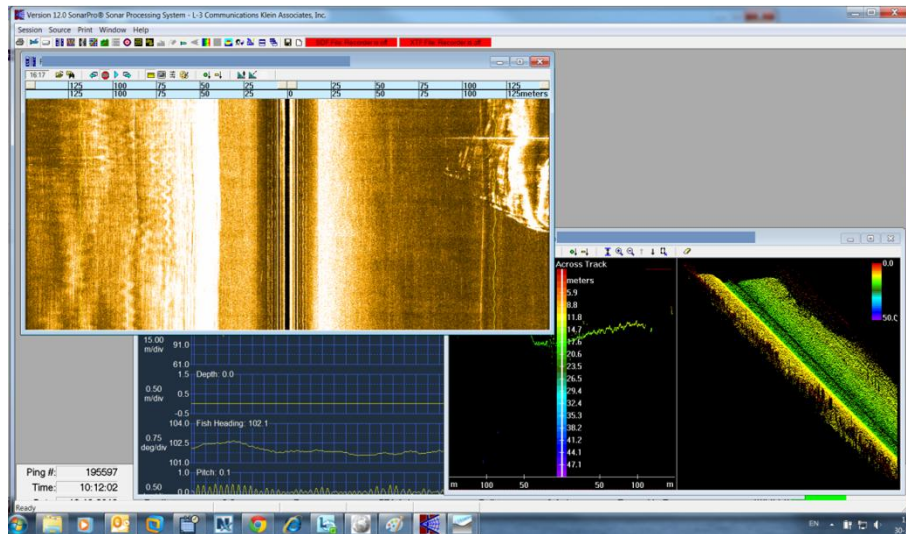
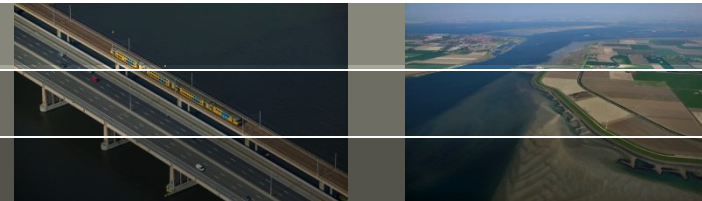


Deltares

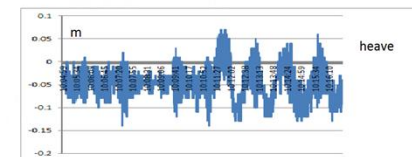
Vessel 20 - before



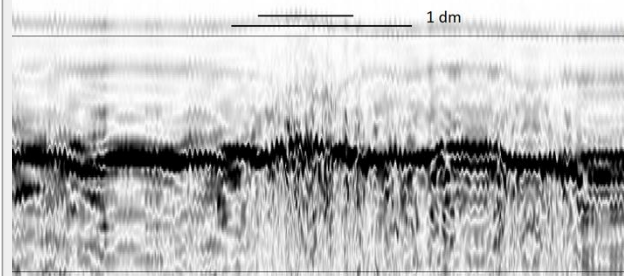
Vessel 20 - passage



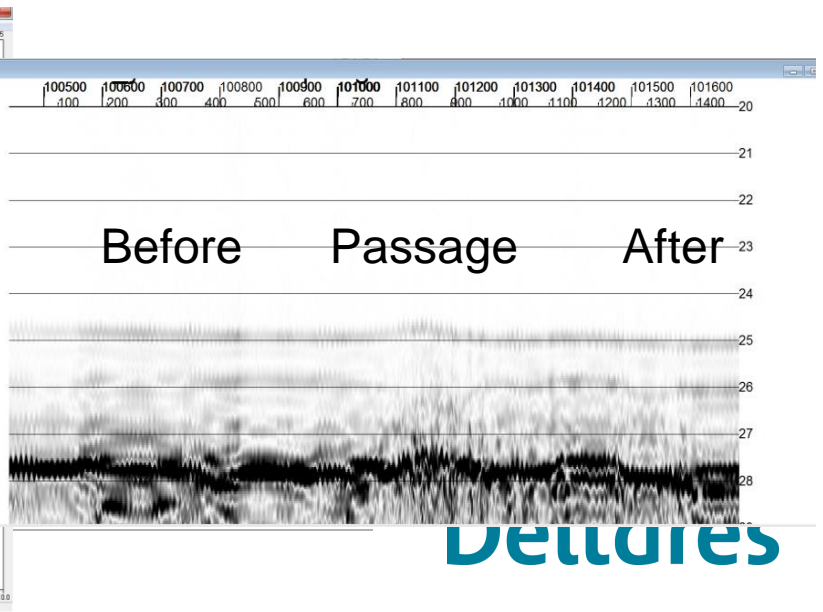
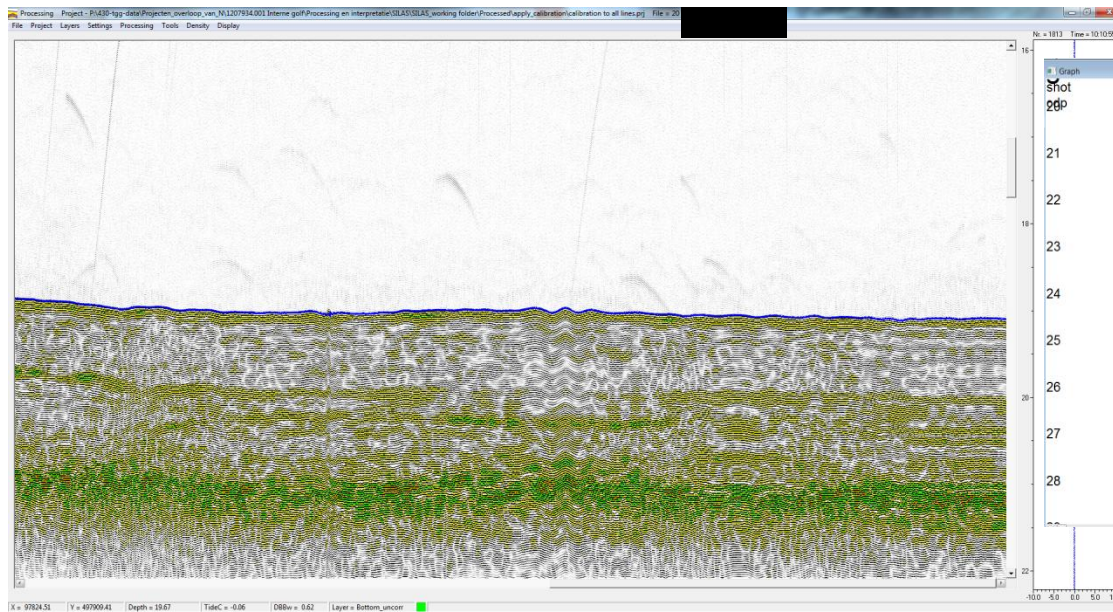
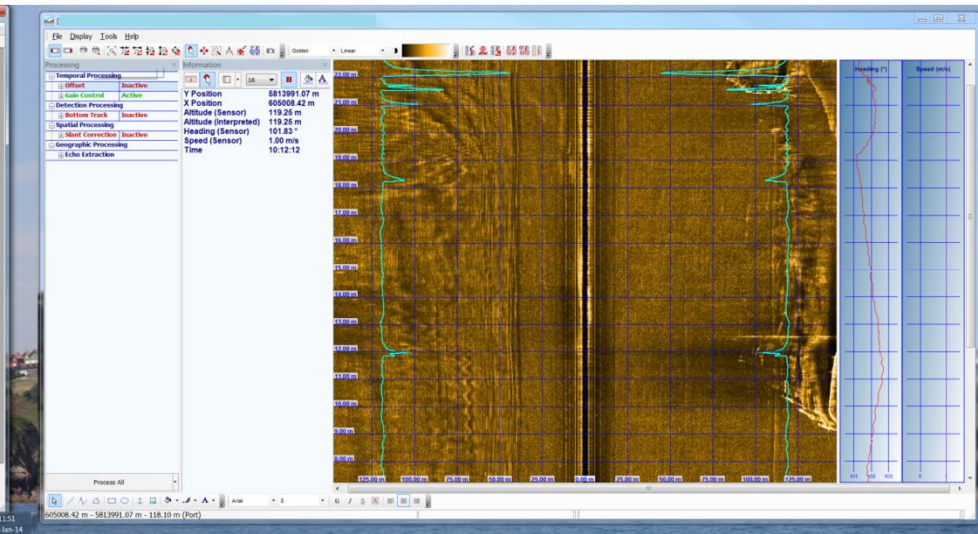
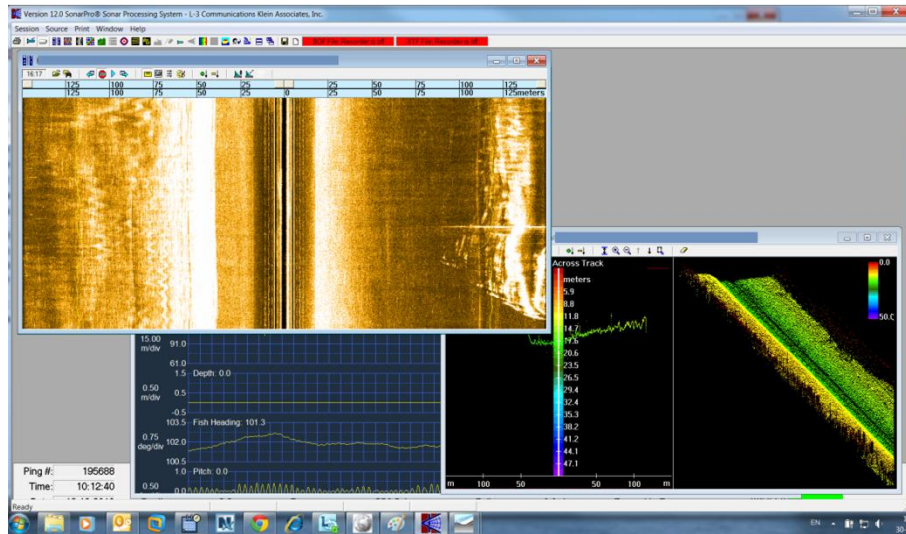
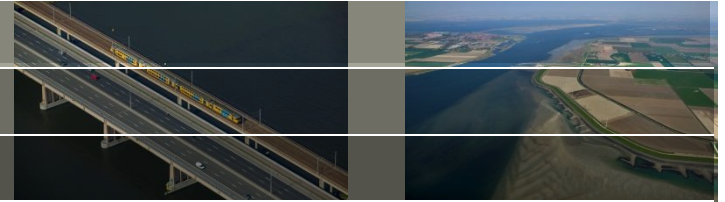
100/00 100800 100900 101000 101100 101200 101300 101400 101500 101600
300 400 500 600 700 800 900 1000 1100 1200 1300 1400 0



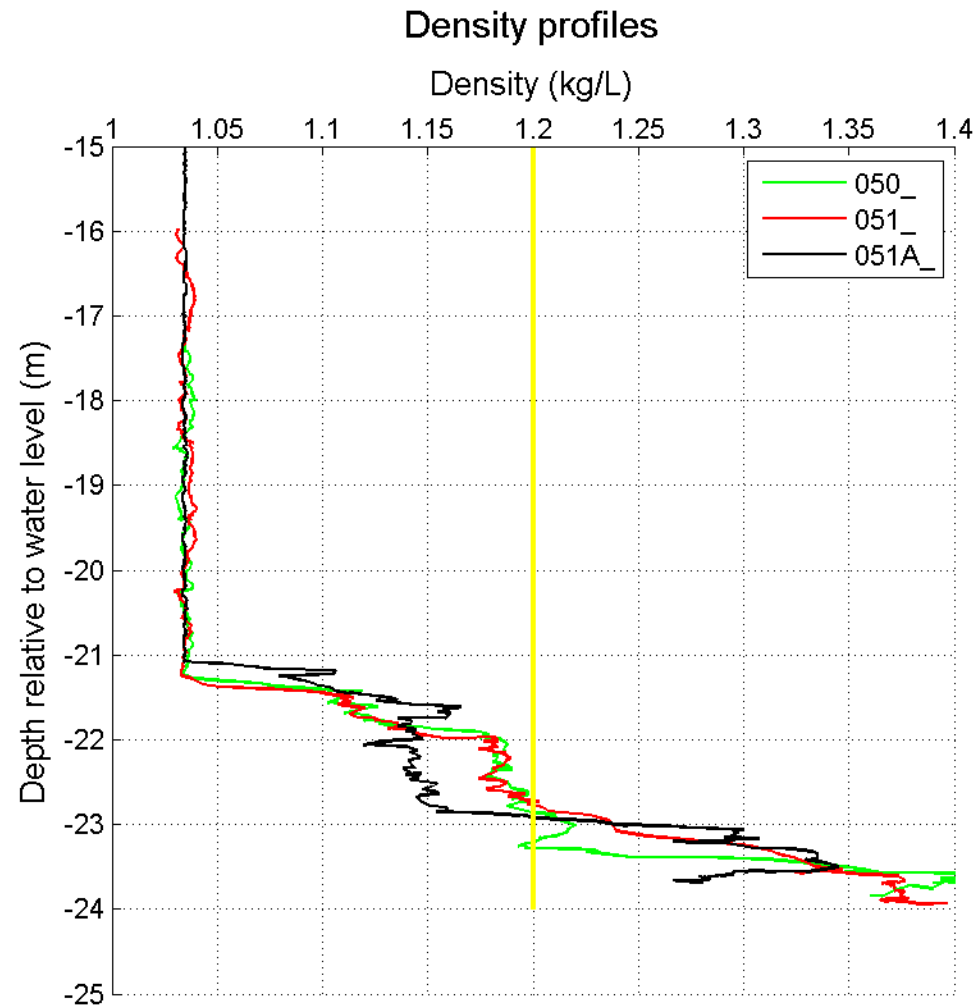
1 dm

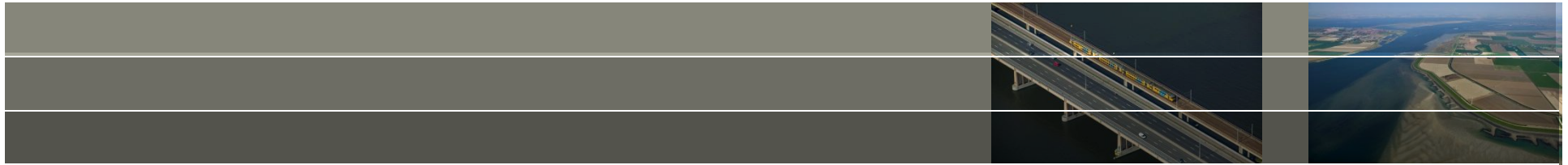


Vessel 20 - after



Vessel 20 – density profiles near Zirfaea





F Navitracker density profiles

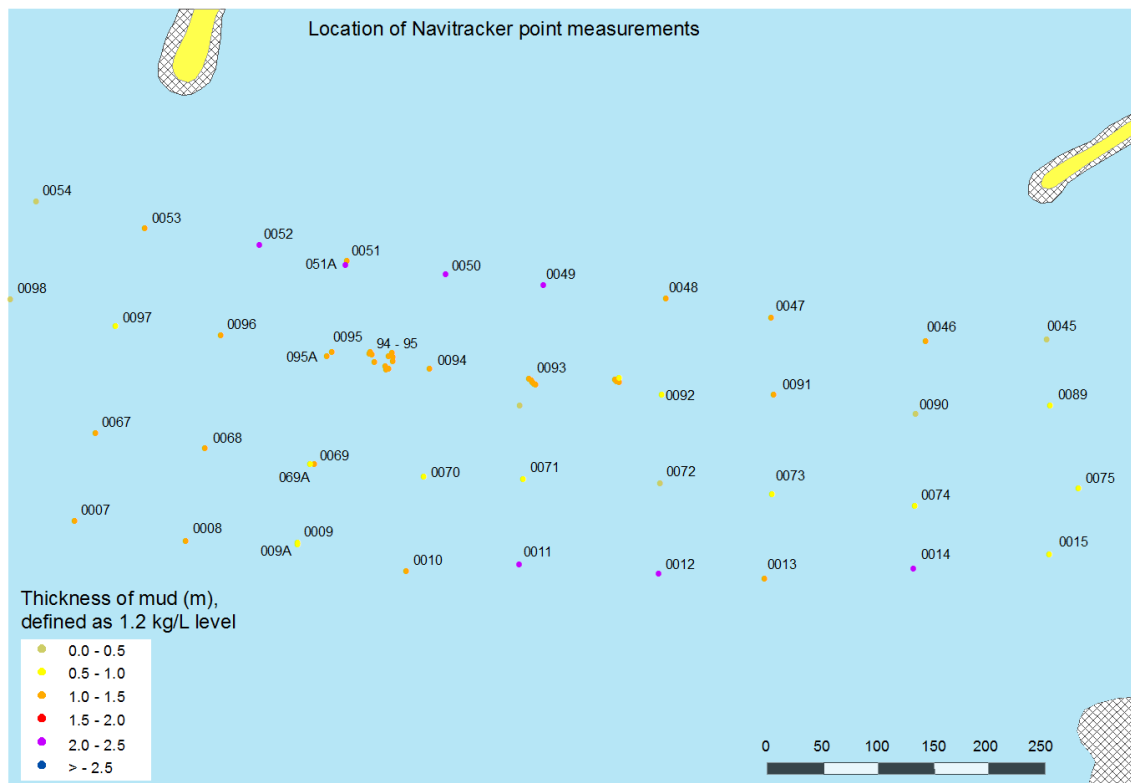


Figure F.1 Location of Navitracker point measurements of density in the survey location. Thickness of the mud, defined as the difference in depth between the top of the mud and the 1.2 kg/L level, is colour coded.

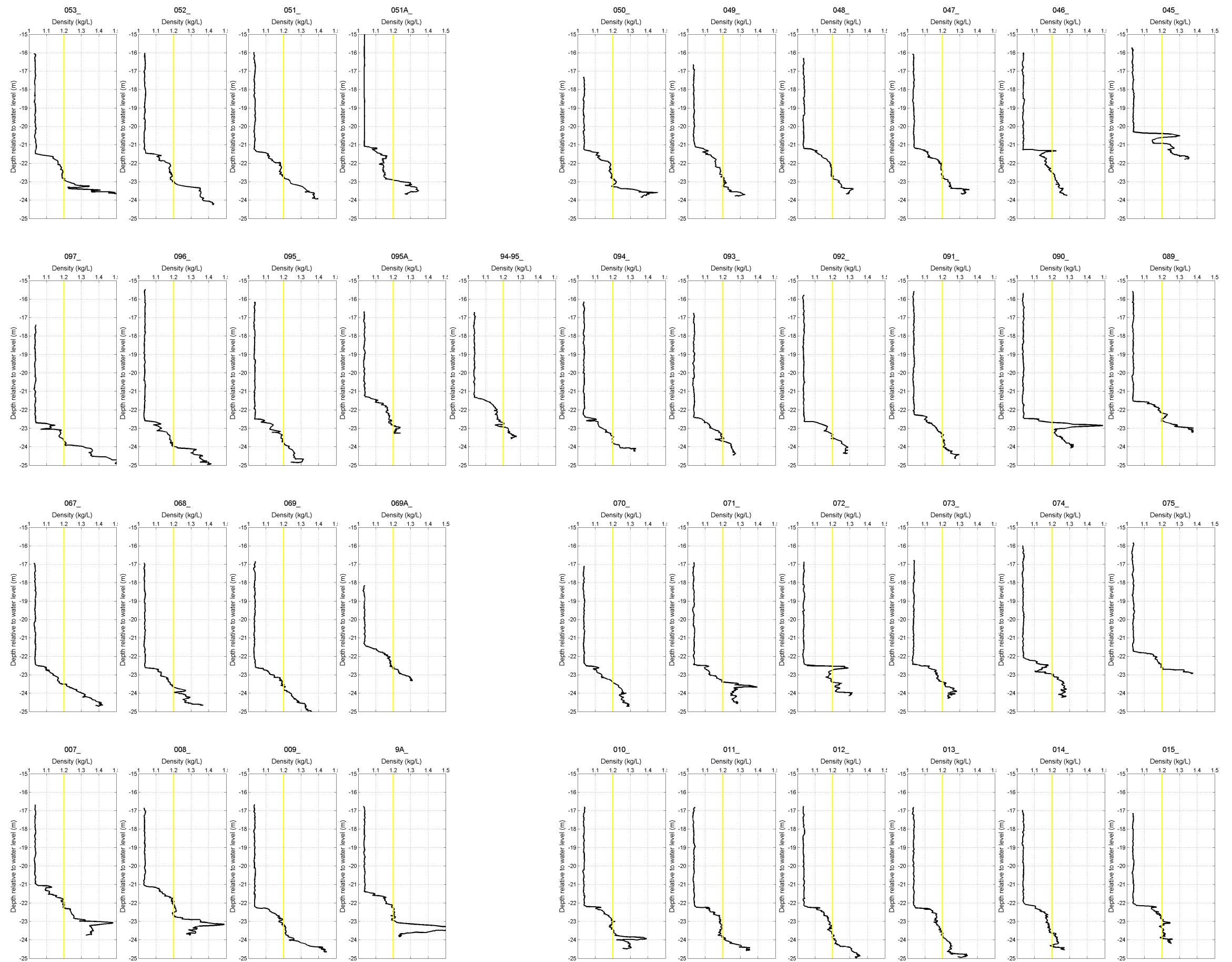
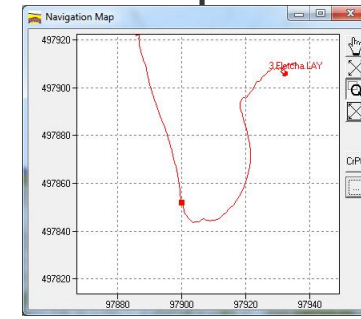
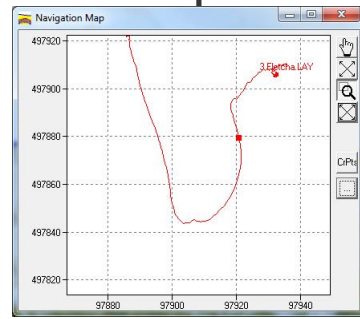
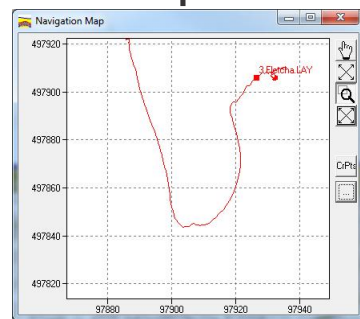
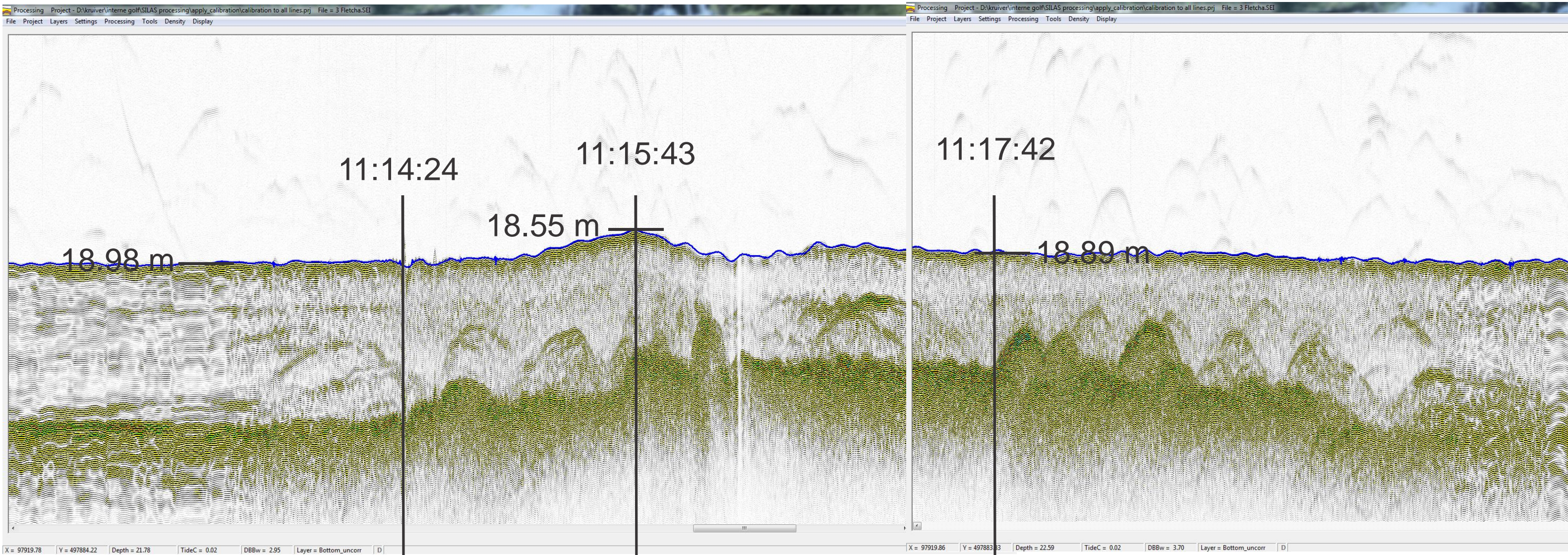


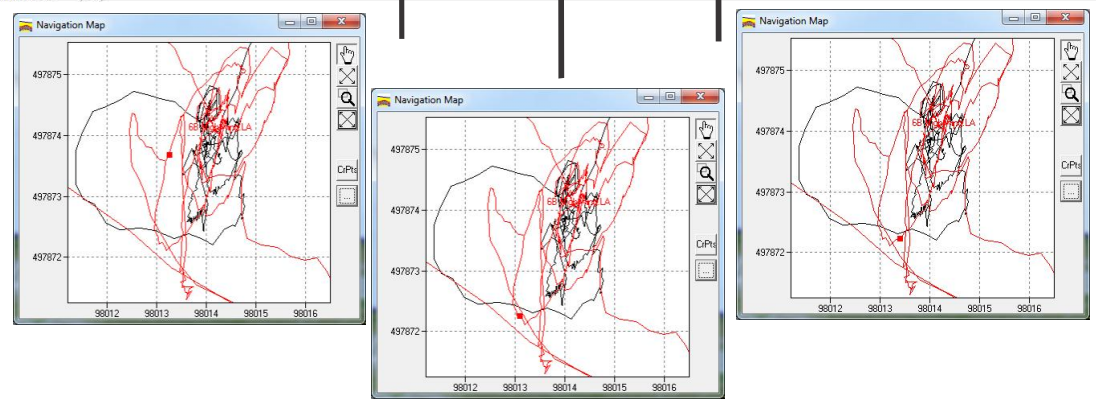
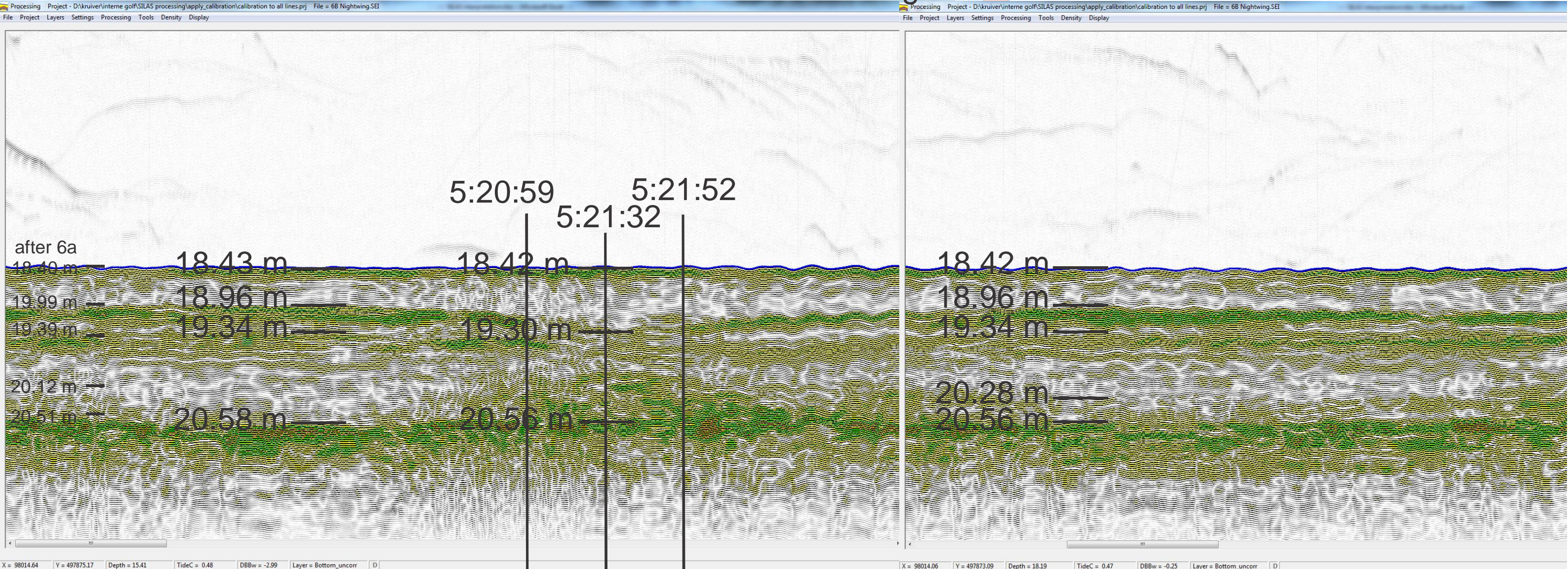
Figure F.2 Navitracker density profiles in the survey area. The standard 1.2 kg/L level is indicated by the yellow lines. The depth is relative to the water level, no tide correction has been applied to the data. The location of the profiles corresponds roughly with the location in Figure F.1.

G Interpretation of SILAS data

Vessel 03

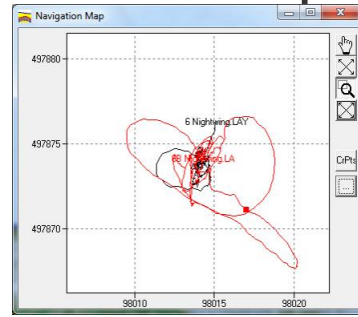
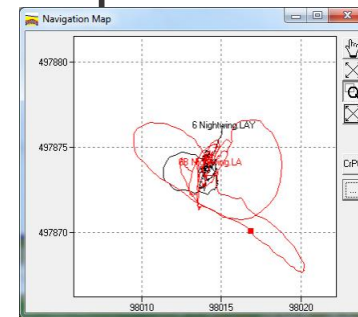
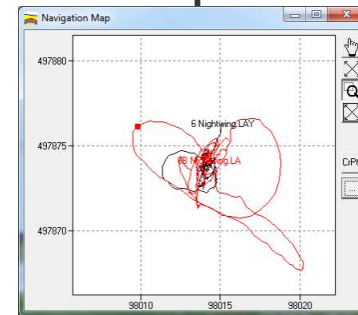
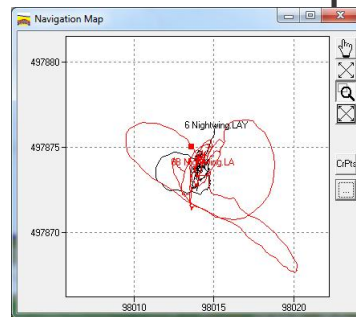
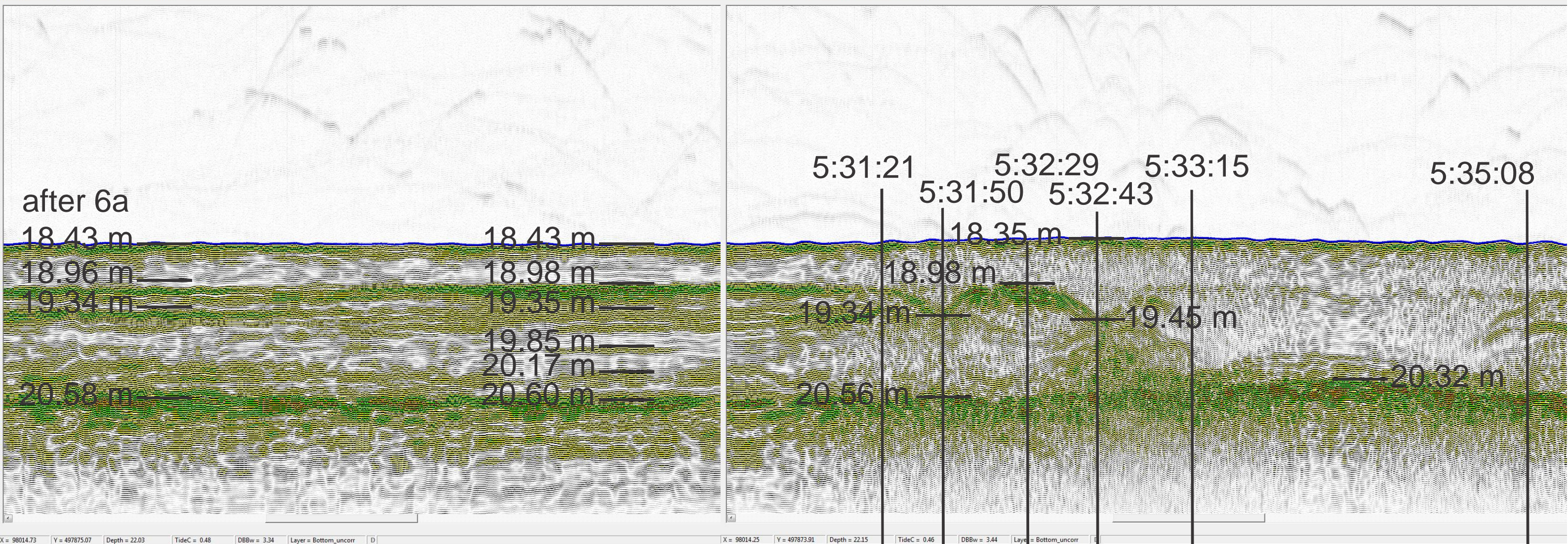


Vessel 6 -another vessel between 6a and 6? Not noted in log

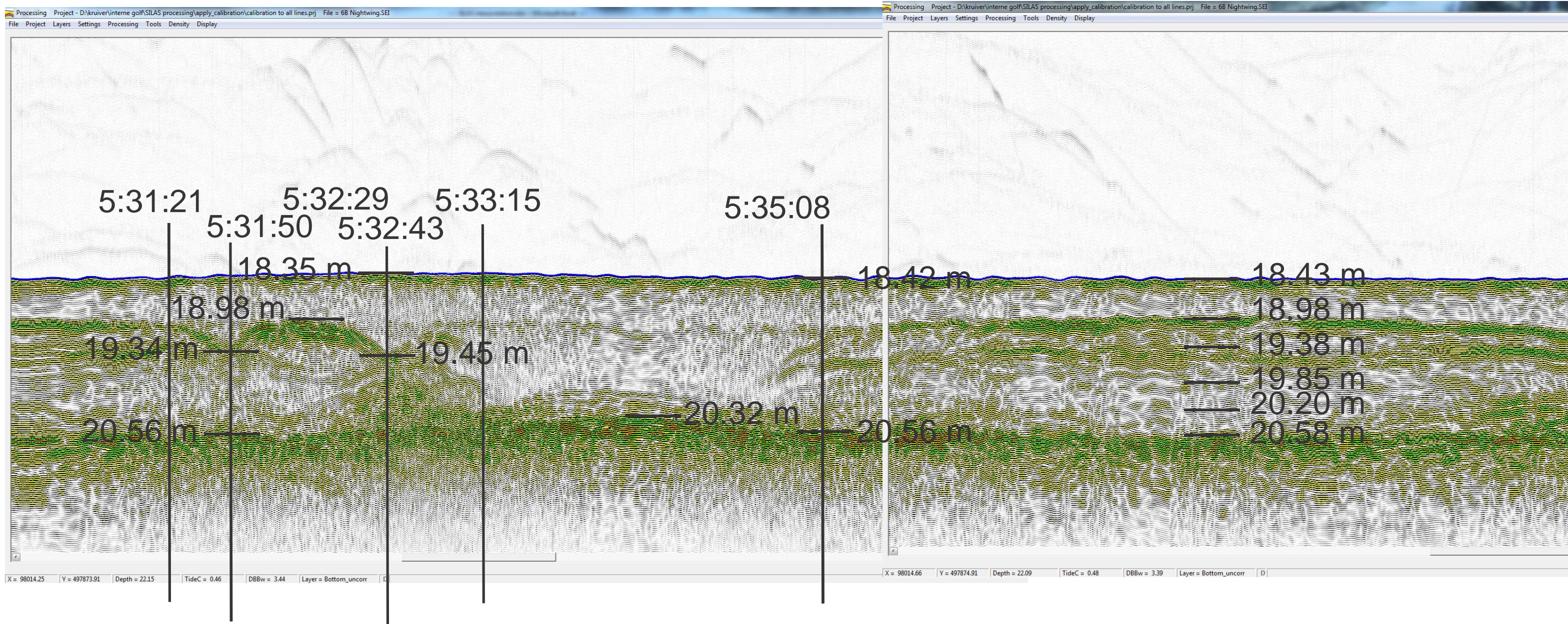


Vessel 6 - first part

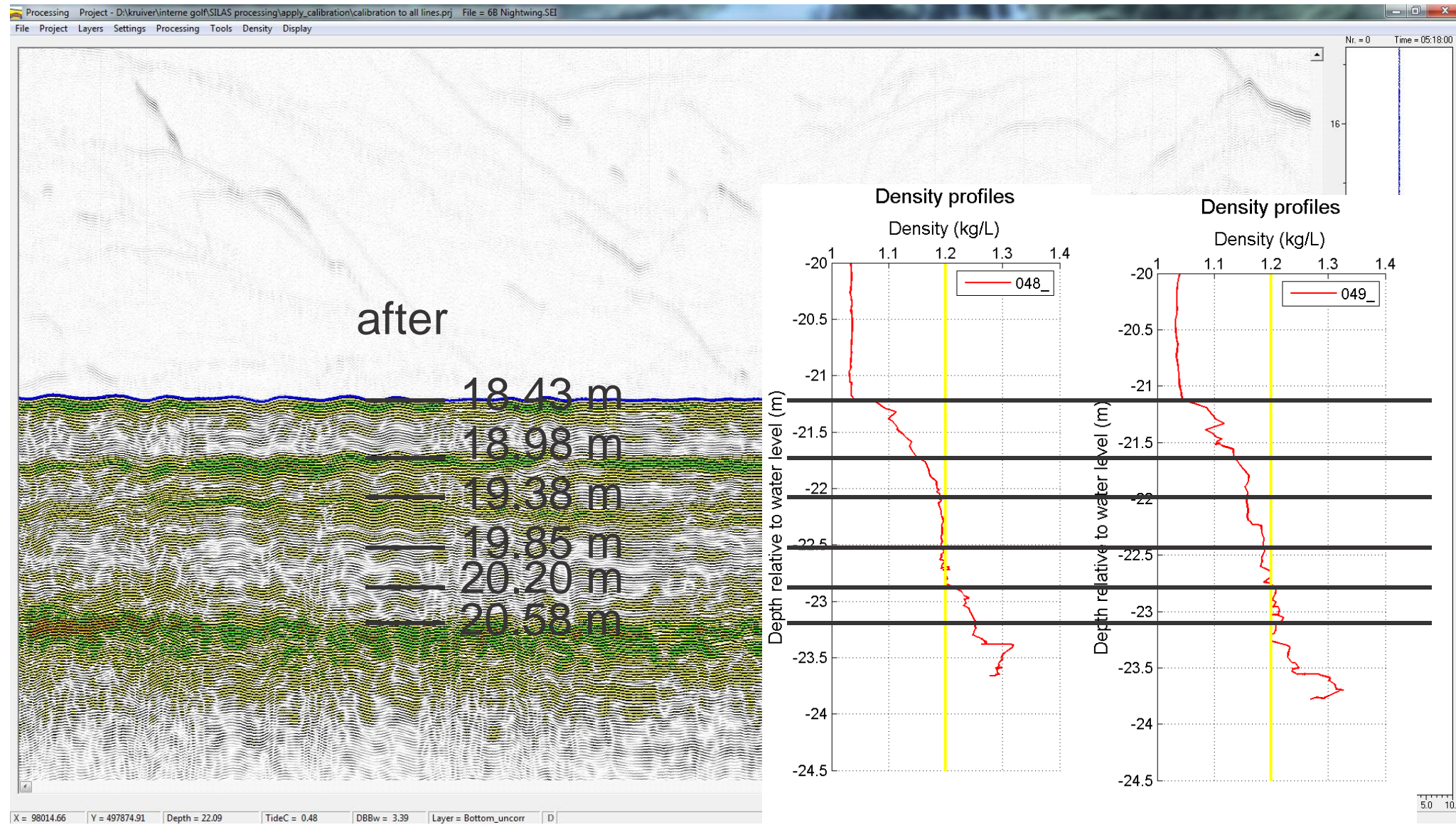
Processing Project - D:\kruiver\interne golf\SILAS processing\apply_calibration\calibration to all lines.prj File = 6B Nightwing.SEI
Processing Project - D:\kruiver\interne golf\SILAS processing\apply_calibration\calibration to all lines.prj File = 6B Nightwing.SEI



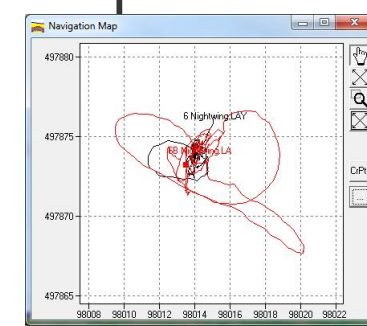
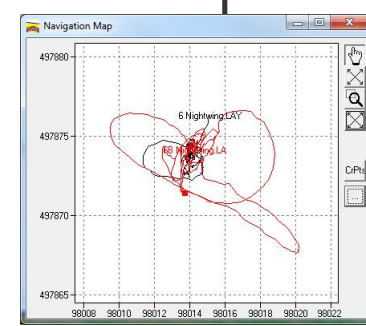
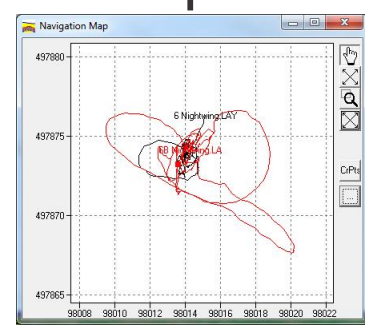
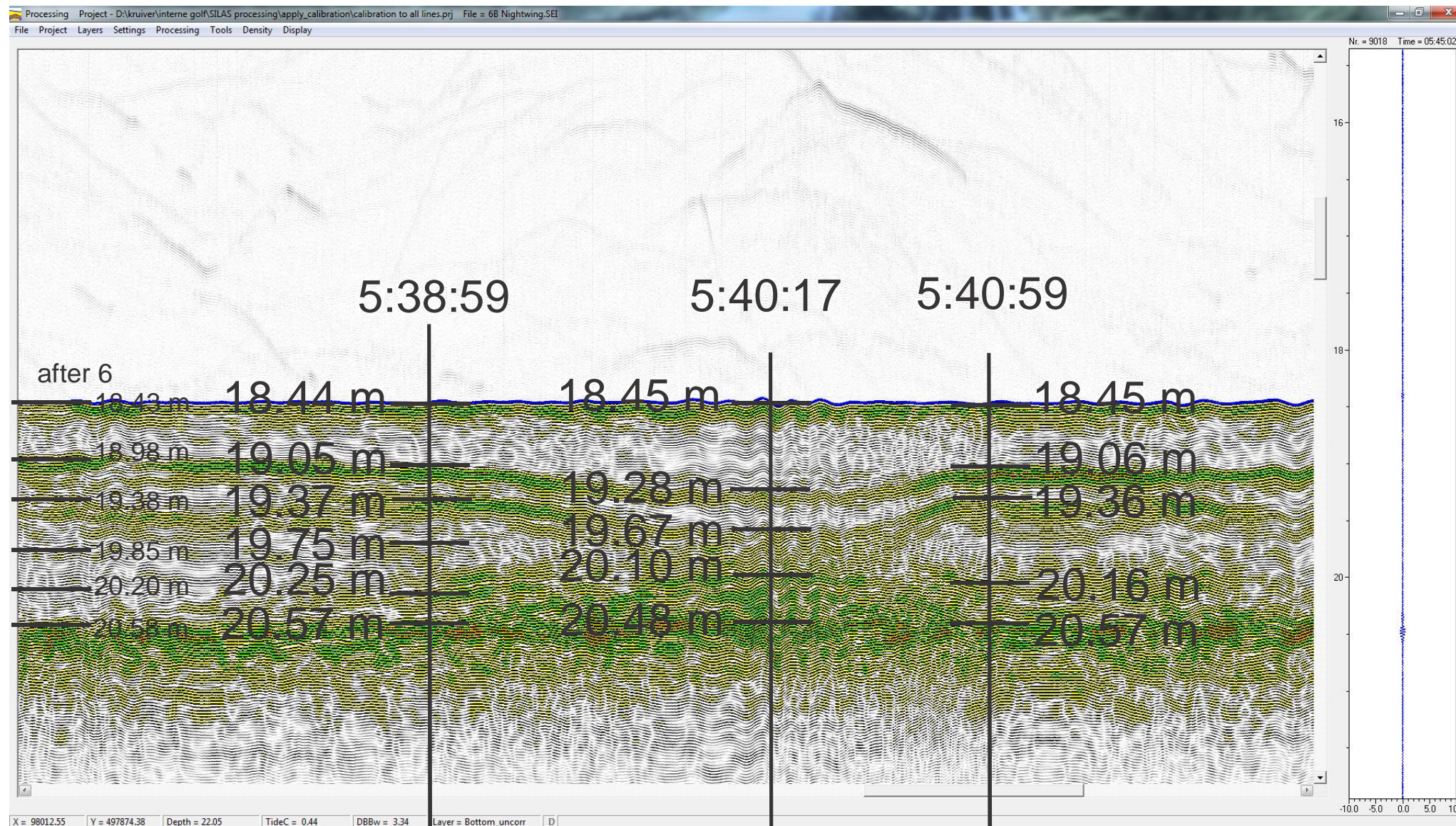
Vessel 6 - second part



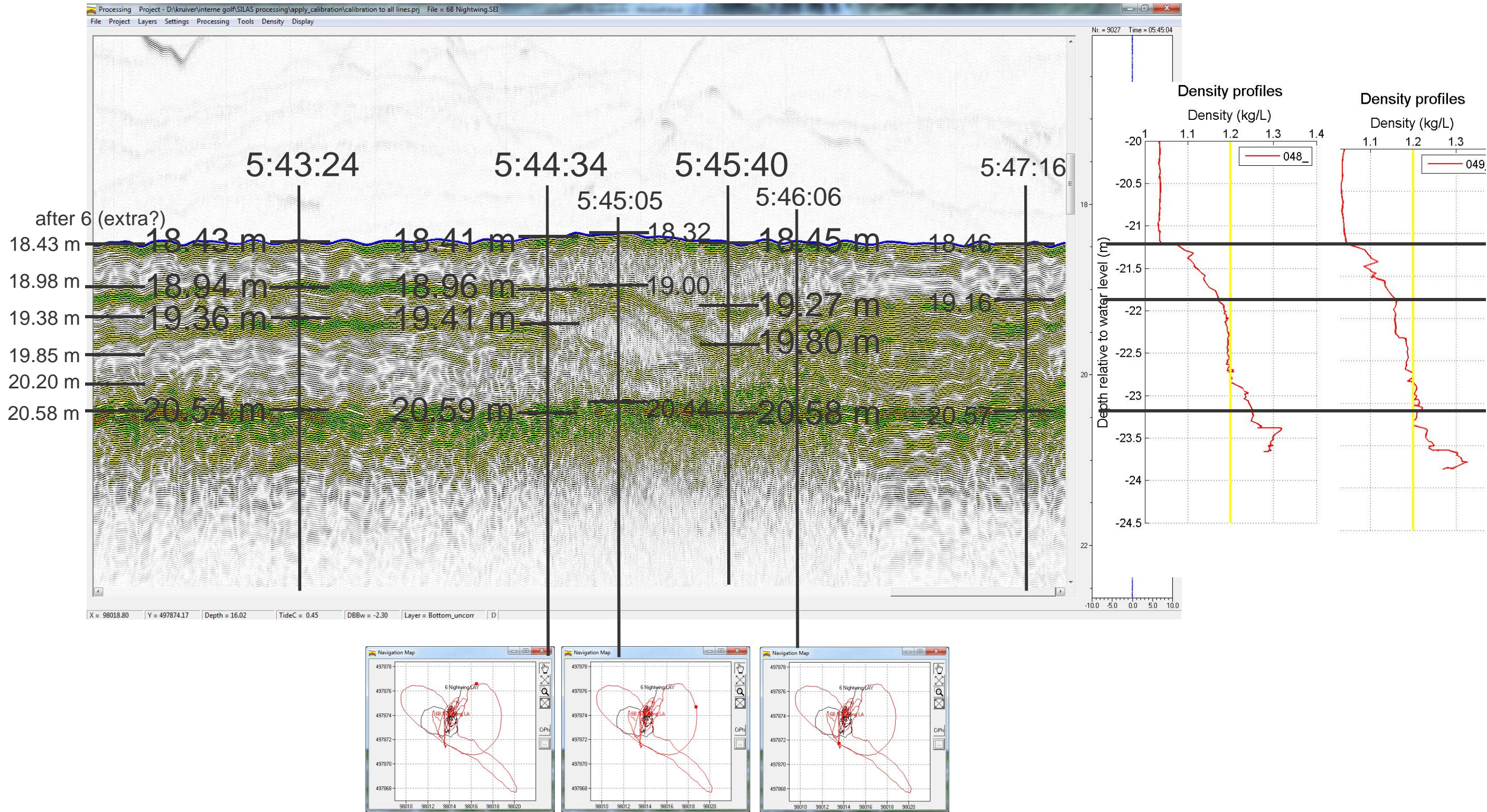
Vessel 6 - density profiles



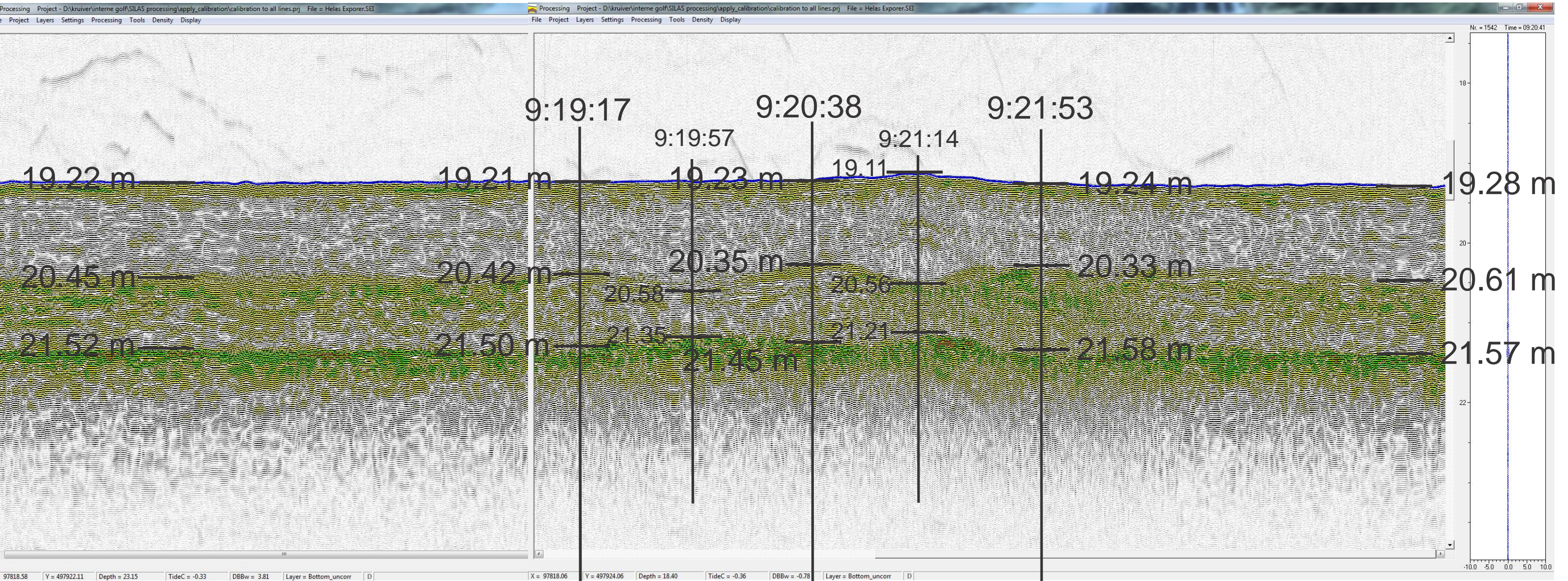
Another vessel between 6 and 6b? In log: pilot vessel at 130 m with lots of bubbles



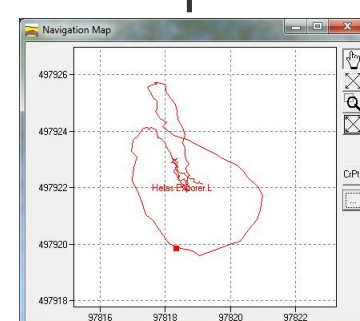
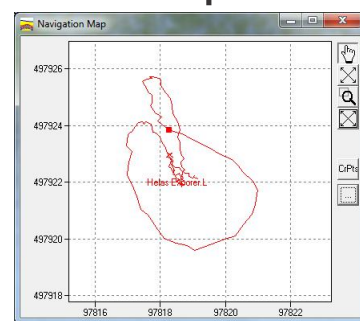
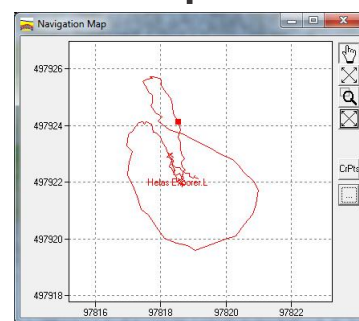
Vessel 6b



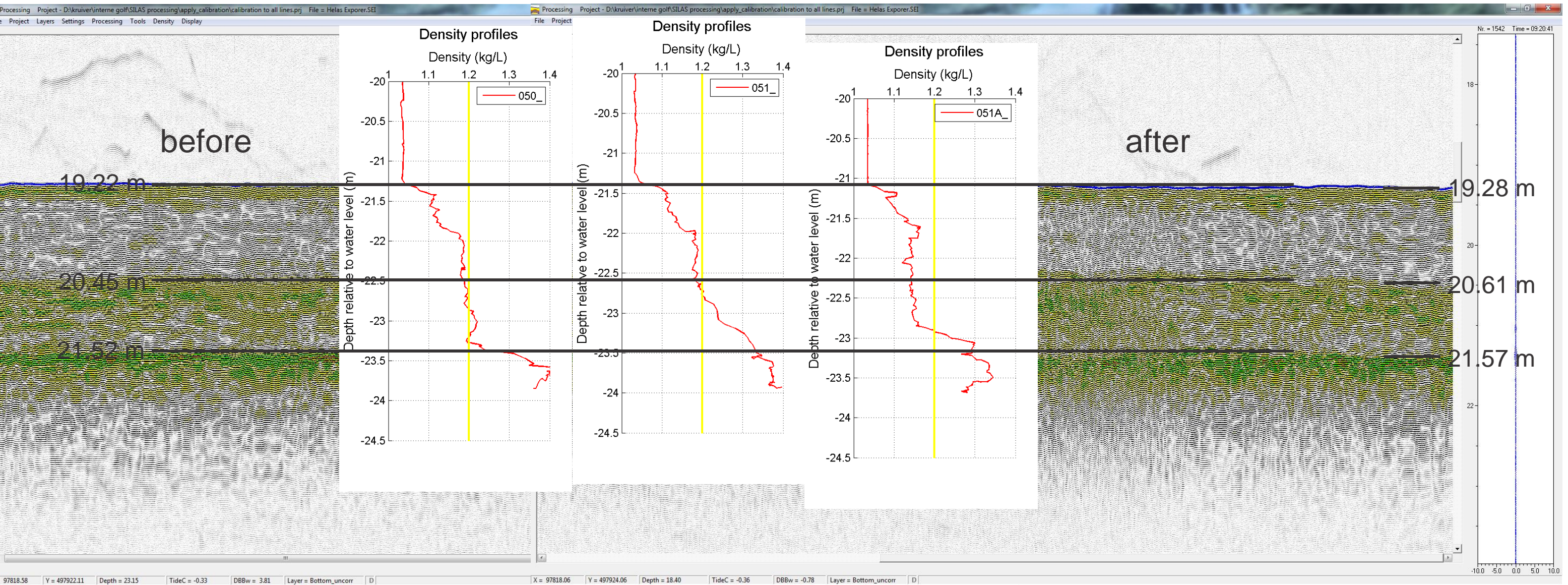
Vessel 15



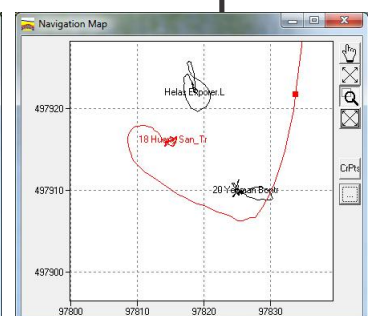
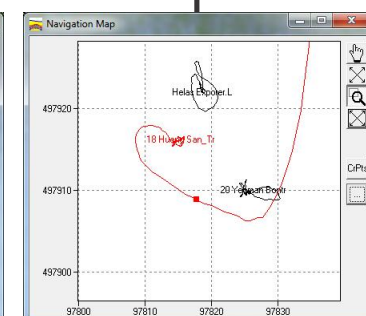
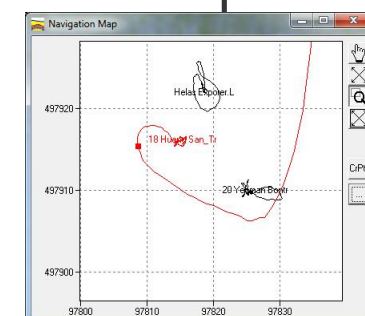
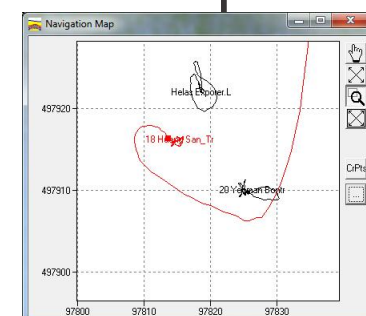
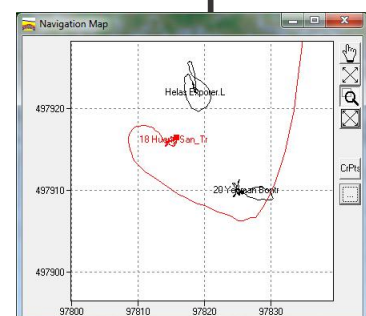
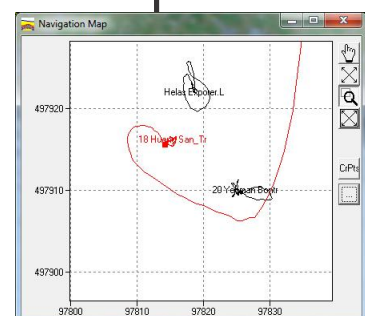
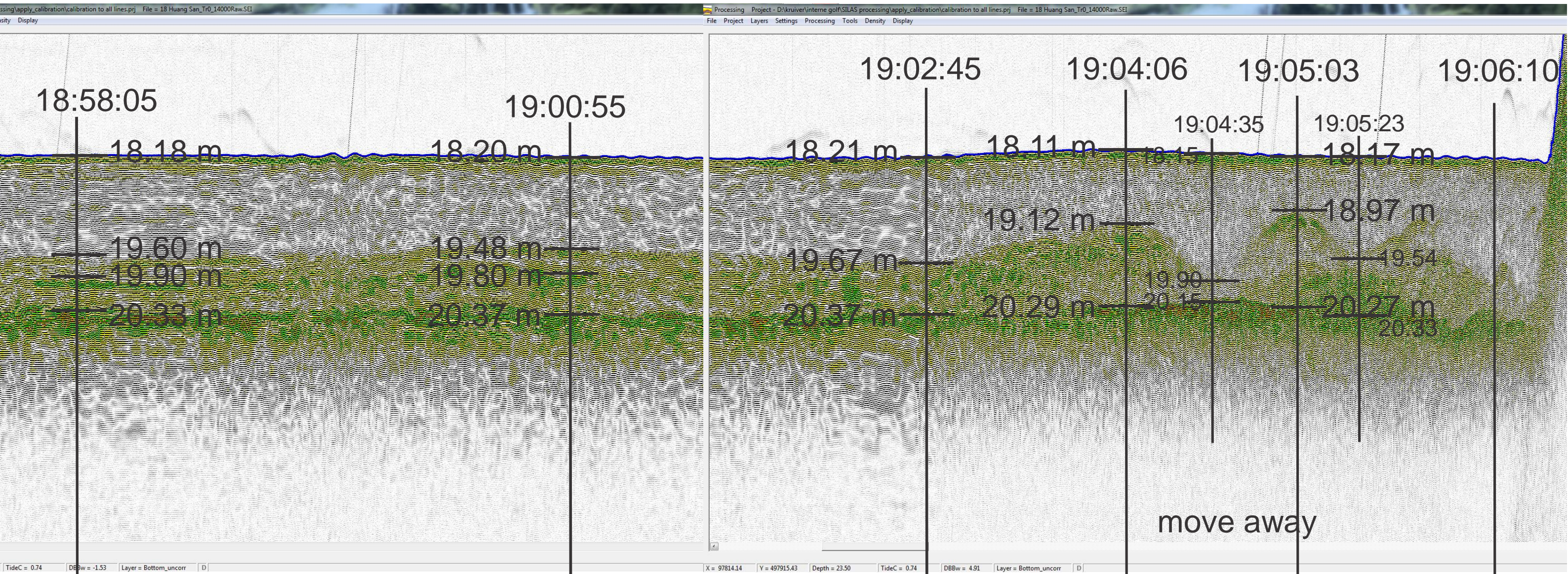
97818.58 | Y = 497922.11 | Depth = 23.15 | TideC = -0.33 | DBBw = 3.81 | Layer = Bottom_uncorr | D | X = 97818.06 | Y = 497924.06 | Depth = 18.40 | TideC = -0.36 | DBBw = -0.78 | Layer = Bottom_uncorr | D | Nr. = 1542 Time = 09:20:41



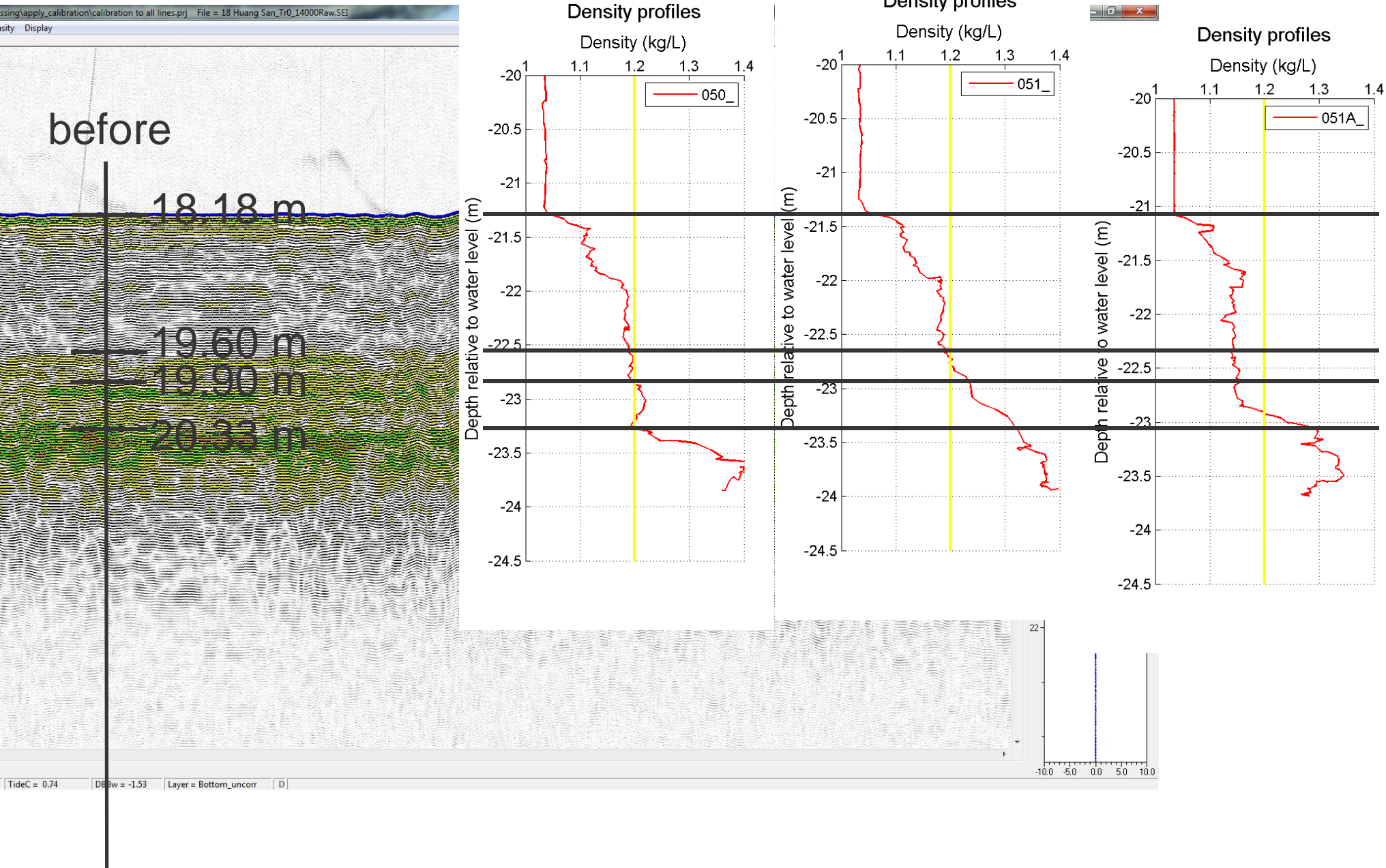
Vessel 15 - density profiles



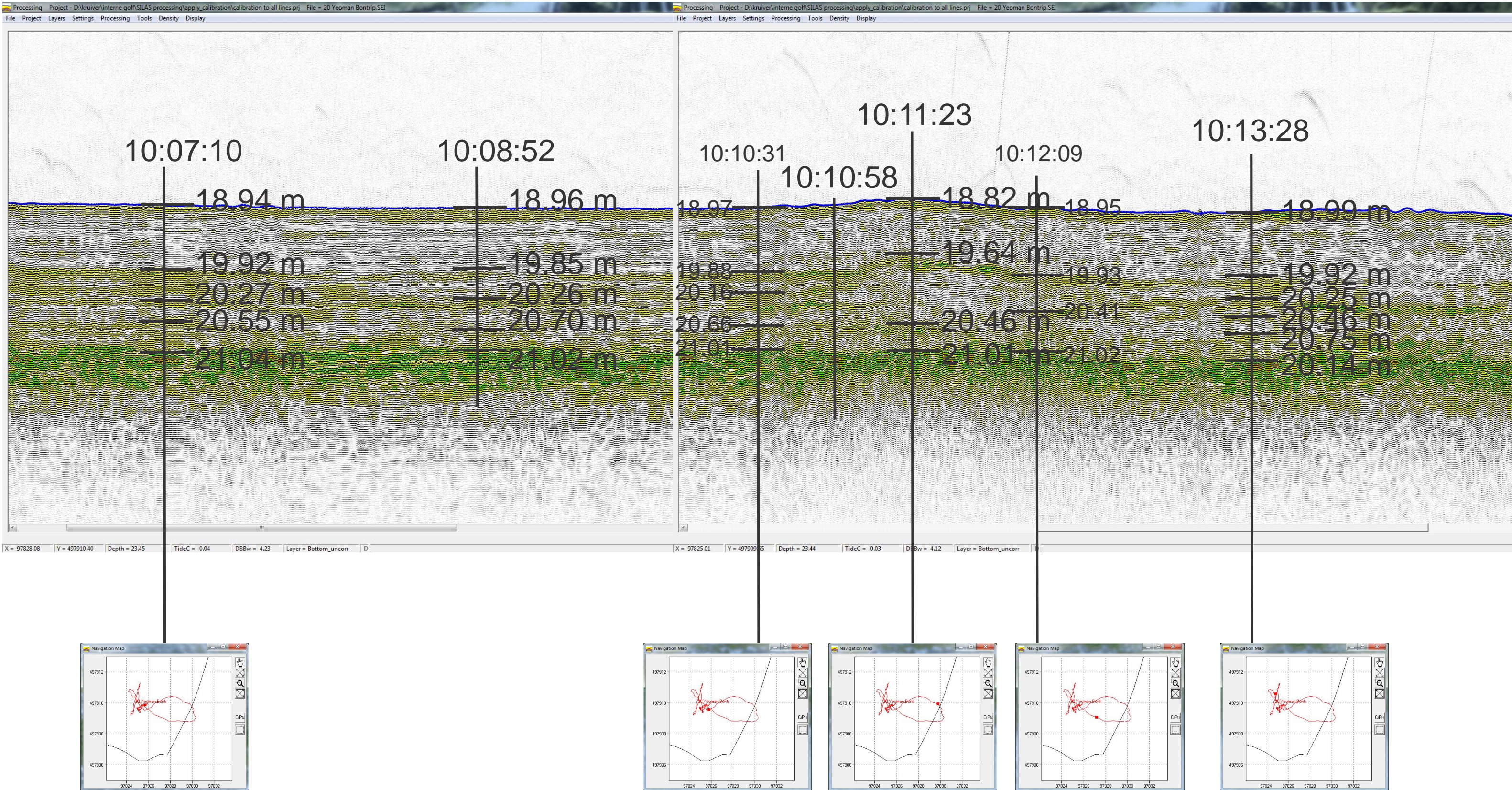
Vessel 18



Vessel 18 density profiles



Vessel 20



Vessel 20 - density profiles

